

PHYTOPLANKTON RESPONSE TO WATER QUALITY THREATS IN MIDWEST  
RESERVOIRS

---

A Dissertation

presented to

the Faculty of the Graduate School

at the University of Missouri-Columbia

---

In Partial Fulfillment

of the Requirements for the Degree

Doctor of Philosophy

---

by

JACOB CIANCI-GASKILL

Dr. Rebecca North, Dissertation Supervisor

JULY 2021

The undersigned, appointed by the dean of the Graduate School, have examined the dissertation entitled

PHYTOPLANKTON RESPONSE TO WATER QUALITY THREATS IN MIDWEST  
RESERVOIRS

presented by Jacob Cianci-Gaskill,

a candidate for the degree of doctor of philosophy,

and hereby certify that, in their opinion, it is worthy of acceptance.

---

Assistant Professor Rebecca North

---

Assistant Professor Alba Argerich

---

Assistant Research Professor Ted Harris

---

Extension Associate Professor John Lory

---

Assistant Research Professor Joanna Whittier

## ACKNOWLEDGEMENTS

This research, and opportunities to present it, were supported by the MU Graduate School, the MU College of Agriculture, Forestry, and Natural Resources, the MU School of Natural Resources, the MU Douglas D. Randall Young Scientists travel award, and the Global Lakes Ecological Observatory Network.

I would like to extend my sincere gratitude to all of the people who helped me to complete this dissertation. Experiencing the generosity of others with their time and willingness to provide assistance well beyond what was required was deeply humbling. From the bottom of my heart, thank you all. To those of you not mentioned specifically by name, please know this is a reflection of the immense amount of help that I received over the past four years and not of my lack of awareness or gratitude for you.

Thank you especially to Chris Brunet, Dan Obrecht, Carol Pollard, and Tony Thorpe for your patience, sense of humor, technical expertise, and willingness to answer my inexhaustible supply of questions. Your assistance was a crucial part of making this dissertation possible and I am, and will always be, grateful.

Thank you to all of the people who assisted me in the field and lab, including Lexy Algieri, Erica Ascani, Jaylen Bragg, Morgann Clinton, Cody Halquist, Josh Horne, Kendall Ivey, Hannah Jaeger, Cody Kimbell, Phillip Klenke, Jannice Newsom, Meghan Schrik, Simon Schroeter, Katharine Smith, and Kiah Wright. Additionally, special thanks to Kyra Florea, Tabitha Gatts, Josh Hagerty, Vanessa Morales, Matt Sauer, and Clare Vanderwerken for always going above and beyond. This would not have been possible without your hard work and dedication.

I would like to thank Ruchi Bhattacharya, Garrett Frandson, Emily Kinzinger, Erin Petty, and Jessi Wilson for all of your help, humor, and support. I am so lucky to be surrounded by such wonderful people and will be forever grateful for your advice and friendship.

Chapter 2 of this dissertation would not have been possible without the help of Steven Baker, LeeAnn Bennett, Scott Campbell, Jerry deNoyelles, Regina Klepikow, Amy Shields, and Laura Webb. Thank you for your hard work, positive attitudes, and generosity with your time.

For chapter 3, Steffanie Abel, Jim Baker, Darby Niswonger, William Schriener, and Jeff Wenzel were a tremendous help collecting and processing fish, analyzing otoliths, and providing expertise on fish consumption advisories. Additionally, I am grateful to Katrina Knott and Becca O'Hearn. You cannot know how important your guidance and encouragement were, and this project would not have been possible without you.

Thank you also to Jack Jones, Bruce Perkins, and the hundreds of volunteers and technicians who contributed to the MU Limnology Lab SLAP and LMVP datasets over the past 40 years. The importance of long-term monitoring data in environmental research cannot be overstated and it was an honor to work with this dataset in chapter 4.

I am grateful to Christie Spinka and Tom Anderson for assistance with statistical analyses, and to Chris Babayco for suggestions and advice about ELISA. Thank you to the MU School of Natural Resources Writing Group for edits and suggestions that greatly improved the quality of this dissertation.

I would also like to thank my advisor, Rebecca North, for your support and encouragement over the past four years, and my committee members for your technical expertise and helpful suggestions throughout my dissertation.

I am thankful for my family, including Ruth Swartswelder, Scott Gaskill, Grace Gaskill, Anne Swartswelder, Joanne Cianci, and Giorgio Cianci. Your love and kind words helped keep me going, and your advice helped keep me sane. I am so grateful to have such a strong, encouraging, and level-headed support network. Thank you also to Nora for being the best writing partner and walking buddy anyone could ask for.

Finally, this dissertation would not have been possible without Daniela Cianci-Gaskill. Daniela, being able to lean on your advice and perspectives was more helpful than you will ever know. I will always be grateful to you for your patience, ceaseless encouragement, and for having confidence in me even when I was not able to have confidence in myself. More importantly, I am so appreciative of the sacrifices you have made which have allowed me to pursue my passion. Your selflessness is deeply humbling and I want you to know that I do not, and will never, take these sacrifices for granted. I could not have gotten here without you. From the bottom of my heart, thank you.

## TABLE OF CONTENTS

ACKNOWLEDGEMENTS .....	ii
LIST OF FIGURES .....	xi
LIST OF TABLES .....	xvii
ABSTRACT .....	xxii
CHAPTER 1: LITERATURE REVIEW .....	1
PROBLEM STATEMENT .....	1
<i>Harmful cyanobacterial blooms</i> .....	1
<i>Cyanotoxins</i> .....	3
<i>Invasive zebra mussels</i> .....	4
FACTORS INFLUENCING PHYTOPLANKTON GROWTH .....	5
<i>Nutrients</i> .....	6
<i>Light</i> .....	8
<i>Water temperature</i> .....	11
<i>Grazers</i> .....	12
MANAGING CYANOBACTERIAL BIOMASS WITH GEOENGINEERING ....	14
<i>Phosphorus inactivation agents</i> .....	15
<i>Aquashade®</i> .....	18
<i>Artificial mixing</i> .....	19
<i>Ultrasonication</i> .....	20
<i>Glacial rock flour</i> .....	21
CONSEQUENCES OF HARMFUL CYANOBACTERIAL BLOOMS .....	25

<i>Microcystin in water</i> .....	27
<i>Microcystin in fish</i> .....	28
<i>Human health risks associated with microcystin</i> .....	30
ZEBRA MUSSELS .....	33
<i>The effects of zebra mussels on phytoplankton</i> .....	33
<i>Environmental factors influencing zebra mussel filtration</i> .....	37
DISSERTATION JUSTIFICATION .....	46
<i>Objectives and hypotheses</i> .....	46
LITERATURE CITED .....	50
CHAPTER 2: PHYTOPLANKTON COMMUNITY RESPONSE TO CHANGES IN LIGHT: CAN GLACIAL ROCK FLOUR BE USED TO CONTROL CYANOBACTERIAL BLOOMS? .....	81
ABSTRACT .....	81
INTRODUCTION .....	82
MATERIALS AND METHODS .....	86
<i>Experimental design and sample collection</i> .....	86
<i>Laboratory analyses</i> .....	91
<i>Statistical analyses</i> .....	96
RESULTS .....	97
<i>Physical parameters</i> .....	97
<i>Water chemistry</i> .....	99
<i>Phytoplankton community biovolume</i> .....	102
<i>Phytoplankton physiology and gross primary productivity</i> .....	104
<i>Zooplankton</i> .....	105

DISCUSSION .....	106
<i>How did the GRF addition affect physical, chemical, and biological parameters in the mesocosm tanks?</i> .....	106
<i>Which functional traits enables cryptophytes to replace cyanophytes</i> .....	110
<i>What implications do our findings have for the nutrient load hypothesis?</i> .....	112
<i>How does GRF compare to other geoengineering strategies?</i> .....	114
<i>Conclusions</i> .....	117
LITERATURE CITED .....	118
TABLES .....	128
FIGURES .....	136
CHAPTER 3: MONITORING MICROCYSTIN ACCUMULATION IN TWO POPULAR SPORTFISH OVER THE COURSE OF A YEAR .....	142
ABSTRACT .....	142
INTRODUCTION .....	143
METHODS .....	146
<i>Site description</i> .....	146
<i>Field collection</i> .....	148
<i>Laboratory analyses</i> .....	150
<i>Statistical analyses</i> .....	156
RESULTS .....	159
<i>Reservoir characteristics</i> .....	160
<i>Water cyanotoxins</i> .....	161
<i>Fish characteristics</i> .....	162
<i>Microcystin in fish by harvest date, species, and tissue</i> .....	163

<i>Fish characteristic cofactors contributing to microcystin variation in fish tissues</i>	163
<i>Combined drivers of microcystin in fish tissues</i>	164
<i>The effects of harvest date and species on microcystin in fish tissues</i>	166
DISCUSSION	167
<i>Temporal patterns of microcystin in fish</i>	168
<i>Differences in microcystin by species</i>	169
<i>Microcystin toxicodistribution in fish</i>	171
<i>Microcystin in water and fish</i>	174
<i>Ecological implications</i>	176
<i>Management implications</i>	178
<i>Conclusions</i>	181
LITERATURE CITED	182
TABLES	192
FIGURES	201
CHAPTER 4: ARE INVASIVE ZEBRA MUSSELS ALWAYS ASSOCIATED WITH AN INCREASE IN WATER CLARITY?	205
ABSTRACT	205
INTRODUCTION	205
METHODS	208
<i>Study reservoirs</i>	208
<i>Water clarity parameters</i>	210
<i>Zebra mussel density and biomass</i>	211
<i>Temperature and dissolved oxygen profiles</i>	213

<i>Statistical analyses</i> .....	214
RESULTS .....	216
<i>Study reservoirs</i> .....	216
<i>Regime shifts in invaded reservoirs</i> .....	217
<i>Regime shifts in reference reservoirs</i> .....	220
<i>Zebra mussel density and biomass</i> .....	222
<i>Habitat suitability</i> .....	223
DISCUSSION .....	223
<i>Zebra mussel populations</i> .....	225
<i>Water temperature</i> .....	227
<i>Suspended inorganic particles</i> .....	228
<i>Dissolved oxygen concentrations</i> .....	230
<i>Zebra mussels along the southern extant of their expansion</i> .....	231
<i>Conclusions</i> .....	233
LITERATURE CITED .....	235
TABLES .....	242
FIGURES .....	256
CHAPTER 5: EXECUTIVE SUMMARY .....	265
LITERATURE CITED .....	272
APPENDIX 1 .....	276
TABLES .....	276
FIGURES .....	306
LITERATURE CITED .....	313

APPENDIX 2 .....	314
SUPPLEMENTARY METHODOLOGY .....	314
<i>Bathymetric measurements</i> .....	314
<i>Phytoplankton identification and enumeration methodology</i> .....	314
<i>Correlation between microcystin and length</i> .....	315
TABLES .....	316
FIGURES .....	320
LITERATURE CITED .....	326
APPENDIX 3 .....	327
FIGURE .....	327
VITA .....	328

## LIST OF FIGURES

**Figure 2.1:** Birds-eye view of mesocosm tank set-up. We added glacial rock flour (GRF) to 14 of the 17 mesocosm tanks used in this experiment. Phytoplankton communities were dominated by either chlorophytes or cyanophytes ( $n=8$ ) at the beginning of the experiment. Of the 9 chlorophyte dominated tanks, a subset ( $n=3$ ) did not receive any nutrient nor GRF amendments and were treated as a control (Con). The remaining chlorophyte dominated tanks ( $n=6$ ) received daily GRF additions. Tanks were kept in a  $\sim 1300\text{ m}^2$  shallow pond that was  $\sim 1\text{ m}$  deep to insulate for changes in air temperatures. The pond was surrounded by low vegetation. Mesocosm tanks were  $\sim 3\text{ m}$  across,  $1.25\text{ m}$  high, and volume of  $11,000\text{ L}$ . Crossbeams were placed across each mesocosm. Sediment traps were suspended from each crossbeam.

**Figure 2.2:** Comparison of the light environment between tanks that received glacial rock flour (GRF) and tanks that did not receive GRF. PAR ratio (0.5 m water/air reading; A) and vertical light attenuation coefficient ( $K_d$ ; B) were measured in all tanks after GRF was added to all ( $n=14$ ) but the control tanks ( $n=3$ ). Both the PAR ratio and  $K_d$  were measured one hour after GRF addition every day of the experiment, 4 hours after addition on days 0, 5, 6, and 7, and 6 hours after addition on day 4. The light ratio was determined by dividing photosynthetically active radiation (PAR) measurements made at 0.5 m depth by PAR measurements from above the water's surface in the air. Among GRF tanks, the light ratio was significantly lower one hour after GRF addition than 4 (Kruskal-Wallis  $p < 0.0001$ ,  $df=2$ ,  $\chi^2=26.46$ ) or 6 hours (Kruskal-Wallis  $p=0.0002$ ,  $df=2$ ,  $\chi^2=26.46$ ), but not significantly different between 4 and 6 hours (Kruskal-Wallis  $p=0.1709$ ,  $df=2$ ,  $\chi^2=26.46$ ; Figure 2).  $K_d$  was significantly higher one hour after GRF addition (Kruskal-Wallis  $p < 0.0001$ ,  $df=2$ ,  $\chi^2=37.10$ ), but not 4 nor 6 hours after addition (Kruskal-Wallis  $p=0.2347$ ,  $df=2$ ,  $\chi^2=37.10$ ). For each time, the light ratio was significantly lower (Kruskal-Wallis  $p < 0.0001$ ,  $df=1$ ,  $\chi^2=75.99$ ) in tanks that received GRF compared to control tanks that did not. For each time,  $K_d$  was significantly higher (Kruskal-Wallis  $p < 0.0001$ ,  $df=1$ ,  $\chi^2=87.88$ ) in tanks that received GRF compared to control tanks that did not.

**Figure 2.3:** Phytoplankton biovolume categorized by functional group. Biovolume for day 0 (A) and day 9 (B) for control tanks, tanks dominated by chlorophytes at the beginning of the experiment, and tanks dominated by cyanophytes at the beginning of the experiment. The chrysophyta\* group includes chrysophyta, bacillariophyta, haptophyta, and ochrophyta.

**Figure 2.4:** Zooplankton abundance in mesocosm tanks. Abundance was measured on day 0 (A) and day 9 (B) for control tanks, tanks dominated by chlorophytes at the beginning of the experiment, and tanks dominated by cyanophytes at the beginning of the experiment.

**Figure 2.5:** Adaptation of the nutrient load hypothesis from Brauer et al., (2012). This hypothesis predicts which phytoplankton dominate based on competition for nitrogen (N), phosphorus (P), and light. The nutrient load hypothesis is based on the assumption that cyanobacteria are superior competitors for light and are able to dominate when N and P concentrations are high (Brauer et al., 2012). We add an additional box to highlight the

nuance that functional traits can add to competition for these resources, specifically light. Our added box, above, connects to Brauer et al. original figure in the area where there is competition for light. While cyanobacteria often dominate when light is the limiting resource, our findings suggest that cryptophytes can outcompete cyanobacteria under specific light levels due to functional traits. Our box shows this by introducing cryptophytes to this figure, showing that as light availability declines, cryptophytes outcompete cyanophytes.

**Figure 3.1:** Correlation-based principal component analysis (PCA) used to investigate the relationship between harvest date and 21 water parameters. The first principal component (PC 1) explains 39.9 % of the variation in this dataset, while the second component (PC 2) explains 24.9 %. Water parameters include: ammonium (NH<sub>4</sub>), chlorophyll-*a* (Chl), dissolved organic carbon (DOC), dissolved oxygen (DO), light attenuation coefficient (K<sub>d</sub>), mean daily mixed layer irradiance (E<sub>24</sub>), microcystin from the upper 0.5 m of the water, natural log of the ratio of total nitrogen to total phosphorus (TN:TP), nitrate (NO<sub>3</sub>), particulate inorganic matter (PIM), particulate organic matter (POM), percent composition of phycocyanin to chlorophyll as measured with a YSI EXO 3 (PC:Chl), pheophytin, pH, Secchi disk depth, temperature (temp), total dissolved nitrogen (TDN), total dissolved phosphorus (TDP), total nitrogen (TN), total phosphorus (TP), and total suspended solids (TSS). Vector length reflects the magnitude of variation explained by that water parameter. Vectors close together are positively correlated while vectors opposite from each other are negatively correlated. Vectors that are orthogonal from each other are unrelated. Harvest date is represented by points.

**Figure 3.2:** Microcystin in water and fish muscles. Microcystin was measured in the upper 0.5 m of water (dashed lines, open circles, right y-axis) and in bluegill (light grey boxes) and largemouth bass (dark grey boxes) muscles (left y-axis). Standard error for water microcystin was never more than 0.4 per Abraxis Microcystin ELISA guidelines. The central box in the 25 - 75 % quartile with median bar, while the upper (lower) lines show the highest (lowest) values that are not considered outliers.

**Figure 3.3:** Boxplots showing wet weight microcystin concentrations, on each harvest date, by species. A two-way ANOVA was used to evaluate differences in microcystin between dates and species ( $\alpha=0.05$ ). The central box in the 25 - 75 % quartile with median bar, while the upper (lower) lines show the highest (lowest) values that are not considered outliers. Letters within each plot show significant differences in microcystin concentrations between species per sampling date as indicated by a Tukey's post hoc test. For muscles (A) and kidneys (C), there was a significant difference between microcystin in bluegill and largemouth bass. The interaction effect between harvest date and species is not significant, so letters in these plots show where significant differences exist in harvest date. For livers (B), the interaction effect between harvest date and species is significant, indicating this relationship depends on harvest date. Letters are placed above each individual box to show significant differences between boxes (Table 3.5).

**Figure 4.1:** Boxplots showing parameters of water clarity for Blue Springs Reservoir. The box shows the 25–75% quartile with median bar, while the upper (lower) lines show the highest (lowest) values that are not considered outliers, which are indicated by black circles. Secchi disk depth (Secchi), total suspended solids (TSS), particulate inorganic

matter (PIM), and chlorophyll-*a* uncorrected for pheophytin (chl-*a*) are shown. Vertical, dashed lines indicate where a regime shift was identified. Gray shading show the probable invasion period for zebra mussels, with the right edge of the box indicating the year when zebra mussels were first observed.

**Figure 4.2:** Boxplots showing parameters of water clarity at 2 sites in Bull Shoals Reservoir. The box shows the 25–75% quartile with median bar, while the upper (lower) lines show the highest (lowest) values that are not considered outliers which are indicated by black circles. Monitoring at site 1 (A), which is closer to the dam than site 2 (B), ended in 2012. Secchi disk depth (Secchi), and chlorophyll-*a* uncorrected for pheophytin (chl-*a*) are shown. Vertical, dashed lines indicate where a regime shift was identified. Gray boxes show the probable invasion period for zebra mussels, with the right edge of the box indicating the year when zebra mussels were first observed.

**Figure 4.3:** Boxplots showing parameters of water clarity in Jacomo Reservoir. The box shows the 25–75% quartile with median bar, while the upper (lower) lines show the highest (lowest) values that are not considered outliers. Secchi disk depth (Secchi), total suspended solids (TSS), particulate inorganic matter (PIM), and chlorophyll-*a* uncorrected for pheophytin (chl-*a*) are shown. Vertical, dashed lines indicate where a regime shift was identified. Gray boxes show the probable invasion period for zebra mussels, with the right edge of the box indicating the year when zebra mussels were first observed.

**Figure 4.4:** Boxplots showing parameters of water clarity in Lake of the Ozarks. The box shows the 25–75% quartile with median bar, while the upper (lower) lines show the highest (lowest) values that are not considered outliers, which are indicated by black circles. Secchi disk depth (Secchi), total suspended solids (TSS), particulate inorganic matter (PIM), and chlorophyll-*a* uncorrected for pheophytin (chl-*a*) are shown. Vertical, dashed lines indicate where a regime shift was identified. Gray boxes show the probable invasion period for zebra mussels, with the right edge of the box indicating the year when zebra mussels were first observed.

**Figure 4.5:** Boxplots showing parameters of water clarity in Lotawana Reservoir. The box shows the 25–75% quartile with median bar, while the upper (lower) lines show the highest (lowest) values that are not considered outliers, which are indicated by black circles. Secchi disk depth (Secchi), total suspended solids (TSS), particulate inorganic matter (PIM), and chlorophyll-*a* uncorrected for pheophytin (chl-*a*) are shown. Vertical, dashed lines indicate where a regime shift was identified. Gray boxes show the probable invasion period for zebra mussels, with the right edge of the box indicating the year when zebra mussels were first observed.

**Figure 4.6:** Boxplots showing parameters of water clarity in Smithville Reservoir. The box shows the 25–75% quartile with median bar, while the upper (lower) lines show the highest (lowest) values that are not considered outliers, which are indicated by black circles. Secchi disk depth (Secchi), total suspended solids (TSS), particulate inorganic matter (PIM), and chlorophyll-*a* uncorrected for pheophytin (chl-*a*) are shown. Vertical, dashed lines indicate where a regime shift was identified. Gray boxes show the probable invasion period for zebra mussels, with the right edge of the box indicating the year when zebra mussels were first observed.

**Figure 4.7:** Boxplots showing parameters of water clarity in Truman Reservoir. The box shows the 25–75% quartile with median bar, while the upper (lower) lines show the highest (lowest) values that are not considered outliers, which are indicated by black circles. Secchi disk depth (Secchi), total suspended solids (TSS), particulate inorganic matter (PIM), and chlorophyll-*a* uncorrected for pheophytin (chl-*a*) are shown. Vertical, dashed lines indicate where a regime shift was identified. Gray boxes show the probable invasion period for zebra mussels, with the right edge of the box indicating the year when zebra mussels were first observed.

**Figure 4.8:** Correlation-based principal component analysis (PCA) biplot. The first principal component explains 50.1 % of the variation in this dataset, while the second component explains 33.7 %. Vectors represent environmental parameters that could influence zebra mussel survival and density. Vector length reflects the amount of variance in the dataset explained by each environmental parameter. Dissolved oxygen and temperature were measured in the epilimnion, while particulate inorganic matter measurements were made in surface water. Anoxia depth is the depth where dissolved oxygen measurements drop below 1 mg L<sup>-1</sup>. Each point represents mean long-term conditions in each study reservoir. Bull Shoals site 2 is not depicted because it lacks dissolved oxygen, temperature, mixing depth, and anoxia depth data. Reservoirs that have been invaded by zebra mussels are indicated by black circles while reservoirs with no known zebra mussels are shown with grey circles.

**Figure A1.1:** Experimental mesocosm tank set up. The trees in the distance are over 100 m away.

**Figure A1.2:** Comparison of the light environment in tanks that received varying amounts of glacial rock flour (GRF). PAR ratio (0.5 m water/air reading) measured in mesocosm tanks that received 0, 5, 10, and 20 kg of GRF. The light ratio was determined by dividing photosynthetically active radiation (PAR) measurements made at 0.5 m depth by PAR measurements from above the water's surface in the air. Bars with the same letter indicate that no significant difference exists between experimental groups while bars with different letters indicate that there is a significant difference in PAR between groups. We found no significant difference in PAR among tanks that received 5, 10, and 20 kg of GRF (Kruskal-Wallis  $p > 0.05$ ). In this dosing experiment, each experimental group consisted of 2 tanks that were not used in the larger, 9-day experiment.

**Figure A1.3:** Slope plots for parameters in experimental mesocosm tanks. Temperature, total suspended solids (TSS), particulate inorganic matter (PIM), particulate organic matter (POM), mean mixed layer irradiance ( $\bar{E}_{24}$ ), and microcystin are presented. Vertical, dashed lines represent measurements taken on day 0 and day 9. Sloped lines represent the change in each parameter for chlorophyte dominated (Chlo, black, dashed line,  $n = 6$ ), cyanophyte-dominated (Cyan, light gray solid, line,  $n = 8$ ), and control (Cont, dark gray, dotted line,  $n = 3$ ) mesocosm tanks. Values to the right of each label are the mean of all tanks within that group.

**Figure A1.4:** Slope plots for chemical parameters in experimental mesocosm tanks. Total phosphorus (TP), total nitrogen (TN), total dissolved phosphorus (TDP), total dissolved nitrogen (TDN), the natural log ratio of TN to TP (TN:TP), ammonium (NH<sub>4</sub><sup>+</sup>), dissolved organic carbon (DOC), and nitrate (NO<sub>3</sub><sup>-</sup>) are presented. Vertical, dashed lines represent

measurements taken on day 0 and day 9. Sloped lines represent the change in each parameter for chlorophyte dominated (Chlo, black, dashed line,  $n=6$ ), cyanophyte-dominated (Cyan, light gray, solid line,  $n=8$ ), and control (Cont, dark gray, dotted line,  $n=3$ ) mesocosm tanks. Values to the right of each label are the mean of all tanks within that group.

**Figure A1.5:** Slope plots for phytoplankton and chlorophyll-*a* concentrations (Chl-*a*) in experimental mesocosm tanks. Vertical, dashed lines represent measurements taken on day 0 and day 9. Sloped lines represent the change in each parameter for chlorophyte dominated (Chlo, black, dashed line,  $n=6$ ), cyanophyte-dominated (Cyan, light gray, solid line,  $n=8$ ), and control (Cont, dark gray, dotted line,  $n=3$ ) mesocosm tanks. Values to the right of each label are the mean of all tanks within that group.

**Figure A1.6:** Slope plots for phytoplankton physiology parameters in experimental mesocosm tanks. Maximum quantum yield of photosystem II ( $\phi_{PSII}$ ), gross primary productivity normalized to chlorophyll-*a* ( $GPP^B$ ), light saturation threshold normalized to chlorophyll-*a* ( $E_k^B$ ), alpha normalized to chlorophyll-*a* ( $\alpha^B$ ), light deficiency parameter ( $\bar{E}_{24}/E_k$ ), and maximum relative electron transport rate ( $rETR_{MAX}$ ) are presented. Vertical, dashed lines represent measurements taken on day 0 and day 9. Sloped lines represent the change in each parameter for chlorophyte dominated (Chlo, black, dashed line,  $n=6$ ), cyanophyte-dominated (Cyan, light gray, solid line,  $n=8$ ), and control (Cont, dark gray, dotted line,  $n=3$ ) mesocosm tanks. Values to the right of each label are the mean of all tanks within that group.

**Figure A1.7:** Slope plots for zooplankton in experimental mesocosm tanks. Vertical, dashed lines represent measurements taken on day 0 and day 9. Sloped lines represent the change in each parameter for chlorophyte dominated (Chlo, black, dashed line,  $n=6$ ), cyanophyte-dominated (Cyan, light gray, solid line,  $n=8$ ), and control (Cont, dark gray, dotted line,  $n=3$ ) mesocosm tanks. Values to the right of each label are the mean of all tanks within that group.

**Figure A2.1:** Bathymetric map of Dairy Farm Lake #1 was created in 2017. Our sampling site for water parameters is indicated by the grey triangle.

**Figure A2.2:** Chlorophyll-*a*, microcystin, and cyanobacterial biovolume measured in Dairy Farm Lake #1 between June 17, 2017 and October 3, 2018. Chlorophyll-*a* concentrations (A) are from the epilimnion (when the reservoir was stratified) or from the surface to 1 m above the sediment (when the reservoir was isothermal). Cyanobacteria (B) are from the epilimnion (when the reservoir was stratified) or from the surface to 1 m above the sediment (when the reservoir was isothermal). Total cyanobacterial biovolume is reported as the percent of total phytoplankton biovolume that are cyanobacteria, while potentially microcystin producing cyanobacteria (PTOX) is reported as the percent of total cyanobacterial biovolume. Potential microcystin producers were classified following Chapman and Foss (2019). Vertical, dotted lines show fish harvest dates that overlap with phytoplankton enumeration.

**Figure A2.3:** Scatterplot of muscle and kidney microcystin displayed as wet weight concentrations. Significant and substantial positive correlations exist between these tissues for both and largemouth bass (Table A2.3).

**Figure A2.4:** Scatterplots of water microcystin and microcystin in fish tissues.  $R^2$  values on each plot represent the  $R^2_{\text{adj}}$  for our final, combined multiple linear regression models that excluded harvest date (Table A2.4). Trendlines indicate that water microcystin concentrations were a significant predictor ( $p < 0.05$ ) for microcystin concentrations in fish muscles (A), livers (B), and kidneys (C). We created models for bluegill (BLG, light grey) and largemouth bass (LMB, dark grey).

**Figure A2.5:** Scatterplot of microcystin and total fish length. Microcystin is reported in wet weight (ww). Trendlines are included only for largemouth bass, as length and microcystin was significantly correlated for largemouth bass and microcystin in muscles (A) and kidneys (B; Table S3).

**Figure A3.1:** Example of site selection in each transect. The first site was always 2 m deeper than the lowest water level recorded over the previous 6 years in the reservoir. Each subsequent site was located at 2 m intervals. The last site in each transect occurred when we did not find any zebra mussels at the previous 2 sites and a depth of 10 m deeper than the 6 year low was reached

## LIST OF TABLES

**Table 2.1:** Experimental design to promote phytoplankton growth through nutrient amendments. Nitrogen (N) and/or phosphorus (P) were added to 11,000 L mesocosm tanks to create bloom conditions and induce nutrient deficiency. A total of 3.08 moles of N was added as ammonium chloride ( $\text{NH}_4\text{Cl}$ ) or sodium nitrate ( $\text{NaNO}_3$ ), and 2.20 moles of P was added as dipotassium phosphate ( $\text{K}_2\text{HPO}_4$ ). Control tanks did not receive nutrient amendments and were dominated by chlorophytes at the beginning of the experiment. The  $\ln(\text{TN}:\text{TP})$  molar ratio is from day 0 of the experiment. Sample size ( $n$ ) refers to the number of mesocosm tanks that received each nutrient form.

**Table 2.2:** Top 3 dominant phytoplankton genera on day 0 and day 9. Percent composition (% Comp.) was calculated for each genera as the percent of total phytoplankton biovolume in each tank. The mean percent composition of all tanks within each group is reported for control ( $n=3$ ), chlorophyte- ( $n=6$ ), and cyanophyte-dominated ( $n=8$ ) mesocosm tanks. Lowest taxonomic identification was down to genus (Table A2.2).

**Table 2.3:** Water quality and phytoplankton physiology parameters. Control (Con), chlorophyte- (Chloro), and cyanophyte- (Cyano) dominated mesocosm tanks prior to glacial rock flour addition (day 0) and at the end of the experiment (day 9). Mean and standard deviation (std dev) are reported. “BDL” indicates that all tanks in a group were below the detection limit as stated in the Methods. Sediment traps were collected only on day 9, so it is not applicable (n/a) to report day 0 sedimentation rates. Significant differences between groups for the change in each parameter from day 0 to day 9 are reported in Table 2.4.

**Table 2.4:** Statistical analyses for each parameter. Analyses were evaluated on the difference between day 9 and day 0 (i.e., day 9 - day 0). We used a one-way analysis of variance (ANOVA) when the parameter followed a normal distribution, or when a normal distribution resulted from a transformation. A Kruskal-Wallis test (KW) was used when the data did not follow a normal distribution. Statistically significant differences between groups ( $p<0.05$ ) are denoted by different letters, while same letters indicate that no significant difference exists. Post Hoc tests were used to identify when the change in each parameter was different between control (Con), chlorophyte- (Chloro), and cyanophyte- (Cyano) dominated mesocosm tanks. A Tukey *post hoc* test was used to identify significant differences for parameters that followed a parametric distribution while Dunn’s test was used on non-parametric parameters.

**Table 3.1:** Characteristics of fish collected from Dairy Farm Lake #1. The sample size ( $n$ ) for bluegill (BLG) and largemouth bass (LMB) are listed underneath each harvest date. For continuous variables, the top value in each cell is the mean of all fish collected on each harvest date, while the bottom value in parentheses is the standard deviation. For sex, which is a categorical variable, the total number of male (m) and female (f) fish are shown for each date. When sex was unable to be determined, fish are reported as undetermined (UD).

**Table 3.2:** Classification of component loadings for water parameters using a correlation based principal component analysis. The percent total variation is listed next to each component loading (CL). Bold values indicate strongly correlated parameters within each CL. One correlated parameter from each CL was retained. For CL 1, we retained chl-a because of its high loading value and relevance to our research questions. We retained water microcystin from CL 2 because of its high loading value and relationship with microcystin in fish. We retained TDN from CL 3 because it had the highest loading value. We also retained DOC and TDP because they had an absolute value  $< 0.6$  for all component loadings, indicating that they did not exhibit multicollinearity with each other or any of the other water parameters. Retained parameters were included in our final, combined model set and are italicized.

**Table 3.3:** Water parameters measured in Dairy Farm Lake #1. Water parameters, including the profiles, are the mean of the sampling date immediately before and immediately after the fish harvest date listed in the top row. “BDL” indicates that parameter was below the detection limit. When fish harvest date fell in between a water sampling date that showed the reservoir to be isothermal and the other to be stratified, we were unable to determine mixing depth nor hypolimnetic dissolved oxygen. This is indicated by “n/a”. We report the maximum depth for mixing depth when the reservoir was isothermal. Parameters measured with a YSI EXO 3 sonde, indicated by “\*”, are averages of the epilimnion when the reservoir was stratified or of the entire water column when the reservoir was isothermal. Hypolimnetic dissolved oxygen is a sonde vertical profile average of the hypolimnion when the reservoir is stratified. Surface water cyanotoxins were collected as an integrated sample between 0 and 0.5 m while bottom water cyanotoxins were collected from 1 m above the sediment.

**Table 3.4:** Correlations between microcystin in muscles, livers, and kidneys for both bluegill and largemouth bass. Spearman’s rank correlation test was used to measure correlations between tissue type. The degrees of freedom (df) and p-value for each correlation are reported, along with the correlation coefficient ( $\rho$ ) when significant correlations exist. Significance, based on an  $\alpha$  value of 0.05, is indicated by \*.

**Table 3.5:** Two-way analysis of variance results showing differences in microcystin concentrations between harvest date and species (Figure 3). Degrees of freedom for harvest date and the interaction between harvest date and species are 7. Degrees of freedom for species is 1. Significance, based on an  $\alpha$  value of 0.05, is indicated by \*.

**Table 3.6:** Known microcystin concentrations in the tissues of largemouth bass, bluegill, and pumpkinseed sunfish. Microcystin is reported as wet weight concentrations.

**Table 4.1:** Characterization for all invaded and reference reservoirs. Latitude and longitude refer to the coordinates near the dam. For all reservoirs except Bull Shoals, this is where water samples are collected. Maximum depth is based on the dam height of each reservoir and volume is the volume of each reservoir at full pool. Trophic status was determined from previous work in Missouri reservoirs (Jones et al. 2008). Flushing rate for Bull Shoals is unknown.

**Table 4.2:** Regime shifts in Secchi disk depth for invaded and reference reservoirs. The year that a regime shift occurs is identified. When no regime shift occurs in a reservoir,

“none” is listed, and when more than one regime shift occurs in a reservoir, multiple years are listed. The number of years is the mean of all years within each period, and the Mann-Kendall p-value indicates whether a significant monotonic trend occurred within a period before and/or after a regime shift, or when no regime shift occurred, the entire data series. When sample size is less than 3, as indicated by “†”, no mean Secchi disk depth nor Mann-Kendall p-value are shown. As an example, Lake of the Ozarks displayed regime shifts in 1986 and 2007. The number of years (10), mean Secchi disk depth of 1.38, and Mann-Kendall p-value of 0.59 correspond with the period before 1986. The sample size of 21, mean Secchi disk depth of 1.65, and Mann-Kendall p-value of 0.65 correspond with the period from 1986 to 2006, and the sample size of 13, mean Secchi disk depth of 1.25, and the Mann-Kendall p-value of 0.08 correspond with the period from 2007 to 2019. When a significant monotonic trend is identified (Mann-Kendall  $<0.05$ , “\*”), the Sen’s slope value identifies the direction and magnitude of the trend.

**Table 4.3:** Regime shifts in total suspended solids (TSS) for invaded and reference reservoirs. The year that a regime shift occurs is identified. When no regime shift occurs in a reservoir, “none” is listed, and when more than one regime shift occurs in a reservoir, multiple years are listed. The number of years is the mean of all years within each period, and the Mann-Kendall p-value indicates whether a significant monotonic trend occurred within a period before and/or after a regime shift, or when no regime shift occurred, the entire data series. When sample size is less than 3, as indicated by “†”, no mean TSS nor Mann-Kendall p-value are. As an example, Lake of the Ozarks displayed regime shifts in 2007 and 2018. The number of years (28), mean TSS of 5.89, and Mann-Kendall p-value of 0.02 correspond with the period before 2007. The sample size of 11, mean TSS of 7.74, and Mann-Kendall p-value of 1 correspond with the period from 2007 to 2017. No mean TSS and Mann-Kendall p-value are reported for the period after 2017 because the sample size for this period is less than 3. When a significant monotonic trend is identified (Mann-Kendall  $<0.05$ , “\*”), the Sen’s slope value identifies the direction and magnitude of the trend. In the previous Lake of the Ozarks example, a Sen’s slope calculation was performed on the period before 2007, and a  $-0.09 \text{ mg L}^{-1} \text{ yr}^{-1}$  slope was identified.

**Table 4.4:** Regime shifts in particulate inorganic matter (PIM) for invaded and reference reservoirs. The year that a regime shift occurs is identified. When no regime shift occurs in a reservoir, “none” is listed, and when more than one regime shift occurs in a reservoir, multiple years are listed. The number of years is the mean of all years within each period, and the Mann-Kendall p-value indicates whether a significant monotonic trend occurred within a period before and/or after a regime shift, or when no regime shift occurred, the entire data series. When sample size is less than 3, as indicated by “†”, no mean POM nor Mann-Kendall p-value are shown. As an example, Lake of the Ozarks does not display a regime shift in PIM. The number of years (41), mean PIM of 3.63, and Mann-Kendall p-value of 0.16 correspond with the entire period. When a significant monotonic trend is identified (Mann-Kendall  $<0.05$ , “\*”), the Sen’s slope value identifies the direction and magnitude of the trend.

**Table 4.5:** Regime shifts in chlorophyll-*a* uncorrected for pheophytin (chl-*a*) for invaded and reference reservoirs. The year that a regime shift occurs is identified. When no regime shift occurs in a reservoir, “none” is listed, and when more than 1 regime shift occurs in a reservoir, multiple years are listed. The number of years is the mean of all

years within each period, and the Mann-Kendall p-value indicates whether a significant monotonic trend occurred within a period before and/or after a regime shift, or when no regime shift occurred, the entire data series. When sample size is less than 3, as indicated by “†”, no mean chl-*a* nor Mann-Kendall p-value are shown. As an example, Lake of the Ozarks displayed regime shifts in 2007 and 2018. The number of years (31), mean chl-*a* of 15.58, and Mann-Kendall p-value of 0.03 correspond with the period before 2007. The sample size of 11, mean chl-*a* of 23.34, and Mann-Kendall p-value of 0.88 correspond with the period from 2007 to 2017. No mean chl-*a* and Mann-Kendall p-value are reported for the period after 2017 because the sample size for this period is less than 3. When a significant monotonic trend is identified (Mann-Kendall <0.05, “\*\*”), the Sen’s slope value identifies the direction and magnitude of the trend. In the previous Lake of the Ozarks example, a Sen’s slope calculation was performed on the period before 2007, and a 0.16 µg L<sup>-1</sup> yr<sup>-1</sup> slope was identified.

**Table 4.6:** Zebra mussel density and biomass from 4 invaded Missouri reservoirs. Density (individuals m<sup>-2</sup>) and biomass (live weight, g m<sup>-2</sup>) are means of all sampling sites within each reservoir. Standard error is also reported. Mussels were collected in the summer of 2019.

**Table 4.7:** Parameters considered for habitat suitability using a principal component analysis (PCA). The top number is the mean for each reservoir, while the bottom number in parentheses is the range (min-max). Temperature and dissolved oxygen (DO) are means of the epilimnion, while total suspended solids (TSS) and particulate inorganic matter (PIM) were measured from surface water samples. We report ratio of PIM to POM as a natural log, ln(PIM):ln(POM), to reduce bias associated with calculating the mean from ratios. Anoxia depth is the depth at which DO concentrations are below 1 mg L<sup>-1</sup>. For Bull Shoals, only site 1 was included in the habitat suitability analysis because no temperature nor dissolved oxygen data exists for Bull Shoals site 2.

**Table A1.1:** Glacial rock flour (GRF) elemental composition, separated by major and minor elements.

**Table A1.2:** Taxonomic composition of phytoplankton within each mesocosm tank. Finest taxonomic identification was down to genus (Guiry and Guiry, 2020). Rare taxa, which are defined as those which total less than 5% of total phytoplankton density in each tank, are excluded. Biovolume (BV) and percent composition is given for all genera that comprise more than 5% of the total phytoplankton biovolume in each tank. Phytoplankton were sampled on day 0 and day 9 in chlorophyte-dominated (*n*= 6), cyanophyte-dominated (*n*= 8) and control (*n*= 3) mesocosm tanks.

**Table A1.3:** Phytoplankton categorization based on functional group. Phytoplankton were identified to genus and placed into one of six functional groups: potentially toxigenic cyanophyta (Chapman and Foss 2019), non-toxin producing cyanophyta, chlorophyta, euglenophyta, cryptophyta and dinoflagellates, and chrysophyta, including bacillariophytes, chrysophytes, ochrophytes, and haptophytes.

**Table A1.4:** Taxonomic composition of zooplankton within each tank. Zooplankton were sampled on days 0 and 9 in chlorophyte-dominated (*n*= 6), cyanophyte-dominated (*n*= 9),

and control ( $n= 3$ ) tanks. Copepods were classified as adults or nauplii. Cladocerans were identified to genus, except those in the family Chydoridae (Thorpe and Covich, 2001).

**Table A2.1:** Assessment of the extraction of microcystin from fish tissue methodology. Both detection limit and extraction efficiency were determined from hatchery raised bluegill, which served as the negative control fish for our study. Negative controls were spiked with a known concentration of microcystin. The extraction efficiency was the percent of this spike that was recovered. We determined the detection limit to be the concentration where negative controls, which are known to lack microcystin came back above the limit of detection, indicating the level where matrix effects are being measured by the analysis. Inter assay variation was determined by including a sample from each species on each plate.

**Table A2.2:** Spearman's rank correlations between fish length and microcystin (MC) in muscles, livers, and kidneys for bluegill and largemouth bass. The degrees of freedom (df) and p-value for each correlation are reported, along with the correlation coefficient ( $\rho$ ) when significant correlations exist.

**Table A2.3.** Microcystin concentrations measured in bluegill and largemouth bass over the course of a year. Microcystin concentrations are reported as  $\text{ng g}^{-1}$  ww. The top value in each cell is the mean of microcystin in all tissues from each harvest date. The middle value, in parentheses, is the standard deviation and the bottom value is the samples size ( $n$ ).

**Table A2.4:** Multiple linear regression models explaining microcystin accumulation in fish fillets, livers, and kidneys. Models were created for all three tissue types for both bluegill (BLG) and largemouth bass (LMB). In the "Fish Characteristic" models, only fish characteristics such as length, age, mass, body condition index, sex, liver organosomatic index (OSI), and gonad OSI (Table 1) were included. The "Combined" models included significant parameters identified in the fish characteristic models, as well as water microcystin (MC), total dissolved phosphorus (TDP), total dissolved nitrogen (TDN), chlorophyll-*a* concentrations (chl-*a*), and dissolved organic carbon, which were identified as un-correlated water quality parameters (Table 2). Both model sets were run twice, the first time including harvest date as a categorical variable with 8 levels. We do not report the individual statistics for harvest date because multiple linear regression determines these based on a reference level for categorical variables. We see no ecological nor experimental benefit to setting any individual date as a reference level, indicated by "-", and instead look for differences in microcystin between dates using a two-way Analysis of Variance (ANOVA, Table 3.5). In the second model set, harvest date was excluded. For each individual model, the p-value and  $R^2$ -adj are listed in the "Species and Tissue" column, while the coefficient, t-value, standard error, and p-value for each significant model parameter are listed in subsequent columns. In each row, "ns" is used to denote when a significant model was not able to be created from the given parameters.

# PHYTOPLANKTON RESPONSE TO WATER QUALITY THREATS IN MIDWEST RESERVOIRS

Jacob Cianci-Gaskill

Dr. Rebecca North, Dissertation Supervisor

## ABSTRACT

Harmful cyanobacterial blooms and invasive species threaten water quality. These threats are expected to worsen in the future, emphasizing the need for creative management solutions and a thorough understanding of their impacts. The objective of this dissertation is to investigate the influence of light on biomass and community composition of phytoplankton with the hypothesis that light will have an impact, regardless of nutrients and grazing. We investigate a novel geoengineering approach designed to control cyanobacteria by reducing light. We demonstrate that daily application of glacial rock flour, a fine particulate that floats on the water's surface, reduces light by half and results in up to a 78 % decrease in cyanobacterial biovolume. We also look at the accumulation of microcystin in the tissues of bluegill and largemouth bass. Microcystin is higher in bluegill, likely because they feed from lower trophic levels. It is also higher in spring and decreases throughout the year, suggesting that time of the year might be an important consideration for microcystin fish consumption advisories. We also find that invasive zebra mussels are not causing an increase in water clarity in MO reservoirs like they are in natural, northern latitude lakes. This could be because reservoir conditions are suboptimal for zebra mussels, thus preventing them from reaching high densities. Understanding how aquatic resources have responded to stressors in the past enables us to predict how they will respond to changes in the future.

## CHAPTER 1

### LITERATURE REVIEW

#### PROBLEM STATEMENT

In recent decades, freshwater resources are becoming increasingly imperiled. Anthropogenic activities like pollution, changes in land use, regulated flow regimes, the introduction of invasive species, and climate change threaten to degrade water quality and reduce biodiversity (Dudgeon et al., 2019). Declines in freshwater biodiversity have outpaced marine and terrestrial biodiversity losses, mainly because of anthropogenic activities (Collen et al., 2009). Emerging stressors, like microplastics and engineered nanomaterials pose additional threats to water quality (Reid et al., 2019). Growing human populations and diminished availability of high quality water resources suggest that there is no sign of an abatement of these anthropogenically induced threats (Vörösmarty et al., 2013), which will likely dominate freshwater systems for decades to come (Settele et al., 2014). Addressing these threats poses an immense management challenge that will require a strong foundation of scientific knowledge of each threat, novel management strategies and techniques, and efficient use of limited management resources. In this dissertation, I investigate three aquatic threats to freshwater, lacustrine ecosystems including harmful cyanobacterial blooms, the cyanotoxins sometimes produced by these blooms, and the impacts of invasive zebra mussels (*Dreissena polymorpha*).

#### *Harmful cyanobacterial blooms*

Harmful cyanobacterial blooms are increasing in frequency and magnitude in lakes and reservoirs across the globe (Huisman et al., 2018) and are one of the most

significant threats to aquatic resources (Brooks et al., 2016). These “blooms” occur when environmental conditions enable the rapid growth of certain cyanobacteria taxa. Elevated temperatures (25 °C for many taxa, Chorus and Welker 2021), and increased phosphorus (P) and nitrogen (N) loading (Downing et al., 2001; Dolman et al., 2012) can lead to larger cyanobacteria blooms. When cells in cyanobacterial blooms die and sink to the hypolimnion, they are decomposed through microbial processes that consume oxygen and leave the bottom of stratified lakes anoxic. This process of excess nutrient loading as a result of anthropogenic activities, called “cultural eutrophication,” costs \$2.2 billion annually in the United States (Dodds et al., 2009) and often leads to cyanobacterial blooms and anoxic hypolimnions. Some cyanobacteria are able to regulate their own buoyancy and partially control their position in the water column, allowing them to move to the top of the water column to access light (Chorus and Welker 2021). Clay particles may prevent colony-forming cyanobacteria from resuspending from the sediment to the water column during spring inoculation (Verspagen et al., 2004). Cyanobacteria require little maintenance energy and are thus able to maintain a higher growth rate than other cyanobacterial groups when light intensities are low (Van Liere et al., 1979). Because of these low light requirements, many cyanobacteria are able to persist in the water column until conditions become favorable. Calm water resulting from low wind enables buoyancy-regulating taxa to rise to the surface and shade other competing phytoplankton (Chorus and Welker 2021). The ability of these taxa to regulate buoyancy is most pronounced when nutrients are readily available as N limitation hinders the ability of some cyanobacteria to expand their gas vesicles (Brookes and Ganf 2001). These

attributes (ability to regulate buoyancy, tolerant of low light intensities) give cyanobacteria a competitive advantage for light over other algae in the water column.

### *Cyanotoxins*

Some cyanobacteria taxa can produce toxins classified as potentially carcinogenic to humans, livestock, and wildlife (Grosse et al., 2006) which can accumulate in organisms across the food web (Ferrão-Filho and Kozlowsky-Suzuki 2011). Toxins from these blooms have been detected in ponds and reservoirs across Missouri (Graham and Jones 2009) and pose a risk to those who use contaminated waters for irrigation, livestock watering, fishing, and recreation. Microcystin is one of the most commonly occurring cyanotoxins and also the most widely studied. It is a hepatotoxin that can cause liver disease in mammals in the form of hepatocellular vacuolation, apoptosis, necrosis, hemorrhage, increased rates of infection by the Hepatitis B virus, and can lead to death (Jochimsen et al., 1998; Miller et al., 2010; Li et al., 2011). These human health risks have prompted several organizations to set advisories for consumption and recreation. The United States Environmental Protection Agency (US EPA) has drafted recreational microcystin concentration advisories to be set at  $4 \mu\text{g L}^{-1}$  while the Missouri Department of Health and Senior Services (DHSS) advises against recreating in waters where microcystin concentrations exceed  $10 \mu\text{g L}^{-1}$ . Microcystin concentrations exhibit a high degree of temporal variability, both throughout the course of a bloom and across years (Park et al., 1998). Microcystin exposure through recreation could come from inhalation of microcystin aerosols (Cheng et al., 2007), swallowing small amounts of pond water while swimming (Lévesque et al., 2014), and consumption of contaminated fish tissues (Schmidt et al., 2013). Microcystins bioaccumulate, or accumulate in lower concentrations

with each increasing trophic level (Ferrão-Filho and Kozlowsky-Suzuki 2011), and have occasionally been observed at concentrations that exceed human consumption guidelines in fish (Poste et al., 2011). Toxin accumulation rates vary by fish taxa and it is unclear how long toxins remain in tissues before degradation or metabolization (Schmidt et al., 2013). Another route of human exposure is through produce irrigated with water where cyanotoxins are present (Corbel et al., 2016). While this is not a major concern for Dairy Farm Pond #1, one of the study sites in this dissertation, which is infrequently used for irrigation during droughts, it may be a concern in other agriculturally dominated ponds where cyanobacteria blooms occur. In addition to the human health concern from exposure to these cyanotoxins, toxic cyanobacterial blooms have economic impacts from livestock deaths (Van Halderen et al., 1995), lake closures (Carmichael and Boyer 2016), pet deaths (Backer et al., 2013), and eutrophication and fish kills associated with high biomass (Dodds et al., 2009).

### *Invasive Zebra Mussels*

The zebra mussel is a notorious aquatic invasive species. Originally from the Caspian Sea region, it was first observed in North America during 1986 in Lake Erie (Carlton 2008). Since then, it has spread as far west as California (Benson et al., 2021), and as far south as Texas (Churchill et al., 2017). While not yet observed in South America, there is concern that if introduced, zebra mussels could spread throughout the southern part of the continent (Petsch et al., 2020). Zebra mussels were first observed in Missouri in 1992 when they were found in the Mississippi River. They have since been transported overland and have been identified in nine Missouri reservoirs, with the most recent invasion occurring in 2017. Due to their high fecundity and filtration rates, zebra

mussels have the ability to dramatically alter systems where they have become established. They remove phytoplankton from the water column, shifting energy and nutrients to the benthos and enabling the proliferation of filamentous algal forms (Feniova et al., 2020). In addition to dramatically altering ecosystem function, they incur economic costs from the fouling of intake pipes, docks, canals, and seawalls, as well as from declines in sport fisheries (MacIsaac 1996; Strayer 2009).

## FACTORS INFLUENCING PHYTOPLANKTON GROWTH

Due to Missouri's latitude, reservoirs throughout the state vary on an annual basis between warm monomictic and dimictic, depending on whether or not ice forms during the winter. If there is ice cover, the reservoir will inversely stratify and nutrient replenishment in the epilimnion will not occur until spring turnover. If ice cover does not form, the reservoir will mix throughout the winter. Traditionally, winter was viewed as an unchanging time when phytoplankton communities were stable and productivity was at an annual low. Recent work shows that there may be more to this traditional view as winter phytoplankton densities are higher than previously thought (Hampton et al., 2016). Throughout the winter, phytoplankton growth and biomass continues to be influenced by temperature (Öterler 2017), light (Gervais 1998), and nutrients (Wen et al., 2020), showing that the traditional view of winter being a dormant state is not always accurate. Currently, our understanding of phytoplankton dynamics until the spring bloom is incomplete. Additional research is required to fully understand phytoplankton succession.

While seasonal succession of the phytoplankton has been demonstrated many times, it is important to note that many taxa compose the phytoplankton community, often at low abundances (Padisák 1992). Environmental conditions change rapidly over

time, depth, and space as water movements and mixing move phytoplankton. Conditions change so frequently that many taxa are able to exist concurrently, even if one may be the superior competitor (Wetzel 2001).

### *Nutrients*

N and P are the nutrients most commonly limiting to phytoplankton growth in many freshwater systems. Thus, their concentrations have a strong influence on lake or reservoir productivity. N and P concentrations are commonly used to evaluate lake trophic status, along with Secchi disk depth and chlorophyll-*a* concentrations (Wetzel 2001; Jones et al., 2008). High algal biomass, especially of cyanobacteria, is often associated with degraded water quality (Dodds et al., 2009). This makes N and P two of the most common pollutants due to their widespread use in fertilizers and as a waste product of wastewater treatment plant effluent (Davis et al., 2009; Paerl and Paul 2012). This cultural eutrophication often results in increased frequency and magnitude of cyanobacterial blooms (Schindler 1974; Paerl and Huisman 2009; Henao et al., 2019). Thus, the reduction of external nutrient loading is frequently the primary goal for water managers (Downing et al., 2001).

Cyanobacteria blooms most commonly occur in eutrophic and hypereutrophic water bodies (Reynolds 1987), but they have been observed in oligotrophic and mesotrophic systems as well (Carrillo et al., 1995; O'Neil et al., 2012). Cyanobacteria growth rates tend to be slower than other phytoplankton at temperatures below 25 °C (Robarts and Zohary 1987). If P is present in high, biologically available concentrations when temperatures warm to this 25 °C threshold, cyanobacteria will typically dominate the phytoplankton (Robarts and Zohary 1987). One reason for this is that some

cyanobacteria are diazotrophs able to fix atmospheric N not available to other phytoplankton, which enables continued growth even in N limited systems (Chorus and Welker 2021). The ability to fix atmospheric N does not always alleviate N limitation, but it does enable cyanobacteria to continue to grow and outcompete other phytoplankton (Anderson et al., 2020). This adaptation is unique in the phytoplankton and even non-diazotrophic cyanobacteria are flexible in the N sources they can utilize (O'Neil et al., 2012). In addition to the absolute concentrations of N and P, there is also evidence suggesting that the ratio of these nutrients (N:P ratio) exerts an influence on cyanobacteria growth and cyanotoxin production. In lakes and reservoirs where the N:P ratio is below 30, cyanobacteria are favored (Smith 1983). There remains some debate as to the importance of N:P ratios versus absolute concentrations of N and P in determining cyanobacteria abundances and both metrics should be considered (Downing et al., 2001). For example, there is some evidence to suggest that cyanobacteria biomass tends to increase between 20 and 25 g L<sup>-1</sup> of total phosphorus (TP; Chorus and Schauser 2011; Vuorio et al., 2020).

Nutrient concentrations also impact cyanotoxin concentrations. N, in particular, is positively correlated with cyanotoxin production (Watanabe and Oishi 1985; Orr and Jones 1998; Horst et al., 2014). For N-rich microcystin, enrichment of nitrate, ammonium, and urea all have been shown to lead to an increase in this cyanotoxin (Chaffin et al., 2018). P, too, influences cyanotoxin production, although this relationship is less clear. While P limitation is associated with a decreased rate of cyanotoxin production (Sivonen 1990), it is linked to a shift to the production of more toxic cyanotoxin congeners (Oh et al., 2000). The N:P ratio, reported as a natural log to reduce

bias associated with taking the mean of a ratio (Isles 2020), also influences cyanotoxin production. Under  $\ln(N:P)$  3.4, microcystin concentrations were more likely to be higher (Harris et al., 2014).

### *Light*

By definition, phytoplankton are photosynthetic organisms and require light to grow. The pigment chlorophyll-*a* enables photosynthesis by collecting red and blue light. Light is crucial in determining the success and survival of phytoplankton, even in systems where mixotrophic taxa, which are able to acquire energy through heterotrophy, dominate (Jansson et al., 1996). Phytoplankton can be co-limited by light and nutrients, but growth can still occur in the absence of light for a limited time (Dubourg et al., 2015). Thus, light is the ultimate limiting factor for phytoplankton and its availability is critical in determining phytoplankton biomass. Light availability decreases with depth in the water column as low-energy red light does not penetrate as deeply as high-energy blue light. The euphotic zone is the area where enough light is available for photosynthesis to exceed respiration. While cells are able to survive outside this zone using stored sugars and starches (Lee 2008), prolonged time spent out of the euphotic zone will result in cell death or cause the cell to enter a resting phase (Bellinger and Sigeo 2010). The amount of time phytoplankton spend in the euphotic zone is also determined by several characteristics of the lake. The amount of suspended particles influences light attenuation and in turn, the depth of the euphotic zone (Jewson 1977; Robarts and Zohary 1984; Cole et al., 1992). Lake stratification patterns also play a role. If the thermocline depth is above the bottom of the euphotic zone, then sinking is the only way phytoplankton will leave this zone. However, during lake mixing, phytoplankton will likely spend some time

below the euphotic zone (Cole et al., 1992). Phytoplankton have developed a variety of adaptations to maintain their position in the euphotic zone including buoyancy-regulation, flagella, forms that reduce sinking (spikes, spines, horns), mucilage secretion, and high surface area to density ratios (Lee 2008). These adaptations all enable phytoplankton to acquire enough light for growth, but there can be tradeoffs from reduced sinking rates. For example, larger cells with higher sinking rates are typically favored in environments with high levels of turbulence. Spending more time deeper in the water, closer to the nutrient-rich hypolimnion can provide an advantage when there is a low likelihood of sinking out of the euphotic zone due to high turbulence (Naselli-Flores et al., 2021). The constantly changing physical environment of lentic systems plays an important role in how much light is available to a phytoplankton at any given time.

Another adaptation is to tolerate a wide range of light intensities. Many cyanobacteria are superior competitors at both high and low light intensities (Yang and Jin 2008). Cyanobacteria are tolerant of low light conditions because of low maintenance energy requirements and their ability to maintain higher growth rates than other phytoplankton under low light levels (Van Liere et al., 1979). This allows them to persist in the water column underneath other phytoplankton groups until conditions become favorable (Chorus and Welker 2021). Several factors can lead to light reduction throughout the water column. High concentrations of dissolved organic carbon can reduce growth by reducing light availability (Bergström and Karlsson 2019). In Lake Kasumigaura (Japan), the cyanobacteria *Microcystis* was still present under light limiting conditions induced from dredging operations, but at lower densities than occurred prior to dredging (Tomioka et al., 2011). Thus a decrease in light, resulting from an increase in

turbidity, was the main factor in determining cyanobacteria abundance (Tomioka et al., 2011). A similar phenomenon occurred in Lake Chagan, China, where elevated total suspended solids concentrations enabled *Microcystis* and *Oscillatoria* to outcompete diatoms and chlorophytes (Liu et al., 2021). Light also influences the ability of buoyancy regulating cyanobacteria to position themselves in a favorable position in the water column. Low light levels induce gas vacuole production, giving a cell positive buoyancy (Deacon and Walsby 1990). In high light intensities, photosynthetic rates increase and cyanobacteria store excess carbohydrates as dense “ballasts,” which accumulate and cause the cell to have a negative buoyancy (Wallace and Hamilton 1999, 2000). Additionally, high light intensities dilute cyanobacteria gas vesicles, also contributing to a decrease in cell buoyancy (Utkilen et al., 1985).

In cyanobacteria, light also influences cyanotoxin production. One theory holds that cyanotoxin production is an adaptation for cyanobacteria to prevent chlorosis during the high light intensities commonly experienced at the water’s surface (Phelan and Downing 2011). Conditions inside a “surface scum” can be harsh during a bloom, especially because cells are exposed to high light intensities for prolonged time periods. While still under debate, evidence exists in the lab to support this claim (Chaffin et al., 2018). A positive correlation between light intensity and microcystin production exists until a threshold intensity of  $40 \mu\text{mol m}^{-2} \text{s}^{-1}$ , after which the correlation becomes negative (Utkilen and Gjølme 1992). Similarly, the number of intercellular cyanotoxin synthetase genes increases with light intensity (Kaebernick et al., 2000). It may be that this threshold is maintained until the light intensity that corresponds with maximum growth rate is exceeded (Wiedner et al., 2003).

### *Water temperature*

Phytoplankton growth is influenced by temperature. The various phytoplankton groups have different temperature requirements and optimum temperatures where they experience their fastest growth rates. Typically, bacillariophyta grow at lower temperatures than other algal groups. While temperature requirements vary from species to species, some bacillariophyta can grow in temperatures as cold as  $-1.8\text{ }^{\circ}\text{C}$  and as warm as  $30\text{ }^{\circ}\text{C}$ , but optimum temperature growth occurs between  $10$  and  $25\text{ }^{\circ}\text{C}$  (Rhee and Gotham 1981; Suzuki and Takahashi 1995), and usually below  $15\text{ }^{\circ}\text{C}$  (Zhang and Prepas 1996). Many cyanobacteria have slower rates of growth relative to other taxa (Chorus and Welker 2021). One of the reasons cyanobacteria are able to form dense blooms later in the summer is because many species experience their highest growth rates at warm temperatures associated with a decline in the growth rates of other phytoplankton groups. This is probably why water temperature is often the best predictor of cyanobacterial blooms in observational field studies (Shin et al., 2021). Once surface water temperatures reach  $25\text{ }^{\circ}\text{C}$ , cyanobacteria blooms are more likely to dominate the phytoplankton (Robarts and Zohary 1987; Paerl and Huisman 2008). Many cyanobacteria native to temperate waters experience their optimum growth rates between  $25.0$  and  $27.5\text{ }^{\circ}\text{C}$  (Mehnert et al., 2010), and can grow and reproduce in temperatures in excess of  $35\text{ }^{\circ}\text{C}$  (Butterwick et al., 2005). Comparatively,  $35\text{ }^{\circ}\text{C}$  is lethal to many other phytoplankton, which cease growing over  $30\text{ }^{\circ}\text{C}$  (Butterwick et al., 2005). Water temperature influences phytoplankton size as well as growth rate. Warmer temperatures select for smaller taxa on the community level, and smaller cells and colonies on the species level (Zohary et al., 2021). Warming causes a stronger temperature gradient to form at the thermocline,

making it less likely for nutrients in hypolimnion to enter the epilimnion (Sommer et al., 2017). This favors smaller phytoplankton because nutrient uptake across the cell membrane is most efficient in smaller cells (Litchman et al., 2007).

### *Grazers*

Grazing pressure and phytoplankton biomass are closely linked. Grazing is widespread in aquatic organisms and is found in zooplankton, mixotrophic phytoplankton, bivalves, larval fish, and planktivorous fish. Whether or not phytoplankton biomass is more closely linked with resource availability or predation pressure has been widely contested. Bottom-up control is when resource limitation results in low phytoplankton biomass, reducing the number of grazers and eventually higher trophic levels in a system (McQueen et al., 1989; George 2021). Top-down control refers to the idea that predation pressure is the driving force behind phytoplankton biomass. With top-down control, grazing pressure is highest when there are few fish to feed on grazing zooplankton (Carpenter et al., 1985; Jeppesen et al., 2020). The debate between whether freshwater ecosystems are controlled more from the bottom-up or top-down has been going on for several decades, but general consensus today is that both forces are important in shaping aquatic communities and ultimately, grazing and phytoplankton biomass closely affect each other (Mao et al., 2020; Rogers et al., 2020). Grazing plays a role in phytoplankton succession, contributing to the clearwater phase many systems experience after the spring diatom bloom (Lampert et al., 1986). While grazing does reduce phytoplankton biomass, it also increases in-lake diversity and may be a greater driver of taxa richness than N:P ratios (Leibold et al., 2017). In addition to directly affecting phytoplankton biomass, grazing can have indirect impacts by altering nutrient

cycling. For example, high densities of filter-feeding mussels can reduce TP concentrations but increase concentrations of biologically available orthophosphate (Hwang et al., 2004). In some instances, grazing from zooplankton can lead to an increase in nutrient sedimentation through the production of fecal pellets (Bloesch and Bürgi 1989) or by selecting for larger taxa with higher sinking rates (Larocque et al., 1996; Vanni 2002). Grazing can also reduce total nutrient concentrations through a reduction in the amount of algal cells present in the water column (Sarnelle 1999). There is also evidence to suggest that whether grazing leads to an increase or decrease in nutrient sedimentation depends on lake productivity (Houser et al., 2000). It is clear that the effects of grazers on nutrient cycling are complex and do not occur ubiquitously throughout freshwater systems. What is clear is that these effects, in addition to direct grazing pressure, can have substantial impacts on phytoplankton.

Phytoplankton have evolved strategies to avoid grazing pressure. Some of these include forming colonies or filaments, growing in morphologically diverse forms such as with spikes/spines, having thicker cell walls, increasing mucilage production, and growing to larger individual cell sizes (Van Donk et al., 2011). These have costs, such as being energetically expensive or resulting in inefficient nutrient assimilation, and many strategies to alleviate grazing pressure represent an evolutionary tradeoff between reducing grazing pressure, acquiring nutrients, and remaining suspended in the euphotic zone (Pančić and KiØrboe 2018; Lürling 2021). For example, grazers favor small, unicellular taxa and in the presence of high grazing pressure, many colonial taxa dominate (Lehman and Sandgren 1985). However, small phytoplankton grow faster than large phytoplankton and will dominate phytoplankton assemblages in the absence of

grazing (Sommer and Sommer 2006). Nutritional content also influences grazing pressure. *Cryptomonas* are desirable due to their high polyunsaturated fatty acid content (Ahlgren et al., 1990). While there are exceptions (Tönno et al., 2016), grazers generally avoid cyanobacteria, which have low levels of polyunsaturated fatty acids, while other food options are available (Ger et al., 2014). In the case of the filter feeding zebra mussel, cyanobacteria are selectively expelled once brought into the mantle (Vanderploeg et al., 2001). Larger phytoplankton, too, are not as nutritious as smaller phytoplankton (Branco et al., 2020). Ultimately, the strategies that phytoplankton have developed to reduce predation pressure make them more difficult to consume or less nutritious to grazers.

## MANAGING CYANOBACTERIAL BIOMASS WITH GEOENGINEERING

Geoengineering approaches, as applied to cyanobacteria, are designed to manipulate the factors required for growth in a way that prevents or curtails blooms. This group of management strategies have gained popularity in recent decades, in part because they often work on much shorter timescales than other management approaches, allowing managers to meet the benchmarks and deadlines set forth in many environmental policies (Mackay et al., 2014). Many geoengineering approaches focus on reducing nutrient loading, although this is not the only approach they take. The selected method should consider lake characteristics like water and nutrient fluxes, biology, and hydrology, as well as logistical considerations like cost, safety, ease of implementation, and efficacy (Lürling and Mucci 2020). While the mechanism behind each strategy differs, the ultimate goal of these management approaches is often to shift freshwater lakes and reservoirs from eutrophic systems where cyanobacteria blooms occur frequently to a lower trophic status where blooms are rare. This alternative stable states hypothesis refers

to the idea that ecosystems maintain resilience and do not experience state change until a dramatic disturbance shifts the ecosystem to a different state with its own resilience (Scheffer et al., 2001; Carpenter and Brock 2006). Lake managers sometimes try to create a disturbance with enough magnitude to shift a eutrophic lake or reservoir to a stable, clearwater state. Traditionally, geoengineering approaches designed to reduce internal nutrient loading have been used for this purpose, although inducing light limitation with glacial rock flour application may also achieve the same results.

### *Phosphorus inactivation agents*

Internal nutrient loading, which refers to the process of sediment-derived nutrient introductions into the water column is a primary obstacle to lake recovery, and often will continue to increase lake P concentrations well after external loads have been reduced (Nürnberg 1988). Many cyanobacteria are poor competitors for P (Baldia et al., 2007) and use excesses of this nutrient to form dense blooms. Several geoengineering approaches have been designed to reduce internal nutrient loading, the most common of which are Phoslock® and alum. These “P-inactivation” techniques are designed to replace iron and manganese as binding agents for P (these are temporary bonds that can be released during anoxic conditions) to permanent binding agents. Often, this approach is paired with a material, usually clays modified with Fe<sup>3+</sup>, polyacrylamide, or chitosan that induced flocculation in cyanobacteria (Pan et al., 2006; Zou et al., 2006). This aids in removing the particulate P that would not otherwise be accessible by the P-inactivation material.

Phoslock® is a lanthanum modified bentonite clay (Douglas 2002) that sinks to the sediment, where it acts as a “cap” by intercepting P released from sediments during

internal nutrient loading (Douglas et al., 2016; Lürling and Mackay 2016). It has been shown to reduce P efflux from the sediments by up to 98 % during extended periods of anoxia, and by up to 88 % during wind-induced resuspension periods (Funes et al., 2021). Application of this material has been attributed to the reduction in algal biomass in numerous instances, making it one of the first geoengineering techniques considered by water managers looking to reduce cyanobacterial blooms (Meis et al., 2012; Noyma et al., 2016; Waajen et al., 2016a, Waajen et al., 2016b). By reducing P concentrations available to phytoplankton, Phoslock® has also been shown to shift some water bodies from being N limited to P limited (Douglas et al., 2016). This shift corresponds with a shift from conditions that favor cyanobacteria to conditions that favor eukaryotic algae which is often a management goal to improve water quality. Phoslock® is especially effective at reducing cyanobacteria in mesocosms where conditions were set to replicate those under simulated climate change scenarios, suggesting that this management strategy will continue to be an important tool for lake managers into the future (Cabrerizo et al., 2020).

Despite its previous successes, there are some drawbacks to relying on Phoslock® to improve water quality. Often, reapplication of materials is required because the binding sites that adsorb P become saturated and materials designed to “cap” nutrient-rich sediments can become buried (Gibbs et al., 2010; Reitzel et al., 2013). Phoslock® is also expensive (\$9.44/kg, <http://www.forestrydistributing.com>). Many of the Phoslock® concentrations used to effectively reduce cyanobacterial blooms fall in the range of 0.046 and 0.085 g L<sup>-1</sup> (van Oosterhout & Lürling 2011; Lürling and van Oosterhout 2012) but often require multiple applications and costs can be high (Epe et al., 2017). In addition to

cost, the effects of Phoslock® on aquatic organisms have been understudied and have focused mostly on zooplankton (van Oosterhout and Lürling 2013). Lanthanum (the element in Phoslock® that adsorbs P) may negatively impact aquatic organisms (Lürling and Tolman 2010). The length of time lanthanum takes to bind with P also influences its impacts on aquatic organisms (Spears et al., 2013). Finally, in-lab experimentation with Phoslock® and other geoengineering materials often yield results and specifications that are not directly transferable to complex, in-lake systems and in-lake “trial and error” is required to achieve desired P reduction results (Mackay et al., 2014).

Aluminum salts are also a way to reduce internal nutrient loading through P-inactivation. The most common of these is aluminum sulfate, or alum ( $\text{Al}_2(\text{SO}_4)_3 \cdot 14.3\text{H}_2\text{O}$ ), which has been applied to over 250 lakes worldwide since 1967 (Cooke et al., 2005; Brattebo et al., 2015). There have been many instances where alum applications reduce internal P loading, alleviate cyanobacterial blooms, and increase water clarity (Pilgram and Brezonik 2005; Brattebo et al., 2017; Wagner et al., 2017). Like Phoslock®, alum provides additional binding sites for mobile P (the fraction of sediment that will likely be released under anoxic conditions) and can also be used to cap sediments. Alum is effective in a variety of conditions (Huser and Pilgrim 2014). However, the longevity of treatment success ranges from 0–45 years and highlights our lack of understanding with regards to application (Huser et al., 2016). Reapplication is often necessary, although the length of time between reapplications varies from as short as annual additions, to as long as 31 years between reapplication (Lewandowski et al., 2003; Rönicke et al., 2021). There is less of a concern that alum will get covered by lake sedimentation over time than for Phoslock® because alum is less dense than some

sediments (James 2017). Despite the documented improvements alum has had on water quality, alum treatment can be only partially effective at reducing internal P loading if rates are underestimated or the effectiveness of the alum is overestimated (James 2017). Additionally, the negative effects of aluminum toxicity to aquatic organisms is a concern with alum, especially in low alkalinity lakes where applied aluminum compounds can induce potentially toxic pH shifts (Wagner et al., 2017). Alum must be buffered because toxic  $\text{Al}^{3+}$  ions will form below pH 6.5 (Cooke et al., 2005).

An important caveat to the effectiveness of P-inactivation techniques is that they are most successful when used in lakes with small watersheds, or in conjunction with efforts to reduce external nutrient loading (Mackay et al., 2014). Otherwise, reductions in P from alum or Phoslock® will be negated as external nutrient loading will raise nutrient concentrations back to what they were. Another drawback to Phoslock® and alum is that they only address internal P loading and do nothing to control N loading. N deficiency has been observed in Missouri reservoirs (Petty et al., 2020) and is not uncommon in other parts of the world (Elser et al., 1990; Maberly et al., 2002; Dzialowski et al., 2005).

#### *Aquashade®*

A less common approach to reducing phytoplankton biomass is to reduce light levels with the colored, insoluble dye Aquashade®. Aquashade® is a product designed to eliminate rooted aquatic macrophytes and filamentous algae. It is composed of the dyes acid blue 9 and acid yellow 23, which absorb light wavelengths critical to plant photosynthesis. This strategy is typically used at a small scale (aquaculture ponds, golf course ponds) and little research has been done to investigate its ability to reduce cyanobacterial blooms. Concentrations of 1,000 to 5,000  $\mu\text{g L}^{-1}$  have been shown to

reduce growth rates of both chlorophyta and cyanobacteria (Spencer 1984), but recent work has shown that cyanobacteria are able to continue to grow in ponds that receive regular dosing (Tucker and Mischke 2019). Aquashade® can reduce photosynthetically active radiation (PAR; Madsen et al., 1999), but its effects on phytoplankton are mixed. While some reports cite a 60 % decline in algal biomass (Batt et al., 2015), others found that Aquashade® had no effect on primary productivity, chlorophyll-*a*, zooplankton, and phytoplankton concentrations (Ludwig et al., 2008; Suski et al., 2018). Aquashade® is not suitable for ponds with an outflow and must be reapplied periodically as it does degrade over time (Suski et al., 2018).

### *Artificial mixing*

Artificial mixing is another method that can shift phytoplankton assemblages from cyanobacteria-dominated to a mixed and diverse community (Visser et al., 1996) and in some cases, may cause a reduction in total algal biomass (Pacheco and Lima Neto 2017). This method is only appropriate when lake depth is sufficiently deep and buoyancy-regulating cyanobacteria dominate the phytoplankton (Ibelings et al., 2016). If these conditions are not met, or if artificial mixing is not high enough to exceed the flotation rates of the buoyancy-regulating cyanobacteria, artificial mixing will not work (Lürling et al., 2016). Sufficient circulation must be supplied to move water that is below the euphotic zone for extended periods of time. In many systems, this requires circulators to mix the entire water column, which is often not done (Han et al., 2020). While artificial mixing has been demonstrated to reduce cyanobacteria in lakes with a maximum depth ranging from 5.2 (Cowell et al., 1987) to 55 m (Becker et al., 2006), water clarity and phytoplankton community will influence the depth at which artificial mixing will be

effective (Ibelings et al., 2016). Additionally, internal nutrient loading is higher in polymictic lakes where frequent lake mixing transports P-rich hypolimnetic waters up to the euphotic zone (Orihel et al., 2015). If lake managers are not careful, artificial mixing can have a similar effect, which may increase cyanobacteria bloom occurrence.

### *Ultrasonication*

Recently, ultrasonication has been proposed as a way to control cyanobacterial blooms. Sound waves with a frequency greater than 20 kHz can cause acoustic cavitation, ultimately lysing cyanobacterial cells, disrupting photosynthetic activity, or causing gas vacuoles to collapse (Phull et al., 1997). Several commercially available units designed to be placed in a pond exist for the purpose of controlling cyanobacteria. These units are largely untested in the field (Park et al., 2017), and, when studies do exist, they suggest that these units are ineffective (Lürling et al., 2014; Wei et al., 2018). Many laboratory studies have attempted to explain the specific parameters that result in the greatest reduction in cyanobacteria, including frequency, duration of exposure, and intensity (Wu et al., 2011). Commercially available ultrasonicator units do not emit sound waves at the same frequency and intensity that has been shown to work in the lab (Lürling et al., 2016). Another concern with ultrasonication is that it can lead to large spikes in dissolved cyanotoxin concentrations (Ressom et al., 1994). Much of the cyanotoxins that cyanobacteria produce are retained within their cell membranes. When these membranes are disrupted and the membranes are lysed, intracellular cyanotoxins are released into the surrounding water (Greenstein et al., 2020). These units can kill zooplankton, which is another criticism of commercially available ultrasonicators (Lürling et al., 2014). As they exist currently, sonication units may be useful, but only in select instances. Custom-made

ultrasound units have been shown to reduce cyanobacteria in mesocosm experiments (Ahn et al., 2003), suggesting that this may one-day be a viable cyanobacteria management strategy if improvements are made to commercially available units.

### *Glacial rock flour*

To the best of our knowledge, this dissertation is the first instance where glacial rock flour is used as a cyanobacteria management strategy. When applied to the water, a portion of the rock flour floats on the surface, reducing light availability throughout the water column. This reduction in light may lead to a decrease in cyanobacteria biomass. More details about the use of glacial rock flour as a geoengineering technique are presented in Chapter 2, but some background about this material, including its occurrence in nature, impact on the ecosystems where it occurs naturally, and physical and chemical characteristics are presented here.

Glacial rock flour occurs naturally as the erosional silt and clay sized particles formed from a glacier passing over bedrock (Rampe et al., 2017). Thus, the composition of glacial rock flour reflects the bedrock from which it was derived (Bischoff and Cummins 2001). As the glacier melts, either from seasonal receding (Casassa et al., 2009) or climate change (Moore et al., 2009), glacial rock flour runs off into a lake, often via a stream. Lakes with high concentrations of glacial rock flour are located where glaciers reside (high latitudes and elevations), and nearness to a glacier determines the amount of glacial rock flour that will occur in a lake. When a glacier is farther away, there are more opportunities for glacial rock flour to become trapped and retained upstream (Saros et al., 2010). Time of year also determines how much glacial rock flour is present in a lake. On a seasonal scale, glacial rock flour inputs will be determined by

temperature and precipitation (Casassa et al., 2009), although variations in glacial rock flour inputs on the scale of tens and hundreds of thousands of years reflect the advancement and retreat of glaciers (Bischoff et al., 1997; Bischoff and Cummins 2001).

A substantial body of work has examined the how glacial rock flour inputs affect conditions in glacially fed alpine lakes. Studies have examined everything from water clarity (Sommaruga et al., 1999; Modenutti et al., 2000), water chemistry (Hood and Berner 2009; Saros et al., 2010; Slemmons and Sarros 2012), light penetration (Rose et al., 2014), and zooplankton communities (Sommaruga, 2015). In lakes near glaciers, glacial rock flour decreases water clarity, but this is less pronounced in large lakes not formed by wind or volcanic activity (Irwin 1974). In glacially fed Lake Tekapo, New Zealand, concentrations of  $2.6 \text{ mg L}^{-1}$  of glacial rock flour contributed to a Secchi disk depth of 1.2 m, and a PAR light attenuation coefficient  $0.51 \text{ m}^{-1}$  (Vant and Davies-Colley 1984). Concentrations of glacial rock flour were measured again in Lake Tekapo 23 years later and were  $1.6 \text{ mg L}^{-1}$  (Gallegos et al., 2008). Comparisons with nearby Lake Pukaki, another glacially fed lake in New Zealand, revealed higher glacial rock flour concentrations of  $11.6 \text{ mg L}^{-1}$  (Gallegos et al., 2008). Maximum total suspended solids concentrations, which were dominated by glacial rock flour, in glacially fed Mascarcardi Lake (Argentina) of the southern Andes Mountains were  $\sim 2.5 \text{ mg L}^{-1}$  (Modenutti et al., 2000). Turbidity in 18 glacially fed lakes in Chile, Canada, and New Zealand varied from 0.3 to 45.5 NTU (mean 14.0 NTU, Rose et al., 2014). As a result of the increased turbidity in glacially fed lakes, the depth at which maximum chlorophyll-*a* occurs is shallower than in oligotrophic, alpine lakes not fed by glaciers (Sommaruga et al., 1999).

Glacial rock flour can alter water chemistry. For example, glacially fed lakes can have nitrate concentrations that are 1–2 orders of magnitude higher than lakes fed by only snowmelt, although this trend is limited to the North American Rocky Mountains (Hood and Berner 2009; Saros et al., 2010; Slemmons and Sarros 2012). This is likely because glacial coverage does not retain N as readily as vegetated soils (Lafreniere and Sharp 2005). P concentrations in glacial rock flour are only  $1.1 \text{ mg g}^{-1}$ , although potassium and magnesium concentrations can be 28.7 and  $26.4 \text{ mg g}^{-1}$ , respectively (Gunnarsen et al., 2019). Glacial meltwater also increases conductivity. Two decades of monitoring in Rasass See in the European Alps revealed an 18-fold increase in conductivity that corresponded with meltwater inputs, which had also increased over this time period as a result of climate change (Thies et al., 2007). Similarly, glacially fed lakes tended to have higher conductivities in Rocky Mountain lakes fed exclusively by snowpack, although this trend does not exist for all alpine lakes (Slemmons and Sarros 2012).

As a result of increasing suspended sediment loads and decreasing water clarity, glacial rock flour reduces light intensity throughout the water column in glacially fed lakes. In British Columbia, glacial rock flour caused the euphotic zone to become 14 m shallower (Barouillet et al., 2019). Many of the studies examining glacially fed alpine lakes are not focused on the glacial rock flour input itself, but rather on the conditions resulting from its presence. Therefore, much of what we know about how the relationship between glacial rock flour concentrations and light is derived from reported light parameters in glacially fed lakes. For example, light attenuation from glacially fed lakes has been measured in lakes across the globe. In these systems, glacial rock flour accounts for 63 % of the total light attenuated, after taking into account the total attenuation from

glacial rock flour, water, dissolved organic matter, and algae (Rose et al., 2014). The effect of glacial rock flour on light attenuation changes based on the proximity of measurements from the river inflow. Compared to immediately next to a glacial inflow in Mascardi Lake, PAR and UV penetration was 20–25% greater ~9000 meters away (Hylander et al., 2011). Along this same gradient (next to the inflow to ~9000 m away), PAR light attenuation decreased from 0.24 to 0.16 m<sup>-1</sup> and total suspended solids decreased from 3.36–3.83 mg L<sup>-1</sup> to 0.59–0.76 mg L<sup>-1</sup> (Laspoumaderes et al., 2013).

Many studies of alpine lakes recognize that glacial rock flour influences the glacially fed systems where it is found, but fewer attempts have been made to characterize the physical and chemical properties of the glacial rock flour particulate. One of the reasons for this is that glacial rock flour is defined broadly as the fine particulate derived from glacial erosion. No standards exist to characterize it by size class or composition because the minerals glacial rock flour is composed of reflect local geology in a lake's catchment (Chanudet and Filella 2009). There are a number of instances where glacial rock flour characterization was made for a specific location, often to aid in paleolimnology studies. For example in Oregon, glacial rock flour derived from the mafic bedrock was composed predominantly of andesine, augite, and pigeonite, with minor amounts of amorphous materials, olivine, hematite, zeolite, magnetite, smectite, and maghemite (Rampe et al., 2017). Lake Brienz in Switzerland is fed by the Aare and Lütschine rivers, which combine to form a mixture of glacial rock flour. This glacial rock flour is composed of 51 % feldspars (albite and orthose), 27 % 2:1 minerals (illite, ti-biotite, biotite), 6 % quartz, 2 % oxides, and 7 % other materials (Chanudet and Filella

2009). These percentages are the means of 8 sampling dates between June 2004 and October 2005 (Chanudet and Filella 2009).

While the mineral composition of glacial rock flour is reported, it is rare to quantify the sediment particle size. When sediment particle size is taken into account, most studies consider only the composition of clay (<2  $\mu\text{m}$ ). The three glacial rock flour brands we considered are composed of 3.5–11.2 % clay, making comparisons with the literature difficult. In Owens Lake of the Sierra Nevada mountains, the clay fraction (<2  $\mu\text{m}$ ) of the glacial rock flour is composed predominantly of quartz, smectite, K-feldspar, and biotite with minor amounts of vermiculite and kaolinite (Bischoff et al., 1997; Bischoff and Cummins 2001). Sediment samples taken from the glacial rock flour rich riverbed of the Copper River (Alaska), were composed of the minerals plagioclase (37 %), quartz (26.3 %), amphibole (ferrotschermakite, 5.9 %), calcite (4.1 %), Kspar (2.4 %), dolomite (1.8%), pyroxene (1.2 %), magnetite (0.2 %), and the clays chlorite (7.5 %), biotite (4.3 %), muscovite (3.7 %), smectite (ferruginous, 2.9 %), and vermiculite (2.7 %, Crusius et al., 2011).

## CONSEQUENCES OF HARMFUL CYANOBACTERIAL BLOOMS

Harmful cyanobacterial blooms occur when one species rapidly increases its biomass at a quicker rate than all or many of the other phytoplankton present in the water (Richardson 1997). Definitions about what constitutes a cyanobacterial bloom vary, including such definitions as a significant increase in the population of one taxon leading to a peak in biomass (Smayda 1997), the presence of phytoplankton in numbers that cause substantial societal impacts (Wells et al., 2015), a visible discoloration of water caused by cyanobacteris (Huisman et al., 2018), and chlorophyll-*a* concentrations either

above a certain threshold (Tett 1987) or significantly higher than baseline concentrations (Carstensen et al., 2007). Others have argued that harmful cyanobacterial blooms should be defined based on the amount of toxins they produce (Watson and Boyer 2013). While what constitutes a cyanobacterial bloom is still being debated, the consequences of increased cyanobacterial densities are clear. Cyanobacterial blooms are unsightly and can result in beach closures, decreased property values, lost recreational opportunities, and interrupted drinking water (Dodds et al., 2009; Bingham et al., 2015; Carmichael and Boyer 2016). Cyanobacterial blooms are considered “harmful” because some taxa can produce secondary metabolites that are recognized as potentially carcinogenic by the International Agency for Research on Cancer (IARC; Grosse et al., 2006). In extreme instances, exposure to these cyanotoxins can result in death for humans (Li et al., 2011), pets (Backer et al., 2013), livestock (Van Halderen et al., 1995), and wildlife (Miller et al., 2010). There are a variety of cyanotoxins which can be classified as neurotoxins, dermal toxins, gastrointestinal inflammatory toxins, and general cytotoxins, but the most commonly occurring cyanotoxin in most freshwater systems is the hepatotoxin microcystin (Carmichael and Boyer 2016). Microcystin is commonly found in lakes, reservoirs, and rivers throughout the world (Sukenik et al., 2015), and has been detected in aquatic and terrestrial organisms including zooplankton (Ferrão-Filho and Kozłowsky-Suzuki 2011), aquatic insects (Toporowska et al., 2014), gastropods (Zurawell et al., 2007), bivalves (Poste and Ozersky 2013), oligochaetes (Xue et al., 2016), fish (Schmidt et al., 2013), turtles (Perrault et al., 2020), bats (Woller-Skar et al., 2015), and birds (McCain et al., 2020). Its distribution and transfer throughout the environment is of particular interest to researchers because of the human health risk it poses.

## *Microcystin in water*

Microcystin occurs in freshwater environments when it is produced by cyanobacteria. There are currently 36 genera of cyanobacteria known to potentially produce microcystin (Chapman and Foss 2019). Within these genera, there are toxin and non-toxin producing strains, depending on whether a cell contains the nonribosomal enzyme complex for the microcystin synthetase (*mcy*) gene cluster (Rantala et al., 2006). When *mcy* is expressed, the cell produces microcystin. Blooms sometimes display high spatial (Kurmayer et al., 2004) and temporal (Tang et al., 2018) variation in toxin production, but it is still unclear what causes *mcy* expression, nor what factors favor toxin-producing and non-toxin producing strains. There is evidence that growth rate is tied to *mcy* expression, as less microcystin is produced during stages of rapid growth compared to bloom maintenance (Tang et al., 2018). Water temperature may also play a role, although whether warming or cooling causes *mcy* gene expression to increase remains unclear (Scherer et al., 2017; Martin et al., 2020). N is another factor that could influence *mcy* expression but like water temperature, this linkage is still unresolved. There is evidence to support that both low and high N concentrations lead to an increase in *mcy* expression and microcystin production (Harke et al., 2016). Determining the environmental factors that contribute to microcystin production will continue to be an important avenue of cyanobacterial research as this knowledge will help us understand and predict water microcystin concentrations. The primary way microcystin enters the water column is through cell lysis of toxin-producing strains (Chorus and Welker 2021). While it is possible that intact cells could release microcystin into the water, no export mechanism has yet been identified and it is likely that, if it exists, this export contributes

only negligibly to dissolved microcystin concentrations (Shi et al., 1995). Instead, dissolved microcystin concentrations are usually highest at the end of a bloom as cells senesce (Wantanabe et al., 1992).

Another potential route for cyanotoxins to enter the water column is from sediments. Microcystin adsorbs to sediment particles (Cousins et al., 1996; Zastepa et al., 2015), which can resuspend through wind, waves, or bioturbation. Sediment microcystin concentrations have been measured as high as  $2.37 \mu\text{g g}^{-1}$  dry weight (Xue et al., 2020). Additionally, chemical changes in overlying water might cause microcystin to be released back into the water column by altering the capacity of sediment particles to adsorb microcystin. Previous work has shown that multiple factors influence the capacity of sediments to adsorb microcystin including changes in pH (Miller et al., 2001; Liu et al., 2008), organic matter content (Mohamed et al., 2007; Wu et al., 2011), and sediment particle size (Miller et al., 2001; Munusay et al., 2012). A decline in sediment adsorption capacity could result in microcystin release and reintroduction into the water column through wind or bioturbation (Song et al., 2015). Either of these scenarios (resuspension of sediment particles or a change in pH of overlying water) could be a source of microcystin in water.

### *Microcystin in fish*

Aquatic organisms can be exposed to microcystin by consuming contaminated food items (Smith and Haney 2006) and by coming into contact with dissolved microcystin in the water (Sieroslawska et al., 2012). In fish, ingested microcystin is transported to the gut after consumption and can then pass into the bloodstream through absorption by intestinal epithelia, although the amount of toxin that passes into the

bloodstream varies by species and microcystin congener (Ernst et al., 2001; Chen et al., 2006). The time between ingestion and when microcystin enters the blood can occur in as little as 3 hours (Tencalla & Dietrich 1997). Microcystin is found at its highest concentrations in the gut, followed by blood-rich organs such as the liver and kidney (Cazenave et al., 2005; Chen et al., 2006). This can be a concern when the entire fish is consumed such as for many small species (Onyango et al., 2020). Microcystin also accumulates in muscle tissues, where it covalently binds to proteins (Smith et al., 2010). The amount of microcystin present in a fish at any given time will depend on the concentration to which the fish is exposed, the length of exposure, and the amount of time that has passed since exposure (Jia et al., 2014; Gurbuz et al., 2016). Unlike many other toxins such as mercury and PCBs, microcystin does not accumulate indefinitely. It can be eliminated through the glutathione metabolic pathway, although the rate of this metabolism is poorly understood (Schmidt et al., 2014). The ability to metabolize this toxin is the main reason that microcystin concentrations decrease as trophic level increases (Ibelings et al., 2005; Ferrão-Filho and Kozlowsky-Suzuki 2011), and is why microcystin concentrations are often highest in planktivorous fish and followed by omnivorous, and then carnivorous taxa (Flores et al., 2018).

Exposure to microcystin can have negative effects on fish health. Exposure can result in histological inflammation, and degeneration and necrosis in tissues throughout the body, but especially the liver (Ibelings et al., 2005). Liver damage seems to be reversible for acute exposure (Kankaanpää et al., 2002). In response to acute microcystin exposure, fish are able to increase the activity of antioxidant enzymes like superoxide dismutase, catalase, glutathione reductase, and glutathione peroxidase (Prieto et al.,

2006). Production of these enzymes and the subsequent detoxification of microcystin exerts an energetic cost, which can be especially harmful to embryonic fish because they have a limited energy reserve contained in the yolk (Cazenave et al., 2006). Chronic exposure to microcystin can also have a negative effect on fish health, resulting in liver and ovary apoptosis, damaged gills, hepatic steatosis, and increased difficulty in maintaining cation-anion homeostasis (Carbis et al., 1997; Zhan et al., 2020; Zhang et al., 2020). These effects are likely a result of cyanotoxin exposure, although it should be noted that exposure to non-toxin producing cyanobacteria can also result in gill damage (Bury et al., 1995, 1998). Microcystin exposure also can cause a change in fish behavior like increased opercular beat rates (Ernst et al., 2006), elevated plasma glucose levels (Ernst et al., 2006), and reduced swimming activity (Baganz et al., 2004). Ultimately, cyanotoxin exposure can result in a greater physiological stress response and reduced fitness, degrading the fishery and reducing its utility to anglers (Ferrão-Filho and Kozlowsky-Suzuki 2011).

#### *Human health risks associated with microcystin*

Human exposure to cyanotoxins can occur through consumption of contaminated fish (Poste et al., 2011), directly through drinking water (Song et al., 2007), or from produce irrigated with contaminated water (Xiang et al., 2019). Exposure can also occur from recreational activities such as aerosol inhalation (Backer et al., 2008), contact with contaminated beach and shoreline sediments (Preece et al 2021), ingestion of small amounts of water while swimming (Stewart et al., 2006), or direct contact with skin (Lévesque et al., 2014). Microcystin inhibits protein phosphatase 2A (PP2A) and 1 (PP1) in hepatocytes, resulting in autophagia, apoptosis, necrosis, hepatocellular vacuolation,

and/or cell proliferation (MacKintosh et al., 1995; Bagu et al., 1997). This can result in liver disease in the form of hemorrhaging, increased rates of infection by the Hepatitis B virus, and even death (Jochimsen et al., 1998; Miller et al., 2010; Li et al., 2011). Other health effects include respiratory problems (Stewart et al., 2006) and gastrointestinal symptoms (Pilotto et al., 1997; Backer et al., 2008; Lévesque et al., 2014). Chronic exposure, while understudied, also can have dramatic human health implications.

Drawing causal links between human health and chronic exposure to materials is difficult because it is often impossible to control for many variables, so instead epidemiologists often rely on correlative and weight-of-evidence approaches (Wyzga and Rohr 2015). Comparisons of people who get their drinking water and consume fish and waterfowl from lakes with varying frequencies of cyanobacterial blooms showed that the people who used the lake with frequent blooms were more likely to use hepatotoxic medicine and test positive for hepatitis B (Li et al., 2011). This suggests that there does seem to be some link between chronic exposure to microcystin and negative health effects. Recent studies conducted on mice have shown that chronic exposure to microcystin can result in increased risk of prostate cancer and kidney injury (Yi et al., 2019; Pan et al., 2021). It is still unclear if these same risks will occur in humans.

As a result of the human health risks associated with microcystin, advisories have been developed for drinking water and fish consumption. These advisories calculate tolerable daily intake (TDI) by applying an uncertainty factor to the no observed adverse effect levels measured in mouse studies (Fawell et al., 1999; Fromme et al., 2000). TDI is the level of microcystin that can be ingested without resulting in negative health effects over some length of time. In the United States, the Environmental Protection Agency has

developed drinking water advisories for microcystin over 10 days of continuous exposure (US EPA 2015). The microcystin advisory for drinking water is  $0.3 \mu\text{g L}^{-1}$  for infants and pre-school children, and  $1.6 \mu\text{g L}^{-1}$  for adults (US EPA 2015). They have also developed recreational guidelines of  $8 \mu\text{g L}^{-1}$  for microcystin (US EPA 2019). Other agencies and organizations around the world have microcystin advisories including the World Health Agency, 16 countries, and 20 individual states (AWWA 2016). For adult drinking water advisories, these range from  $1 \mu\text{g L}^{-1}$  to  $1.6 \mu\text{g L}^{-1}$  (AWWA 2016). Drinking water advisories are developed based on TDIs because people require drinking water on a daily basis. The World Health Organization has used the same chronic exposure TDI that they use to set their drinking water advisory for fish consumption as well (WHO 2006). Many agencies and organizations use this same TDI to set their own recommendation for fish consumption and microcystin exposure (Testai et al., 2016). TDIs might be appropriate for people who consume fish as a regular part of their diet, but not for those who consume fish for short periods, such as recreationally (Ibelings and Chorus 2007). To account for this discrepancy in frequency of exposure, the most comprehensive microcystin advisory for fish consumption is divided into acute, seasonal, and daily exposure (Ibelings and Chorus 2007). Acute exposure represents a single event where microcystin is consumed, such as eating fish caught at a single fishing trip. For acute exposure, no negative health effects should occur if exposure does not exceed  $25 \mu\text{g}$  per exposure for a 10 kg child and  $190 \mu\text{g}$  per exposure for a 75 kg adult (Ibelings and Chorus 2007). For seasonal tolerable daily intake advisories, limits are calculated based on per day exposure because this advisory assumes per day exposure over the course of several weeks. These limits are  $4 \mu\text{g day}^{-1}$  for a 10 kg child and  $30 \mu\text{g day}^{-1}$  for a 75 kg

adult (Ibelings and Chorus 2007). For daily exposure for several months at a time, lifetime tolerable daily intake advisories are listed as  $0.4 \mu\text{g day}^{-1}$  for a 10 kg child and  $3 \mu\text{g day}^{-1}$  for a 75 kg adult (Ibelings and Chorus 2007). Other fish consumption advisories relating to microcystin are more general, recommending against consuming fish with microcystin concentrations higher than a set threshold value. For example, the state of California also has a general fish consumption advisory for microcystin, warning consumers to avoid eating fish with microcystin concentrations exceeding  $0.01 \mu\text{g g}^{-1}$  wet weight (Testai et al., 2016). Ohio and Illinois both recommend that consumers avoid fish when microcystin concentrations exceed  $0.028 \mu\text{g g}^{-1}$  (Testai et al., 2016), and the Australian government recommends avoiding fish with microcystin concentrations greater than  $0.024 \mu\text{g g}^{-1}$  wet weight (Mulvenna et al., 2012).

## ZEBRA MUSSELS

### *The effects of zebra mussels on phytoplankton*

Many of the impacts zebra mussels have on the systems to which they invade result from their prolific filtering capacity. They can filter up to  $21.7 \text{ mL mg}^{-1} \text{ hr}^{-1}$  (Fanslow et al., 1995), although this rate likely varies based on phytoplankton availability (Smith et al., 1998), cyanobacteria abundance (Gardner et al., 1995; Lavrentyev et al., 1995), water temperature (Fanslow et al., 1995), zebra mussel densities (Fanslow et al., 1995), and lake stratification patterns (Schwalb et al., 2013). Zebra mussel filtration rates can be limited by phytoplankton quantity (Smith et al., 1998) and quality (Gardner et al., 1995, Lavrentyev et al., 1995). Zebra mussels can selectively reject nutrient-poor and/or toxic cyanobacteria in their pseudofeces (Vanderploeg et al. 2001), and high phytoplankton densities may still be associated with decreased filtration rates if

cyanobacteria make up a large percentage of the community (Gardner et al., 1995; Lavrentyev et al., 1995). Zebra mussels are able to filter a broad range of particle sizes (~1–750  $\mu\text{m}$ ) which contributes to their ability to assimilate up to 40% of their body carbon per day (Vanderploeg et al., 2001). Energy and nutrients are shifted to benthic areas nearshore (Hecky et al., 2004; Cha et al., 2011; North et al., 2012; Ozersky et al., 2012; Kim et al., 2015). Approximately a third of the P filtered out of water column is egested as feces or pseudofeces, much of which is composed of N and P in bioavailable forms easily taken up by benthic organisms (Conroy et al., 2005; Ozersky et al., 2013; Vanderploeg et al., 2017; Vanni 2021). The increase in benthic nutrient availability can dramatically alter ecosystem structure in invaded lakes and is often associated with an increase in macroinvertebrate populations (Ward and Ricciardi, 2007). This also reduces nutrients and energy availability for planktivores, resulting in smaller young-of-the-year fish (Hansen et al., 2020). Improved light conditions and increased nutrient availability in the benthos also have led to an increase in filamentous algae and periphyton after zebra mussel establishment (Lowe and Pillsbury 1995; Sakharova et al., 2018). In some instances, zebra mussel densities have become high enough to reduce dissolved oxygen (DO) concentrations in the water column (Caraco et al., 2000; Effler et al., 2004). Zebra mussels also outcompete native mussels and displace them through suffocation (Schloesser et al., 1991; Dzierżyńska-Białończyk et al., 2018). While the full economic impacts of zebra mussels has not been fully quantified, they are likely in excess of \$100 million (Strayer, 2009) and may be as high as \$1 billion annually (Pimentel et al., 2005). Most of this cost comes from the clogging of intake pipes. Between 1989 and 2004, North American drinking water and power plants spent a combined \$267 million on

removing and trying to prevent zebra mussel colonization on intake pipes (Connelly et al., 2007). Increased nutrient concentrations have been associated with an increase in zebra mussel densities, so the cost of this invader will likely increase as it continues to spread and cultural eutrophication occurs at increasing rates (Schuler et al., 2020).

Zebra mussel fecundity is over one million eggs per female per spawning event (Ludyanskiy et al., 1993) and mussels are able to reproduce twice per year under favorable conditions (Chase and Bailey 1999; Locklin et al., 2020). Veligers are planktonic for the first 18–90 days of their life before attaching to a surface with byssal threads (Ackerman et al., 1994). Zebra mussels readily colonize any hard surface, which along with the aforementioned life history traits (high fecundity, planktonic veligers), have contributed to the overland spread of zebra mussels via the ballast water and hulls of personal watercraft. In lotic systems, zebra mussels spread when planktonic veligers are transported downstream (Jin and Zhao 2021). The high fecundity, ability to colonize a variety of substrates, and planktonic veliger stage that enables wide dispersal often leads to high mussel densities in the lakes, reservoirs, and rivers where zebra mussels become established, often within 2 years of introduction (Ludyanskiy et al., 1993; Strayer et al 2019). Zebra mussels are currently considered invasive in 33 European countries, 3 Canadian provinces, and 33 states in the US (Dölle and Kurzmann 2020; Benson et al., 2021). High zebra mussel densities, and their associated collective filtering capacity, can filter the entire volume of a water body in as little a time scale as hours to days. In Lake Simcoe (ON), which has a volume of 11.6 km<sup>3</sup>, conservative estimates for the rate dreissenids filter the water column is 0.24 times per day (North et al., 2013). The 7.9 km<sup>3</sup> of the inner part of Saginaw Bay (Lake Huron, MI) gets filtered by dreissenids 0.2–1.3

times per day (Fanslow et al., 1995), and Lake St. Clair (MI/ON), volume 4.2 km<sup>3</sup>, gets filtered twice per day (Herbert et al., 1991). Such high fecundity and filtering capacity are some of the reasons that this invader can have such substantial impacts in systems where it becomes established.

It is well documented that zebra mussels increase water clarity in the water bodies where they become established. A meta-analysis of almost 200 studies revealed an increase in water clarity in nearly all systems after the invasion of zebra mussels (Higgins and Vander Zanden, 2010). This was evident by a mean 38.5 % increase in Secchi disk depth, 40.7 % decrease in turbidity, 39.7 % decrease in suspended solids, 47.3 % decrease in chlorophyll-*a* concentrations, 58.5 % decrease in phytoplankton, and 51.3 % decrease in zooplankton (Higgins and Vander Zanden, 2010). Many of these trends were corroborated in Lake Simcoe (ON; North et al., 2013), which experienced a decrease in chlorophyll-*a* concentrations and phytoplankton biovolume during all four seasons of the first 12 years post- zebra mussel invasion (Baranowska et al., 2013). In Hargus Lake (OH), decreases in phytoplankton biomass (and increases in water clarity) after the introduction of zebra mussels resulted in a 1.2 m increase in thermocline depth over a three year span (Yu and Culver, 2000). As zebra mussels reduced the concentrations of suspended seston, light attenuation decreased and the epilimnion thickened due to an increased heating rate (Yu and Culver, 2000). Water clarity in Saginaw Bay (Lake Huron, MI) increased and a muting effect on the seasonal phenomenon (spring Saginaw River discharge, summer cyanobacterial blooms, autumnal wind-driven resuspension) that typically influence turbidity was also observed post- zebra mussel invasion (Fahnenstiel et al., 1995; Budd et al., 2001). There were negative correlations between zebra mussel

biomass and both turbidity and phytoplankton biomass in Lake Michigan (US, Ransibrahmanakul et al., 2018). In Oneida Lake (NY), the introduction of zebra mussels likely contributed to a greater increase in Secchi disk depth than did the reduction of total P loading (Zhu et al., 2006). Lake Ontario (NY/ON) also experienced increases in water clarity. However, this shift likely originated from decreased calcium loading from Lake Erie, where rapidly growing zebra mussel populations use calcium for cell construction (Barbiero et al., 2006). As a result, fewer “whiting,” or calcite precipitation, events occurred in Lake Ontario during this study, which may increase water clarity more than mussel filtration (Barbiero et al., 2006). Zebra mussels increase water clarity in rivers as well. In the Seneca River (NY), Secchi disk depth increased 2.5 times and chlorophyll-*a* concentrations decreased 16 times post- zebra mussel invasion (Effler et al., 2004). In the Hudson River Estuary (NY), phytoplankton biomass declined by 85 % post- zebra mussel establishment (Caraco et al., 1997). Incidences where zebra mussels do not lead to an increase in water clarity are rare and seem to be the exception, not the rule. In Green Bay (Lake Michigan, WI), chlorophyll-*a* concentrations increased post- zebra mussel invasion while phytoplankton biomass remained unchanged (De Stasio et al., 2014). Phytoplankton communities shifted as the bay saw a decrease in chlorophyta and an increase in grazing resistant cyanobacteria and bacillariophyta, which may attribute to the increase in chlorophyll-*a* concentrations (De Stasio et al., 2014).

#### *Environmental factors influencing zebra mussel filtration*

Few aquatic invaders can have as much of an impact on ecosystems where they become established as can zebra mussels. This invasive bivalve is notorious for reducing phytoplankton biomass in systems where it becomes established because of its filter-

feeding behavior. The collective filtering capacity, and thus the impact these mussels have on invaded systems, is ultimately determined by the densities they are able to attain. Many organisms are able to persist in sub-optimal conditions even if they are not able to reach the same densities that they otherwise might have had conditions been more favorable (Lockwood et al., 2013). Environmental factors occurring outside of the optimal range for zebra mussels may limit the densities they are able to form, and thus limit their collective filtering capacity. For zebra mussels, some of these factors include water temperatures, DO concentrations, calcium concentration, and concentrations of suspended inorganic particles. Understanding the range of these conditions that zebra mussels are able to tolerate is an important factor in assessing the risk of invasion that individual water bodies face. While zebra mussel tolerance thresholds for many conditions have been established, the combined effects of multiple stressors is not well understood. Preliminary work has shown that the likelihood of zebra mussel mortality increases when multiple stressors are introduced, compared to when a single parameter is suboptimal (Mathai et al., 2020). Recent work has also shown that zebra mussels are able to adapt to conditions outside of their optimum, both behaviorally (Ouellette-Plante et al., 2017) and because of selection pressure (Elderkin and Klerks 2005; De Ventura et al., 2016). The extent of zebra mussels' adaptive capacities should be a continued area of research, especially as they continue to push the boundaries of their predicted range expansion in North America (Drake and Bossenbroek 2004; Locklin et al., 2020; Benson et al., 2021; Vanderbush et al., 2021). Our current understanding of zebra mussel dynamics is not adequate to meet research and management needs and investigations into

how this invader responds to different environmental conditions remain necessary (Strayer et al., 2019).

### *Water temperature*

Temperature is an important variable in zebra mussel life history and many studies have examined how temperature changes affect growth and survival. Temperature determines when zebra mussels spawn, how often they spawn, how quickly veligers develop, and veliger and adult zebra mussel growth rates. Spawning rates are maximized at 18 °C (McMahon, 1996), but a lower limit of 12 °C is commonly accepted as the minimum temperature required for spawning (Neumann et al., 1992). If temperatures warm quickly enough in the spring, zebra mussels are able to spawn twice in the same season (Chase and Bailey 1999). In Texas, near the southern extent of zebra mussel distributions, spawning was initiated early enough that the spring cohort was able to spawn by autumn (Churchill 2013; Locklin et al., 2020). Peaks in larval development and veliger settlement onto substrates are also optimized at 18 °C (Piesik 1983; Afanas'yev and Protasov 1987; Sprung 1987). Optimal zebra mussel growth rate is between 10–15 °C (Walz 1978), while optimal temperatures for filtration are 10–22 °C (Reeders and Bij de Vaate 1990). Multiple spawning events in a season, along with higher growth rates at elevated temperatures, could compensate for increased mortality associated with temperatures above 25 °C, enabling zebra mussels to continue to expand along the southern extent of their range (Churchill et al., 2017).

An upper temperature threshold to zebra mussel growth and survival could limit the spread of zebra mussels. While mussels are able to persist beyond 25 °C, some evidence suggests that temperatures above this threshold cause growth rates to decline

(Thorp et al., 1998), respiration rates to increase (Alexander et al., 1994), and a reduction in byssus thread production and foot activity (Rajagopal et al., 1997). Similarly, a stress response, indicated by increased mortality and reduced growth rates, occurred in zebra mussels in 30 °C water compared to 20 °C water (Jost et al., 2015). Zebra mussels are able to survive beyond 30 °C for limited periods. The thermal tolerance for zebra mussels seems to be between 31–32 °C, with 100% mortality occurring in as little as 2 and as many as 47 days at these temperatures (McMahon et al., 1994; Elderkin and Klerks, 2005). Continual exposure to elevated temperatures seems to be especially deadly. Even brief, 8 hour reductions in temperature to below 32 °C can result in 20 % survival compared to 0 % survival when temperatures are kept above 32 °C (Mathai et al., 2020). Zebra mussels are also able to survive temperatures as high as 37–39 °C, but only for up to 75 minutes (McMahon et al., 1994, Spidle et al., 1995).

Most of the work investigating thermal limits of zebra mussels has been conducted in the lab and may not completely explain some of the regional differences that are observed in zebra mussels and temperature. Zebra mussels located in areas with warmer climate can survive in elevated temperatures for longer (McMahon, 1996, Elderkin and Klerks, 2005, Morse et al., 2009). In Lake Texoma (OK/TX), near the southern extant of this species' range, zebra mussels have highest growth rates at 27–28 °C, much warmer than the 17–23 °C optimal temperature range described previously (Ludyanskiy et al., 1993; Churchill et al., 2017), and the thermal tolerance of zebra mussels in southern Kansas is 32 °C (Morse et al., 2009). Zebra mussels in the mouth of the Mississippi River can survive for an average of 20 hours longer than zebra mussels in the Mississippi's headwaters at water temperatures of 32 °C (Elderkin and Klerks 2005).

These examples suggest that zebra mussels at southern latitudes can evolve thermal tolerance due to the selection pressure of elevated water temperatures (Morse et al., 2009; Locklin et al., 2020). It seems that cooler temperatures also influence regional temperature tolerances of zebra mussels. In Gull Lake, Michigan, *in situ* experiments revealed that 25 °C was the lethal limit for zebra mussels (White et al. 2015). This is cooler than the 30–32 °C lethal limit reported in many laboratory studies (McMahon et al., 1994; Elderkin and Klerks, 2005; White et al., 2015). Zebra mussel distributions in Lake Winnipeg, Manitoba, are reduced in areas of the lake where cooler temperatures resulting from shallower water depths limit mussel establishment and spread (Depew et al., 2020). The range of thermal adaptation that zebra mussels are able to show will ultimately determine how far they will spread. Our ability to understand this extent will enable us to accurately predict this spread and assess its impacts (Feng et al., 2020).

#### *Dissolved oxygen*

Zebra mussels are one of the least tolerant bivalves to anoxic conditions (McMahon, 1996). In the Ponto-Caspian region where they are native, zebra mussels use byssal threads to remain attached to surfaces in turbulent, oxygenated littoral areas of large lakes (Farr and Payne 2010). There is some evidence to suggest that populations from different geographic regions can adapt to local dissolved DO conditions (De Ventura et al., 2016). This has only been investigated in Europe, but it could have implications for assessing the potential range of zebra mussels in North America as well. To date, our understanding of zebra mussel DO tolerance depends mostly on laboratory studies conducted several decades ago. Zebra mussel DO tolerance depends on temperature and it is easier to understand the relationship between these variables in a

controlled, laboratory environment. At warmer temperatures, mussels require more DO to meet metabolic demands (Alexander and McMahon, 2004). Zebra mussels are able to survive anoxic conditions, but only for limited periods. For example, when DO concentrations are below  $0.7 \text{ mg L}^{-1}$ , zebra mussel mortality is 100 % after 6 days when water temperatures are  $17\text{--}18 \text{ }^{\circ}\text{C}$ , 4 days at temperatures between  $20\text{--}21 \text{ }^{\circ}\text{C}$ , and 3 days when temperatures are  $23\text{--}24 \text{ }^{\circ}\text{C}$  (Mikheev, 1964). Others have found that in anoxic conditions, 100 % mortality happens after 5 days when temperatures are  $18 \text{ }^{\circ}\text{C}$  (Karatayev et al., 1998). Zebra mussels can survive anoxic environments for much longer at colder temperatures. Below DO concentrations of  $0.4 \text{ mg L}^{-1}$ , zebra mussels can survive for 38–42 days at  $5 \text{ }^{\circ}\text{C}$  compared to 3–4 days at  $25 \text{ }^{\circ}\text{C}$  (Mathews and McMahon, 1999). Zebra mussel size also influences the length of time individual mussels are able to survive in reduced DO environments with larger mussels surviving for longer in anoxic environments than smaller ones (Mikheev 1964; Mathews and McMahon, 1999).

Several field studies have also identified DO as playing an important role in zebra mussel survival, distribution, and health, although these have not been able to directly verify the specific survival thresholds measured in lab studies due to variable environmental parameters. In Hargus Lake (OH), no decrease in zebra mussel survival occurred until the lower metalimnion, where DO concentrations reached  $1.7 \text{ mg L}^{-1}$  and temperatures were  $18 \text{ }^{\circ}\text{C}$  (Yu and Culver 1999). Below these DO concentrations, zebra mussel survival dropped from 75 to 0 %, and many of the mussels expired during the third (and final) month of stratification when hypoxic conditions were most pronounced (Yu and Culver 1999). It is difficult to attribute this mortality exclusively to low DO concentrations, as other environmental changes, such as increased ammonia or nitrate

concentrations, could also play a role (Yu and Culver 1999). DO concentrations can limit zebra mussel distributions to above the depth of stratification, at least in systems that often experience anoxia in the hypolimnion. In larger lakes, zebra mussel densities are higher in basins that are deeper and have higher DO concentrations (Depew et al., 2020). Cohorts from the previous spring, or previous years depending on DO conditions at the time, can be wiped out during years when stratification persists for several months (Garton and Johnson 2008; Locklin et al., 2020). Zebra mussels might be prevented from reaching high densities in systems that experience frequent and prolonged stratification. This is more common at southern latitudes where mixing depths tend to be shallower and anoxia in the hypolimnion tends to last longer than water bodies to the north (Jones et al., 2011; Churchill et al., 2017). High DO concentrations also can influence zebra mussel health. Zebra mussel production of glutathione, an antioxidant that reduces oxidative stress, is positively correlated with DO concentrations (Wojtal-Frankiewicz et al., 2017). High DO concentrations do not seem to be a prerequisite for zebra mussel establishment as high densities have been observed in systems where DO concentrations are  $\sim 6 \text{ mg L}^{-1}$  throughout much of the summer (Effler et al., 1996).

### *Calcium*

Calcium (Ca) is necessary for zebra mussel shell construction and osmoregulation (Vinogradov et al., 1993; McMahon, 1996). Calcium carbonate ( $\text{CaCO}_3$ ) is the most usable form of Ca for zebra mussels. A minimum threshold for  $\text{CaCO}_3$  is required for mussel survival, but the exact concentration of this threshold is debated. Based on a meta-analysis of laboratory and field studies, Ca concentrations of  $12.0 \text{ mg Ca L}^{-1}$  represent a functional threshold for zebra mussel establishment, although zebra mussels have been

observed in water bodies with lower Ca concentrations (Cohen 2007). Zebra mussels have been observed at Ca concentrations as low as 8.0 mg Ca L<sup>-1</sup> in the St. Lawrence River (Jones and Ricciardi 2005), and 8.5 mg Ca L<sup>-1</sup> in Ontario (Canada) lakes (Hincks and Mackie 1997). Field studies may underestimate the Ca threshold necessary for zebra mussel survival as Ca concentrations can fluctuate from when they are measured. In the lab, CaCO<sub>3</sub> concentrations of 13 mg Ca L<sup>-1</sup> have been identified as the threshold for survival and reproduction (Baldwin et al., 2012). Zebra mussel growth rate is highest at concentrations of 32 mg Ca L<sup>-1</sup> (Hincks and Mackie 1997). No upper toxicity of Ca concentrations have been identified, but zebra mussel densities decline when exposed to calcium chloride (CaCl<sub>2</sub>, Coldsnow et al., 2021). CaCO<sub>3</sub> concentrations have been used to model the potential range of zebra mussels in North America, and waterbodies with concentrations above 20 mg Ca L<sup>-1</sup> are classified as having a moderate risk of invasion (Whittier et al., 2008). In the United States, water bodies in regions such as the Pacific Northwest and parts of New England likely have a low risk of zebra mussel invasion, due to their low CaCO<sub>3</sub> concentrations (Strayer 2009). In 80 % of Missouri reservoirs, mean Ca concentrations are above 20 mg L<sup>-1</sup>, and CaCO<sub>3</sub> are above 70 mg L<sup>-1</sup> (Wylie and Jones 1991). In only 4 % of reservoirs are concentrations below 20 mg L<sup>-1</sup> (Wylie and Jones 1991).

#### *Inorganic suspended solids*

Inorganic suspended solids can clog inhalant siphons and gills which can reduce zebra mussel respiration, clearance, and ingestion rates (Madon et al., 1998; Tuttle-Raycraft et al., 2017). Many bivalves address elevated concentrations of inorganic particles by reducing their filtering rates and/or producing pseudofaeces to clear their

gills from inorganic particles, but this exerts an energetic cost (Chapman et al., 2017; Goldsmith et al., 2021). Previous research has tried to determine a level of inorganic suspended solids under which zebra mussels display a negative response, but with mixed results. Some studies suggest that the impacts of inorganic particles on zebra mussel fitness is substantial, while others argue that zebra mussels are only minimally impacted. Of the former, 5.0 inorganic: organic particles in the seston has been proposed as a ratio beneath which zebra mussel ingestion, assimilation, water processing, and clearance rates are substantially reduced (Madon et al., 1998; Schneider et al., 1998). Others have found that threshold concentrations are more appropriate for assessing the impacts of inorganic solids on zebra mussels because underneath these thresholds, zebra mussels begin to display negative responses. For example, bentonite clay in 31 mg L<sup>-1</sup> concentrations resulted in a significant decrease in respiration rates of zebra mussels in mesocosm tanks (Alexander et al., 1994), and inorganic suspended solids exceeding 27 mg L<sup>-1</sup> caused zebra mussels to produce an increased amount of pseudofeces (Lei et al., 1996). One reason for the lack agreement about the precise threshold might be because zebra mussels are able to adapt their behavior to reduce the impacts of chronic levels of high suspended inorganic solids (Ouellette-Plante et al., 2017). This makes understanding the exact effects of inorganic suspended solids on zebra mussel behavior a challenge.

There is evidence suggesting that zebra mussels are only minimally impacted by high concentrations of inorganic suspended particles. During benthic sediment resuspension in Lake Druzno (Poland), zebra mussels stopped filtering until all but the smallest particles settled out of suspension, a process that only took 10–30 minutes (Wiśniewski 1990). For these mussels, total ingestion rates over a four hour period were

the same as mussels that did not experience sediment resuspension, suggesting that brief periods of exposure to fine inorganic particles do not cause a negative impact (Wiśniewski 1990). The respiration rate of zebra mussels exposed to high turbidity derived from bentonite clay (80 NTU) decreased, but this decrease was smaller in mussels that had previously been acclimated to similar turbidity levels (Summers et al., 1996). Behaviorally, zebra mussels can close their inhalant siphons under high concentrations of illitesmectite clay for brief time periods and can selectively reject inorganic materials in pseudofaeces before digestion (MacIsaac and Rocha 1995; Baker et al., 1998). Physiologically, zebra mussels exposed to chronically high concentrations of suspended sediments are able to increase their palp to gill surface area ratio to increase their ability to sort food and non-food particles (Payne et al., 1995). At this point, more work is needed to better understand the impacts of inorganic sediments on zebra mussels and their ability to adapt to the suboptimal conditions.

## DISSERTATION JUSTIFICATION

### *Objectives and Hypotheses*

The objective of this dissertation is to investigate the influence of light on phytoplankton. Traditional management of phytoplankton biomass has focused on controlling nutrient loading while light availability is considered unchangeable and is largely ignored. This dissertation looks at how decreased light availability, resulting from GRF application, influences phytoplankton communities in mesocosm tanks. It also looks at microcystin accumulation in the tissues of bluegill and largemouth bass. Microcystin is a secondary metabolite produced by some species of cyanobacteria, possibly as a way to protect the cell from high UV radiation (Phelan and Downing 2011). Finally, this

dissertation investigates how increased light availability influences phytoplankton by looking at water clarity before and after the introduction of filter feeding zebra mussels in Missouri reservoirs.

H<sub>0</sub>: Light does not control phytoplankton biomass independent of nutrient concentrations, water temperature, and grazing.

H<sub>1</sub>: Light controls phytoplankton biomass independent of nutrient concentrations, water temperature, and grazing.

This dissertation focuses on studying some of the aquatic threats in Missouri's reservoirs. In Chapter 2, we used a novel geoengineering approach, glacial rock flour, to control cyanobacterial blooms by limiting light availability. Despite being a crucial factor to cyanobacterial growth, light is rarely considered as a cyanobacterial management strategy. To the best of our knowledge, glacial rock flour has never before been used for this purpose. We applied glacial rock flour to chlorophyte- and cyanophyte-dominated mesocosm tanks and measured phytoplankton taxonomic composition and phytoplankton biovolume before and after glacial rock flour additions. Our objective was to see if we could reduce light availability throughout the water column and, in doing so, control cyanobacterial growth. We hypothesized that decreased light availability would reduce cyanobacterial biomass. Our findings from this study are published in *Frontiers in Environmental Science* (Gaskill et al. 2020).

In Chapter 3, we study how microcystin, one of the most commonly produced cyanotoxins, accumulates in fish. Microcystin has been shown to transfer between trophic levels, ultimately ending up in fish tissues (Ibelings et al., 2005). This creates a potential human health risk for anglers who consume the fish they catch. Currently, only California (Butler et al., 2012), Illinois (Illinois EPA, 2012), Nebraska (Walker et al., 2008), Ohio (Ohio, 2010), Oregon (Oregon Health Authority, 2015), and Washington (Trainer and Hardy, 2015) have microcystin guidelines or advisories for fish consumption in the United States. We measured microcystin concentrations in the filets, livers, and kidneys of two recreationally valuable sportfish in Missouri, bluegill (*Lepomis macrochirus*) and largemouth bass (*Micropterus salmoides*), over the course of 12 months in a reservoir that frequently experiences cyanobacterial blooms. We measured water parameters once every two weeks throughout this 12-month period as well. Our objectives for this study were to investigate whether any fish characteristics or water quality parameters were linked with cyanotoxin accumulation in fish tissues. We hypothesized that there would be no relationship between microcystin concentrations in fish tissues and fish characteristics, and also that there would be no relationship between microcystin in fish and water quality parameters.

Chapter 4 looks at the effects of invasive zebra mussels in Missouri reservoirs. There is substantial evidence showing that zebra mussels increase water clarity of water bodies in northern latitudes, but this has not been investigated in Missouri where many reservoirs are characterized by warm water temperatures, high turbidities, and anoxic hypolimnions throughout most of the summer. While water temperatures in southern latitudes often exceed experimental tolerance levels for zebra mussels, there is some

evidence that zebra mussel populations can adapt to local temperature regimes (Elderkin and Klerks 2005). The ability to withstand higher temperatures might lead to faster growth rates and more frequent reproduction events, which may ultimately increase the impact zebra mussels have in southern reservoirs (Locklin et al., 2020). Our objective for this study was to determine whether zebra mussels are causing an increase in water clarity in Missouri reservoirs. We predict that the presence of zebra mussels will result in an increase in water clarity due to the filter-feeding behavior of zebra mussels. Our hypothesis is that zebra mussel presence and water clarity are related in Missouri reservoirs.

Chapters 2 through 4 are written with the intent to publish in peer-reviewed journals and an independent literature cited section follows each chapter. Formatting for these chapters follows the requirements outlined by the journal to which each chapter was (or will be) submitted. This was *Frontiers in Environmental Science* for Chapter 2, *Aquatic Toxicology* for Chapter 3, and will be *Biological Invasions* for Chapter 4. Writing in these chapters uses plural pronouns (i.e., “we” and “our”) to reflect the contribution of coauthors. Additionally, some of the introductory materials may overlap between chapters.

## LITERATURE CITED

- Ackerman, J.D., B. Sim & S.J. Nichols, 1994. A review of the early life history of zebra mussels (*Dreissena polymorpha*): comparisons with marine bivalves. *Canadian Journal of Zoology* 72:1169–1179.
- Afanas'yev, S.A. & A.A. Protasov, 1987. Characteristics of a *Dreissena* population in the periphyton of a nuclear power plant cooling pond. *Hydrobiological Journal* 23:42–49.
- Ahlgren, G., L. Lundstedt, M. Brett & C. Forsberg, 1990. Lipid composition and food quality of some freshwater phytoplankton for cladoceran zooplankters. *Journal of Plankton Research* 12:809–818.
- Ahn, C.Y., M.H. Park, S.H. Joung, H.S. Kim, K.Y. Jang & H.M. Oh, 2003. Growth inhibition of cyanobacteria by ultrasonic radiation: laboratory and enclosure studies. *Environmental Science and Technology* 37:3031–3037.
- Alexander, J.E., J.H. Thorp & R.D. Fell, 1994. Turbidity and temperature effect on oxygen consumption in the zebra mussel (*Dreissena polymorpha*). *Canadian Journal of Fisheries and Aquatic Sciences* 51:179–184.
- Alexander, J.E. & R.F. McMahon, 2004. Respiratory response to temperature and hypoxia in the zebra mussel *Dreissena polymorpha*. *Comparative Biochemistry and Physiology Part A: Molecular & Integrative Physiology* 137:425–434.
- American Water Works Association (AWWA), 2016. Cyanotoxins in US Drinking Water: Occurrence, Case Studies and State Approaches to Regulation. [https://www.awwa.org/Portals/0/AWWA/Government/201609\\_Cyanotoxin\\_Occurrence\\_States\\_Approach.pdf?ver=2018-12-13-101832-037](https://www.awwa.org/Portals/0/AWWA/Government/201609_Cyanotoxin_Occurrence_States_Approach.pdf?ver=2018-12-13-101832-037)
- Anderson, I.M., T.J. Williamson, M.J. González & M.J. Vanni, 2020. Nitrate, ammonium, and phosphorus drive seasonal nutrient limitation of chlorophytes, cyanobacteria, and diatoms in a hyper-eutrophic reservoir. *Limnology and Oceanography* 65: 962–978.
- Backer, L.C., W. Carmichael, B. Kirkpatrick, C. Williams, M. Irvin, Y. Zhou, T.B. Johnson, K. Nierenberg, V.R. Hill, S.M. Kieszak & Y.-S. Cheng, 2008. Recreational exposure to low concentrations of microcystins during an algal bloom in a small lake. *Marine Drugs* 6:389–406.
- Backer, L.C., J.H. Landsberg, M. Miller, K. Keel & T.K. Taylor, 2013. Canine cyanotoxin poisonings in the United States (1920s–2012): Review of suspected and confirmed cases from three data sources. *Toxins* 5:1597–1628.
- Baganz, D., G. Staaks, S. Pflugmacher & C.E.W. Steinberg, 2004. Comparative study of microcystin-LR-induced behavioral changes of two fish species, *Danio rerio* and *Leucaspis delineatus*. *Environmental Toxicology* 19:564–570.

- Bagu J.R., B. Sykes, M. Craig, C.F.B. Holmes, 1997. A molecular basis for different interactions of marine toxins with protein phosphatase 1. *Journal of Biological Chemistry* 272:5087–5097.
- Baker, S.M., J.S. Levinton, J.P. Kurdziel & S.F. Shumway, 1998. Selective feeding and biodeposition by zebra mussels and their relation to changes in phytoplankton composition and seston load. *Journal of Shellfish Research* 17:1207–1213.
- Baldia, S.F., A.D. Evangelista, E.V. Aralar & A.E. Santiago, 2007. Nitrogen and phosphorus utilization in the cyanobacterium *Microcystis aeruginosa* isolated from Laguna de Bay, Philippines. *Journal of Applied Phycology* 19:607–613.
- Baldwin, B.S., M. Carpenter, K. Rury & E. Woodward, 2012. Low dissolved ions may limit secondary invasion of inland waters by exotic round gobies and dreissenid mussels in North America. *Biological Invasions* 14:1157–1175.
- Baranowska, K.A., R.L. North, J.G. Winter & P.J. Dillon, 2013. Long-term seasonal effects of dreissenid mussels on phytoplankton in Lake Simcoe, Ontario, Canada. *Inland Waters* 3:285–296.
- Barbiero, R.P., M.L. Tuchman & E.S. Millard, 2006. Post-dreissenid increases in transparency during summer stratification in the offshore waters of Lake Ontario: is a reduction in whiting events the cause? *Journal of Great Lakes Research* 32:131–141.
- Barouillet, C., B.F. Cumming, K.R. Laird, C.J. Perrin & D.T. Selbie, 2019. Influence of glacial flour on the primary and secondary production of sockeye salmon nursery lakes: a comparative modern and paleolimnological study. *Canadian Journal of Fisheries and Aquatic Sciences* 76:2165–2432.
- Batt, R.D., S.R. Carpenter, J.J. Cole, M.L. Pace, R.A. Johnson, J.T. Kurtzweil & G.M. Wilkinson, 2015. Altered energy flow in the food web of an experimentally darkened lake. *Ecosphere* 6:33.
- Becker, A., A. Herschel & C. Wilhelm, 2006. Biological effects of incomplete destratification of hypertrophic freshwater reservoir. *Hydrobiologia* 559:85–100.
- Bellinger, E.G. & D.C. Sigee, 2010. *Freshwater Algae: Identification and Use as Bioindicators*. John Wiley & Sons, Ltd, Chichester, 271 pp.
- Benson, A.J., D. Raikow, J. Larson, A. Fusaro, A.K. Bogdanoff & A. Elgin, 2021, *Dreissena polymorpha* (Pallas, 1771): U.S. Geological Survey, <https://nas.er.usgs.gov/queries/FactSheet.aspx?speciesID=5>.
- Bergström, A. & J. Karlsson, 2019. Light and nutrient control phytoplankton biomass responses to global change in northern lakes. *Global Change Biology* 25: 2021–2029.
- Bingham, M., S.K. Sinha & F. Lupi, 2015. *Economic benefits of reducing harmful algal blooms in Lake Erie*. Gainesville, FL: Environmental Consulting and Technology Inc.

- Bischoff, J.L., K.M. Menking, J.P. Fitts & J.A. Fitzpatrick, 1997. Climate oscillations 10,000 – 155,000 yr B.P. at Owens Lake, California reflected in glacial rock flour abundance and lake salinity in core OL-92. *Quaternary Research* 48:313–325.
- Bischoff, J.L. & K. Cummins, 2001. Wisconsin Glaciation of the Sierra Nevada (79,000–15,000 yr B.P.) as recorded by rock flour in sediments of Owens Lake, California. *Quaternary Research* 55:14–24.
- Bloesch J. & H.R. Bürgi, 1989. Changes in phytoplankton and zooplankton biomass and composition reflected by sedimentation. *Limnology and Oceanography* 34:1048–1061.
- Branco, P., M. Egas, S.R. Hall & J. Huisman, 2020. Why do phytoplankton evolve large size in response to grazing? *The American Naturalist* 195: <https://doi.org/10.1086/706251>
- Brattebo, S.B., E.B. Welch & H.G. Gibbons, 2015. Nutrient inactivation with alum: What has worked and why? *Lake Line* 35:30–34.
- Brattebo, S.K., E.B. Welch, H.L. Gibbons, M.K. Burghdoff, G.N. Williams & J.L. Oden, 2017. Effectiveness of alum in a hypereutrophic lake with substantial external loading. *Lake and Reservoir Management* 33:108–118.
- Brauer, V.S., M. Stomp, & J. Huisman, 2012. The nutrient-load hypothesis: Patterns of resource limitation and community structure driven by competition for nutrients and light. *The American Naturalist* 179:721–740.
- Brookes, J.D. & G.G. Ganf, 2001. Variations in the buoyancy response of *Microcystis aeruginosa* to nitrogen, phosphorus and light. *Journal of Plankton Research* 23:1399–1411.
- Brooks, B.W., J.M. Lazorchak, M.D.A. Howard, M.V. Johnson, S.L. Morton, D.A.K. Perkins, E.D. Reavie, G.I. Scott, S.A. Smith & J.A. Steevens, 2016. Are harmful algal blooms becoming the greatest inland water quality threat to public health and aquatic ecosystems? *Environmental Toxicology and Chemistry* 35:6–13.
- Budd, J.W., T.D. Drummer, T.F. Nalepa & G.L. Fahnenstiel, 2001. Remote sensing of biotic effects: zebra mussels (*Dreissena polymorpha*) influence on water clarity in Saginaw Bay, Lake Huron. *Limnology and oceanography* 46:213–223.
- Bury, N.R., F.B. Eddy & G.A. Codd, 1995. The effects of the cyanobacterium *Microcystis aeruginosa*, the cyanobacterial hepatotoxin microcystin-LR, and ammonia on growth-rate and ionic regulation of brown trout. *Journal of Fish Biology* 46:1042–1054.
- Bury, N.R., G.A. Codd, S.E.W. Bonga & G. Flik, 1998. Fatty acids from the cyanobacterium *Microcystis aeruginosa* with potent inhibitory effects of fish gill  $\text{Na}^+/\text{K}^+$ -ATPase activity. *Journal of Experimental Biology* 201:81–89.
- Butler, C.J. & R. Linville, 2012. Toxicological summary and suggested action levels to reduce potential adverse health effects of six cyanotoxins. Office of

Environmental Health Hazard Assessment, California Environmental Protection Agency, Sacramento.

- Butterwick, C., S.I. Heaney & J.F. Talling, 2005. Diversity in the influence of temperature on the growth rates of freshwater algae, and its ecological relevance. *Freshwater Biology* 50:291–300.
- Cabrerizo, M.J., M.I. Álvarez-Manzaneda, E. León-Palmero, G. Guerrero-Jiménez, L.N. de Senerpont Domis, S. Teurlincx & J.M. González-Olalla, 2020. Warming and CO<sub>2</sub> effects under oligotrophication on temperate phytoplankton communities. *Water Research* 173:115579.
- Caraco, N.F., J.J. Cole, P.A. Raymond, D.L. Strayer, M.L. Pace, S.E.G. Findlay & D.T. Fischer, 1997. Zebra mussel invasion in a large, turbid river: phytoplankton response to increased grazing. *Ecology* 78:588–602.
- Caraco N.F., J.J. Cole, S.E.G. Findlay, D.T. Fischer, G.G. Lampman, M.L. Pace & D.L. Strayer, 2000. Dissolved oxygen declines in the Hudson River associated with the invasion of the zebra mussel (*Dreissena polymorpha*). *Environmental Science and Technology* 34:1204–1210.
- Carbis, C.R., G.T. Rawlin, P. Grant, G.F. Mitchell, J.W. Anderson & I. McCauley, 1997. A study of feral carp, *Cyprinus carpio* L., exposed to *Microcystis aeruginosa* at Lake Mokoan, Australia, and possible implications for fish health. *Journal of Fish Diseases* 20:81–91.
- Carlton, J.T., 2008. The zebra mussel *Dreissena polymorpha* found in North America in 1986 and 1987. *Journal of Great Lakes Research* 34:770–773.
- Carmichael, W.W. & G.L. Boyer, 2016. Health impacts from cyanobacteria harmful algae blooms: Implications for the North American Great Lakes. *Harmful Algae* 54:194–212.
- Carpenter, S.R., J.F. Kitchell & J.R. Hodgson, 1985. Cascading trophic interactions and lake productivity. *BioScience* 35:634–639.
- Carpenter, S.R. & W.A. Brock, 2006. Rising variance: A leading indicator of ecological transition. *Ecology Letters* 9:311–318.
- Carrillo, P., I. Reche, P. Sanchez-Castillo & L. Cruz-Pizarro, 1995. Direct and indirect effects of grazing on the phytoplankton seasonal succession in an oligotrophic lake. *Journal of Plankton Research* 17:1363–1379.
- Carstensen, J., P. Henriksen & A.S. Heiskanen, 2007. Summer algal blooms in shallow estuaries: definition, mechanisms, and link to eutrophication. *Limnology and Oceanography* 52:370–384.
- Casassa, G., P. López, B. Pouyaud & F. Escobar, 2009. Detection of changes in glacial run-off in alpine basins: Examples from North America, the Alps, central Asia and the Andes. *Hydrological Processes* 23:31–41.

- Cazenave, J., D.A. Wunderlin, M.D.L.A. Bistoni, M.V. Amé, E. Krause, S. Pflugmacher & C. Wiegand, 2005. Uptake, tissue distribution and accumulation of microcystin-RR in *Corydoras paleatus*, *Jenynsia multidentata* and *Odontesthes bonariensis*: a field and laboratory study. *Aquatic Toxicology* 75:178–190.
- Cazenave, J., M.A. Bistoni, E. Zwirnmann, D.A. Wunderlin & C. Wiegand, 2006. Attenuating effects of natural organic matter on microcystin toxicity in zebra fish (*Danio rerio*) embryos—benefits and costs of microcystin detoxication. *Environmental Toxicology* 21:22–32.
- Cha, Y., C.A. Stow, T.F. Nalepa & K.H. Reckhow, 2011. Do invasive mussels restrict offshore phosphorus transport in Lake Huron? *Environmental Science and Technology* 45:7226–7231.
- Chaffin, J.D., T.W. Davis, D.J. Smith, M.M. Baer & G.J. Dick, 2018. Interactions between nitrogen form, loading rate, and light intensity on *Microcystis* and *Planktothrix* growth and microcystin production. *Harmful Algae* 73:84–97.
- Chanudet, V. & M. Filella, 2009. Size and composition of inorganic colloids in a peri-alpine, glacial flour-rich lake. *Geochimica et Cosmochimica Acta* 72:1466–1479.
- Chapman, A. & A. Foss, 2019. Potentially toxigenic (PTOX) cyanobacteria list. Palatka, FL: GreenWater Laboratories.
- Chapman P.M., A. Hayward & J. Faithful, 2017. Total suspended solids effects on freshwater lake biota other than fish. *Bulletin of Environmental Contamination and Toxicology* 99:423–427.
- Chase, M.E. & R.C. Bailey, 1999. The ecology of the zebra mussel (*Dreissena polymorpha*) in the Lower Great Lakes of North America: I. Population Dynamics and Growth. *Journal of Great Lakes Research* 25:107–121.
- Chen, J., P. Xie, D. Zhang, Z. Ke & H. Yang, 2006. *In situ* studies on the bioaccumulation of microcystins in the phytoplanktivorous silver carp (*Hypophthalmichthys molitrix*) stocked in Lake Taihu with dense toxic *Microcystis* blooms. *Aquaculture* 261:1026–1038.
- Cheng, Y.S., Y. Zhou, C.M. Irvin, B. Kirkpatrick & L.C. Backer, 2007. Characterization of aerosols containing microcystin. *Marine Drugs* 5:136–150.
- Churchill, C.J., 2013. Spatio-temporal spawning and larval dynamics of a zebra mussel (*Dreissena polymorpha*) population in a North Texas Reservoir: Implications for invasions in the southern United States. *Aquatic Invasions* 8:389–406.
- Churchill, C.J., D.J. Hoeinghaus, & T.W. La Point, 2017. Environmental conditions increase growth rates and mortality of zebra mussels (*Dreissena polymorpha*) along the southern invasion front in North America. *Biological Invasions* 19:2355–2373.
- Chorus, I. & M. Welker, 2021. Toxic Cyanobacteria in Water: A guide to their public health consequences, monitoring and management. CRC Press, London, 858 pp.

- Chorus, I. & I. Schauser, 2011. Oligotrophication of Lake Tegel and Schlachtensee, Berlin - analysis of system components, causalities and response thresholds compared to responses of other waterbodies. Technical report (45/2011) of the Federal Environment Agency (Umweltbundesamt).
- Cohen, A.N., 2007. Potential Distribution of Zebra Mussels (*Dreissena Polymorpha*) and Quagga Mussels (*Dreissena Bugensis*) in California: Phase 1 Report. San Francisco Estuary Institute, Oakland, CA, USA.
- Coldsnow, K.D., W.D. Hintz, M.S. Schuler, A.B. Stoler & R.A. Relyea, 2021. Calcium chloride pollution mitigates the negative effects of an invasive clam. *Biological Invasions* 23:1349–1366.
- Cole, J.J., N.F. Caraco & B.L. Peierls, 1992. Can phytoplankton maintain a positive carbon balance in a turbid, freshwater, tidal estuary? *Limnology and Oceanography* 37:1608–1617.
- Collen, B., J. Loh, S. Whitmee, L. McRae, R. Amin & J.E.M. Baillie, 2009. Monitoring change in vertebrate abundance: the Living Planet Index. *Conservation Biology* 23:317–327.
- Connelly N.A., C.R. O’Neill, B.A. Knuth & T.L. Brown, 2007. Economic impacts of zebra mussels on drinking water treatment and electric power generation facilities. *Environmental Management* 4400:105–112.
- Conroy, J.D., W.J. Edwards, R.A. Pontius, D.D. Kane, H. Zhang, J.F. Shea, J.N. Richey & D.A. Culver, 2005. Soluble nitrogen and phosphorus excretion of exotic freshwater mussels (*Dreissena* spp.): potential impacts for nutrient remineralization in western Lake Erie. *Freshwater Biology* 50:1146–1162.
- Cooke, G.D., E.B. Welch, S.A. Peterson & S.A. Nichols, 2005. Restoration and management of lakes and reservoirs. Boca Raton, CRC Press. 616 pp.
- Corbel, S., C. Mougin, S. Nélieu, G. Delarue & N. Bouaïcha, 2016. Evaluation of the transfer and the accumulation of microcystins in tomato (*Solanum lycopersicum* cultivar MicroTom) tissues using a cyanobacterial extract containing microcystins and the radiolabeled microcystin-LR (<sup>14</sup>C-MC-LR). *Science of The Total Environment* 541:1052–1058.
- Cousins, I.T., D.J. Bealing, H.A. James & A. Sutton, 1996. Biodegradation of microcystin-LR by indigenous mixed bacterial populations. *Water Research* 30:481–485.
- Cowell, B.C., C.J. Dawes, W.E. Gardiner & S.M. Sceda, 1987. The influence of whole lake aeration on the limnology of a hypereutrophic lake in central Florida. *Hydrobiologia* 148:3–24.
- Crusius, J., A.W. Schroth, S. Gassó, C.M. Moy, R.C. Levy & M. Gatica, 2011. Glacial flour dust storms in the Gulf of Alaska: Hydrologic and meteorological controls and their importance as a source of bioavailable iron. *Geophysical Research Letters* 38:L06602.

- Davis, T.W., D.L. Berry, G.L. Boyer & C.J. Gobler, 2009. The effects of temperature and nutrients on the growth and dynamics of toxic and non-toxic strains of *Microcystis* during cyanobacteria blooms. *Harmful Algae* 8:715–725.
- De Stasio, B.T., M.B. Schimpf & B.H. Cornwell, 2014. Phytoplankton communities in Green Bay, Lake Michigan after invasion by dreissenid mussels: increased dominance by cyanobacteria. *Diversity* 6:681–704.
- De Ventura, L., D. Sarpe, K. Kopp & J. Joke, 2016. Variability in phenotypic tolerance to low oxygen in invasive populations of quagga and zebra mussels. *Aquatic Invasions*. *Aquatic Invasions* 11:267–276.
- Deacon, C. & A.E. Walsby, 1990. Gas vesicle formation in the dark, and in the light of different irradiances, by the cyanobacterium *Microcystis* sp. *British Phycological Journal* 25:133–139.
- Depew, D.C., E. Krutzelmann, K.E. Watchorn, A. Caskenette & E.C. Enders, 2020. The distribution, density, and biomass of the zebra mussel (*Dreissena polymorpha*) on natural substrates in Lake Winnipeg 2017–2019. *Journal of Great Lakes Research* In Press.
- Dodds, W.K., W.W. Bouska, J.L. Eitzmann, T.J. Pilger, K.L. Pitts, A.J. Riley, J.T. Schloesser & D.J. Thornbrugh, 2009. Eutrophication of U.S. freshwaters: analysis of potential economic damages. *Environmental Science and Technology* 43:12–19.
- Dölle, K. & D.E. Kurzmann, 2020. The freshwater mollusk *Dreissena polymorpha* (zebra mussel) - a review: living, prospects and jeopardies. *Asian Journal of Environment and Ecology* 13:1–17.
- Dolman, A.M., J. Rucker, F.R. Pick, J. Fastner, T. Rohrlack, U. Mischke & C. Weidner, 2012. Cyanobacteria and cyaontoxins: the influence of nitrogen versus phosphorus. *PLoS ONE* 7:e38757.
- Douglas, G.B., 2002. US Patent 6350383: Remediation material and remediation process for sediments.
- Douglas, G.B., M. Lürling & B.M. Spears, 2016. Assessment of changes in potential nutrient limitation in an impounded river after application of lanthanum-modified bentonite. *Water Research* 97:47–54.
- Downing, J.A., S.B. Watson & E. McCauley, 2001. Predicting cyanobacteria dominance in lakes. *Canadian Journal of Fisheries and Aquatic Sciences* 58:1905–1908.
- Drake, J.M., & J.M. Bossenbroek, 2004. The potential distribution of zebra mussels in the United States. *BioScience* 54:931–941.
- Dudgeon, D., 2019. Multiple threats imperil freshwater biodiversity in the Anthropocene. *Current Biology* 29:R960–R967.
- Dubourg, P., R.L. North, K. Hunter, D. Vandergucht, O. Abirhire, G.M. Silsbe, S. Guildford & J.J. Hudson, 2015. Light and nutrient co-limitation of phytoplankton

- communities in a large reservoir: Lake Diefenbaker, Saskatchewan, Canada. *Journal of Great Lakes Research* 42:129–143.
- Dzialowski, A.R., S.-H. Wang, N.-C. Lim, W.W. Spotts & D.G. Huggins, 2005. Nutrient limitation of phytoplankton growth in central plains reservoirs, USA. *Journal of Plankton Research* 27:587–595.
- Dzierżyńska-Białończyk, A., Ł. Jermacz, T. Maćkiewicz, J. Gajewska & J. Kobak, 2018. Mechanisms and impact of differential fouling of the zebra mussel *Dreissena polymorpha* on different unionid bivalves. *Freshwater Biology* 63:687–699.
- Effler, S.W., C.M. Brooks, K. Whitehead, B. Wagner, S.M. Doerr, M. Perkins, C.A. Siegfried, L. Walrath & R.P. Canale, 1996. Impact of Zebra mussel invasion on river water quality. *Water Environment Research* 68:205–214.
- Effler, S.W., D.A. Matthews, C.M. Brooks-Matthews, M.G. Perkins, C.A. Siegfried & J.M. Hassett, 2004. Water quality impacts and indicators of metabolic activity of the zebra mussel invasion of the Seneca River. *Journal of the American Water Resources Association* 40:737–754.
- Elderkin, C.L. & P.L. Klerks, 2005. Variation in thermal tolerance among three Mississippi River populations of the zebra mussel, *Dreissena polymorpha*. *Journal of Shellfish Research* 24:221–226.
- Elser, J.J., E.R. Marzolf & C.R. Goldman, 1990. Phosphorus and nitrogen limitation of phytoplankton growth in the freshwaters of North America; A review and critique of experimental enrichment. *Canadian Journal of Fisheries and Aquatic Sciences* 47:1468–1477.
- Epe, T.S., K. Finsterle & S. Yasseri, 2017. Nine years of phosphorus management with lanthanum modified bentonite (Phoslock) in a eutrophic, shallow swimming lake in Germany. *Lake and Reservoir Management* 33:119–129.
- Ernst, B., B. Hitzfeld & D. Dietrich, 2001. Presence of *Planktothrix* sp. And cyanobacterial toxins in Lake Ammersee, Germany and their impact on whitefish (*Coregonus lavaretus* L.). *Environmental Toxicology* 16:483–488.
- Ernst, B., S.J. Hoeger, E. O'Brien & D.R. Dietrich, 2006. Oral toxicity of the microcystin-containing cyanobacterium *Planktothrix rubescens* in European whitefish (*Coregonus lavaretus*). *Aquatic Toxicology* 79:31–40.
- Fahnenstiel, G.L., G.A. Lang, T.F. Nalepa & T.H. Johengen, 1995. Effects of zebra mussel (*Dreissena polymorpha*) colonization on water quality parameters in Saginaw Bay, Lake Huron. *Journal of Great Lakes Research* 21:435–448.
- Fanslow, D.L., T.F. Nalepa & G.A. Lang, 1995. Filtration rates of the zebra mussel (*Dreissena polymorpha*) on natural seston from Saginaw Bay, Lake Huron. *Journal of Great Lakes Research* 21:489–500.
- Farr, M.D. & B.S. Payne, 2010. Environmental habitat conditions associated with freshwater dreissenids. In *Aquatic Nuisance Species Research Program, US Army Corps of Engineers*.

- Fawell, J.K., R.E. Mitchell, D.J. Everett & R.E. Hill, 1999. The toxicity of cyanobacterial toxins in the mouse: I Microcystin-LR. *Human and Experimental Toxicology* 18:162–167.
- Feng, X., Y. Liang, B. Gallardo & M. Papeş, 2020. Physiology in ecological niche modeling: using zebra mussel's upper thermal tolerance to refine model predictions through Bayesian analysis. *Ecography* 43: 270–282.
- Feniova, I., E.G. Sakharova, Z.I. Gorelysheva, M. Karpowicz, A. Górniak, V. Petrosyan, A.R. Dzialowski, 2020. Effects of zebra mussels (*Dreissena polymorpha*) on phytoplankton community structure under eutrophic conditions. *Aquatic Invasions* 15:435–454.
- Ferrão-Filho, A.S. & B. Kozłowsky-Suzuki, 2011. Cyanotoxins: bioaccumulation and effects on aquatic animals. *Marine Drugs* 9:2729–2772.
- Flores, N.M., T.R. Miller & J.D. Stockwell, 2018. A global analysis of the relationship between concentrations of microcystins in water and fish. *Frontiers in Marine Science* 5:30.
- Fromme, H., A. Kohler, R. Krause & D. Fuhring, 2000. Occurrence of cyanobacterial toxins – microcystins and anatoxin-a – in Berlin water bodies with implications to human health and regulations. *Environmental Toxicology* 15:120–130.
- Funes, A., I. Álvarez-Manzaneda, A. del Arco, J. de Vicente & I. de Vicente, 2021. Evaluating the effect of CFH-12® and Phoslock® on phosphorus dynamics during anoxia and resuspension in shallow eutrophic lakes. *Environmental Pollution* 269:116093.
- Gallegos, C.L., R.J. Davies-Colley & M. Gall, 2008. Optical closure in lakes with contrasting extremes of reflectance. *Limnology and Oceanography* 53:2021–2034.
- Gardner, W.S., J.F. Cavaletto, T.H. Johengen, J.R. Johnson, R.T. Heath, & J.B. Cotner Jr., 1995. Effects of the zebra mussel, *Dreissena polymorpha*, on community nitrogen dynamics in Saginaw Bay, Lake Huron. *Journal of Great Lakes Research* 21:529–544.
- Garton, D.W. & L.E. Johnson, 2008. Variation in growth rates of the zebra mussel, *Dreissena polymorpha*, within Lake Wawasee. *Freshwater Biology* 45:443–451.
- Gaskill, J.A., T.D. Harris & R.L. North, 2020. Phytoplankton response to changes in light: can glacial rock flour be used to control cyanobacterial blooms? *Frontiers in Environmental Science* 8:540607.
- George, D.G., 2021. Top-down versus bottom-up control in planktonic systems: some case studies from the English Lake District. *Hydrobiologia* 848:219–236.
- Gervais, F., 1998. Ecology of cryptophytes coexisting near a freshwater chemocline. *Freshwater Biology* 39:61–78.

- Ger, K.A., L.A. Hansson & M. Lürling, 2014. Understanding cyanobacteria-zooplankton interactions in a more eutrophic world. *Freshwater Biology* 59:1783–1798.
- Gibbs, M.M., C.W. Hickey, & D. Özkundakci, 2010. Sustainability assessment and comparison of efficacy of four P-inactivation agents for managing internal phosphorus loads in lakes: sediment incubations. *Hydrobiologia* 658:253–275.
- Goldsmith, A.M., F. Jaber, H. Ahmari & C.R. Randklev, 2021. Clearing up cloudy waters: a review of sediment impacts to unionid freshwater mussels. *Environmental Reviews* 29:100–108.
- Graham, J.L. & J.R. Jones, 2009. Microcystin in Missouri Reservoirs. *Lake and Reservoir Management*, 25:253–263.
- Greenstein, K.E., R. Zamyadi, C.M. Glover, C. Adams, E. Rosenfeldt & E.C. Wert, 2020. Delayed release of intracellular microcystin following partial oxidation of cultured and naturally occurring cyanobacteria. *Toxins* 12:335.
- Grosse, Y., R. Baan, K. Straif, B. Secretan, F.E. Ghissassi & V. Coglianò, 2006. Carcinogenicity of nitrate, nitrite, and cyanobacterial peptide toxins. *The Lancet Oncology* 7:628–629.
- Gunnarsen, K.C., L.S. Jensen, B. Gómez-Muñoz, M.T. Rosing & A. de Neergaard, 2019. Glacially abraded rock flour from Greenland: potential for macronutrient supply to plants. *Journal of Plant Nutrition and Soil Science* 182:846–856.
- Gurbuz, F., O.Y. Uzunmehmetoğlu, Ö. Diler, J.S. Metcalf & G.A. Codd, 2016. Occurrence of microcystins in water, bloom, sediment and fish from a public water supply. *Science of the Total Environment* 562:860–868.
- Hampton, S.E., A.W.E. Galloway, S.M. Powers, T. Ozersky, K.H. Woo, R.D. Batt, S.G. Labou, C.M. O'Reilly, S. Sharma, N.R. Lottig, E.H. Stanley, R.L. North, J.D. Stockwell, R. Adrian, G.A. Weyhenmeyer, L. Arvola, H.M. Baulch, I. Bertani, L.L. Bowman Jr., C.C. Carey, J. Catalan, W. Colom-Montero, L.M. Domine, M. Felip, I. Granados, C. Gries, H.P. Grossart, J. Haberman, M. Haldna, B. Hayden, S.N. Higgins, J.C. Jolley, K.K. Kahilainen, E. Kaup, M.J. Kehoe, S. MacIntyre, A.W. Mackay, H.L. Mariash, R.M. McKay, B. Nixdorf, P. Nöges, T. Nöges, M. Palmer, D.C. Pierson, D.M. Post, M.J. Pruet, M. Rautio, J.S. Read, S.L. Roberts, J. Rücker, S. Sadro, E.A. Silow, D.E. Smith, R.W. Sterner, G.E.A. Swann, M.A. Timofeyev, M. Toro, M.R. Twiss, R.J. Vogt, S.B. Watson, E.J. Whiteford & M.A. Xenopoulos, 2016. Ecology under lake ice. *Ecology Letters* 20:98–111.
- Han, Y., J.W. Smithheart, R.L. Smyth, T.N. Aziz & D.R. Obenour, 2020. Assessing vertical diffusion and cyanobacteria bloom potential in a shallow eutrophic reservoir. *Lake and Reservoir Management* 36:169–185.
- Hansen, G.J.A., T.D. Ahrenstorff, B.J. Bethke, J.D. Dumke, J. Hirsch, K.E. Kovalenko, J.F. LeDuc, R.P. Maki, H.M. Rantala & T. Wagner, 2020. Walleye growth declines following zebra mussel and *Bythotrephes* invasion. *Biological Invasions* 22:1481–1495.

- Harke, M.J., M.M. Steffen, C.J. Gobler, T.G. Otten, S.W. Wilhelm, S.A. Wood & H.W. Paerl, 2016. A review of the global ecology, genomics, and biogeography of the toxic cyanobacterium, *Microcystis* spp. *Harmful Algae* 54:4–20.
- Harris, T.D., F.M. Wilhelm, J.L. Graham & K.A. Loftin, 2014. Experimental manipulation of TN:TP ratios suppress cyanobacterial biovolume and microcystin concentration in large-scale *in situ* mesocosms. *Lake and Reservoir Management* 30:72–83.
- Hecky, R.E., R.E.H. Smith, D.R. Barton, S.J. Guildford, W.D. Taylor, M.N. Charlton & T. Howell, 2004. The nearshore phosphorus shunt: A consequence of ecosystem engineering by dreissenids in the Laurentian Great Lakes. *Canadian Journal of Fisheries and Aquatic Sciences* 61:1285–1293.
- Henaou, E., P. Rzymiski & M.N. Waters, 2019. A review on the study of cyanotoxins in paleolimnological research: current knowledge and future needs. *Toxins* 12:6.
- Herbert, P.D.N., C.C. Wilson, M.H. Murdoch & R. Lazar, 1991. Demography and ecological impacts of the invading mollusk *Dreissena polymorpha*. *Canadian Journal of Zoology* 69:405–409.
- Higgins, S.N. & M.J. Vander Zanden, 2010. What a difference a species makes: a meta-analysis of dreissenid mussel impacts on freshwater ecosystems. *Ecological Monographs* 80:179–196.
- Hincks, S.S., & G.L. Mackie, 1997. Effects of pH, calcium, alkalinity, hardness, and chlorophyll on the survival, growth, and reproductive success of zebra mussel (*Dreissena polymorpha*) in Ontario lakes. *Canadian Journal of Fisheries and Aquatic Sciences* 54:2049–2057.
- Hood, E. & L. Berner, 2009. Effects of changing glacial coverage on the physical and biogeochemical properties of coastal streams in southeastern Alaska. *Journal of Geophysical Research* 114:1–10.
- Horst, G.P., O. Sarnelle, J.D. White, S.K. Hamilton, R.B. Kaul & J.D. Bressie, 2014. Nitrogen availability increases the toxin quota of a harmful cyanobacterium, *Microcystis aeruginosa*. *Water Research* 54:188–198.
- Houser, J.N., S.R. Carpenter & J.J. Cole, 2000. Food web structure and nutrient enrichment: effects on sediment phosphorus retention in whole-lake experiments. *Canadian Journal of Fisheries and Aquatic Sciences* 57:1524–1533.
- Hozumi, A., I. Ostrovsky, A. Sukenik & H. Gildor, 2019. Turbulence regulation of *Microcystis* surface scum formation and dispersion during a cyanobacteria bloom event. *Inland Waters* 10:51–70.
- Huisman, J., G.A. Codd, H.W. Paerl, B.W. Ibelings, J.M.H. Verspagen & P.M. Visser, 2018. Cyanobacterial blooms. *Nature Reviews Microbiology* 16:471–483.
- Huser, B.J. & K.M. Pilgrim, 2014. A simple model for predicting aluminum bound phosphorus formation and internal loading reduction in lakes after aluminum addition to lake sediment. *Water Research* 53:378–385.

- Huser, B.J., S. Egemose, H. Harper, M. Hupfer, H. Jensen, K.M. Pilgrim, K. Reitzel, E. Rydin & M. Futter, 2016. Longevity and effectiveness of aluminum addition to reduce sediment phosphorus release and restore lake water quality. *Water Research* 97:122–132.
- Hwang, S.J., H.S. Kim, J.K. Shin, J.M. Oh & D.S. Kong, 2004. Grazing effects of a freshwater bivalve (*Corbicula leana* Prime) and large zooplankton on phytoplankton communities in two Korean lakes. *Hydrobiologia* 515:161–179.
- Hylland, S., T. Jephson, K. Lebet, J. Einem, T. Fagerberg, E. Balseiro, B. Modenutti, M. Sol Souza, C. Laspoumaderes, M. Jönsson, P. Ljungberg, A. Nicolle, P. Anders Nilsson, L. Ranaker & L.A. Hansson, 2011. Climate-induced input of turbid glacial meltwater affects vettcle distribution and community composition of phyto- and zooplankton. *Journal of Plankton Research* 33:1239–1248.
- Ibelings, B.W., K., Bruning, J. Jonge, K. Wolfstein, L.M. Dionisio, J. Postma, & T. Burger, 2005. Distribution of microcystins in a lake foodweb: no evidence for biomagnification. *Microbial Ecology* 49:487–500.
- Ibelings, B.W. & I. Chorus, 2007. Accumulation of cyanobacterial toxins in freshwater seafood and its consequence for public health: a review. *Environmental Pollution* 150:177–192.
- Ibelings, B.W., M. Bormans, J. Fastner & P.M. Visser, 2016. CYANOCOST special issue on cyanobacterial blooms: synopsis – a critical review of the management options for their prevention, control and mitigation. *Aquatic Ecology* 50:595–605.
- Illinois Environmental Protection Agency, 2012. Algal toxins in fish - Fish consumption guidance memo.
- Irwin, J., 1974. Water clarity records from twenty-two New Zealand lakes. *New Zealand Journal of Marine and Freshwater Research* 8:223–227.
- Isles, P.D.F., 2020. The misuse of ratios in ecological stoichiometry. *Ecology* 101:e03153.
- James, W.F., 2017. Phosphorus binding dynamics in the aluminum floc layer of Half Moon Lake, Wisconsin. *Lake and Reservoir Management* 33:130-142.
- Jansson, M., P. Blomqvist, A. Jonsson & A.K. Bergström, 1996. Nutrient limitation of bacterioplankton, autorophic and mixotrophic phytoplankton, and heterotrophic nanoflagellates in Lake Öträsket. *Limnology and Oceanography* 41:1552–1559.
- Jeppesen, E., D.E. Canfield, R.W. Bachmann, M. Søndergaard, K.E. Havens, L.S. Johansson, T.L. Lauridsen, T. Sh, R.P. Rutter, G. Warren, G. Ji & M.V. Hoyer, 2020. Toward predicting climate change effects on lakes: a comparison of 1656 shallow lakes from Florida and Denmark reveals substantial differences in nutrient dynamics, metabolism, trophic structure, and top-down control. *Inland Waters* 10:197–211.
- Jewson D.H., 1977. Light penetration I relation to phytoplankton content of the euphotic zone of Lough Neagh, N. Ireland. *Oikos* 28:74–83.

- Jia, J., W. Luo, Y. Lu & J.P. Giesy, 2014. Bioaccumulation of microcystins (MCs) in four fish species from Lake Taihu, China: assessment of risks to humans. *Science of the Total Environment* 487:224–232.
- Jin, Y. & X. Zhao, 2021. The spatial dynamics of a zebra mussel model in river environments. *Discrete and Continuous Dynamical Systems Series B* 26:1991–2010.
- Jochimsen, E.M., W.W. Carmichael, J. An, D.M. Cardo, S.T. Cookson, C.E.M. Holmes, M. B. D.C. Antunes, D.A.D.M. Filho, T.M. Lyra, V.S.T. Barreto, S.M.F.O. Azevedo & W.R. Jarvis, 1998. Liver failure and death after exposure to microcystins at a hemodialysis center in Brazil. *The New England Journal of Medicine* 338:873–878.
- Jones, L.A. & A. Ricciardi, 2005. Influence of physiochemical factors on the distribution and biomass of invasive mussels (*Dreissena polymorpha* and *Dreissena bugensis*) in the St. Lawrence River. *Canadian Journal of Fisheries and Aquatic Sciences* 62:1953–1962.
- Jones, J.R., D.V. Obrecht, B.D. Perkins, M.F. Knowlton, A.P. Thorpe, S. Watanabe & R.R. Bacon, 2008. Nutrients, seston, and transparency of Missouri reservoirs and oxbow lakes: An analysis of regional limnology. *Lake and Reservoir Management* 24:155–180.
- Jones, J.R., M.F. Knowlton, D.V. Obrecht & J.L. Graham, 2011. Temperature and oxygen in Missouri reservoirs. *Lake and Reservoir Management* 27:173–182.
- Jost, J.A., E.N. Soltis, M.R. Moyer & S.S. Keshwani, 2015. Linking zebra mussel growth and survival with two cellular stress indicators during chronic temperature stress. *Invertebrate Biology* 134:189–202.
- Kaebnick, M., B.A. Neilan, T. Borner & E. Dittmann, 2000. Light and transcriptional response of the microcystin biosynthesis gene cluster. *Applied Environmental Microbiology* 66:3387–3392.
- Kankaanpää, H., P.J. Vuorinen, V. Sipia & M. Keinanen, 2002. Acute effects and bioaccumulation of nodularin in sea trout (*Salmo trutta* L.) exposed orally to *Nodularia spumigena* under laboratory conditions. *Aquatic Toxicology* 61:155–168.
- Karatayev, A.Y., L.E. Burlakova & D.K. Padilla, 1998. Physical factors that limit the distribution and abundance of *Dreissena polymorpha* (PALL.). *Journal of Shellfish Research* 17:1219–1235.
- Kim, T.Y., R.L. North, S.J. Guildford, P. Dillon & R.E.H. Smith, 2015. Phytoplankton productivity and size composition in Lake Simcoe: The nearshore shunt and the importance of autumnal production. *Journal of Great Lakes Research* 41:1075–1086.

- Kurmayer, R., G. Christiansen, J. Fastner & T. Börner, 2004. Abundance of active and inactive microcystin genotypes in populations of the toxic cyanobacterium *Planktothrix* spp. *Environmental Microbiology* 6:831–841.
- Lafreniere, M.J. & M.J. Sharp, 2005. A comparison of solute fluxes and sources from glacial and non-glacial catchments over contrasting melt seasons. *Hydrological Processes* 19:2991–3012.
- Lampert, W., W. Fleckner, H. Rai & B.E. Taylor, 1986. Phytoplankton control by grazing zooplankton: a study on the spring clear-water phase. *Limnology and Oceanography* 31:478–490.
- Larocque I., A. Mazumder, M. Proulx, D.R.S Lean & F.R. Pick, 1996. Sedimentation of algae: relationships with biomass and size distribution. *Canadian Journal of Fisheries and Aquatic Sciences* 53:1133–1142.
- Laspoumaderes, C., B. Modenutti, M. Sol Souza, M.B. Navarro, F. Cuassolo, & E. Balseiro, 2013. Glacier melting and stoichiometric implications for lake community structure: Zooplankton species distributions across a natural light gradient. *Global Change Biology* 19:316–326.
- Lavrentyev, P.J., W.S. Gardner, J.F. Cavaletto, & J.R. Beaver, 1995. Effects of the zebra mussel (*Dreissena polymorpha*) on protozoa and phytoplankton from Saginaw Bay, Lake Huron. *Journal of Great Lakes Research* 21:545–557.
- Lee, R.E., 2008. *Phycology*. Cambridge University Press, Cambridge, 547 pp.
- Lehman, J.T. & C.D. Sandgren, 1985. Species-specific rates of growth and grazing loss among freshwater algae. *Limnology and Oceanography* 30:34–46.
- Lei J., B.S. Payne & S.Y. Wang, 1996. Filtration dynamics of the zebra mussel, *Dreissena polymorpha*. *Canadian Journal of Fisheries and Aquatic Sciences* 53:29–37.
- Leibold, M.A., S.R. Hall, V.H. Smith & D.A. Lytle, 2017. Herbivory enhances the diversity of primary producers in pond ecosystems. *Ecology* 98:48–56.
- Lévesque, B., M. Gervais, P. Chevalier, D. Gauvis, E. Anassour-Laouan-Sidi, S. Gingras, N. Fortin, G. Brisson, C. Greer & D. Bird, 2014. Prospective study of acute health effects in relation to exposure of cyanobacteria. *Science of the Total Environment* 466/467:397–403.
- Lewandowski, I., I. Schauser & M. Hupfer, 2003. Long term effects of phosphorus precipitations with alum in hypereutrophic Lake Susser See (Germany). *Water Research* 33:3617–3627.
- Li, Y., J. Chen, Q. Zhao, C. Pu, Z. Qiu, R. Zhang & W. Shu, 2011. A cross-sectional investigation of chronic exposure to microcystin in relationship to childhood liver damage in the Three Gorges Reservoir Region, China. *Environmental Health Perspectives* 119:1483–1488.

- Liu, G., Y. Qian, S. Dai & N. Feng, 2008. Adsorption of microcystin LR and LW on suspended particulate matter (SPM) at different pH. *Water, Air, and Soil Pollution* 192:67–76.
- Litchman, E., C.A. Klausmeier, O.M. Schofield & P.G. Falkowski, 2007. The role of functional traits and trade-offs in structuring phytoplankton communities: scaling from cellular to ecosystem level. *Ecology Letters* 10:1170–1181.
- Liu, X., L. Chen, G. Zhang, J. Zhang, Y. Wu & H. Ju, 2021. Spatiotemporal dynamics of succession and growth limitation of phytoplankton for nutrients and light in a large shallow lake. *Water Research* 194:116910.
- Locklin, J.L., D.N. Corbitt & R.F. McMahon, 2020. Settlement, density, survival and shell growth of zebra mussels, *Dreissena polymorpha*, in a recently invaded low latitude, warm water Texas reservoir. *Aquatic Invasions* 15:408–434.
- Lockwood, J.L., M.F. Hoopes & M.P. Marchetti, 2013. *Invasion Ecology* 2<sup>nd</sup> Edition. Wiley-Blackwell, Chichester, UK, pp. 462.
- Lowe, R.L. & R.W. Pillsbury, 1995. Shifts in benthic algal community structure and function following the appearance of zebra mussels (*Dreissena polymorpha*) in Saginaw Bay, Lake Huron. *Journal of Great Lakes Research* 21:558–566.
- Ludwig, G.R., P. Perschbacher & R. Edziyie, 2008. The effect of the dye Aquashade® on water quality, phytoplankton, zooplankton, and sunshine bass, *Morone chrysops x M-saxatilis*, fingerling production in fertilized culture ponds. *Journal of the World Aquaculture Society* 41:40–48.
- Ludyanskiy M.L., D. McDonald, & D. MacNeill, 1993. Impact of the zebra mussel, a bivalve invader – *Dreissena polymorpha* is rapidly colonizing hard surfaces throughout waterways of the United States and Canada. *Bioscience* 43:533–544.
- Lürling, M. & Y. Tolman, 2010. Effects of lanthanum and lanthanum-modified clay on growth, survival and reproduction of *Daphnia magna*. *Water Research* 44:309–319.
- Lürling, M. & F. van Oosterhout, 2012. Case study on the efficacy of a lanthanum-enriched clay (Phoslock®) in controlling eutrophication in Lake Het Groene Eiland (The Netherlands). *Hydrobiologia* 710:253–263.
- Lürling, M. & Y. Tolman, 2014. Beating the blues: is there any music in fighting cyanobacteria with ultrasound? *Water Research* 66:361–373.
- Lürling, M., G. Waajen & L.N. de Senerpont Domis, 2016. Evaluation of several end-of-pipe measures proposed to control cyanobacteria. *Aquatic Ecology* 50:499–519.
- Lürling, M., & M. Mucci, 2020. Mitigating eutrophication nuisance: in-lake measures are becoming inevitable in eutrophic waters in the Netherlands. *Hydrobiologia* 847:4447–4467.
- Lürling, M., 2021. Grazing resistance in phytoplankton. *Hydrobiologia* 848:237–249.

- Maberly, S.C., L. King, M.M. Dent, R.I. Jones & C.E. Gibson, 2002. Nutrient limitation of phytoplankton and periphyton growth in upland lakes. *Freshwater Biology* 47:2136–2152.
- MacIsaac, H.J. & R. Rocha, 1995. Effects of suspended clay on zebra mussel (*Dreissena polymorpha*) faeces and pseudofaeces production. *Archiv für Hydrobiologie* 135:53–64.
- MacIsaac, H.J., 1996. Potential abiotic and biotic impacts of zebra mussels on the inland waters of North America. *American Zoologist* 36:287–299.
- Mackay, E.B., S.C. Maberly, G. Pan, K. Reitzel, A. Bruere, N. Corker, G. Douglas, S. Egemose, D. Hamilton, T. Hatton-Ellis, B. Huser, W. Li, S. Meis, B. Moss, M. Lürling, G. Phillips, S. Yasseri & B.M. Spears, 2014. Geoengineering in lakes: welcome attraction or fatal distraction? *Inland Waters* 4:349–356.
- MacKintosh, R.V., K.N. Dalby, D.G. Campbell, P.T. Cohen, P. Cohen & C. MacKintosh, 1995. The cyanobacterial toxin microcystin binds covalently to cysteine-273 on protein phosphatase-1. *FEBS Letters* 371:236–240.
- Madsen, J.D., K.D. Getsinger, R.M. Stewart, J.G. Skogerboe, D.R. Honnell & C.S. Owens, 1999. Evaluation of Transparency and Light Attenuation by Aquashade®. *Lake and Reservoir Management* 15:142–147.
- Madon, S.P., D.W. Schneider, J.A. Stoeckel & R.E. Sparks, 1998. Effects of inorganic sediment and food concentrations on energetic processes of the zebra mussel, *Dreissena polymorpha*: Implications for growth in turbid rivers. *Canadian Journal of Fisheries and Aquatic Sciences* 55:401–413.
- Mao, Z., X. Gu, Y. Cao, M. Zhang, Q. Zeng, H. Chen, R. Shen & E. Jeppesen, 2020. The role of top-down and bottom-up control for phytoplankton in a subtropical shallow eutrophic lake: evidence based on a long-term monitoring and modeling. *Ecosystems* 23:1449–1463.
- Martin, R.M., M. Moniruzzaman, G.F. Stark, E.R. Gann, D.S. Derminio, B. Wei, F.L. Hellweger, A. Pinto, G.L. Boyer & S.W. Wilhelm, 2020. Episodic decrease in temperature increases *mcy* gene transcription and cellular microcystin in continuous cultures of *Microcystis aeruginosa* PCC 7806. *Frontiers in Microbiology* 11:601864.
- Mathai, P.P., J.H. Bertram, S.K. Padhi, V. Singh, I.E. Tolo, A. Primus, S.K. Mor, N.B.D. Phelps & M.J. Sadowsky, 2020. Influence of environmental stressors on the microbiota of zebra mussels (*Dreissena polymorpha*). *Invertebrate Microbiology* 81:1042–1053.
- Mathews, M.A. & R.F. McMahon, 1999. Effects of temperature and temperature acclimation on survival of zebra mussels (*Dreissena polymorpha*) and Asian clams (*Corbicula fluminea*) under extreme hypoxia. *Journal of Molluscan Studies* 65:317–325.

- McCain, S., R.R. Sim, E.W. Howerth, S. Aschenbroich, S.G.M. Kirejczyk, B. McHale, C. Jerry, J.J. Kottwitz, A.E. Wilson & R. McManamon, 2020. Myonecrosis and death due to presumed microcystin toxicosis in American white pelicans (*Pelecanus erythrorhynchos*). *Journal of Zoo and Wildlife Medicine* 51:407–415.
- McMahon, R.E., M.A. Matthews, T.H. Ussery, R. Chase, & M. Clarke, 1994. Further studies of heat tolerance in zebra mussels: Effects of temperature acclimation and chronic exposure to lethal temperatures. In *Proceedings: Forth international zebra mussel conference '94*, pp. 251–272. Wisconsin Sea Grant Institute, Madison, Wisconsin.
- McMahon, R.F., 1996. The physiological ecology of the zebra mussel, *Dreissena polymorpha*, in North America and Europe. *Amer. Zool.* 36:339–363.
- McQueen, D.J., M.R.S. Johannes, J.R. Post, T.J. Stewart & D.R.S. Lean, 1989. Bottom-up and top-down impacts on freshwater pelagic community structure. *Ecological Monographs* 59:289–309.
- Mehnert, G., F. Leunert, S. Cirés, K.D. Jöhnk, J. Rucker, B. Nixdorf & C. Wiedner, 2010. Competitiveness of invasive and native cyanobacteria from temperate freshwaters under various light and temperature conditions. *Journal of Plankton Research* 32:1009–1021.
- Meis, S., B.M. Spears, S.C. Maberly, M.B. O'Malley & R.G. Perkins, 2012. Sediment amendment with Phoslock® in Clatto Reservoir (Dundee, UK): Investigating changes in sediment elemental composition and phosphorus fractionation. *Journal of Environmental Management* 93:185–193.
- Mikheev, V.P., 1964. Linear growth of *Dreissena polymorpha* Pallas in some reservoirs of the European USSR. *Trudy Instituta Biologii Vnutrennikh Vod Akademii Nauk SSSR* 7:55–65.
- Miller, M.J., M.M. Critchley, J. Hutson & H.J. Fallowfield, 2001. The adsorption of cyanobacterial hepatotoxins from water onto soil during batch experiments. *Water Research* 35:1461-1468.
- Miller, M.A., R.M. Kudela, A. Mekebri, D. Crane, S.C. Oates, M. T. Tinker, M. Staedler, W.A. Miller, S. Toy-Choutka, C. Dominik, D. Hardin, G. Langlois, M. Murry, K. Ward & D.A. Jessup, 2010. Evidence for a novel marine harmful algal bloom: cyanotoxin (microcystin) transfer from land to sea otters. *PLoS ONE* 5:e12576.
- Modenutti, B., G. Pérez, E. Balseiro & C. Queimalinos, 2000. The relationship between light attenuation, chlorophyll a and total suspended solids in a Southern Andes glacial lake. *Verhandlungen des Internationalen Verein Limnologie* 27:1–4.
- Mohamed, Z.A., H.M. El-Sharouny & W.S.M. Ali, 2007. Microcystin production in benthic mats of cyanobacteria in the Nile River and irrigation canals, Egypt. *Toxicon* 47:584–590.
- Morse, J.T., 2009. Thermal tolerance, physiological condition, and population genetics of dreissenid mussels (*Dreissena polymorpha* and *D. rostriformis bugensis*) relative

- to their invasion of waters in the Western United States. Dissertation, University of Texas at Arlington.
- Moore, R.D., S.W. Fleming, B. Menounos, R. Wheate, A. Fountain, K. Stahl, K. Holm & M. Jakob, 2009. Glacier change in western North America: Influences on hydrology, geomorphic hazards and water quality. *Hydrological Processes* 23:42–61.
- Mulvenna, V., K. Dale, B. Priestly, U. Mueller, A. Humpage, G. Shaw, G. Allinson & I. Falconer, 2012. Health risk assessment for cyanobacterial toxins in seafood. *International Journal of Environmental Research and Public Health* 9:807–820.
- Munusay, T., Y. Hu & J. Lee, 2012. Adsorption and photodegradation of microcystin-LR onto sediments collected from reservoirs and rivers in Taiwan: a laboratory study to investigate the fate, transfer, and degradation of microcystin-LR. *Environmental Science and Pollution Research* 19:2390–2399.
- Naselli-Flores, L., T. Zohary & J. Padisák, 2021. Life in suspension and its impact on phytoplankton morphology: an homage to Colin S. Reynolds. *Hydrobiologia* 848:7-30.
- Neumann, D., J. Borcharding, & B. Jantz, 1992. Growth and seasonal reproduction of *Dreissena polymorpha* in the Rhine River and adjacent waters. In T.E. Nalepa & D.W. Schloesser (eds.), *Zebra mussels: Biology, impacts, and control*, pp. 95–109. Lewis Publishers, CRC Press, Boca Raton, Florida.
- North, R.L., R.E.H. Smith, R.E. Hecky, D.C. Depew, L.F. León, M.N. Charlton & S.J. Guildford, 2012. Distribution of seston and nutrient concentrations in the eastern basin of Lake Erie pre- and post-dreissenid mussel invasion. *Journal of Great lakes Research* 38:463–476.
- North, R.L., D. Barton, A.S. Crowe, P.J. Dillon, R.M.L. Dolson, D.O. Evans, B.K. Ginn, L. Håkanson, J. Hawryshyn, H. Jarjanazi, J.W. King, J.K.L. La Rosa, L. León, C.F.M. Lewis, G.E. Liddle, Z.H. Lin, F.J. Longstaffe, R.A. Macdonald, L. Molot, T. Ozersky, M.E. Palmer, R. Quinlan, M.D. Rennie, M.M. Robillard, D. Rodé, K.M. Rühland, A. Schwalb, J.P. Smol, E. Stainsby, J.J. Trumpickas, J.G. Winter & J.D. Young, 2013. The state of Lake Simcoe (Ontario, Canada): The effects of multiple stressors on phosphorus and oxygen dynamics. *Inland Waters* 3:51–74.
- Noyma, N.P., L. de Magalhaes, L.L. Furtado, M. Mucci, F. van Oosterhout, V.L.M. Huszar, M.M. Marinho & M. Lürling, 2016. Controlling cyanobacterial blooms through effective flocculation and sedimentation with combined use of flocculants and phosphorus adsorbing natural soil and modified clay. *Water Research* 97:26–38.
- Nürnberg, G.K., 1988. Prediction of phosphorus release rates from total and reductant-soluble phosphorus in anoxic lake sediments. *Canadian Journal of Fisheries and Aquatic Sciences* 45:453–462.

- O’Neil, J.M., T.W. Davis, M.A. Burford & C.J. Gobler, 2012. The rise of harmful cyanobacteria blooms: The potential roles of eutrophication and climate change. *Harmful Algae* 14:313–334.
- Oh, H.M., S.J. Lee, M.H. Jang & B.D. Yoon, 2000. Microcystin production by *Microcystis aeruginosa* in a phosphorus-limited chemostat. *Applied Environmental Microbiology* 66:176–179.
- Ohio, 2010. Cooperative fish tissue monitoring program, State of Ohio, Sport Fish Tissue Consumption Advisory Program.
- Onyango, D.M., P.S. Orina, R.C. Ramkat, C. Kowenje, C.M. Githukia, D. Lusweti & H.B.O. Lung’aya, 2020. Review of current state of knowledge of microcystin and its impact on fish in Lake Victoria. *Lakes and Reservoirs* 25:350–361.
- Oregon Health Authority, 2015. Public health advisory guidelines harmful algae blooms in freshwater bodies.
- Orihel, D.M., D.W. Schindler, N.C. Ballard, M.D. Graham, D.W. O’Connell, L.R. Wilson & R.D. Vinebrooke, 2015. The “nutrient pump:” Iron-poor sediments fuel low nitrogen-to-phosphorus ratios and cyanobacterial blooms in polymictic lakes, 2015. *Limnology and Oceanography* 00:1–25.
- Orr, P.T. & G.J. Jones, 1998. Relationship between microcystin production and cell division rates in nitrogen-limited *Microcystis aeruginosa* cultures. *Limnology and Oceanography* 43:1604–1614.
- Öterler, B., 2017. Winter phytoplankton composition occurring in a temporarily ice-covered lake: a case study. *Polish Journal of Environmental Studies* 26:2677–2688.
- Ouellette-Plante, J., A.L. Morden, L.E. Johnson, A.L. Martel & A. Ricciardi, 2017. Acclimation by invasive mussels: spatiotemporal variation in phenotypic response to turbidity. *Freshwater Science* 36:325–337.
- Ozersky, T., D.O. Evans & D.R. Barton, 2012. Invasive mussels alter the littoral food web of a large lake: stable isotopes reveal drastic shifts in sources and flow of energy. *PlosOne* 7:e51249.
- Ozersky, T., D.R. Barton, R.E. Hecky & S.J. Guildford, 2013. Dreissenid mussels enhance nutrient efflux, periphyton quantity and production in the shallow littoral zone of a large lake. *Biological Invasions* 15:2799–2810.
- Pacheco, C.H.A. & I.E. Lima Neto, 2017. Effect of artificial circulation on the removal kinetics of cyanobacteria in a hypereutrophic shallow lake. *Journal of Environmental Engineering* 143:06017010.
- Padisák, 1992. Seasonal succession of phytoplankton in a large shallow lake (Balaton, Hungary) – a dynamic approach to ecological memory, its possible role and mechanisms. *Journal of Ecology* 80:217–230.
- Paerl, H.W. & J. Huisman, 2008. Blooms like it hot. *Science* 320:57–58.

- Paerl, H.W. & J. Huisman, 2009. Climate change: A catalyst for global expansion of harmful cyanobacterial blooms. *Environmental Microbiology Reports* 1:27–37.
- Paerl, H.W. & V.J. Paul, 2012. Climate change: Links to global expansion of harmful cyanobacteria. *Water Research* 46:1349–1363.
- Pan, G., H. Zou, H. Chen & X. Yuan, 2006. Removal of harmful cyanobacterial blooms in Taihu Lake using local soils III. Factors affecting the removal efficiency and an in situ field experiment using chitosan-modified local soils. *Environmental Pollution* 141:206–212.
- Pan, C., L. Zhang, X. Meng, H. Qin, Z. Xiang, W. Gong, W. Luo, D. Li & X. Han, 2021. Chronic exposure to microcystin-LR increases the risk of prostate cancer and induces malignant transformation of human prostate epithelial cells. *Chemosphere* 263:128295.
- Pančić, M. & T. KiØrboe, 2018. Phytoplankton defense mechanisms: traits and trade-offs. *Biological Reviews* 93:1269–1303.
- Park, H., C. Iwami, M.F. Watanabe, K. Harada, T. Okino & H. Hayashi, 1998. Temporal variabilities of the concentrations of intra- and extracellular microcystin and toxic *Microcystis* species in a hypertrophic lake, Lake Suwa, Japan (1991–1994). *Environmental Toxicology* 13:61–72.
- Park, J., J. Church, Y. Son, K.T. Kim, W.H. Lee, 2017. Recent advances in ultrasonic treatment: challenges and field applications for controlling harmful algal blooms (HABs). *Ultrasonics Sonochemistry* 38:326–334.
- Payne, B.S., A.C. Miller, E.D. Hubertz & J. Lei, 1995. Adaptive variation in palp and gill size of the zebra mussel (*Dreissena polymorpha*) and Asian clam (*Corbicula fluminea*). *Canadian Journal of Fisheries and Aquatic Sciences*. 52:1130–1134.
- Phelan, R.R. & T.G. Downing, 2011. A growth advantage for microcystin production by *Microcystis* PCC7806 under high light. *Journal of Phycology* 47:1241–1246.
- Phull, S.S., A.P. Newman, J.P. Lorimer, B. Pollet & T.J. Mason, 1997. The development and evaluation of ultrasound in the biocidal treatment of water. *Ultrasonics Sonochemistry* 4:157–164.
- Piesik, Z., 1983. Biology of *Dreissena polymorpha* (Pall.) settling on stylon nets and the role of this mollusc in eliminating the seston and the nutrients from the water course. *Polskie Archiwum Hydrobiologii* 30:353–361.
- Pilgram, K.M. & P.L. Brezonik, 2005. Treatment of lake inflows with alum for phosphorus removal. *Lake and Reservoir Management* 21:1–9.
- Pilotto, L.S., R.M. Douglas, M.D. Burch, S. Cameron, M. Beers, G.J. Rouch, P. Robinson, M. Kirk, C.T. Cowie, S. Hardiman, C. Moore & R.G. Attwell, 1997. Health effects of exposure to cyanobacteria (blue-green algae) during recreational water-related activities. *Australian and New Zealand Journal of Public Health* 21:562–566.

- Pimentel, D., R. Zuniga & D. Morrison, 2005. Update on the environmental and economic costs associated with alien-invasive species in the United States. *Ecological Economics* 52:273–288.
- Perrault, J.R., C.R. Perkins, M.J. Ajemian, M.J. Bresette, C.R. Mott & A. Page-Karjian, 2020. Harmful algal and cyanobacterial toxins in foraging green turtles (*Chelonia mydas*) in Florida's Big Bend. *Toxicon*: X 5:100020.
- Petsch, D.K., L.G. Ribas, T. Mantovano, M.M. Pulzatto, A.T. Alves, G.D. Pinha & S.M. Thomaz, 2020. Invasive potential of golden and zebra mussels in present and future climatic scenarios in the new world. *Hydrobiologia* 848:2319–2330.
- Petty, E.L., D.V. Obrecht & R.L. North, 2020. Filling in the flyover zone: high phosphorus in Midwestern (USA) reservoirs results in high phytoplankton biomass but not high primary productivity. *Frontiers in Environmental Science* 8:11.
- Poste, A.E., R.E. Hecky & S.J. Guildford, 2011. Evaluating microcystin exposure risk through fish consumption. *Environmental Science and Technology* 45:5806–5811.
- Poste, A.E. & T. Ozersky, 2013. Invasive dreissenid mussels and round gobies: a benthic pathway for the trophic transfer of microcystin. *Environmental Toxicology and Chemistry* 32:2159–2164.
- Preece, E.P., W. Hobbs, F.J. Hardy, L. O'Garro, E. Frame & F. Sweeny, 2021. Prevalence and persistence of microcystin in shoreline lake sediments and porewater, and associated potential for human health risk. *Chemosphere* 272:129581.
- Prieto, A.I., A. Jos, S. Pichardo, I. Moreno & A.M. Cameán, 2006. Differential oxidative stress responses to microcystins LR and RR in intraperitoneally exposed tilapia fish (*Oreochromis* sp.). *Aquatic Toxicology* 77:314–321.
- Rajagopal, S., G. Van der Velde & H.A. Jenner, 1997. Response of zebra mussel, *Dreissena polymorpha*, to elevated temperatures in the Netherlands. In: F.M. D'Itri (ed.), *Zebra mussels and aquatic nuisance species*. Ann Arbor Press, Chelsea. pp 257–273.
- Rampe, E.B., B. Horgan, N. Scudder, R.J. Smith & A.M. Rutledge, 2017. Mineralogy of rock flour in glaciated volcanic terrains: An analog for a cold and icy early Mars. NASA Technical Report JSC-CN-38727.
- Ransibrahmanakul, V., S.J. Pittman, D.E. Pirhalla, S.C. Sheridan, C.C. Lee, B.B. Barnes, C. Hu & K. Shein, 2018. Linking weather patterns, water quality and invasive mussel distributions in the development and application of a water clarity index for the Great Lakes. 38th Annual IEEE International Geoscience and Remote Sensing Symposium, pp. 120–123.
- Rantala, A., P. Rajaniemi-Wacklin, C. Lyra, L. Lepistö, J. Rintala, J. Mankiewicz-Boczek & K. Sivonen, 2006. Detection of microcystin-producing cyanobacteria in

- Finnish lakes with genus-specific microcystin synthetase gene E (*mcyE*) PCR and associations with environmental factors. *Applied and Environmental Microbiology* 72:6101–6110.
- Reeders, H.H., & A. Bij de Vaate, 1990. Zebra mussels (*Dreissena polymorpha*): a new perspective for water quality management. *Hydrobiologia* 200/201:437–450.
- Reid, A.J., A.K. Carlson, I.F. Creed, E.J. Eliason, P.A. Gell, P.T.J. Johnson, K.A. Kidd, T.J. MacCormack, J.D. Olden, S.J. Ormerod, J.P. Smol, W.W. Taylor, K. Tockner, J.C. Vermaire, D. Dudgeon & S.J. Cooke, 2019. Emerging threats and persistent conservation challenges for freshwater biodiversity. *Biological Reviews* 94:849–873.
- Reitzel, K., F.Ø. Andersen, S. Egemose & H.S. Jensen, 2013. Phosphate adsorption by lanthanum modified bentonite clay in fresh and brackish water. *Water Research* 47:2787–2796.
- Ressom, R., F.S. Soong, J. Fitzgerald, L. Turczynowicz, O. El Saadi, D. Roder, T. Maynard & I. Falconer, 1994. Health effects of toxic cyanobacteria (blue-green algae). National Health and Medical Research Council, Canberra, Australia.
- Reynolds, C.S., 1987. The response of phytoplankton communities to changing lake environments. *Aquatic Sciences* 49:220–236.
- Rhee, G.Y. & I.J. Gotham, 1981. The effect of environmental factors on phytoplankton growth: Light and the interactions of light with nitrate limitation. *Limnology and Oceanography* 26:649–659.
- Richardson, K., 1997. Harmful or exceptional phytoplankton blooms in the marine ecosystem. *Advances in Marine Biology* 31:301–385.
- Robarts, R.D. & T. Zohary, 1984. *Microcystis aeruginosa* and underwater light attenuation in a hypereutrophic lake (Hartbeespoort Dam, South Africa). *Journal of Ecology* 72:1001–1017.
- Robarts, R.D. & T. Zohary, 1987. Temperature effects on photosynthetic capacity, respiration, and growth rates of bloom-forming cyanobacteria. *New Zealand Journal of Marine and Freshwater Research* 21:391–399.
- Rogers, T.L., S.B. Munch, S.D. Stewart, E.P. Palkovacs, A. Giron-Nava, S.S. Matsuzaki & C.C. Symons, 2020. Trophic control changes with season and nutrient loading in lakes. *Ecology Letters* 23: 1287–1297.
- Rönicke, H., M.A. Frassl, K. Rinke, J. Tittel, M. Beyer, B. Kormann, F. Gohr & M. Schultze, 2021. Suppression of bloom-forming colonial cyanobacteria by phosphate precipitation: a 30 years case study in Lake Barleber (Germany). *Ecological Engineering* 162:106171.
- Rose, K.C., D.P. Hamilton, C.E. Williamson, C.G. McBride, J.M. Fischer, M.H. Olson, J.E. Saros, M.G. Allan & N. Cabrol, 2014. Light attenuation characteristics of glacially-fed lakes. *Journal of Geophysical Research: Biogeosciences* 119:1446–1457.

- Sakharova, E.G., A.V. Krylov, V.G. Petrosyan, D.G. Seleznev, I. Kostshevska-Shlakovska, I.Y. Feniova, M. Rzepecki & N.S. Zilitinkevich, 2018. Experimental study of the effects of bivalve *Dreissena polymorpha* on phytoplankton under eutrophic conditions. *Russian Journal of Ecology* 49:428–433.
- Sagrane, S. & B. Oudra, 2009. CyanoHAB occurrence and water irrigation cyanotoxin contamination: Ecological impacts and potential health risks. *Toxins* 1:113–122.
- Sarnelle O., 1999. Zooplankton effects on vertical particulate flux: testable models and experimental results. *Limnology and Oceanography*. 44:357–70.
- Saros, J.E., K.C. Rose, D.W. Clow, V.C. Stephensm A.B. Nurse, H.A. Arnett, J.R. Stone, C.E. Williamson & A.P. Wolfe, 2010. Melting alpine glaciers enrich high-elevation lakes with reactive nitrogen. *Environmental Science and Technology* 44:4891–4896.
- Scheffer, M., S. Carpenter, J.M. Foley, C. Folke & B. Walker, 2001. Catastrophic shifts in ecosystems. *Nature* 413:591–596.
- Scherer, P.I., U. Raeder, J. Geist & K. Zwirgmaier, 2017. Influence of temperature, mixing, and addition of microcystin-LR on microcystin gene expression in *Microcystis aeruginosa*. *Microbiology* 6:e00393.
- Schindler, D.W., 1974. Eutrophication and recovery in experimental lakes: Implications for lake management. *Science* 184:897–899.
- Schloesser, D.W. & W.P. Kovalak, 1991. Infestation of native unionids by *Dreissena polymorpha* in a power plant intake canal in Lake Erie. *Journal of Shellfish Research* 10:355–359.
- Schmidt, J.R., M. Shaskus, J.F. Estenik, C. Oesch, R. Khidekel & G. Boyer, 2013. Variations in the microcystin content of different fish species collected from a eutrophic lake. *Toxins* 5:992–1009.
- Schmidt, J.R., S.W. Wilhelm & G.L. Boyer, 2014. The fate of microcystins in the environment and challenges for monitoring. *Toxins* 6:3354–3387.
- Schneider, D.W., S.P. Madon, J.A. Stoeckel & R.E. Sparks, 1998. Seston quality controls zebra mussel (*Dreissena polymorpha*) energetics in turbid rivers. *Oecologia* 117:331–341.
- Schuler, M.S., W.D. Hintz, D.K. Jones, B.M. Mattes, A.B. Stoler & R.A. Relyea, 2020. The effects of nutrient enrichment and invasive mollusks on freshwater environments. *Freshwater Ecology* 11: e03196.
- Schwalb, A.N., D. Bouffard, T. Ozersky, L. Boegman & R.E.H. Smith, 2013. Impacts of hydrodynamics and benthic communities on phytoplankton distributions in a large, dreissenid-colonized lake (Lake Simcoe, Ontario, Canada). *Inland Waters* 3:269–284.
- Settele, J., R. Scholes, R. Betts, S. Bunn, P. Leadley, D. Nepstad, J.T. Overpeck, & M.A. Taboada, 2014. Terrestrial and inland water systems. In B. Field, V.R. Barros,

- D.J. Dokken, K.J. Mach, M.D. Mastrandrea, T.E. Bilir, M. Chatterjee, K.L. Ebi, Y.O. Estrada, R.C. Genova, B. Girma, E.S. Kissel, A.N. Levy, S. MacCracken, P. R. Mastrandrea & L.L. White (eds.), *Climate Change 2014: Impacts, Adaptation, and Vulnerability. Part A: Global and Sectoral Aspects*. pp. 271–359. Contribution of Working Group II to the Fifth Assessment Report of the Intergovernmental Panel on Climate Change, Cambridge University Press, Cambridge, UK.
- Shi, L., W.W. Carmichael & I. Miller, 1995. Immuno-gold localization of hepatotoxins in cyanobacterial cells. *Archives of Microbiology* 163:7–15.
- Shin, J., S. Yoon, Y. Kim, T. Kim, B. Go & Y. Cha, 2021. Effects of class imbalance on resampling and ensemble learning for improved predication of cyanobacterial blooms. *Ecological Informatics* 61:101201.
- Sieroslawska, A., A. Rymuszka, J. Velisek, B. Pawlik-Skowrońska, Z. Svobodova & T. Skowroński, 2012. Effects of microcystin-containing cyanobacterial extract on hematological and biochemical parameters of common carp (*Cyprinus carpio* L.). *Fish Physiology and Biochemistry* 38:1159–1167.
- Sivonen, K., 1990. Effects of light, temperature, nitrate, orthophosphate, and bacteria on growth of and hepatotoxin production by *Oscillatoria agardhii* strains. *Applied Environmental Microbiology* 56:2658–2666.
- Slemmons, K.E.H. & J.E. Saros, 2012. Implications of nitrogen-rich glacial meltwater for phytoplankton diversity and productivity in alpine lakes. *Limnology and Oceanography* 57:1651–1663.
- Smayda, T.J., 1997. What is a bloom? A commentary. *Limnology and Oceanography* 42:1132–1136.
- Smith, V.H., 1983. Low nitrogen to phosphorus ratios favor dominance by blue-green algae in lake phytoplankton. *Science* 12:669–671.
- Smith, T.E., R.J. Stevenson, N.F. Caraco & J.J. Cole, 1998. Changes in phytoplankton community structure during the zebra mussel (*Dreissena polymorpha*) invasion of the Hudson River (New York). *Journal of Plankton Research* 20:1567–1579.
- Smith, J.L. & J.F. Haney, 2006. Foodweb transfer, accumulation, and depuration of microcystins, a cyanobacterial toxin, in pumpkinseed sunfish (*Lepomis gibbosus*). *Toxicon* 48:580–589.
- Smith, J.L., K.L. Schulz, P.V. Zimba & G.L. Boyer, 2010. Possible mechanism for the foodweb transfer of covalently bound microcystins. *Ecotoxicology and Environmental Safety* 73:757–761.
- Sommaruga, R., R. Psenner, E. Schafferer, K.A. Koinig & S. Sommaruga-Wögrath, 1999. Dissolved organic carbon concentration and phytoplankton biomass in high-mountain lakes of the Austrian Alps: potential effect of climatic warming on UV underwater attenuation. *Arctic, Antarctic, and Alpine Research* 31:247–253.

- Sommaruga, R., 2015. When glaciers and ice sheets melt: consequences for planktonic organisms. *Journal of Plankton Research* 37:509–518.
- Sommer, U. & F. Sommer, 2006. Cladocerans versus copepods: the cause of contrasting top-down controls on freshwater and marine phytoplankton. *Oecologia* 147:183–194.
- Sommer, U., E. Charalampous, S. Genitsaris & M. Moustaka-Gouni, 2017. Benefits, costs and taxonomic distribution of marine phytoplankton body size. *Journal of Plankton Research* 39:494–508.
- Song, L., W. Chen, L. Peng, N. Wan, N. Gan & X. Zhang, 2007. Distribution and bioaccumulation of microcystins in water columns; A systematic investigation into the environmental fate and risks associated with microcystins in Meiliang Bay, Lake Taihu. *Water Research* 41:2853v2864.
- Song, H., L.X. Coggins, E.S. Reichwaldt & A. Ghadouani, 2015. The importance of lake sediments as a pathway for microcystin dynamics in shallow eutrophic lakes. *Toxins* 7:900–918.
- Spears, B.M., M. Lüring, S. Yasserli, A.T. Castro-Castellon, M. Gibbs, S. Meis, C. McDonald, J. McIntosh, D. Sleep & F. van Oosterhout, 2013. Lake responses following lanthanum-modified bentonite clay (Phosplock®) application: An analysis of water column lanthanum data from 16 case study lakes. *Water Research* 47:5930–5942.
- Spencer, D.F., 1984. Influence of Aquashade® on growth, photosynthesis, and phosphorus uptake of microalgae. *Journal of Aquatic Plant Management* 22:80–84.
- Spidle, A.P., E.L. Mills & B. May, 1995. Limits to tolerance of temperature and salinity in the quagga mussel (*Dreissena bugensis*) and the zebra mussel (*Dreissena polymorpha*). *Canadian Journal of Fisheries and Aquatic Sciences* 52:2108–2119.
- Sprung, M., 1987. Ecological requirements for developing *Dreissena polymorpha* eggs. *Archiv fur Hydrobiologie Supplements* 79:69–86.
- Stewart, I., P.M. Webb, P.J. Schluter & G.R. Shaw, 2006. Recreational and occupational field exposure to freshwater cyanobacteria – a review of anecdotal and case reports, epidemiologic studies, and the challenges for epidemiologic assessment. *Environmental Health* 5:6.
- Strayer, D.L., 2009. Twenty years of zebra mussels: Lessons from the mollusk that made headlines. *Frontiers in Ecology and the Environment* 7:135–141.
- Strayer, D.L., B.V. Adamovich, R. Adrian, D.C. Aldridge, C. Balogh, L.E. Burlakova, H.B. Fried-Petersen, L.G. Tóth, A.L. Hetherington, T.S. Jones, A.Y. Karatayev, J.B. Madill, O.A. Makarevich, J.E. Marsden, A.L. Martel, D. Minchin, T.F. Nalepa, R. Noordhus, T.J. Robinson, L.G. Rudstam, A.N. Schwalb, D.R. Smith, A.D. Steinman & J.M. Jeschke, 2019. Long-term population dynamics of

- dreissenid mussels (*Dreissena polymorpha* and *D. rostriformis*): A cross-system analysis. *Ecosphere* 10:e02701.
- Sukenik, A., A. Quesada & N. Salmaso, 2015. Global expansion of toxic and non-toxic cyanobacteria: effect on ecosystem funding. *Biodiversity and Conservation* 24:889–908.
- Summers, R.B., J.H. Thorp, J.E. Alexander Jr. & R.D. Fell, 1996. Respiratory adjustment of dreissenid mussels (*Dreissena polymorpha* and *Dreissena bugensis*) in response to chronic turbidity. *Canadian Journal of Fisheries and Aquatic Sciences* 53:1626–1631.
- Suski, J.G., C.M. Swan, C.J. Salice & C.F. Wahl, 2018. Effects of pond management on biodiversity patterns and community structure of zooplankton in urban environments. *Science of the Total Environment* 619-620:1441–1450.
- Suzuki, Y., & M. Takahashi, 1995. Growth responses of several diatom species isolated from various environments to temperature. *Journal of Phycology* 31:880–888.
- Tang, X., L.E. Krausfeldt, K. Shao, G.R. LeClerc, J.M.A. Stough, G. Gao, G.L. Boyer, Y. Zhang, H.W. Paerl, B. Qin & S.W. Wilhelm, 2018. Seasonal gene expression and the ecophysiological implications of toxic *Microcystis aeruginosa* blooms in Lake Taihu. *Environmental Science and Technology* 52:11049–11059.
- Tencalla, F. & D. Dietrich, 1997. Biochemical characterization of microcystin toxicity in rainbow trout (*Oncorhynchus mykiss*). *Toxicol* 35:583–595.
- Testai, E., F.M. Burati, E. Funari, M. Manganelli, S. Vichi, N. Arnich, R. Biré, V. Fessard & A. Sialehaamo, 2016. Review and analysis of occurrence, exposure and toxicity of cyanobacteria toxins in food. *EFSA Supporting Publications* 13:998E.
- Tett, P., 1987. The ecophysiology of exceptional blooms. *Rapport et Proces-verbaux des Reunions Conseil international pour l'Exploration de la Mer* 187:47–60.
- Thies, H., U. Nickus, V. Mair, R. Tessadri, D. Tait, B. Thaler & R. Psenner, 2007. Unexpected response of high alpine lake waters to climate warming. *Environmental Science and Technology* 41:7424–7429.
- Thorp, J.H., J.E. Alexander, Jr., B.L. Bukaveckas, G.A. Cobbs & K.L. Bresko, 1998. Responses of Ohio River and Lake Erie dreissenid molluscs to changes in temperature and turbidity. *Canadian Journal of Fisheries and Aquatic Sciences* 55:220–229.
- Tomioka, N., A. Imai, & K. Komatsu, 2011. Effect of light availability on *Microcystis aeruginosa* blooms in shallow hypereutrophic Lake Kasumigaura. *Journal of Plankton Research* 33:1263–1273.
- Tønno, I., H. Agasild, T. Kõiv, R. Freiberg, P. Nõges & T. Nõges, 2016. Algal diet of small-bodied crustacean zooplankton in a cyanobacteria-dominated eutrophic lake. *PLoS ONE* 11:e0154526.

- Toporowska, M., B. Pawlik-Skowrońska & R. Kalinowska, 2014. Accumulation and effects of cyanobacterial microcystins and anatoxin-a on benthic larvae of *Chironomus* spp. (Diptera: Chironomidae). *European Journal of Entomology* 111:83–90.
- Trainer, V.L. & F.J. Hardy, 2015. Integrative monitoring of marine and freshwater harmful algae in Washington State for public health protection. *Toxins* 7:1206–1234.
- Tucker, C.S. & C.C. Mischke, 2019. The pond dye, Aquashade, does not prevent cyanobacterial off-flavors in pond-grown channel catfish. *North American Journal of Aquaculture* 82:101–107.
- Tuttle-Raycraft, S., T.J. Morris & J.D. Ackerman, 2017. Suspended solid concentration reduces feeding in freshwater mussels. *Science of the Total Environment* 598:1160–1168.
- US EPA, 2015. Drinking water health advisory for the cyanobacterial microcystin toxins. United States Environmental Protection Agency, Washington DC.
- US EPA, 2019. Recommended human health recreational ambient water quality criteria or swimming advisories for microcystins and cylindrospermopsin. United States Environmental Protection Agency, Washington DC.
- Utkilen, H.C., R.L. Oliver & A.E. Walsby, 1985. Buoyancy regulation in a red *Oscillatoria* unable to collapse gas vacuoles by turgor pressure. *Archiv für Hydrobiologie* 102:319–329.
- Utkilen, H. & N. Gjølme, 1992. Toxin production by *Microcystis aeruginosa* as a function of light in continuous cultures and its ecological significance. *Applied Environmental Microbiology* 58:1321–1325.
- Van Donk, E., A. Ianora & M. Vos, 2011. Induced defences in marine and freshwater phytoplankton: a review. *Hydrobiologia* 668:3–19.
- Van Halderen, A., W.R. Harding, J.C. Wessels, D.J. Schneider, E.W.P. Heine, J. Van Der Merwe & J.M. Fourie, 1995. Cyanobacterial (blue-green algae) poisoning of livestock in the Western Cape Province of South Africa. *Journal of the South African Veterinary Association* 66:260–264.
- van Liere, L., L.R. Mur, C.E. Gibson & M. Herdman, 1979. Growth and physiology of *Oscillatoria agardhii* and some related species, a survey. *Hypereutrophic Ecosystems* 2:67–77.
- van Oosterhout, F. & M. Lürling, 2011. Effects of the novel ‘Flock & Lock’ lake restoration technique on *Daphnia* in Lake Rauwbraken (The Netherlands). *Journal of Plankton Research* 33:255–263.
- van Oosterhout, F. & M. Lürling, 2013. The effect of phosphorus binding clay (Phoslock®) in mitigating cyanobacterial nuisance: a laboratory study on the effects on water quality variables and plankton. *Hydrobiologia* 710:265–277.

- Vanderbush, B., C. Longhenry, D.O. Luccesi & M.E. Barnes, 2021. A review of zebra mussel biology, distribution, aquatic ecosystem impacts, and control with specific emphasis on South Dakota, USA. *Open Journal of Ecology* 11:163–182.
- Vanderploeg, H.A., J.R. Liebig, W.W. Carmichael, M.A. Agy, T.H. Johengen, G.L. Fahnenstiel & T.F. Nalepa, 2001. Zebra mussel (*Dreissena polymorpha*) selective filtration promoted toxic *Microcystis* blooms in Saginaw Bay (Lake Huron) and Lake Erie. *Canadian Journal of Fisheries and Aquatic Sciences* 58:1208–1221.
- Vanderploeg H.A., O. Sarnelle, J.R. Liebig, N.R. Morehead, S.D. Robinson, T.H. Johengen & G.P. Horst, 2017. Seston quality drives feeding, stoichiometry and excretion of zebra mussels. *Freshwater Biology* 62:664–680.
- Vanni, M.J., 2002. Nutrient cycling by animals in freshwater ecosystems. *Annual Review of Ecology and Systematics* 33:341–370.
- Vanni, M.J., 2021. Invasive mussels regulate nutrient cycling in the largest freshwater ecosystem on Earth. *PNAS* 118: e2100275118.
- Vant, V.N. & R.J. Davies-Colley, 1984. Factors affecting clarity of New Zealand lakes. *New Zealand Journal of Marine and Freshwater Research* 18:367–377.
- Verspagen, J.M.H., E.O.F.M. Snelder, P.M. Visser, J. Huisman, L.R. Mur & B.W. Ibelings, 2004. Recruitment of benthic *Microcystis* (Cyanophyceae) to the water column: Internal buoyancy changes or resuspension? *Journal of Phycology* 40:260–270.
- Vinogradov, G.A., N.F. Smirnova, V.A. Sokova & A.A. Bruznitsky, 1992. Influence of chemical composition of the water on the mollusk *Dreissena polymorpha*. In T.F. Nalepa and D.W. Schloesser (eds.), *Zebra mussels: Biology, impacts, and control*. Lewis Publishers, CRC Press, Boca Raton, FL. 283–293 pp.
- Visser P.M., B.W. Ibelings, B. Vanderveer, J. Koedood & L.R. Mur, 1996. Artificial mixing prevents nuisance blooms of the cyanobacterium *Microcystis* in Lake Nieuwe Meer, the Netherlands. *Freshwater Biology* 2:435–450.
- Vörösmarty, C.J., C. Pahl-Wostl, S.E. Bunn & R. Lawford, 2013. Global water, the Anthropocene and the transformation of a science. *Current Opinion in Environmental Sustainability* 5:539–550.
- Vuorio, K., M. Järvinen, & N. Kotamäki, 2020. Phosphorus thresholds for bloom-forming cyanobacterial taxa in boreal lakes. *Hydrobiologia* 847: 4389–4400.
- Waajen, G., F. van Oosterhout, G. Douglas & M. Lürling, 2016a. Management of eutrophication in Lake De Kuil (The Netherlands) using combined flocculant – Lanthanum modified bentonite treatment. *Water Research* 97:83–95.
- Waajen, G., F. van Oosterhout, G. Douglas, M. Lürling, 2016b. Geo-engineering experiments in two urban ponds to control eutrophication. *Water Research* 97:60–82.

- Wagner, K.J., D. Meringolo, D.F. Mitchell, E. Moran & S. Smith, 2017. Aluminum treatments to control internal phosphorus loading in lakes on Cape Cod, Massachusetts. *Lake and Reservoir Management* 33:171–186.
- Walker, S.R., J.C. Lund, D.G. Schumacher, P.A. Brakhage, B.C. McManus, J.D. Miller, M.M. Augustine, J.J. Carney, R.S. Holland, K.D. Hoagland, J.C. Holz, T.M. Barrow, D.C. Rundquist & A.A. Gitelson, 2008. Nebraska experience. *Advances in Experimental Medicine and Biology* 619:139–152.
- Wallace, B.B. & D.P. Hamilton, 1999. The effect of variations in irradiance on buoyancy regulation in *Microcystis aeruginosa*. *Limnology and Oceanography* 44:272–281.
- Wallace, B.B. & D.P. Hamilton, 2000. Simulation of water-bloom formation in the cyanobacterium *Microcystis aeruginosa*. *Journal of Plankton Research* 22:1127–1138.
- Walz, N., 1973. Studies on the biology of *Dreissena polymorpha* in the Lake of Constance. *Archiv fur Hydrobiologie, Supplement* 42:452–482.
- Walz, N. 1978. The energy balance of the freshwater mussel *Dreissena polymorpha* Pallas in laboratory experiments and in Lake Constance. *Archiv fur Hydrobiologie* 55:121–141.
- Wantanabe, M.F., K. Tsuji, Y. Wantanabe, K. Harada & M. Suzuki, 1992. Release of heptapeptide toxin (microcystin) during the decomposition process of *Microcystis aeruginosa*. *Natural Toxins* 1:48–53.
- Watanabe, M.F. & S. Oishi, 1985. Effects of environmental factors on toxicity of a cyanobacterium (*Microcystis aeruginosa*) under culture conditions. *Applied Environmental Microbiology* 49:1342–1344.
- Watson, S.B. & G.L. Boyer, 2013. Harmful and Nuisance Algae. IJC Working Group (Ed.), Technical report on ecosystem indicators assessment of progress towards restoring the Great Lakes, International Joint Commission.
- Ward, J.M. & A. Ricciardi, 2007. Impacts of *Dreissena* invasions on benthic macroinvertebrate communities: a meta-analysis. *Diversity and Distributions* 13:155–65.
- Wei, Y., W. Yang, T.W. Simon, K. Lu, H. Zhang, J. Wang & J. Zhu, 2018. Selective control of cyanobacteria by a combined method of sonication and modified clay: an enclosure study. *Fundamental and Applied Limnology* 191:199–212.
- Wells, M.L., V.L. Trainer, T.J. Smayda, B.S.O. Karlson, C.G. Trick, R.M. Kudela, A. Ishikawa, S. Bernard, A. Wulff, D.M. Anderson & W.P. Cochlan, 2015. Harmful algal blooms and climate change: learning from the past and present to forecast the future. *Harmful Algae* 49:68–93.
- Wen, Z., K. Song, Y. Shang, L. Lyu, Q. Yang, C. Fang, J. Du, S. Li, G. Liu, B. Zhang & S. Cheng, 2020. Variability of chlorophyll and the influence factors during winter in seasonally ice-covered lakes. *Journal of Environmental Management* 267:111338.

- Wetzel, R.G., 2001. Limnology: Lake and River Ecosystems. Academic Press, San Diego, 1006 pp.
- White, J.D., S.K. Hamilton & O. Sarnelle, 2015. Heat-induced mass mortality of invasive zebra mussels (*Dreissena polymorpha*) at sublethal water temperatures. *Canadian Journal of Fisheries and Aquatic Sciences* 72: 1221–1229.
- Whittier, T.R., P.L. Ringold, A.T. Herlihy & S.M. Pierson, 2008. A calcium-based invasion risk assessment for zebra and quagga mussels (*Dreissena* spp). *Frontiers in Ecology and the Environment* 6:180–184.
- Wiśniewski, R., 1990. Shoals of *Dreissena polymorpha* as bio-processor of seston. *Hydrobiologia* 200/201:451–458.
- World Health Organization (WHO), 2006. Guidelines for drinking-water quality, third edition, incorporating first addendum. [http://www.who.int/water\\_sanitation\\_health/dwq/gdwq3rev/en/index.html](http://www.who.int/water_sanitation_health/dwq/gdwq3rev/en/index.html).
- Wiedner, C., P.M. Visser, J. Fastner, J.S. Metcalf, G.A. Codd & L.R. Mur, 2003. Effects of light on the microcystin content of *Microcystis* strain PCC 7806. *Applied Environmental Microbiology* 69:1475–1481.
- Wiśniewski, R., 1990. Shoals of *Dreissena polymorpha* as bio-processor of seston. *Hydrobiologia* 200/201:451–458.
- Wojtal-Frankiewicz, A., J. Bernasińska, P. Frankiewicz, K. Gwoździński & T. Jurczak, 2017. The role of environmental factors in the induction of oxidative stress in zebra mussel (*Dreissena polymorpha*). *Aquatic Ecology* 51:289–306.
- Woller-Skar, M.M., D.N. Jones, M.R. Luttenton & A.L. Russell, 2015. Microcystin detected in little brown bats (*Myotis lucifugus*). *American Midland Naturalist* 174:331–334.
- Wu, X., E.M. Joyce & T.J. Mason, 2011. The effects of ultrasound on cyanobacteria. *Harmful Algae* 10:738–743.
- Wylie, G.D. & J.R. Jones, 1991. Assessment of the sensitivity of Missouri reservoirs to acidification. *Journal of Freshwater Ecology* 6:431–437.
- Wyzga, R.E. & A.C. Rohr, 2015. Long-term particulate matter exposure: attributing health effects to individual PM components. *Journal of the Air and Waste Management Association* 65:523–543.
- Xiang, L., Y.W. Li, B.L. Liu, H.M. Zhao, H. Li, Q.Y. Cai, C.H. Mo, M.H. Wong & Q.X. Li, 2019. High ecological and human health risks from microcystins in vegetable fields in southern China. *Environment International* 133:105142.
- Xue, Q., X. Su, A.D. Steinman, Y. Cai, Y. Zhao & L. Xie, 2016. Accumulation of microcystins in a dominant Chironomid Larvae (*Tanytus chinensis*) of a large, shallow and eutrophic Chinese lake, Lake Taihu. *Scientific Reports* 6:3109.

- Xue, Q., A.D. Steinman, L. Xie, L. Yao, X. Su, Q. Cao, Y. Zhao & Y. Cai, 2020. Seasonal variation and potential risk assessment of microcystins in the sediments of Lake Taihu, China. *Environmental Pollution* 259:113884.
- Yang, S. & X. Jin, 2008. Critical light intensities for *Microcystis aeruginosa*, *Scenedesmus quadricauda* and *Cytoclotella* sp. and competitive growth patterns under different light:N:P ratios. *Journal of Freshwater Ecology* 23:387–396.
- Yi, X., S. Xu, F. Huang, C. Wen, S. Zheng, H. Feng, J. Guo, J. Chen, X. Feng & F. Yang, 2019. Effects of chronic exposure to microcystin-LR on kidney in mice. *International Journal of Environmental Research and Public Health* 16:5030.
- Yu, N. & D.A. Culver, 1999. In situ survival and growth of zebra mussels (*Dreissena polymorpha*) under chronic hypoxia in a stratified lake. *Hydrobiologia* 392:205–215.
- Yu, N. & D.A. Culver, 2000. Can zebra mussels change stratification patterns in a small reservoir? *Hydrobiologia* 431:175–184.
- Zastepa, A., F.R. Pick, J.M. Blais & A. Saleem, 2015. Analysis of intracellular and extracellular microcystin variants in sediments and pore waters by accelerated solvent extraction and high performance liquid chromatography-tandem mass spectrometry. *Analytica Chimica Acta* 872:26–34.
- Zhan, C., W. Liu, F. Zhang & X. Zhang, 2020. Microcystin-LR triggers different endoplasmic reticulum stress pathways in the liver, ovary, and offspring of zebrafish (*Danio rerio*). *Journal of Hazardous Materials* 386:15.
- Zhang, Y. & E.E. Prepas, 1996. Regulation of the dominance of planktonic bacillariophyta and cyanobacteria in four eutrophic hardwater lakes by nutrients, water column stability, and temperature. *Canadian Journal of Fisheries and Aquatic Sciences* 53:621–633.
- Zhang, D., W. Lin, Y. Liu, H. Guo, L. Wang, L. Yang, L. Li, D. Li & R. Tang, 2020. Chronic microcystin-LR exposure induces abnormal lipid metabolism via endoplasmic reticulum stress in male zebrafish. *Toxins* 12:107.
- Zhu, B., D.G. Fitzgerald, C.M. Mayer, L.G. Rudstam & E.L. Mills, 2006. Alteration of ecosystem function by zebra mussels in Oneida Lake: Impacts on submerged macrophytes. *Ecosystems* 9:1017–1028.
- Zohary, T., G. Flaim & U. Sommer, 2021. Temperature and the size of freshwater phytoplankton. *Hydrobiologia* 848:143–155.
- Zou, H., G. Pan, H. Chen & X. Yuan, 2006. Removal of cyanobacterial blooms in Taihu Lake using local soils II. Effective removal of *Microcystis aeruginosa* using local soils and sediments modified by chitosan. *Environmental Pollution* 141:201–205.
- Zurawell, R.W., J.I. Goldberg, C.F. Holmes & E.E. Prepas, 2007. Tissue distribution and oral dose effects of microcystin in the freshwater pulmonate snail *Lymnaea stagnalis jugularis* (Say). *Journal of Toxicology and Environmental Health, Part A* 70:620–626.

## CHAPTER 2

# PHYTOPLANKTON COMMUNITY RESPONSE TO CHANGES IN LIGHT: CAN GLACIAL ROCK FLOUR BE USED TO CONTROL CYANOBACTERIAL BLOOMS?

This work is published in *Frontiers in Environmental Science* (Gaskill et al. 2020).

Gaskill, J.A., T.D. Harris & R.L. North, 2020. Phytoplankton response to changes in light: can glacial rock flour be used to control cyanobacterial blooms? *Frontiers in Environmental Science* 8:540607.

## ABSTRACT

Cyanobacterial harmful algal blooms are one of the most prominent threats to water quality in freshwater ecosystems and are expected to become more common as the climate continues to change. While traditional strategies to manage algal blooms have focused on controlling nutrients, manipulating light as a way to reduce cyanobacteria is less frequently explored. Here, we propose the addition of glacial rock flour (GRF), a fine particulate that floats on the water's surface and remains suspended in the water column, to reduce light availability and in turn, phytoplankton biomass dominated by cyanobacteria. To determine if a sustained reduction in light could lower cyanobacteria biomass and microcystin concentrations, we applied GRF to large-scale (11 kL) mesocosm tanks for 9 consecutive days. Mesocosm tanks were amended by adding nitrogen and phosphorus to generate chlorophyte- and cyanophyte- dominated

experimental tanks. To assess how the phytoplankton community was impacted in each tank, we measured photosynthetic irradiance parameters, the maximum quantum yield of photosystem II, gross primary productivity (GPP), phytoplankton biovolume, and phytoplankton community composition before and after the addition of GRF. GRF effectively reduced cyanophyte biovolume by 78% in the cyanophyte-dominated tanks, despite no significant change in total phytoplankton community biovolume. Cyanophytes were replaced by cryptophytes, which increased by 106% in the chlorophyte-dominated tanks and by 240% in the cyanophyte-dominated tanks. The change in photosynthetic irradiance parameters and GPP after the addition of GRF was not significantly different between any of the treatment or control groups, suggesting that either the cyanophytes will likely recover if light availability increases, or that the new cryptophyte-dominated community was well suited to a reduced light environment. Cyanobacterial blooms are expected to increase in frequency and magnitude as climate change progresses, but our study suggests that light manipulation may be a useful in-lake management strategy for controlling these blooms and warrants further investigation.

## INTRODUCTION

Cyanobacterial harmful algal blooms often occur in lakes and reservoirs with high nutrient concentrations (Heisler et al., 2008). These blooms are increasing in frequency and magnitude across the globe and are a threat to aquatic resources (Brooks et al., 2016). Cyanobacteria are of poor nutritional food quality compared to other phytoplankton taxa for zooplankton grazers, which rely on foods high in polyunsaturated fatty acids, and can cause inefficiencies in trophic transfers (Brett et al., 2009; Grosbois et al., 2017). Some cyanobacteria produce secondary metabolites, the most common of which is the

cyanotoxin microcystin, that are toxic to animals and have been identified as potentially carcinogenic to humans (Grosse et al., 2006). Cyanotoxins have caused livestock (Van Halderen et al., 1995), pet (Backer et al., 2013), and wildlife (Miller et al., 2010) mortality and in extreme instances can result in human fatalities (Carmichael et al., 2001). Given the human and animal health hazard posed by cyanobacterial blooms, water body advisories and closures are common during bloom events, which can strain local economies during cyanobacterial outbreaks (Dodds et al., 2009).

Light is a critical resource for all phytoplankton. Phytoplankton use stored sugars and starches or rely on mixotrophy to temporarily survive in the absence of light (Lee, 2008), but prolonged light limitation can result in cell death or cause the cell to enter a resting phase (Bellinger and Sigee, 2010). Light requirements vary among individual taxa, and many cyanobacteria can be superior competitors at both low and high light intensities (Yang and Jin, 2008). Cyanobacteria are tolerant of reduced light conditions because of low maintenance energy requirements and their ability to maintain higher growth rates at lower light levels than many other phytoplankton (Van Liere and Mur, 1980). This tolerance allows them to persist deeper in the water column underneath other phytoplankton groups until conditions become favorable (Chorus and Bartram, 1999). Light also influences the ability of buoyancy regulating cyanobacteria to position themselves at a favorable depth in the water column. Low light levels induce gas vacuole production, giving the cell positive buoyancy (Deacon and Walsby, 1990), while high light intensities increase photosynthetic rates, allowing cells to store dense carbohydrate ballasts (Wallace and Hamilton, 2000). Cyanobacteria are also superior competitors under high light conditions due to their ability to withstand high levels of UV radiation

(Paerl et al., 1983; Sinha and Häder, 2008). The ability to withstand variable light intensities may be allowing cyanobacteria to adapt to a changing climate more favorably compared to eukaryotic algae.

Cyanobacteria are anticipated to benefit from climate-induced environmental changes. Warmer water temperatures will favor cyanobacteria, many of which have peak growth rates at temperatures between 25 and 34 °C (Robarts and Zohary, 1987; but see Lurling et al., 2013). Warming waters will result in earlier and stronger thermal stratification, which will benefit buoyancy regulating taxa (Paerl and Huisman, 2009). Projected climate change scenarios indicate that some states will experience more severe droughts while others will have higher rates of precipitation (U.S. Environmental Protection Agency, 2016). Extended droughts can increase the salinity of surface waters, which may favor cyanobacteria over other phytoplankton taxa (Paerl and Paul, 2012; Lehman et al., 2013). Higher rates of precipitation will result in increased nutrient runoff from the landscape, potentially leading to an increase in cyanobacterial blooms (Paerl and Paul, 2012). These impending climatic changes emphasize the need for a reliable method to mitigate cyanobacterial blooms.

A commonality among cyanobacterial management strategies is to reduce water column nutrient availability. Each management strategy has tradeoffs and no single strategy has been successful at controlling all types of cyanobacterial blooms (Ibelings et al., 2016). For example, beneficial management practices (BMPs) are often used to reduce external nutrient loading and subsequent cyanobacteria biomass (Sharpley et al., 2000). While BMPs can be effective, it can take several decades before noticeable improvements to water quality are observed (Osgood, 2017). Another strategy to control

cyanobacterial blooms is to lower in-lake phosphorus (P) concentrations. Commercially available solid-phase P sorbents can reduce available P, and in turn cyanobacterial biomass, but these reductions are not permanent unless external nutrient loading is also reduced (Mackay et al., 2014). Where it is not always practical to reduce nutrient availability, other approaches could provide a more realistic way to reduce cyanobacterial blooms. One strategy is to negate the advantage that buoyancy regulation provides some taxa with approaches such as artificial mixing or lake flushing (Visser et al., 2016).

When nutrient reduction methods are not feasible, light reduction management strategies may help mitigate cyanobacterial blooms. To the best of our knowledge, the only management strategy designed to control algal growth by altering the light environment is the application of artificial dye products. These dyes come in a variety of colors, but all are designed to absorb incoming photosynthetically active radiation (PAR), thus reducing the amount available for aquatic photosynthesizers. These dyes are touted as environmentally friendly and published research shows they have no effect on fish, crayfish, nor tadpoles (Spencer, 1984; Bristow et al., 1996; Bartson et al., 2018), but can reduce zooplankton diversity (Suski et al., 2018). The main drawback to these dyes is that they are designed to control rooted macrophytes and have limited effectiveness in controlling cyanophyta, bacillariophyta, euglenophyta, or chlorophyta biomass (Ludwig et al., 2008). In this study, we designed an experiment to test the efficacy of an alternative way to reduce light availability through the addition of glacial rock flour (GRF).

GRF is defined broadly as fine particulate derived from glacial erosion and occurs naturally as the erosional silt- and clay-sized particles formed from a glacier passing over bedrock (Rampe et al., 2017). No standards exist to characterize it by size class or

composition because GRF is composed of minerals reflecting the local geology in a lake catchment (Chanudet and Filella, 2009). As the glacier melts, either from seasonal receding (Casassa et al., 2009) or climate change (Moore et al., 2009), GRF runs off into the lake, often via a tributary. In glacial lakes, GRF attenuates 63% of the total water column PAR (Rose et al., 2014). Lakes that receive glacial meltwater have reduced primary productivity due to the decreased light availability, although mixotrophic phytoplankton are less sensitive to this change in light than those who rely solely on photosynthesis (Slemmons et al., 2013; Sommaruga and Kandolf, 2014).

We conducted an experiment where we reduced light through the addition of GRF with the objective of decreasing cyanophyta biomass and microcystin concentrations. Phytoplankton growth was stimulated in mesocosm tanks with amendments of P, nitrogen (N), or a combination of both to produce phytoplankton communities dominated by either chlorophytes or cyanophytes. The light environment in experimental tanks was manipulated through the addition of GRF. We hypothesize that cyanophyte biovolume and microcystin concentrations would be impacted by GRF additions, and that this change would be reflected in the physiology and primary productivity of the phytoplankton community. Our results have important implications for the future management of our changing water bodies.

## MATERIALS AND METHODS

### *Experimental Design and Sample Collection*

This experiment was conducted at the University of Kansas field station in Lawrence, KS, USA (39.049674°N, 95.190777°W) in closed bottom, fiberglass

mesocosm tanks. Each was filled to a volume of 11,000 L and depth of 1.25 m. To insulate from fluctuations in air temperatures, mesocosm tanks were kept in a ~1,300 m<sup>2</sup> shallow pond and were surrounded with ~1 m of water (Figure 1). The insulation pond was surrounded by low vegetation, mainly grasses and wildflowers that were mowed periodically throughout the summer (Figure A2.1). The closest trees were over 100 m away from the mesocosm tank set. Tanks were positioned within 50 cm of each other and were accessed via anchored walkways. On July 23, 2018, we filled each tank with 10,840 L of water from an on-site storage impoundment, then inoculated each tank with 160 L of surface water from a nearby reservoir (Milford Lake, KS, USA) with a well-documented history of cyanobacterial harmful algal blooms (Harris et al., 2020). For 8 consecutive weeks prior to the beginning of our experiment, 20 of the 23 mesocosm tanks received weekly N and P amendments. Treatments were designed to result in tanks with N- or P-deficient conditions for phytoplankton growth. Three tanks were maintained as ambient control tanks and received no nutrient nor GRF additions (Table 2.1). Each tank was randomly assigned a nutrient amendment, or in the case of the controls, no nutrient amendment.

A preliminary experiment was conducted on 6 of the 20 amended tanks to assess the quantity of GRF required to achieve the greatest reduction in light. We compared light conditions in tanks that received zero ( $n=3$ ), 5 ( $n=2$ ), 10 ( $n=2$ ), and 20 ( $n=2$ ) kg of GRF and determined that adding more than 5 kg of GRF did not result in any additional reduction in light based on no significant difference in PAR among tanks that received the 3 doses of GRF (Kruskal-Wallis  $p=0.2551$ ,  $df=3$ ,  $\chi^2=18.01$ ). We chose 5 kg of GRF as the optimum quantity to add in our subsequent experiment (Figure A1.2). The 6 tanks

that received GRF during this preliminary experiment were then removed from the experiment described below.

The GRF used was commercially available from Vital Earth's®. Its elemental composition was determined in triplicate by Activation Laboratories Ltd. (ActLabs, Ancaster, ON) via lithium metaborate/tetraborate fusion followed by aqueous phase analyses using inductively coupled plasma (ICP)–optical emission spectrometry (OES) and ICP–mass spectrometry (MS) for major and trace elements, respectively (Table A1.1). We determined GRF sediment particle fractionation using a hydrometer (Gee and Bauder, 1979). Sediment particles were measured in the following size fractions: 0.5 – 2 mm (sand), 0.002 – 0.05 mm (silt), and <0.002 mm (clay). GRF was 18.3% sand, 70.7% silt, and 11.2% clay. We did not explicitly test for any biota associated with GRF.

Before our main experiment began, we grew algal communities in the mesocosms, and assessed light reduction resulting from GRF application to mesocosms. Algal communities were created by adding different forms of nutrients so that algal communities would vary (Table 2.1). We kept tanks that received the same nutrient forms together, even if a single tank in the group was not dominated by the same phytoplankton. We included 1 tank in the chlorophyte-dominated group where chlorophytes only comprised 9.2% of the total biovolume (Tank #3, Table A1.2). Cryptophytes were the dominant taxa in this tank on day 0 (71.2%), but we decided to include it with the other tanks that received the same nutrient amendments because we do not believe excluding it would have changed our results. If this tank were excluded, cryptophyte biovolume would have increased in the 5 remaining chlorophyte-dominated tanks by 111.0% between day 0 and day 9, compared to an increase of 105.7% if the tank

were included. In 1 of the cyanophyte-dominated tanks as well, cyanophytes were not the dominant taxa on day 0, comprising only 14.3% (Tank #11, Table A1.2). We included this tank for the same reasons. When it was included, cryptophytes increased by 240.0% between day 0 and day 9. When this tank was excluded, they increased by 408.0%.

Ultimately, we considered phytoplankton dominance to be the taxa with the highest biovolume, averaged across all tanks within the group. On day 0, 6 of the 17 tanks were included in the chlorophyte-dominated group (biovolume mean and range = 1.51, 0.06 – 3.11 mm<sup>3</sup> L<sup>-1</sup>; % of total phytoplankton biovolume mean and range = 51.4, 9.2 – 89.4%) and 8 were included in the cyanophyte-dominated group (biovolume mean and range = 28.17, 0.98 – 71.87 mm<sup>3</sup> L<sup>-1</sup>; % of total biovolume mean and range = 71.3, 14.3 – 92.0%). *Oocystis* was the most prevalent phytoplankton in chlorophyte-dominated tanks, comprising a mean 35.4% of total phytoplankton biovolume (range = 0 – 86.9%), while *Aphanizomenon*, which comprised a mean 22.8% total phytoplankton biovolume (range = 0 – 49.4%), was the most prevalent phytoplankton in cyanophyte-dominated tanks (Tables 2.2 and A1.2). Control tanks ( $n=3$ ) were also dominated by chlorophytes (biovolume mean and range= 3.17, 0.28 – 8.08 mm<sup>3</sup> L<sup>-1</sup>; % of total biovolume mean and range = 52.3, 25.1 – 82.0%) when the experiment began, particularly from the genus *Tetraedron*, which comprised a mean 26.2% of total phytoplankton biovolume (range = 0 – 78.5%, Table 2.2 and A1.2). We added GRF to each of the chlorophyte- and cyanophyte-dominated treatment tanks, exclusive of the 3 control tanks. For 9 consecutive mornings between 9:00-10:30 AM (CST), we distributed 5 kg of GRF evenly across the surface of each tank with a sifter. GRF was allowed to float on the tank surface, although some mixed into the water column over the next 24 hrs. PAR

measurements were taken in the air above the water surface, just below the water's surface, 0.5, and 1 m below the surface in each tank using a cosine Li-Cor underwater quantum sensor (LI-192). To account for changes in PAR from the time we measured the first tank to the time that we measured the last, we corrected each underwater PAR measurement by dividing it by the air PAR measurement we made above the water's surface. We report this value as the PAR ratio (0.5 m water/air reading). To ensure that a reduction in light was maintained throughout the entire day, light was measured one hour after GRF addition on all experimental days, 4 hours after GRF addition on days 0, 5, 6, and 7, and 6 hours after GRF addition on day 4. PAR measurements from just below the surface, 0.5, and 1 m below the surface, were used to determine the light attenuation coefficient ( $K_d$ ) in all tanks from the natural logarithm of irradiance versus depth (Kirk, 1994). Temperature profiles were collected from just below the surface, 0.5, and 1 m below the surface using a Yellow Springs Instrument EXO3, which is accurate to  $\pm 0.01$  °C.

During our main experiment, we collected water samples from each tank on days 0 and 9 with a PVC integrated sampler with a check valve from the surface to a depth of 1.0 m to avoid collecting or resuspending any material that had settled to the tank bottom. We then filtered water samples onto pre-combusted, 1.2  $\mu\text{m}$ , GF/C filters for total suspended solids (TSS), which were frozen until analysis. Integrated whole water for total P (TP) and total N (TN) analyses were stored in glass digestion test tubes. Filtrate from 0.7  $\mu\text{m}$  glass fiber filters (GFF) was also stored in glass digestion test tubes within 30 hrs of collection to measure total dissolved P (TDP) and total dissolved N (TDN). Filtrate from 0.45  $\mu\text{m}$  nitrocellulose membrane filters was frozen for nitrate ( $\text{NO}_3^-$ ) and

ammonium ( $\text{NH}_4^+$ ) analysis. Dissolved organic carbon (DOC) samples were stored frozen as filtrate from pre-combusted,  $0.7 \mu\text{m}$  GFF filters. A subset of the integrated water sample was immediately frozen at  $-20 \text{ }^\circ\text{C}$  in amber, HDPE bottles for microcystin analysis. Samples for phytoplankton identification and enumeration were collected by taking a subset of the integrated water sample and preserving it with 1% Lugols solution in amber vials. Within 30 hrs of collection, water filtered onto  $0.7 \mu\text{m}$  GF/F filters were frozen until they were analyzed for chlorophyll-*a* (chl-*a*) and the phytoplankton pigment absorption coefficient ( $\alpha_\phi$ ). Whole water for P-E parameters, gross primary production (GPP), and the maximum quantum yield of photosystem II ( $\phi_{\text{PSII}}$ ) were stored in the dark prior to running on the Water-Pulse Amplitude Modulated fluorometer (PAM, Heinz Walz GmbH) within 30 hrs of collection.

We collected samples for zooplankton identification and enumeration throughout the entire water column of each tank (1.25 m deep) using a  $243 \mu\text{m}$  Wisconsin net (diameter = 200 mm) raised at approximately one-third of a meter per second. Zooplankton samples were immediately preserved with 4% formalin for enumeration.

We used sediment traps, positioned 0.5 m below the water's surface, to determine sedimentation rates in each tank. Sediment traps were constructed from PVC with a 7.6 cm diameter and 6:1 height to aspect ratio (Bloesch and Burns, 1980). On each sampling date, the entire 2 L sediment trap was emptied into a HDPE collection bottle and homogenized by inverting 3 times. A portion of homogenized water was retained on pre-combusted,  $1.2 \mu\text{m}$ , GF/C filters and later analyzed for TSS.

### *Laboratory Analyses*

We measured TSS from both whole water integrated samples and sediment traps using standard methods (Section 2540 D and E; APHA 2017). Pre-weighed filters with retained material were dried at 105 °C for 30 minutes and then weighed. Filters were then incinerated at 550 °C for 20 minutes to burn off organic material before being weighed again. This loss-on-ignition analysis allowed us to differentiate TSS by subtracting the mass left after incineration, which is particulate inorganic matter (PIM), from the total filter mass before incineration, which is TSS. The difference is particulate organic matter (POM). TSS had a detection limit of 0.1 mg L<sup>-1</sup>. We determined sedimentation rates from the TSS measured in our sediment traps using (Kalff, 2002):

#### Sedimentation Rate

$$= \frac{\text{Subsample Dry Weight (mg)} \times \text{Total Sample Vol. (cm}^3\text{)}}{10 \times \text{Subsample Vol. (cm}^3\text{)} \times \text{Trap Area (cm}^2\text{)} \times \text{Period (day)}}$$

Total sample volume was always 2000 cm<sup>3</sup>, sediment trap area was 45.6 cm<sup>2</sup>, and the period that traps were deployed was 9 days.

Mean daily mixed layer irradiance ( $\bar{E}_{24}$ ) is a measure of the amount of light phytoplankton in the mixed layer are exposed to over 24 hrs. It was calculated using the formula:

$$\bar{E}_{24} = \bar{E}_0 \times (1 - \exp(-1 \times K_d \times Z_{mix})) \times (K_d \times Z_{mix})^{-1}$$

Incident irradiance,  $\bar{E}_0$ , was calculated as the 24 hr mean of PAR measurements taken at an onsite meteorological station (Natural Resources Conservation Service, site Ku-Nesa, <https://wcc.sc.egov.usda.gov/nwcc/site?sitenum=2147>) on day 0 (9/24/18) and day 9 (10/2/18). Mixing depth within each tank,  $Z_{mix}$ , was calculated from temperature profiles

using the rLakeAnalyzer package (Winslow et al., 2017). Profiles were taken one hour after GRF addition on all experimental days, 4 hours after GRF addition on days 0, 5, 6, and 7, and 6 hours after GRF addition on day 4. Occasionally, tanks would temporarily stratify in the afternoon between the water's surface and 0.5 m. Tanks were isothermal every morning, indicating that even if a tank did stratify at the end of the previous day, it mixed during the night. We used the maximum depth of each tank, 1.25 m, as the value for  $Z_{\text{mix}}$  when calculating  $\bar{E}_{24}$ .

TP and TDP were measured spectrophotometrically using the ascorbic acid colorimetric method (Section 4500-P E; APHA, 2017) with a detection limit of 0.03  $\mu\text{mol L}^{-1}$ . TN and TDN were measured with the second derivative spectroscopy procedure (Crumpton et al., 1992) with a detection limit of 2.50  $\mu\text{mol L}^{-1}$ . Total and total dissolved P and N samples were measured in triplicate.  $\text{NO}_3^-$ , which was measured in duplicate on a Lachat QuikChem Flow Injection Analyzer (Lachat Method 10-107-04-1-B/C), had a detection limit of 0.36  $\mu\text{mol L}^{-1}$ . This method reports  $\text{NO}_3^-$  as  $\text{NO}_3^-$  plus nitrite ( $\text{NO}_2^-$ ) based on the assumption that environmental  $\text{NO}_2^-$  concentrations are minimal. We measured  $\text{NH}_4^+$  in duplicate on a Lachat QuikChem Flow Injection Analyzer (Lachat Method 10-107-06-1-K) based on the Berthelot reaction with a limit of detection of 0.71  $\mu\text{mol L}^{-1}$ . We report  $\text{NH}_4^+$  as  $\text{NH}_3$  plus  $\text{NH}_4^+$ . We measured DOC in duplicate using a Shimadzu total organic C analyzer with the high-temperature combustion method (Section 5310B; APHA 2017), with a limit of detection of 16.7  $\mu\text{mol L}^{-1}$ . Intracellular microcystin was extracted via 3 freeze-thaw cycles from whole water samples, which were then filtered through 0.45  $\mu\text{m}$  GFFs. We measured total microcystin, both the intracellular microcystin previously released from freeze-thaw

cycles and the extracellular microcystin present in the water, using indirect competitive ELISA (Enzyme Linked Immunosorbent Assay) kits from Abraxis LLC, which have a limit of detection of  $0.15 \mu\text{g L}^{-1}$ . Chl-*a* concentrations were quantified fluorometrically with a Turner Design Fluorometer (TD-700) after ethanol extraction and phaeophytin acid-correction (Knowlton, 1984; Sartory and Grobbelaar, 1986). The chl-*a* detection limit was  $0.09 \mu\text{g L}^{-1}$ .

Phytoplankton were identified to genus (Table A1.2) by BSA Environmental Services Inc. (Guiry and Guiry, 2020), and enumerated using the Ütermohl method (Lund et al., 1958). Phytoplankton were allowed to settle for at least 20 hrs in a dark enclosure protected from vibrations and temperature changes prior to enumeration (Burkholder and Wetzel, 1989). Cell biovolume estimates are based on measurements from 10 cells in each taxon and were calculated using the formula of Hillebrand et al., (1999) for solid geometric shapes that most closely match cell shape. All enumerations were conducted using a LEICA DMiL inverted microscope at  $800\times$  and  $1260\times$  magnification, depending on the size of the dominant taxa, particulates, and variation in the range of taxon sizes. Heterocyte abundance was calculated for all phytoplankton samples. It is beneficial to group phytoplankton into functional groups when trying to understand ecological function (Salmaso et al., 2015). For example, both cryptophytes and dinoflagellates have 2 flagella, are known to participate in diel vertical migrations to take advantage of both the nutrient-rich hypolimnion and light-replete surface waters, and can supplement metabolic requirements with mixotrophy (Raven and Richardson, 1984; Lee, 2008). We classified the phytoplankton by the following 6 taxonomic groups: 1) potentially toxigenic cyanophyta (Chapman and Foss, 2019), 2) non-toxin producing cyanophyta, 3)

chlorophyta, 4) euglenophyta, 5) cryptophyta and dinoflagellates, and 6) chrysophyta, including chrysophytes, bacillariophyta, ochrophytes, and haptophytes (Table A1.3).

We assessed phytoplankton physiology, including  $\phi_{PSII}$ , P–E parameters (alpha normalized to chl-*a* [ $\alpha^B$ ], the light saturation threshold normalized to chl-*a*, [ $E_k^B$ ], and the maximum relative electron transport rate [ $rETR_{MAX}$ ]), and gross primary productivity normalized to chl-*a* ( $GPP^B$ ) following the procedures outlined in Petty et al., (2020).

Within 30 hrs of collection, we measured  $\phi_{PSII}$  in triplicate with a Water-PAM fluorometer on whole, integrated water that had been dark adapted for 30 minutes. Water samples were corrected for background fluorescence with 0.2  $\mu m$  PTFE sample water filtrate. We also used the Water-PAM to perform rapid light curves. For each light curve, the light limited slope ( $\alpha$ ) and light saturation threshold ( $E_k$ ) were defined as  $\phi_{PSII}$  fit against irradiance to a light intensity ( $E$ ) using the normalized version of Webb et al., (1974):

$$\alpha \times E_k \times (1 - e(-E \times E_k)) \times E^{-1}$$

where  $rETR_{MAX}$  was the product of  $\alpha$  and  $E_k$ . We divided  $\bar{E}_{24}$  by  $E_k$  to assess light deficiency within each tank. When this ratio is above 1, light availability is greater than phytoplankton light saturation and light does not limit photosynthesis. Below 1, phytoplankton do not receive enough light to reach saturation and may experience light deficiency (Hecky and Guildford, 1984). The areal pigment absorption coefficient ( $\alpha_\phi$ ), a factor in our calculation of  $GPP^B$ , was quantified using the quantitative filter technique by measuring absorbance at 350 – 750 with a scanning spectrophotometer (Agilent Cary60 UV/VIS) before and after depigmentation with a sodium hypochlorite solution (4.00 – 4.99% available chlorine). We then calculated  $a_\phi$  using:

$$a_{\phi} = 2.303 \times (A_P - A_{NAP}) \times \beta^{-1} \times (V_f/A_f)^{-1}$$

where  $A_P$  is absorption before and  $A_{NAP}$  is absorption after depigmentation,  $\beta$  is the path-length amplification factor to adjust for differences in absorption between water and filter, and  $V_f/A_f$  is the ratio of volume of water filtered to the filter area (Silsbe et al., 2012). We determined GPP using the R package *phytotools* (Silsbe and Malkin, 2015). This package is based on the primary production model of Fee (1990) and incorporates chl-*a*, P-E parameters,  $a_{\phi}$ ,  $K_d$ , and  $\bar{E}_0$ .

Zooplankton were enumerated by the Central Plains Center for Bioassessment to the following taxonomic groups: cladocerans, adult copepods, and copepod nauplii (Thorp and Covich, 2001). Before being photographed, samples were switched from the 4% fixation preservative from the field to 80% ethanol. Images of each zooplankton were taken using a Motic Plus 2.0 digital camera at 10× magnification (87.7 pixels mm<sup>-1</sup>) using Image-J software (National Institutes of Health, Bethesda, Maryland). All abundance calculations of each zooplankton taxa assumed 100% net filtering efficiency.

### *Statistical Analyses*

A Shapiro-Wilk test was used to test for normality and a Levene's test to assess homoscedasticity. The alpha value for all statistical tests was set at 0.05. All statistical analyses were performed in Program R (R Core Team, 2019) and all figures were created using the *ggplot2* package (Wickham, 2009).

We tested for a significant difference in  $K_d$  and the PAR ratio (0.5 m water/air reading) between tanks that received GRF and the control tanks that did not receive GRF. We took the mean of control ( $n= 3$ ) and GRF ( $n= 14$ ) tanks. Neither parameter was

normally distributed, even after transformation, so we used a Kruskal-Wallis test to look for significant differences at one, 4, and 6 hours after GRF addition and a Dunn's *post hoc* test to identify where significant differences existed.

Unless stated otherwise, statistical analyses were performed on the change in each parameter between days 0 and 9. We calculated this change by subtracting the value for each parameter on day 9 from the value for that parameter on day 0 (i.e., day 9 - day 0). Positive values indicate an increase in the parameter on day 9, while negative values indicate a decrease. We used a One-Way Analysis of Variance (ANOVA) to test whether the change in each parameter was significantly different between the control ( $n= 3$ ), chlorophyte-dominated ( $n= 6$ ), and cyanophyte-dominated ( $n= 8$ ) tanks. In instances where a parameter was not normally distributed, even after transformation, we used a Kruskal-Wallis test. When a significant difference did exist, we used a Tukey *post hoc* to identify significant differences for parameters that followed a parametric distribution, and a Dunn's test on parameters that did not follow a normal distribution. For tanks where the microcystin concentrations were below the limit of detection, we used the limit of detection,  $0.15 \mu\text{g L}^{-1}$ , for statistical analyses. We compared chl-*a* concentrations and phytoplankton biovolume to assess photoacclimation. Neither chl-*a* nor biovolume were normally distributed, even after transformation, so we used the non-parametric Spearman's Rank correlation to assess the relationship between these 2 variables.

## RESULTS

### *Physical Parameters*

We assessed water clarity by measuring  $K_d$  and the PAR ratio (0.5 m water/air reading) in each tank.  $K_d$  was significantly higher (Kruskal-Wallis  $p < 0.0001$ ,  $df = 1$ ,  $\chi^2 = 118.84$ ) and the PAR ratio (Kruskal-Wallis  $p < 0.0001$ ,  $df = 1$ ,  $\chi^2 = 112.18$ ) was significantly lower in tanks that received GRF. The PAR ratio was significantly lower one hour after GRF addition than 4 (Kruskal-Wallis  $p < 0.0001$ ,  $df = 2$ ,  $\chi^2 = 26.46$ ) or 6 hours (Kruskal-Wallis  $p = 0.0002$ ,  $df = 2$ ,  $\chi^2 = 26.46$ ), but not significantly different between 4 and 6 hours (Kruskal-Wallis  $p = 0.1709$ ,  $df = 2$ ,  $\chi^2 = 26.46$ ; Figure 2.2). In tanks that received GRF,  $K_d$  was significantly higher one hour after GRF addition than 4 (Kruskal-Wallis  $p < 0.0001$ ,  $df = 2$ ,  $\chi^2 = 37.10$ ) or 6 (Kruskal-Wallis  $p < 0.0001$ ,  $df = 2$ ,  $\chi^2 = 37.10$ ) hours, but not significantly different between 4 and 6 hours (Kruskal-Wallis  $p = 0.2347$ ,  $df = 2$ ,  $\chi^2 = 37.10$ ; Figure 2.2).  $K_d$  was  $\sim 3\times$  higher in tanks that received GRF compared to the control tanks (Figure 2.2). Tanks that received GRF had PAR ratios 86.4, 60.4, and 67.7% lower, and mean  $K_d$ s 80.5, 73.6, and 68.8% higher, compared to control tanks for one, 4, and 6 hours after GRF application, respectively.

Water temperatures remained below 25 °C throughout the experiment (Table 2.3). The change in temperature over the course of the experiment was not significantly different between control, chlorophyte-, and cyanophyte- dominated tanks (Table 2.4, Figure A1.3).

Mean TSS sedimentation rates were  $0.1 \text{ g m}^{-2} \text{ day}^{-1}$  (range= below detection limit [BDL] –  $0.1 \text{ g m}^{-2} \text{ day}^{-1}$ ) in control,  $1.9 \text{ g m}^{-2} \text{ day}^{-1}$  (range=  $0.8 - 2.9 \text{ g m}^{-2} \text{ day}^{-1}$ ) in chlorophyte-dominated, and  $2.3 \text{ g m}^{-2} \text{ day}^{-1}$  (range=  $1.0 - 3.4 \text{ g m}^{-2} \text{ day}^{-1}$ ) in cyanophyte-dominated tanks. Mean PIM sedimentation rates were BDL (range= BDL –  $0.1 \text{ g m}^{-2} \text{ day}^{-1}$ ) in control,  $1.9 \text{ g m}^{-2} \text{ day}^{-1}$  (range=  $0.8 - 2.8 \text{ g m}^{-2} \text{ day}^{-1}$ ) in chlorophyte-dominated, and

2.2 g m<sup>-2</sup> day<sup>-1</sup> (range= BDL – 0.1 g m<sup>-2</sup> day<sup>-1</sup>) in cyanophyte-dominated tanks. Mean POM sedimentation rates were always BDL in control and 0.1 g m<sup>-2</sup> day<sup>-1</sup> (range= BDL – 0.1 g m<sup>-2</sup> day<sup>-1</sup>) in both chlorophyte- and cyanophyte-dominated tanks (Table 2.3).

Between days 0 and 9,  $\bar{E}_{24}$  increased from 106.67 to 115.45  $\mu\text{mol photons m}^{-2} \text{ s}^{-1}$  in control, and from 57.14 to 64.36  $\mu\text{mol photons m}^{-2} \text{ s}^{-1}$  in cyanophyte-dominated tanks.  $\bar{E}_{24}$  decreased from 114.16 to 110.66  $\mu\text{mol photons m}^{-2} \text{ s}^{-1}$  in chlorophyte-dominated tanks (Table 2.3, Figure A1.3). The change in  $\bar{E}_{24}$  throughout the experiment was not significantly different between the control, chlorophyte-, and cyanophyte- dominated tanks (Table 2.4). The  $\bar{E}_{24}$  values we observed throughout the experiment were above the light deficiency threshold of 41.7  $\mu\text{mol photons m}^{-2} \text{ s}^{-1}$  (Hecky and Guildford, 1984) in all tanks.

### *Water Chemistry*

We report all water chemistry parameters as the mean of control, chlorophyte-, and cyanophyte- dominated mesocosm tanks (Table 2.3). To determine the influence of GRF on water chemistry, we examined the change in each parameter between day 9 and day 0 and tested to see if this change was different between the control, chlorophyte-, and cyanophyte- dominated tanks, but in most cases it was not (Tables 2.3 and 2.4). The change in water column TSS, PIM, and POM was not significantly different between any of the experimental groups. TSS increased from 0.8 to 3.1 mg L<sup>-1</sup>, from 1.5 to 7.3 mg L<sup>-1</sup>, and from 4.5 to 20.2 mg L<sup>-1</sup> in the control, chlorophyte-, and cyanophyte- dominated tanks, respectively. PIM decreased from 0.4 to 0.3 mg L<sup>-1</sup> in the control, but increased from 1.0 to 5.5 mg L<sup>-1</sup> and from 2.2 to 10.5 mg L<sup>-1</sup> in the chlorophyte- and cyanophyte-dominated tanks, respectively. POM increased in the control and cyanophyte-dominated

tanks from 0.9 to 2.8 mg L<sup>-1</sup> and from 6.6 to 9.7 mg L<sup>-1</sup>, respectively, but decreased in the chlorophyte-dominated tanks from 2.9 to 1.8 mg L<sup>-1</sup> (Table 2.3, Figure A1.3).

TP concentrations decreased from 0.74 to 0.67 μmol L<sup>-1</sup> in the control and from 5.89 to 3.85 μmol L<sup>-1</sup> in the cyanophyte-dominated tanks. All cyanophyte-dominated tanks received P amendments for 8 weeks prior to the beginning of the experiment (Table 2.1). The change in TP concentrations was not significantly different between the control and chlorophyte-dominated, nor the control and cyanophyte-dominated tanks (Table 2.4). TP concentrations were unchanged over the course of the experiment in the chlorophyte-dominated tanks (mean= 0.57 μmol L<sup>-1</sup>; Table 2.3, Figure A1.4). The change in TP concentrations between days 9 and 0 in the cyanophyte-dominated tanks was significantly greater than the change between days 9 and 0 in the chlorophyte-dominated tanks.

The change in TN concentrations between days 9 and 0 was not significantly different between the control, chlorophyte-, and cyanophyte- dominated tanks (Table 2.4). TN concentrations were stable in the control and chlorophyte-dominated, but decreased from 163.06 to 153.54 μmol L<sup>-1</sup> in the cyanophyte-dominated tanks (Table 2.3, Figure A1.4).

The TN:TP molar ratio can serve as an indicator of phytoplankton nutrient deficiency. We report the natural log (ln) of the TN:TP ratio as this transformation reduces bias inherent with calculating the mean of a ratio (Isles, 2020). If the ln(TN:TP) molar ratio exceeds 3.91, then the phytoplankton community is P-deficient, and if it is lower than 3.00 then the phytoplankton community is N-deficient (Guildford and Hecky, 2000). Between 3.00 and 3.91, it could be N, P, or some other factor restricting growth

(Guildford and Hecky, 2000). The mean  $\ln(\text{TN}:\text{TP})$  molar ratios for control and chlorophyte-dominated tanks on day 0 were 4.61 (range= 4.07 – 4.96) and 4.74 (range= 4.30 – 5.47), respectively, indicating P-deficient conditions (Tables 2.1 and 2.3; Guildford and Hecky, 2000). Cyanophyte-dominated tanks had a mean  $\ln(\text{TN}:\text{TP})$  molar ratio of 3.39 (range= 2.74 – 4.23) on day 0 (Tables 2.1 and 2.3, Figure A1.4). This value was between P-deficient and N-deficient conditions, suggesting that these tanks could have been either N or P deficient. Alternatively, cyanophyte-dominated tanks could have been growth-limited by other factors such as light (Guildford and Hecky, 2000). Heterocytes were only present in the cyanophyte-dominated tanks. They were identified in 6 tanks on day 0 and only 4 tanks on day 9 in low densities (mean= 5,850, range= 27 – 13,800 cells  $\text{L}^{-1}$ ). The change in the  $\ln(\text{TN}:\text{TP})$  ratio between days 9 and 0 was not significantly different between the control, chlorophyte- and cyanophyte- dominated tanks (Table 2.4).

The change in TDN, TDP,  $\text{NO}_3^-$ , and  $\text{NH}_4^+$  concentrations were not significantly different between any of the experimental groups (Table 2.4). TDN and TDP concentrations were stable in all tanks throughout the experiment, although a notable deviation was the decrease in TDP from 1.52 to 1.27  $\mu\text{mol L}^{-1}$  in the cyanophyte-dominated tanks (Table 2.3).  $\text{NO}_3^-$  concentrations were never above the limit of detection in control, and decreased from 3.94 to 2.78  $\mu\text{mol L}^{-1}$  and from 1.75 to 0.45  $\mu\text{mol L}^{-1}$  in chlorophyte- and cyanophyte- dominated tanks, respectively (Table 2.3).  $\text{NH}_4^+$  concentrations increased from 1.51 to 1.83  $\mu\text{mol L}^{-1}$  and from 8.53 to 12.17  $\mu\text{mol L}^{-1}$  in the control and cyanophyte-dominated tanks, respectively, but decreased from 3.49 to 3.03  $\mu\text{mol L}^{-1}$  in the chlorophyte-dominated tanks (Table 2.3, Figure A1.4).

Over the course of the experiment, DOC concentrations increased from 1009.25 to 1063.20  $\mu\text{mol L}^{-1}$  in the control, from 1015.00 to 1030.73  $\mu\text{mol L}^{-1}$  in the chlorophyte-dominated, and from 1032.98 to 1081.02  $\mu\text{mol L}^{-1}$  in the cyanophyte-dominated tanks (Table 2.3, Figure A1.4). The difference between day 9 and day 0 DOC concentrations in the cyanophyta-dominated tanks were significantly larger than in the chlorophyte-dominated tanks (Table 2.4), but there was no significant difference between the control and neither the chlorophyte- nor cyanophyte-dominated tanks (Table 2.4).

Microcystin concentrations ranged from BDL to 4.04  $\mu\text{g L}^{-1}$  (Table 2.3). Over this 9-day experiment, they increased from 0.17 to 0.19  $\mu\text{g L}^{-1}$  in the control, from 0.16 to 0.19  $\mu\text{g L}^{-1}$  in the chlorophyte-dominated, and from 0.70 to 0.87  $\mu\text{g L}^{-1}$  in the cyanophyte-dominated tanks (Table 2.3). The change in microcystin concentrations between days 9 and 0 was not significantly different among any of the experimental groups (Table 2.4, Figure A1.3).

#### *Phytoplankton Community Biovolume*

Photoacclimation is a photosynthesizer's physiological response to changes in light and displays as an increase or decrease in chl-*a* concentrations relative to phytoplankton biomass (Falkowski and LaRoche, 1991). To check if photoacclimation was occurring in the experimental tanks to which we added GRF, we examined the relationship between chl-*a* concentrations and phytoplankton biovolume. There was a significant positive correlation between these parameters prior to GRF addition (day 0; Spearman's Rank,  $p= 0.0023$ ,  $\rho= 0.76$ ,  $n= 14$ ) and on day 9 (Spearman's Rank,  $p= 0.0038$ ,  $\rho= 0.74$ ,  $n= 14$ ), indicating that the phytoplankton did not exhibit photoacclimation. Chl-*a* concentrations decreased from 3.54 to 2.09  $\mu\text{g L}^{-1}$  and from 2.97

to  $1.53 \mu\text{g L}^{-1}$  in the control and chlorophyte-dominated tanks, respectively, but increased from 48.7 to  $63.52 \mu\text{g L}^{-1}$  in the cyanophyte-dominated tanks (Table 2.3, Figure A1.5). The change in chl-*a* concentrations and phytoplankton biovolume between days 9 and 0 was not significantly different between the control, chlorophyte- and cyanophyte-dominated tanks (Table 2.4). Total phytoplankton biovolume decreased from 4.43 to  $2.64 \text{ mm}^3 \text{ L}^{-1}$  and from 35.31 to  $28.13 \text{ mm}^3 \text{ L}^{-1}$  in the control and cyanophyte-dominated tanks, respectively. Total phytoplankton biovolume remained unchanged in the chlorophyte-dominated tanks (mean=  $2.55 \text{ mm}^3 \text{ L}^{-1}$ ; Table 2.3). Within all tanks, dinoflagellates comprised only 23.0, 13.3, and 0.1%, respectively, of the cryptophyte and dinoflagellate functional group. Throughout the rest of this study, we refer to the group containing cryptophytes and dinoflagellates as the cryptophyte functional group.

Within the chlorophyte- and cyanophyte-dominated tanks, declines in cyanophytes (49.4 and 77.9%, respectively) were compensated by an increase in cryptophytes (105.7 and 240%, respectively; Figure 2.3). Much of this cryptophyte increase can be attributed to the genus *Cryptomonas*, which comprised 32.2 and 37.1% of total phytoplankton biovolume on day 9 in chlorophyte- and cyanophyte-dominated tanks, respectively (Tables 2.2 and A1.2). The change in potentially toxigenic cyanophyta biovolume was significantly different in the cyanophyte-dominated tanks compared to the control and chlorophyte-dominated tanks (Table 2.4). Potentially toxigenic cyanophytes increased by 16.7% in control, and declined by 100 and 76.2% in chlorophyte and cyanophyte-dominated tanks, respectively. All cyanobacteria (potentially toxigenic taxa and non-toxin producing taxa combined) declined by 22.8, 49.4, and 77.9% in the control, chlorophyte- and cyanophyte-dominated tanks, respectively, between days 0 and

9. While the change in biovolume between sampling dates for all other taxonomic groups was not significantly different between experimental tanks, cryptophytes increased by 18.8, 105.7, and 240.0% in the control, chlorophyte- and cyanophyte-dominated tanks, respectively.

#### *Phytoplankton Physiology and Gross Primary Productivity*

Phytoplankton samples with  $\phi_{PSII}$  values below 0.65 can indicate that the communities are physiologically stressed due to light, nutrients, or some combination thereof (Kromkamp et al., 2008). At no point on days 0 nor 9 did  $\phi_{PSII}$  exceed the empirical optimum threshold of  $\sim 0.65$  in any tank (Table 2.3, Figure A1.6).  $\phi_{PSII}$  decreased from 0.57 to 0.53 and from 0.61 to 0.56 in the control and chlorophyte-dominated tanks, respectively, but increased from 0.34 to 0.48 in the cyanophyte-dominated tanks (Table 2.3, Figure A1.6). We observed no significant difference in the change in  $\phi_{PSII}$  between the control, chlorophyte-, and cyanophyte- dominated tanks.

Additional indicators of phytoplankton physiology also remained largely unchanged after the addition of GRF (Table 2.4). The light utilization efficiency parameter ( $\alpha^B$ ) increased from 0.51 to 0.58 and from 0.48 to 0.65 in the control and chlorophyte-dominated tanks, respectively, but decreased from 0.07 to 0.05 in the cyanophyte-dominated tanks. The light saturation parameter ( $E_k^B$ ) increased from 153.23 to 377.22  $\mu\text{mol photons } (\mu\text{g Chl-}a^{-1}) \text{ m s}^{-1}$  in the control, but decreased in both the chlorophyte- and cyanophyte- dominated tanks from 428.24 to 388.69 and from 80.90 to 32.34  $\mu\text{mol photons } (\mu\text{g Chl-}a^{-1}) \text{ m s}^{-1}$ , respectively (Table 2.3).  $rETR_{MAX}$  decreased from 315.69 to 291.40 in the control, but increased from 175.63 to 222.69 and from 136.12 to 197.21 photons reemitted photons absorbed<sup>-1</sup> in the chlorophyte- and cyanophyte-

dominated tanks, respectively (Table 2.3). The light deficiency parameter ( $\bar{E}_{24}/E_k$ ) decreased in control, chlorophyte-, and cyanophyte-dominated tanks from 0.85 to 0.45, 0.55 to 0.43, and from 0.20 to 0.18, respectively (Table 2.3, Figure A1.6). We observed no significant difference in the change in  $\alpha^B$ ,  $E_k^B$ ,  $rETR_{MAX}$ , nor  $\bar{E}_{24}/E_k$ , between the control, chlorophyte- and cyanophyte- dominated tanks.

Gross primary productivity normalized to chl-*a* ( $GPP^B$ ) increased from 25.9 to 33.3, from 15.4 to 18.2, and from 15.2 to 22.8 mmol O<sub>2</sub> ( $\mu\text{g Chl-a}^{-1}$ ) m day<sup>-1</sup> in the control, chlorophyte- and cyanophyte- dominated tanks, respectively (Table 2.3, Figure A1.6). We did not observe a significant difference in the change in  $GPP^B$  between any of the tanks (Table 2.4).

### *Zooplankton*

To evaluate whether zooplankton dynamics were influenced by GRF addition and/or if grazing was impacting phytoplankton populations differently between tanks and over the course of the experiment, we compared total zooplankton, cladoceran, and copepod abundance between days 0 and 9 (Table A1.4, Figure 2.4). Copepods were separated into adults and nauplii. Between days 9 and 0, the change in total zooplankton, cladoceran, adult copepod, and copepod nauplii abundance was not significantly different in any of the tanks (Table 2.4). While not significant (Table 2.3, Figure A1.7), total zooplankton abundance increased from 70.85 to 111.87 in control, but decreased from 79.56 to 31.78 and from 211.84 to 126.04 in chlorophyte- and cyanophyte-dominated tanks, respectively. Adult copepod abundance increased from 14.82 to 16.00 individuals L<sup>-1</sup> in the control, but decreased from 17.36 to 12.73 and from 89.05 to 59.59 individuals L<sup>-1</sup> in chlorophyte- and cyanophyte- dominated tanks, respectively. Copepod nauplii

abundance decreased from 26.73 to 16.59 in control, from 31.46 to 12.75 in chlorophyte-dominated, and from 63.54 to 39.01 individuals L<sup>-1</sup> in cyanophyte-dominated tanks. Cladocerans increased from 29.30 to 79.27 in control tanks, but decreased from 30.75 to 6.30 and from 59.25 to 27.43 individuals L<sup>-1</sup> in chlorophyte- and cyanophyte- dominated tanks, respectively (Table 2.3, Figure A1.7).

## DISCUSSION

Light availability throughout the water column was significantly reduced in all mesocosm tanks that received GRF relative to the control tanks. This reduction in light was maintained throughout the 9-day experiment and resulted in a 77.9% decline in cyanophyte biovolume in tanks dominated by cyanophytes. While total phytoplankton biovolume did not change after the addition of GRF, cryptophytes increased by 240.0% in cyanophyta-dominated tanks. In the chlorophyte-dominated tanks, cyanophytes decreased by 49.4% while cryptophytes increased by 105.7%. Changes in cyanophytes and cryptophytes were less in the control tanks where cyanophytes decreased by 22.8% and cryptophytes increased by 18.8% between days 0 and 9.

### *How Did the GRF Addition Affect Physical, Chemical, and Biological Parameters in the Mesocosm Tanks?*

The addition of GRF to mesocosm tanks significantly reduced PAR by half and maintained this relatively low light level throughout the 9-day experiment. PIM concentrations increased by ~80% from day 0 to day 9 in the chlorophyte- and cyanophyte-dominated tanks that received GRF. POM decreased by 37.9% in chlorophyte-dominated tanks and increased by only 32.0% in cyanophyte-dominated

tanks between day 0 and day 9, suggesting that the reduction in light is due to increases in suspended inorganic particles derived from the GRF. In tanks that received GRF, the mean  $K_d$  value was  $3.77 \text{ m}^{-1}$ . This was higher than what occurs in many glacially-fed, natural lakes. Glacially-fed lakes in New Zealand, Chile, and Canada have mean  $K_{ds}$  of  $0.96 \text{ m}^{-1}$  and a maximum of  $2.28 \text{ m}^{-1}$  (Rose et al., 2014). Lakes in the US Rocky Mountains do not exceed  $K_d$  of  $0.30 \text{ m}^{-1}$  (Slemmons and Sarros, 2012) and  $K_d$  in glacially-fed Mascaridi Lake in Argentina is often between  $0.40$  and  $0.75 \text{ m}^{-1}$  (Modenutti et al., 2000; Hylander et al., 2011). Our  $K_d$  values are likely higher than those that occur in water bodies, due to the smaller scale of our experiment, the lack of flow in our mesocosm tanks, and the higher rate of GRF addition. In natural systems, GRF inputs are relatively constant due to consistent tributary inflows creating horizontal gradients in turbidity as particles fall out of suspension with increasing distance from tributary inflows (Laspoumaderes et al., 2013).

Our experimental approach was to manipulate light while maintaining nutrient concentrations. We wanted to ensure that the GRF additions were not adding or precipitating nutrients in the experimental tanks. TN, TDN,  $\text{NO}_3^-$ ,  $\text{NH}_4^+$ , and TDP concentrations remained largely unchanged throughout this 9-day experiment. The change in TP from days 9 to 0 was significantly different in the chlorophyte-dominated tanks compared to the cyanophyte-dominated tanks, but not compared to the control tanks. If the addition of GRF precipitated P from the water column, we would have expected to see a decline in TP in all of the GRF tanks, including both the chlorophyte- and cyanophyte- dominated tanks. This was not the case as TP only declined by  $0.01 \mu\text{mol L}^{-1}$  in the chlorophyte-dominated tanks. We believe the decrease in cyanophyta and

increase in cryptophyta can be attributed to reduced light and not an increase in P deficiency because we also saw no significant change in the ln(TN:TP) molar ratio in any of the tanks.

Microcystin concentrations were low throughout the experiment but increased in all tanks between days 0 and 9. The decline in cyanophyta in the chlorophyte- and cyanophyte- dominated tanks could explain the increase in microcystin concentrations. As cyanobacterial cells lyse, they can release intracellular microcystin into the water column (Greenfield et al., 2014). Microcystin concentrations never exceeded  $4.04 \mu\text{g L}^{-1}$  on day 9 and increases in microcystin between days 0 and 9 were never more than  $0.17 \mu\text{g L}^{-1}$ , despite the declines we observed in cyanophyta. Non-toxic strains of the cyanobacterium *Microcystis* outcompete toxic strains at low light levels (Kardinaal et al., 2007), which could be why we did not see a greater increase in microcystin concentrations following the addition of GRF.

We anticipated that increased turbidity resulting from GRF additions would negatively impact zooplankton abundance and diversity, especially for filter-feeding cladocerans (Sommaruga, 2015). High concentrations of suspended particles can make it difficult for filter-feeding cladocerans to obtain food and they are often absent from lakes with high GRF inputs (Barouillet et al., 2019). Copepods are able to survive higher turbidities than other zooplankton (Sommaruga, 2015). We observed a decline in cladoceran, adult copepod, and copepod nauplii abundance in the chlorophyte- and cyanophyte- dominated tanks. The decline in cladocerans could be the result of an increase in fine particulates, which interferes with their ability to filter organic particles out of the water (Sommaruga, 2015; Barouillet et al., 2019). In our experiment,

cladocerans declined in tanks that received GRF, but increased in the control tanks. A longer study period is necessary to properly evaluate whether the decline in zooplankton we observed is a direct result of GRF application, or simply natural variation in the population. Our 9-day experiment was not long enough to see a dramatic change in the zooplankton community life cycle as cladocerans can live for 15 – 50 days depending on species (Sarma et al., 2002), and lay new egg clutches every 3 – 7 days (Dodson and Frey, 1991). It is not uncommon for many copepods to live up to a year (Allan, 1976), and it can take a month before nauplii reach sexual maturity (Gilbert and Williamson, 1983). The additional time it would take for at least one generation of zooplankton to be born likely explains why we did not see a significant change in zooplankton abundance by day 9 of our experiment. Our findings suggest that additional work is needed over a longer time period to better understand how the addition of GRF impacts zooplankton communities.

The dominant cyanophyte in cyanophyte-dominated tanks at the beginning of the experiment was *Aphanizomenon*. While *Aphanizomenon* has been shown to persist at light levels as low as 50  $\mu\text{mol photons m}^{-2} \text{ s}^{-1}$  in culture, its highest growth rates occur above 150  $\mu\text{mol photons m}^{-2} \text{ s}^{-1}$  (Hadas et al., 2002; Üveges et al., 2012) and it is often outcompeted in reduced light environments (Huisman et al., 1999). *Cryptomonas*, the most common cryptophyte on day 9, can dominate algal communities when light levels are as low as 15  $\mu\text{mol photons m}^{-2} \text{ s}^{-1}$  (Lizotte and Priscu, 1992). The reduced light environment created from GRF addition could have enabled *Cryptomonas* to replace *Aphanizomenon* as the most prevalent genera.

The switch from a cyanophyte-dominated community to one where cryptophytes are the dominant taxon is efficient and beneficial for trophic interactions. Cyanophytes create inefficient trophic transfers due to their low composition of polyunsaturated fatty acids (Brett et al., 2009). Zooplankton meet most of their polyunsaturated fatty acid requirements from eukaryotic phytoplankton and are not able to survive long periods when these fatty acids are unavailable (Grosbois et al., 2017). Cyanophytes can be too large for many gape-limited grazers to consume, either because they form mucilaginous colonies or long filaments (Haney, 1987). The production of cyanotoxins can also be detrimental to grazers, but the magnitude of these effects are debated (Rohrlack et al., 2001; Paes et al., 2016). Conversely, cryptophytes are highly nutritious and are an important component of aquatic food webs (Stemberger and Gilbert, 1985; Sarnelle, 1993). Thus, the switch from cyanophyte- to cryptophyte-dominated phytoplankton communities likely provided a net benefit to the treated mesocosms by creating a highly edible phytoplankton community for primary consumers.

#### *Which Functional Traits Enabled Cryptophytes to Replace Cyanophytes?*

Both cryptophytes and cyanophytes can tolerate low light, but in our study, cryptophytes replaced cyanophytes when GRF was added. Cryptophytes, especially of the genus *Cryptomonas*, are better suited to sustained periods of reduced light availability and are often the dominant phytoplankton in permanently ice-covered lakes (Gervais, 1998). *Cryptomonas* was the most common cryptophyte we observed on day 9 in tanks that were originally dominated by cyanophytes on day 0 (Table A1.2). Cryptophytes can position themselves at favorable light intensities using their 2 flagella, and many are mixotrophs that can supplement their metabolic (Porter, 1988) and nutrient (Urabe et al.,

2000) requirements with heterotrophy. This is consistent with existing projections that protists sometimes use phagotrophy to survive and outcompete phototrophs at low irradiance levels (Jones, 2000; Schwaderer et al., 2011). The ability to acquire energy through both heterotrophy and autotrophy provides mixotrophs with a competitive advantage (Tittle et al., 2003). Some models even suggest a positive relationship between mixotrophy and primary productivity (Hammer and Pitchford, 2005; Stoecker et al., 2017) because mixotrophs can use phagotrophy to relieve nutrient stress, enabling them to be productive in nutrient-deficient conditions (Jost et al., 2004). None of our tanks were nutrient sufficient (Guildford and Hecky, 2000). Phagotrophy might explain why  $GPP^B$  increased in all of them, albeit at low rates. Our maximum increases of  $7.6 \text{ mmol O}_2 [\mu\text{g Chl-a}^{-1}] \text{ m day}^{-1}$  are consistent with low increases in GPP for phagocytic phytoplankton (Hammer and Pitchford, 2005).

The increase in  $GPP^B$  over the course of the experiment also suggests that the new cryptophyte-dominated community used light more efficiently than the previous chlorophyte- or cyanophyte- dominated communities. Phycobiliproteins, secondary pigments present in both cyanophytes and cryptophytes, can lead to an inverse relationship between  $\alpha^B$  and PAR that is contrary to the positive relationship observed in other phytoplankton groups (MacIntyre et al., 2002; Overkamp et al., 2014). This could explain why  $\alpha^B$  in the chlorophyte-dominated tanks, which switched from a chlorophyte- to a cryptophyte- dominated community increased, and why  $\alpha^B$  in the cyanophyte-dominated tanks did not change. Cyanophyta can have  $E_k$  values between 150.82 and  $783.30 \mu\text{mol photons m}^{-2} \text{ s}^{-1}$  (Zhang et al., 2011), while cryptophytes under ice cover have been between 15 and  $45 \mu\text{mol photons m}^{-2} \text{ s}^{-1}$  (Lizotte and Priscu, 1992). Our

cyanophyte-dominated tanks experienced a 2.5-fold decrease in  $E_K^B$  from day 0 to 9, suggesting that the shift to dominance by cryptophytes impacted P–E parameters.

Eukaryotic phytoplankton are physiologically stressed at  $\phi_{PSII}$  values below 0.65, while cyanophyta thresholds are lower, typically between 0.4 and 0.6 (Campbell et al., 1998; Kromkamp et al., 2008). In our cyanophyte-dominated tanks,  $\phi_{PSII}$  increased from 0.34 to 0.48 over the course of the experiment, corresponding with a decline in prokaryotic cyanophyta and an increase in eukaryotic cryptophytes. The control and chlorophyte tanks remained dominated by eukaryotes throughout the experiment and exhibited little change in  $\phi_{PSII}$ . Phytoplankton communities in all tanks were physiologically stressed throughout the experiment.

#### *What Implications do our Findings Have for the Nutrient Load Hypothesis?*

Our findings provide important insights for the nutrient load hypothesis (Brauer et al., 2012), which predicts phytoplankton dominance based on nutrient concentrations and light availability. It postulates that in low-nutrient environments, the  $\ln(\text{TN}:\text{TP})$  ratio will determine phytoplankton composition while in high-nutrient systems, absolute nutrient concentrations explain which species dominate (Brauer et al., 2012). Increased nutrient enrichment leads to an increase in algal biomass, which in turn reduces light availability through self-shading. Thus, when absolute nutrient concentrations are high, light becomes the single limiting resource. This hypothesis assumes that cyanophyta are superior competitors for light and will dominate the community unless light limitation is reached, at which point total phytoplankton biomass is expected to decline (Brauer et al., 2012). Our results suggest the assumption that cyanophytes will be sole “winners” in this scenario should be revised to include phytoplankton functional traits (Figure 2.5). These

functional traits could enable certain taxa to thrive in the reduced light environment created by bloom formation and self-shading.

The nutrient load hypothesis does consider some functional traits for cyanophyta such as their ability to fix atmospheric N<sub>2</sub> or regulate their buoyancy with gas vacuoles. In our experiment, heterocystous N<sub>2</sub> fixation rates were insubstantial given the low (mean= 5,850 cells L<sup>-1</sup>) number enumerated. The ln(TN:TP) ratios were lowest in the cyanophyte-dominated tanks, but were always between the N- and P- deficiency thresholds where it can be N, P, or something else that limits growth (Guildford and Hecky, 2000). This, along with the increase in NH<sub>4</sub><sup>+</sup> concentrations observed from days 0 to 9, suggest that the cyanophyte-dominated tanks were not N-deficient. Functional traits for other phytoplankton groups, such as mixotrophy or flagella, both of which might enable other phytoplankton to dominate in low light environments, are not considered (Brauer et al., 2012). Contrary to predictions from the nutrient load hypothesis (Brauer et al., 2012), cyanophyta were not the dominant taxa at the end of our experiment. Cryptophytes were, suggesting that at high nutrient concentrations, functional traits add nuance to competition for light not previously considered.

While cyanobacteria often dominate when light is the limiting resource, our findings suggest that cryptophytes can outcompete cyanobacteria under low light levels. In Lake Peipsi, Estonia/Russia, cyanobacteria are replaced by cryptophytes shortly after the formation of ice and its associated reduction in light availability (Blank et al., 2009). Further experimentation is required to quantify the thresholds where this shift from nutrient stoichiometry to functional traits occurs, but the importance of functional traits in determining phytoplankton community composition should not be overlooked.

### *How does GRF Compare to Other Geoengineering Strategies?*

One of the challenges faced by lake managers and drinking water treatment plant operators is mitigating or controlling harmful algal blooms. In 2014, a toxic cyanobacterial bloom in Lake Erie cost the Toledo drinking water plant ~\$4 million and had a total economic impact of ~\$65 million (Bingham et al., 2015). Reductions in external nutrient loading can successfully lower cyanobacterial biomass, but it usually takes years after government regulations have been enacted before declines in biomass are observed (Osgood, 2017). Sometimes, managers need to reduce phytoplankton biomass over a much shorter time scale if, for example, the resource is being used for drinking water. In other instances, it might not always be feasible to reduce external nutrient loading, such as in water bodies with watersheds dominated by agriculture or urban areas. In these situations, alternative geoengineering strategies can be used. Solid-phase P sorbents may be the most common geoengineering approach. These materials are clays enriched with aluminum (Gibbs et al., 2010), iron (Zamparas et al., 2012), or lanthanum (Haghseresht et al., 2009) and work by binding to any soluble reactive P they contact as they sink through the water column.

One benefit of GRF over other geoengineering techniques is its effectiveness on a short timescale. We saw a 49.4 and 77.6% decline in cyanobacteria in chlorophyte- and cyanophyte-dominated tanks, respectively, after 9 days. This decline occurred more quickly than the several months to a year phytoplankton biomass declines after the addition of solid-phase P sorbents (Epe et al., 2017; Wagner et al., 2017). Re-application of solid-phase P sorbents can be required in as short as a couple of years to as long as a decade, depending on lake morphology, nutrient inputs, inorganic particle inputs, and

sedimentation rates (Lürling and van Oosterhout, 2012; Mackay et al., 2014; Wagner et al., 2017). Another benefit of GRF is that it results in a decrease in cyanobacteria, but not total phytoplankton biovolume, while solid-phase P sorbents are typically associated with a decline in total phytoplankton biomass (Epe et al., 2017). Maintaining phytoplankton biomass is important in systems where fish yield is a concern (Downing and Plante, 1993).

A consideration to using GRF is that it adds inorganic particles into the water, a concern in reservoirs with limited storage capacity (deNoyelles and Kastens, 2016). Of the 14 tanks that received GRF, the highest TSS sedimentation rate was  $3.4 \text{ g m}^{-2} \text{ day}^{-1}$ . This rate is well within the range of natural sedimentation and is lower than some rates found in the North American Midwest. Sedimentation rates in Iowa lakes can range from 11.6 to as high as  $203.0 \text{ g m}^{-2} \text{ day}^{-1}$  during the summer (Canfield et al., 1982). We added GRF based on tank surface area at a rate of  $0.68 \text{ kg m}^{-2} \text{ day}^{-1}$ . For the average small impoundment of  $0.027 \text{ km}^2$  (Downing et al., 2006), this would come to  $39,706 \text{ kg day}^{-1}$ . At this application rate, it would cost \$35,854 USD, based on the \$18.06 USD per kg price at which we purchased GRF. Such a high application rate and cost likely makes GRF an untenable management strategy in large systems. Using surface area from our mesocosms to calculate cost for a pond is a rough estimation and assumes that application rates are constant based on surface area. Other factors, such as wind blowing the GRF to one side of the impoundment, or disruptions to the water's surface from animals could influence the amount of GRF required for an impoundment compared to a mesocosm.

Another consideration to the use of GRF is that it must be applied more frequently than most other geoengineering techniques, at least initially. Frequent GRF additions may

not be required if the phytoplankton community shifts to an alternative stable state. The alternative stable state hypothesis posits that ecosystems maintain resilience and do not experience state change until a dramatic disturbance shifts the ecosystem to a different state with its own resilience (Scheffer et al., 2001; Carpenter and Brock, 2006).

Disturbances can include modifications to habitat or changes in resource availability (Shurin et al., 2004). Competition for one such resource, light, could create an alternate stable state, especially if the existing phytoplankton community was replaced (Brauer et al., 2012). We were able to shift a cyanophyte- dominated phytoplankton community to dominance by cryptophytes in 9 days but we did not continue the experiment long enough to see if an alternate stable state was achieved, nor the time point at which further GRF additions would be unnecessary. In Shidou Reservoir, China, cyanophyta made up ~100% of the phytoplankton biovolume before an abrupt reduction in the human population within the watershed shifted the phytoplankton community to dominance by chlorophytes (Yang et al., 2017). This shift was sustained for ~3 years, during which time cyanophytes made up less than 20% of phytoplankton biomass, before a climatic disturbance event shifted the community back to dominance by cyanophytes (Yang et al., 2017). Additional experimentation should investigate long-term trends in the phytoplankton community to determine if GRF application is able to shift the phytoplankton community to an alternative stable state.

The effects of GRF to higher trophic levels will be important when determining whether it should be used in cyanoHAB management. The reduction in light availability from GRF additions could reduce the foraging efficiency of visual predators (Minor and Stein, 1996; Vogel and Beauchamp, 1999). GRF also increases the amount of suspended

inorganic particles, which can have a negative impact on fish by damaging gills (Lake and Hinch, 1999) or reducing the filtering efficiency of filter-feeders (Sommaruga, 2015). These effects to biota might not be substantial if short periods of GRF application result in a shift to an alternate stable state. In addition to aquatic biota, the extraction of GRF might impact the terrestrial environment. Commercial GRF is mined from terminal moraines located in the northwestern United States and southwestern Canada, and is sold as a soil amendment for micronutrients. Additional studies should evaluate the long-term effects of GRF addition to higher trophic levels and on the terrestrial environment before its adoption as a widespread management strategy.

### *Conclusions*

We demonstrate GRF application reduces light availability, resulting in a decline in cyanophytes and replacement by cryptophytes. Our findings provide valuable insights to the nutrient load hypothesis (Brauer et al., 2012), suggesting that cryptophytes might outcompete cyanophytes for light when nutrients are abundant. Further iterations of this hypothesis should consider incorporating functional traits into predictions of phytoplankton community composition. Before GRF can be advocated as a harmful algal bloom management strategy, further investigation is needed to determine whether an alternative stable state was reached after cryptophytes became the dominant taxa. Regardless, we believe that manipulating light is an important, overlooked strategy for algal bloom management. As the effects of climate change become more pronounced, algal blooms will continue to increase in frequency and magnitude (Paerl and Paul, 2012), and it will become even more important for lake managers to have a variety of techniques to address this challenge.

## LITERATURE CITED

- Allan, J.D., 1976. Life history patterns in zooplankton. *The American Naturalist*. 110:165–180.
- APHA, 2017. *Standard Methods for the Examination of Water and Wastewater*. 23<sup>rd</sup> ed., eds. Baird, R.B., Eaton, A.D., Rice, E.W. Washington DC: American Public Health Association, Denver: American Water Works Association, Alexandria: Water Environment Federation.
- Backer, L.C., J.H. Landsberg, M. Miller, K. Keel & T.K. Taylor, 2013. Canine cyanotoxin poisonings in the United States (1920s–2012): review of suspected and confirmed cases from three data sources. *Toxins* 5:1597–1628.
- Bartson, S., J. Ogilvie, A.J. Petroff, G.R. Smith & J.E. Rettig, 2018. Effect of pond dye on the response of Southern Leopard Frog tadpoles (*Lithobates sphenoccephalus*) to Western Mosquitofish (*Gambusia affinis*) cues. *Basic and Applied Herpetology* 32:71–76.
- Barouillet, C., B.F. Cumming, K.R. Laird, C.J. Perrin & D.T. Selbie, 2019. Influence of glacial flour on the primary and secondary production of sockeye salmon nursery lakes: a comparative modern and paleolimnological study. *Canadian Journal of Fisheries and Aquatic Sciences* 76:2303–2314.
- Bellinger, E.G. & D.C. Sigeo, D.C., 2010. *Freshwater Algae: Identification and Use as Bioindicators*. Chichester: Chichester John Wiley & Sons, Ltd.
- Bingham, M., S.K. Sinha & F. Lupi, 2015. Economic benefits of reducing harmful algal blooms in Lake Erie: Environmental Consulting and Technology Inc., Technical Report.
- Blank, K., J. Haberman, M. Haldna & R. Laugaste, 2009. Effect of winter conditions on spring nutrient concentrations and plankton in a large shallow Lake Peipsi (Estonia/Russia). *Aquatic Ecology* 43:745–753.
- Bloesch, J. & N.M. Burns, 1980. A critical review on sedimentation trap technique. *Aquatic Sciences* 42:15–55.
- Brauer, V.S., M. Stomp & J. Huisman, 2012. The nutrient-load hypothesis: Patterns of resource limitation and community structure driven by competition for nutrients and light. *The American Naturalist* 179:721–740.
- Brett, M.T., M.J. Kainz, S.J. Taipale & H. Seshan, 2009. Phytoplankton, not allochthonous carbon, sustains herbivorous zooplankton production. *Proceedings of the National Academy of Sciences* 106:21197–21201.
- Bristow, B.T., R.C. Summerfelt & R.D. Clayton, 1996. Comparative performance of intensively cultured larval walleye in clear, turbid, and colored water. *The Progressive Fish-Culturist* 58:1–10.

- Brooks, B.W., J.M. Lazorchak, M.D.A. Howard, M.V. Johnson, S.L. Morton, D.A.K. Perkins, E.D. Reavie, G.I. Scott, S.A. Smith & J.A. Steevens, 2016. Are harmful algal blooms becoming the greatest inland water quality threat to public health and aquatic ecosystems? *Environmental Toxicology and Chemistry* 35:6–13.
- Burkholder, J.M. & R.G. Wetzel, 1989. Epiphytic microalgae on natural substrata in a hardwater lake: Seasonal dynamics of community structure, biomass and ATP content. *Archiv fur Hydrobiologie* 83:1–56.
- Campbell, D., V. Hurry, A.K. Clarke, P. Gustafsson & G. Öquist, 1998. Chlorophyll fluorescence analysis of cyanobacterial photosynthesis and acclimation. *Microbiology and Molecular Biology Reviews* 62:667–683.
- Canfield, D.E., J.R. Jones & R.W. Bachmann, 1982. Sedimentary losses of phosphorus in some natural and artificial Iowa lakes. *Hydrobiologia* 87:65–76.
- Carmichael, W.W., S.M. Azevedo, J.S. An, R.J. Molica, E.M. Jochimsen, S. Lau, K.L. Renhart, G.R. Shaw & G.K. Eaglesham, 2001. Human fatalities from cyanobacteria: chemical and biological evidence for cyanotoxins. *Environmental Health Perspectives* 109:663–668.
- Carpenter, S.R. & W.A. Brock, 2006. Rising variance: a leading indicator of ecological transition. *Ecology Letters* 9:311–318.
- Casassa, G., P. López, B. Pouyaud & F. Escobar, 2009. Detection of changes in glacial run-off in alpine basins: examples from North America, the Alps, central Asia and the Andes. *Hydrological Processes* 23:31–41.
- Chanudet, V. & M. Filella, 2009. Size and composition of inorganic colloids in a peri-alpine, glacial flour-rich lake. *Geochimica et Cosmochimica Acta* 72:1466–1479.
- Chapman, A. & A. Foss, 2019. Potentially Toxicogenic (PTOX) Cyanobacteria List. GreenWater Laboratories Technical Report.
- Chorus, I. & J. Bartram, 1999. *Toxic Cyanobacteria in Water: A guide to their public health consequences, monitoring and management*. London: E & FN Spon.
- Crumpton, W.G., T.M. Isehart & P.D. Mitchell, 1992. Nitrate and organic N analyses with second derivative spectroscopy. *Limnology and Oceanography* 37:907–913.
- Deacon, C. & A.E. Walsby, 1990. Gas vesicle formation in the dark, and in the light of different irradiances, by the cyanobacterium *Microcystis* sp. *British Phycological Journal* 25:133–139.
- deNoyelles, F. & J.H. Kastens, 2016. Reservoir sedimentation challenges Kansas. *Transactions of the Kansas Academy of Science* 119:69–81.
- Dodds, W.K., W.W. Bouska, J.L. Eitzmann, T.J. Pilger, K.L. Pitts, A.J. Riley, J.T. Schloesser & D.J. Thornbrugh, 2009. Eutrophication of U.S. freshwaters: analysis of potential economic damages. *Environmental Science and Technology*. 43:12–19.

- Dodson, S.I. & D.G. Frey, 1991. "Cladocera and other Banchiopoda," in Ecology and Classification of North American Freshwater Invertebrates, eds. J.H. Thorp, & A.P. Covich (London, Eng: Academic Press), 723–763.
- Downing, J.A. & C. Plante, 1993. Production of fish populations in lakes. *Canadian Journal of Fisheries and Aquatic Sciences* 50:110–120.
- Downing, J.A., Y.T. Prairie, J.J. Cole, C.M. Duarte, L.J. Tranvik, R.G. Striegl, W.H. McDowell, P. Kortelainen, N.F. Caraco, J.M. Melack & J.J. Middelburg, 2006. The global abundance and size distribution of lakes, ponds, and impoundments. *Limnology and Oceanography* 51:2388–2397.
- Epe, T.S., K. Finsterle & S. Yasseri, 2017. Nine years of phosphorus management with lanthanum modified bentonite (Phoslock in a eutrophic, shallow swimming lake in Germany). *Lake and Reservoir Management* 33:119–129.
- Falkowski, P.G. & J. LaRoche, 1991. Acclimation to spectral irradiance in algae. *Journal of Phycology* 27:8–14.
- Fee, E.J., 1990. Computer programs for calculating in-situ phytoplankton photosynthesis. Canadian Technical Report of Fisheries and Aquatic Sciences No. 1740.
- Gee, G.W. & J.W. Bauder, 1979. Particle size analysis by hydrometer: A simplified method for routine textural analysis and a sensitivity test of measurement parameters. *Soil Science Society of America Journal* 43:1004–1007.
- Gervais, F., 1998. Ecology of cryptophytes coexisting near a freshwater chemocline. *Freshwater Biology* 39:61–78.
- Gibbs, M.M., C.W. Hickey & D. Özkundakci, 2010. Sustainability assessment and comparison of efficacy of four P-inactivation agents for managing internal phosphorus loads in lakes: sediment incubations. *Hydrobiologia* 658:253–275.
- Gilbert, J.J. & C.E. Williamson, 1983. Sexual dimorphism in zooplankton (Copepoda, Cladocera, and Rotifera). *Annual Review of Ecology, Evolution, and Systematics* 14:1–33.
- Greenfield, D.I., A. Duquette, A. Goodson, C.J. Keppler, S.H. Williams, L.M. Brock, K.D. Stackley, D. White & S.B. Wilde, 2014. The effects of three chemical algaecides on cell numbers and toxin content of the cyanobacteria *Microcystis aeruginosa* and *Anabaenopsis* sp. *Environ. Manage.* 54, 1110–1120.
- Grosbois, G., H. Mariash, T. Schneider & M. Rautio, 2017. Under-ice availability of phytoplankton lipids is key to freshwater zooplankton winter survival. *Scientific Reports* 7:11543.
- Grosse, Y., R. Baan, K. Straif, B. Secretan, F.E. Ghisassi & V. Coglianò, 2006. Carcinogenicity of nitrate, nitrite, and cyanobacterial peptide toxins. *The Lancet Oncology* 7:628–629.

- Guildford, S.J. & R.E. Hecky, 2000. Total nitrogen, total phosphorus, and nutrient limitation in lakes and oceans: is there a common relationship? *Limnology and Oceanography* 45:1213–1223.
- Guiry, M.D. & G.M. Guiry, 2020. AlgaeBase. World-wide electronic publication, National University of Ireland, Galway. <https://www.algaebase.org>
- Hadas, O., R. Pinkas, N. Malinsky-Rushansky, G. Shalev-Alon, E. Delphine, T. Berner, A. Sukenik & A. Kaplan, 2002. Physiological variables determined under laboratory conditions may explain the bloom of *Aphanizomenon ovalisporum* in Lake Kinneret. *European Journal of Phycology* 37:259–267.
- Haghsereht, F., S. Wang & D. Do, 2009. A novel lanthanum-modified bentonite, Phoslock®, for phosphate removal from wastewaters. *Applied Clay Science* 46:369–375.
- Hammer, A.C. & J.W. Pitchford, 2005. The role of mixotrophy in plankton bloom dynamics, and the consequences for productivity. *ICES J. Mar. Sci.* 5, 833–840.
- Haney, J.F., 1987. Field studies on zooplankton-cyanobacteria interactions. *New Zealand Journal of Marine and Freshwater Research* 21:467–475.
- Harris, T., J. Yun, D.S. Baker, J. Kastens, B. Sturm, P. Leavitt, M. Ketterer & A.S. Amand, 2020. Phytoplankton and water quality in Milford Reservoir: results of paleolimnological sediment core and historical data analyses. Kansas Biological Survey Report No. 197.
- Hecky, R.E. & S.J. Guildford, 1984. Primary productivity of Southern Indian Lake before, during, and after impoundment and Churchill River diversion. *Canadian Journal of Fisheries and Aquatic Sciences* 41:591–604.
- Heisler, J., P.M. Glibert, J.M. Burkholder, D.M. Anderson, W. Cochlan, W.C. Dennison, Q. Dortch, C.J. Gobler, C.A. Heil, E. Humphries, A. Lewitus, R. Magnien, H.G. Marshall, K. Sellner, D.A. Stockwell, D.K. Stoecker & M. Suddleson, 2008. Eutrophication and harmful algal blooms: a scientific consensus. *Harmful Algae* 8:3–13.
- Hillebrand, H., C.D. Dürselen, D. Kirschtel, U. Pollinger & T. Zohary, 1999. Biovolume calculation for pelagic and benthic microalgae. *Journal of Phycology* 35:403–424.
- Huisman, J., R.R. Jonker, C. Zonneveld & F.J. Weissing, 1999. Competition for light between phytoplankton species: experimental tests of mechanistic theory. *Ecology* 80:211–222.
- Hylander, S., T. Jephson, K. Lebet, J. Einem, T. Fagerberg, E. Balseiro, B. Modenutti, M.S. Souza, C. Laspoumaderes, M. Jönsson, P. Ljungberg, A. Nicolle, P.A. Nilsson, L. Ranåker & L.-A. Hansson, 2011. Climate-induced input of turbid glacial meltwater affects vertical distribution and community composition of phyto- and zooplankton. *Journal of Plankton Research* 33:1239–1248.

- Ibelings, B.W., M. Bormans, J. Fastner & P.M. Visser, 2016. CYANOCOST special issue on cyanobacterial blooms: synopsis – a critical review of the management options for their prevention, control and mitigation. *Aquat. Ecol.* 50, 595–605.
- Isles, P.D.F., 2020. The misuse of ratios in ecological stoichiometry. *Ecology* 101:e03153.
- Jones, R.I., 2000. Mixotrophy in planktonic protists: an overview. *Freshwater Biology* 45:219–226.
- Jost, C., C.A. Lawrence, F. Campolongo, W. van de Bund, S. Hill, & D.L. DeAngelis, 2004. The effects of mixotrophy on the stability and dynamics of a simple planktonic food web model. *Theoretical Population Biology* 66:37–51.
- Kalff, J., 2002. *Limnology: Inland Water Ecosystems*. New Jersey: Prentice Hall.
- Kardinaal, W.E.A., L. Tonk, I. Janse, S. Hol, P. Slot, J. Huisman & P.M. Visser, 2007. Competition for light between toxic and nontoxic strains of the harmful cyanobacterium *Microcystis*. *Applied and Environmental Microbiology* 73:2939–2946.
- Kirk, J.T., 1994. *Light and Photosynthesis in Aquatic Ecosystems*. Oxford: Oxford University Press.
- Knowlton, M.F., 1984. Flow-through microcuvette for fluorometric determination of chlorophyll. *Water Resources Bulletins* 20:795–799.
- Kromkamp, J.C., N.A. Dijkman, J. Peene, S.G.H. Simms & H.J. Gons, 2008. Estimating phytoplankton primary production in Lake IJsselmeer (The Netherlands) using variable fluorescence (PAM-FRRF) and C-uptake technique. *European Journal of Phycology* 43:327–344.
- Lake, R.G. & S.G. Hinch, 1999. Acute effects of suspended sediment angularity on juvenile coho salmon (*Oncorhynchus kisutch*). *Canadian Journal of Fisheries and Aquatic Sciences* 56:862–867.
- Laspoumaderes, C., B. Modenutti, M.S. Souza, M.B. Navarro, F. Cuassolo & E. Balseiro, 2013. Glacier melting and stoichiometric implications for lake community structure: Zooplankton species distributions across a natural light gradient. *Global Change Biology* 19:316–326.
- Lee, R.E., 2008. *Phycology*. Cambridge: Cambridge University Press.
- Lehman, P.W., K. Marr, G.L. Boyer, S. Acuna & S.J. Teh, 2013. Long-term and causal factors associated with *Microcystis* abundance and toxicity in San Francisco Estuary and implication for climate change impacts. *Hydrobiologia* 718:141–158.
- Lizotte, M.P. & J.C. Prisco, 1992. Photosynthesis–Irradiance relationships in phytoplankton from the physically stable water column of a perennially ice-covered lake (Lake Bonney, Antarctica). *Journal of Phycology* 28:179–185.

- Ludwig, G.R., P. Perschbacher R. Edziyie, 2008. The effect of the dye Aquashade® on water quality, phytoplankton, zooplankton, and sunshine bass, *Morone chrysops* x *M-saxatilis*, fingerling production in fertilized culture ponds. *Journal of the World Aquaculture Society* 41:40–48.
- Lund, J.W.G., C. Kipling & E.D. LeCren, 1958. The inverted microscope method of estimating algal numbers and the statistical basis of estimates by counting. *Hydrobiologia* 11:143–170.
- Lürling, M. & F. van Oosterhout, 2012. Case study on the efficacy of a lanthanum-enriched clay (Phoslock®) in controlling eutrophication in Lake Het Groene Eiland (The Netherlands). *Hydrobiologia* 710:253–263.
- Lürling, M., F. Eshetu, E.J. Faassen, S. Kosten & V.L.M. Husza, 2013. Comparison of cyanobacterial and green algal growth rates at different temperatures. *Freshwater Biology* 58:552–559.
- MacIntyre, H.L., T.M. Kana, T. Anning & R.J. Geider, 2002. Photoacclimation of photosynthesis irradiance response curves and photosynthetic pigments in microalgae and cyanobacteria. *Journal of Phycology* 38:17–38.
- Mackay, E.B., S.C. Maberly, G. Pan, K. Reitzel, A. Bruere, N. Corker, G. Douglas, S. Egemose, D.P. Hamilton, T. Hatton-Ellis, B.J. Huser, W. Li, S. Meis, B. Moss, M. Lürling, G. Phillips, S. Yasseri & B.M. Spears, 2014. Geoengineering in lakes: welcome attraction or fatal distraction? *Inland Waters* 4:349–356.
- Miller, M.A., R.M. Kudela, A. Mekebri, D. Crane, S.C. Oates, M.T. Tinker, M. Staedler, W.A. Miller, S. Yoy-Choutka, C. Dominik, D. Hardin, G. Langlois, M. Murray, K. Ward & D.A. Jessup, 2010. Evidence for a novel marine harmful algal bloom: cyanotoxin (microcystin) transfer from land to sea otters. *PLoS ONE* 5:e12576.
- Miner, J.G. & R.A. Stein, 1996. Detection of predators and habitat choice by small bluegills: Effect of turbidity and alternative prey. *Transactions of the American Fisheries Society* 125:97–103.
- Moore, R.D., S.W. Fleming, B. Menounos, R. Wheate, A. Fountain, K. Stahl, K. Holm & M. Jakob, 2009. Glacier change in western North America: influences on hydrology, geomorphic hazards and water quality. *Hydrological Processes* 23:42–61.
- Modenutti, B., G. Pérez, E. Balseiro & C. Queimalinos, 2000. The relationship between light attenuation, chlorophyll a and total suspended solids in a Southern Andes glacial lake. *Verhandlung des Internationalen Verein Limnologie* 27:1–4.
- Osgood, R.A., 2017. Inadequacy of best management practices for restoring eutrophic lakes in the United States: guidance for policy and practice. *Inland Waters* 7:401–407.
- Overkamp, K.E., R. Gasper, K. Kock, C. Herrmann, E. Hofmann & N. Frankenberg-Dinkel, 2014. Insights into the biosynthesis and assembly of cryptophycean phycobiliproteins. *Journal of Biological Chemistry* 289:26691–26707.

- Paerl, H.W., J. Tucker & P.T. Bland, 1983. Carotenoid enhancement and its role in maintaining blue-green algal (*Microcystis aeruginosa*) surface blooms. *Limnology and Oceanography* 28:847–857.
- Paerl, H.W. & J. Huisman, 2009. Climate change: a catalyst for global expansion of harmful cyanobacterial blooms. *Environmental Microbiology Reports* 1:27–37.
- Paerl, H.W. & V.J. Paul, 2012. Climate change: links to global expansion of harmful cyanobacteria. *Water Research* 46:1349–1363.
- Paes T.A.S.V., I.A.S. Costa, A.P.C. Silva & E.M. Eskinazi-Sant’Anna, 2016. Can microcystins affect zooplankton structure community in tropical eutrophic reservoirs? *Brazilian Journal of Biology* 76:450–460.
- Petty, E.L., D.V. Obrecht, D.V. & R.L. North, 2020. Filling in the flyover zone: high phosphorus in midwestern (USA) reservoirs results in high phytoplankton biomass but not high primary productivity. *Frontiers in Environmental Science* 8:111.
- Porter, K.G., 1988. Phagotrophic phytoflagellates in microbial food webs. *Hydrobiologia* 159:89–97.
- R Core Team, 2019. R: a language and environment for statistical computing. R Foundation for Statistical Computing, Vienna, Austria. URL <https://www.R-project.org/>.
- Rampe, E.B., B. Horgan, N. Scudder, R.J. Smith & A.M. Rutledge, 2017. Mineralogy of rock flour in glaciated volcanic terrains: an analog for a cold and icy early Mars. NASA Technical Report JSC-CN-38727.
- Raven, J.A. & K. Richardson, 1984. Dinophyte flagella: a cost-benefit analysis. *New Phytologist* 98:259–276.
- Robarts, R.D. & T. Zohary, 1987. Temperature effects on photosynthetic capacity, respiration, and growth rates of bloom-forming cyanobacteria. *New Zealand Journal of Marine and Freshwater Research* 21:391–399.
- Rohrlack, T., E. Dittmann, T. Börner & K. Christoffersen, 2001. Effects of cell-bound microcystins on survival and feeding of *Daphnia* spp. *Applied and Environmental Microbiology* 67:3523–3529.
- Rose, K.C., D.P. Hamilton, C.E. Williamson, C.G. McBride, J.M. Fischer, M.H. Olson, J.E. Saros, M.G. Allan & N. Cabrol, 2014. Light attenuation characteristics of glacially-fed lakes. *Journal of Geophysical Research Biogeosciences* 119:1446–1457.
- Salmaso, N., L. Naselli-Flores & J. Padisák, 2015. Functional classifications and their applications in phytoplankton ecology. *Freshwater Biology* 60:603–619.
- Sarma, S.S.S., S. Nandini & R.D. Gulati, 2002. Cost of reproduction in selected species of zooplankton (rotifers and cladocerans). *Hydrobiologia* 481:89–99.

- Sarnelle, O., 1993. Herbivore effects on phytoplankton succession in a eutrophic lake. *Ecological Monographs* 63:129–149.
- Sartory, D.P. & J.U. Grobbelaar, 1986. Extraction of chlorophyll-*a* from freshwater phytoplankton for spectrophotometric analysis. *Hydrobiologia* 114:117–187.
- Scheffer, M., S. Carpenter, J.M. Foley, C. Folke & B. Walker, 2001. Catastrophic shifts in ecosystems. *Nature* 413:591–596.
- Schwaderer, A.S., K. Yoshiyama, P. Pinto, N.G. Swenson, C.A. Klausmeier & E. Litchman, 2011. Eco-evolutionary differences in light utilization traits and distributions of freshwater phytoplankton. *Limnology and Oceanography* 56:589–598.
- Sharpley, A., B. Foy & P. Withers, 2000. Practical and innovative measures for the control of agricultural phosphorus losses to water: an overview. *Journal of Environmental Quality* 29:1–9.
- Shurin, J.B., P. Amarasekare, J.M. Chase, R.D. Holt, M.F. Hoopes & M.A. Leibold, 2004. Alternative stable states and regional community structure. *Journal of Theoretical Biology* 227:359–368.
- Silsbe, G.M., R.E. Hecky & R.E.H. Smith, 2012. Improved estimation of carbon fixation rates from active fluorometry using spectral fluorescence in light-limited environments. *Limnology and Oceanography Methods* 10:736–751.
- Silsbe, G.M. & S.Y. Malkin, 2015. phytotools: Phytoplankton Production Tools. R package version 1.0. <https://CRAN.R-project.org/package=phytotools>
- Sinha, R.P. & D.P. Häder, 2008. UV-protectants in cyanobacteria. *Plant Science* 174:278–289.
- Slemmons, K.E.H. & J.E. Saros, 2012. Implications of nitrogen-rich glacial meltwater for phytoplankton diversity and productivity in alpine lakes. *Limnology and Oceanography* 57:1651–1663.
- Slemmons, K.E.H., J.E. Saros & K. Simon, 2013. The influence of glacial meltwater on alpine aquatic ecosystems: a review. *Environmental Science Processes and Impacts* 15:1794–1806.
- Sommaruga, R. & G. Kandolf, 2014. Negative consequences of glacial turbidity for the survival of freshwater planktonic heterotrophic flagellates. *Scientific Reports* 4:4113.
- Sommaruga, R., 2015. When glaciers and ice sheets melt: consequences for planktonic organisms. *Journal of Plankton Research* 37:509–518.
- Spencer, D.F., 1984. Oxygen consumption by the crayfish *Orconectes propinquus* (Girard) exposed to Aquashade. *Bulletin of Environmental Contamination and Toxicology* 33:373–378.

- Stemberger, R.S. & J.J. Gilbert, 1985. Body size, food concentration, and population growth in planktonic rotifers. *Ecology* 66:1151–1159.
- Stoecker, D.K., P.J. Hansen, D.A. Caron & A. Mitra, 2017. Mixotrophy in the marine plankton. *Annual Review of Marine Science* 9:311–335.
- Suski, J.G., C.M. Swan, C.J. Salice & C.F. Wahl, 2018. Effects of pond management on biodiversity patterns and community structure of zooplankton in urban environments. *Science of the Total Environment* 619:1441–1450.
- Tittle, J., V. Bissinger, B. Zipple, U. Gaedke, E. Bell, A. Lorke & N. Kamjunke, 2003. Mixotrophs combine resource use to outcompete specialists: Implications for aquatic food webs. *Proceedings of the National Academy of Science* 100:12776–12781.
- Thorp, J.H. & A.P. Covich, 2001. *Ecology and Classification of North American Freshwater Invertebrates*. San Diego: Academic Press.
- Urabe, J., T.B. Gurung, T. Yoshida, T. Sekino & M. Nakanishi, 2000. Diel changes in phagotrophy by *Cryptomonas* in Lake Biwa. *Limnology and Oceanography* 45:1558–1563.
- Üveges, V., K. Tapolczai, L. Krienitz & J. Padisák, 2012. Photosynthetic characteristics and physiological plasticity of an *Aphanizomenon flos-aquae* (Cyanobacteria, Nostocaceae) winter bloom in a dep oligo-mesotrophic lake (Lake Stechlin, Germany). *Hydrobiologia* 698:263–272.
- U.S. Environmental Protection Agency, 2016. Climate change indicators in the United States, 2016. Fourth edition. EPA 430-R-16-004. [www.epa.gov/climate-indicators](http://www.epa.gov/climate-indicators).
- Van Halderen, A., W.R. Harding, J.C. Wessels, D.J. Schneider, E.W.P. Heine, J. Van Der Merwe & J.M. Fourie, 1995. Cyanobacterial (blue-green algae) poisoning of livestock in the Western Cape Province of South Africa. *Journal of the South African Veterinary Association* 66:260–264.
- Van Liere L. & L.R. Mur, 1980. “Occurrence of *Oscillatoria Agardhii* and some related species, a survey,” in *Hypertrophic Ecosystems: Developments in Hydrobiology* vol 2, eds. J. Barica & L.R. Mur (Dordrecht, NL: Springer), 66–77.
- Visser, P.M., B.W. Ibelings, M. Bormans & J. Huisman, 2016. Artificial mixing to control cyanobacterial blooms: a review. *Aquatic Ecology* 50:423–441.
- Vogel, J.L. & D.A. Beauchamp, 1999. Effects of light, prey size, and turbidity on reaction distances of lake trout (*Salvelinus namaycush*) to salmonid prey. *Canadian Journal of Fisheries and Aquatic Sciences* 56:1293–1297.
- Wagner, K.J., D. Meringolo, D.F. Mitchell, E. Moran & S. Smith, 2017. Aluminum treatments to control internal phosphorus loading in lakes on Cape Cod, Massachusetts. *Lake and Reservoir Management* 33:171–186.

- Wallace, B.B. & D.P. Hamilton, 2000. Simulation of water-bloom formation in the cyanobacterium *Microcystis aeruginosa*. *Journal of Plankton Research* 22:1127–1138.
- Webb, W.L., M. Newton & D. Starr, 1974. Carbon dioxide exchange of *Alnus rubra*: a mathematical model. *Oecologia* 17:281–291.
- Wickham, H., 2009. *ggplot2: elegant graphics for data analysis*. Springer New York.
- Winslow, L., J. Read, R. Woolway, J. Brentrup, T. Leach, J. Zward, S. Albers & D. Collinge, 2017. *rLakeAnalyzer: Lake Physics Tools*. Available at: <https://cran.r-project.org/package=rLakeAnalyzer>.
- Yang, J.R., H. Lv, A. Isabwe, L. Liu, X. Yu, H. Chen & J. Yang, 2017. Disturbance-induced phytoplankton regime shifts and recovery of cyanobacteria dominance in two subtropical reservoirs. *Water Research* 120:52–63.
- Yang, S. & X. Jin, 2008. Critical light intensities for *Microcystis aeruginosa*, *Scenedesmus quadricauda* and *Cytoclotella* sp. and competitive growth patterns under different light:N:P ratios. *Journal of Freshwater Ecology* 23:387–396.
- Zamparas, M., A. Gianni, P. Stathi, Y. Deligiannakis & I. Zacharias, 2012. Removal of phosphate from natural waters using innovative modified bentonites. *Applied Clay Science* 62:101–106.
- Zhang, M., X. Shi, Y. Yu & F. Kong, 2011. The acclimative changes in photochemistry after colony formation of the cyanobacteria *Microcystis aeruginosa*. *Journal of Phycology* 47:524–532.

TABLES

**Table 2.1.** Experimental design to promote phytoplankton growth through nutrient amendments. Nitrogen (N) and/or phosphorus (P) were added to 11,000 L mesocosm tanks to create bloom conditions and induce nutrient deficiency. A total of 3.08 moles of N was added as ammonium chloride (NH<sub>4</sub>Cl) or sodium nitrate (NaNO<sub>3</sub>), and 2.20 moles of P was added as dipotassium phosphate (K<sub>2</sub>HPO<sub>4</sub>). Control tanks did not receive nutrient amendments and were dominated by chlorophytes at the beginning of the experiment. The ln(TN:TP) molar ratio is from day 0 of the experiment. Sample size (*n*) refers to the number of mesocosm tanks that received each nutrient form.

<b>Nutrient forms added</b>	<b>Amount N and/or P added (moles)</b>	<b>Experimental group</b>	<b>ln(TN:TP ) (molar ratio)</b>
NH <sub>4</sub> Cl + K <sub>2</sub> HPO <sub>4</sub> ( <i>n</i> =3)	3.08N + 2.20P	cyanophyte-dominated	3.73
NaNO <sub>3</sub> + K <sub>2</sub> HPO <sub>4</sub> ( <i>n</i> =3)	3.08N + 2.20P	cyanophyte-dominated	3.12
K <sub>2</sub> HPO <sub>4</sub> ( <i>n</i> =2)	2.20	cyanophyte-dominated	3.29
NH <sub>4</sub> Cl ( <i>n</i> =3)	3.08	chlorophyte-dominated	4.52
NaNO <sub>3</sub> ( <i>n</i> =3)	3.08	chlorophyte-dominated	4.95
None ( <i>n</i> =3)	0	control	4.61

**Table 2.2:** Top 3 dominant phytoplankton genera on day 0 and day 9. Percent composition (% Comp.) was calculated for each genera as the percent of total phytoplankton biovolume in each tank. Mean percent composition of all tanks within each group is reported for control ( $n= 3$ ), chlorophyte- ( $n= 6$ ), and cyanophyte-dominated ( $n= 8$ ) mesocosms. Lowest identification was to genus (Table A2.2).

Experimental Group	Dominant Algal Genus on Day 0			Dominant Algal Genus on Day 9		
	Functional Group	Genus	% Comp.	Functional Group	Genus	% Comp.
Control	Chlorophyta	<i>Tetraedron</i>	26.2	Chlorophyta	<i>Tetraedron</i>	23.4
	Chlorophyta	<i>Scenedesmus</i>	13.8	Chlorophyta	<i>Scenedesmus</i>	12.5
	Cryptophyta & Dinoflagellates	<i>Cryptomonas</i>	13.6	Cryptophyta & Dinoflagellates	<i>Plagioselmis</i>	12.0
Chlorophyte-Dominated	Chlorophyta	<i>Oocystis</i>	35.4	Cryptophyta & Dinoflagellates	<i>Cryptomonas</i>	32.2
	Cryptophyta & Dinoflagellates	<i>Cryptomonas</i>	9.6	Chrysophyta	<i>Chrysochromulina</i>	14.7
	Chrysophyta	<i>Chrysochromulina</i>	7.3	Chlorophyta	<i>Oocystis</i>	10.7
Cyanophyte-Dominated	Potentially Toxigenic Cyanophyta	<i>Aphanizomenon</i>	22.8	Cryptophyta & Dinoflagellates	<i>Cryptomonas</i>	37.1
	Potentially Toxigenic Cyanophyta	<i>Dolichospermum</i>	22.1	Potentially Toxigenic Cyanophyta	<i>Aphanizomenon</i>	13.8
	Non-toxin Producing Cyanophyta	<i>Pseudanabaena</i>	13.3	Chlorophyta	<i>Scenedesmus</i>	9.8

**Table 2.3:** Water quality and phytoplankton physiology parameters. Control (Con), chlorophyte- (Chloro), and cyanophyte- (Cyano) dominated mesocosm tanks prior to glacial rock flour addition (day 0) and at the end of the experiment (day 9). Mean and standard deviation (std dev) are reported. “BDL” indicates that all tanks in a group were below the detection limit as stated in the Methods. Sediment traps were collected only on day 9, so it is not applicable (n/a) to report day 0 sedimentation rates. Significant differences between groups for the change in each parameter from day 0 to day 9 are reported in Table 2.4.

	Day 0 Mean $\pm$ Std Dev			Day 9 Mean $\pm$ Std Dev		
	Con n=3	Chloro n=6	Cyano n=8	Con n=3*	Chloro n=6	Cyano n=8†
<b>Physical Parameters</b>						
Temperature (°C)	21.1 $\pm$ 0.1	21.2 $\pm$ 0.1	20.8 $\pm$ 0.1	18.6 $\pm$ 0.1	18.6 $\pm$ 0.2	18.4 $\pm$ 0.1
Total Suspended Solids, TSS (mg L <sup>-1</sup> )	0.8 $\pm$ 0.6	1.5 $\pm$ 0.6	4.5 $\pm$ 1.7	3.1 $\pm$ 1.2	7.3 $\pm$ 2.2	20.2 $\pm$ 7.7
Particulate Inorganic Matter, PIM (mg L <sup>-1</sup> )	0.4 $\pm$ 0.3	1.0 $\pm$ 0.5	2.2 $\pm$ 0.6	0.3 $\pm$ 0.2	5.5 $\pm$ 1.8	10.5 $\pm$ 5.2
Particulate Organic Matter, POM (mg L <sup>-1</sup> )	0.9 $\pm$ 1.0	2.9 $\pm$ 2.4	6.6 $\pm$ 6.7	2.8 $\pm$ 1.2	1.8 $\pm$ 0.7	9.7 $\pm$ 5.2
TSS Sedimentation Rate (g m <sup>-2</sup> day <sup>-1</sup> )	n/a	n/a	n/a	0.1 $\pm$ 0.0	1.9 $\pm$ 0.8	2.3 $\pm$ 0.9
PIM Sedimentation Rate (g m <sup>-2</sup> day <sup>-1</sup> )	n/a	n/a	n/a	0.0 $\pm$ 0.0	1.9 $\pm$ 0.8	2.2 $\pm$ 0.9
POM Sedimentation Rate (g m <sup>-2</sup> day <sup>-1</sup> )	n/a	n/a	n/a	0.0 $\pm$ 0.0	0.1 $\pm$ 0.0	0.1 $\pm$ 0.0
Mean daily mixed layer irradiance, $\bar{E}_{24}$ ( $\mu$ mol photons m <sup>-2</sup> s <sup>-1</sup> )	106.67 $\pm$ 11.64	114.16 $\pm$ 10.69	57.14 $\pm$ 19.64	115.45 $\pm$ 9.55	110.66 $\pm$ 14.07	64.36 $\pm$ 22.67
<b>Chemical Parameters</b>						
Total Nitrogen:Total Phosphorus, ln(TN:TP) (molar ratio)	4.61 $\pm$ 0.39	4.74 $\pm$ 0.40	3.39 $\pm$ 0.40	4.67 $\pm$ 0.33	4.70 $\pm$ 0.28	3.72 $\pm$ 0.22
Total Phosphorus, TP ( $\mu$ mol L <sup>-1</sup> )	0.74 $\pm$ 0.42	0.57 $\pm$ 0.18	5.89 $\pm$ 2.05	0.67 $\pm$ 0.34	0.56 $\pm$ 0.09	3.85 $\pm$ 1.53
Total Dissolved Phosphorus, TDP ( $\mu$ mol L <sup>-1</sup> )	0.25 $\pm$ 0.10	0.16 $\pm$ 0.01	1.52 $\pm$ 1.61	0.23 $\pm$ 0.04	0.18 $\pm$ 0.03	1.27 $\pm$ 0.58

Total Nitrogen, TN ( $\mu\text{mol L}^{-1}$ )	65.43 $\pm$ 9.25	62.09 $\pm$ 5.63	163.06 $\pm$ 35.41	64.45 $\pm$ 9.58	61.68 $\pm$ 7.83	153.54 $\pm$ 46.67
Total Dissolved Nitrogen, TDN ( $\mu\text{mol L}^{-1}$ )	49.92 $\pm$ 4.12	53.71 $\pm$ 6.82	93.20 $\pm$ 22.17	51.80 $\pm$ 4.74	55.88 $\pm$ 8.83	91.16 $\pm$ 23.28
Nitrate, $\text{NO}_3^-$ ( $\mu\text{mol L}^{-1}$ )	BDL	3.94 $\pm$ 5.53	1.75 $\pm$ 2.51	BDL	2.78 $\pm$ 2.05	0.45 $\pm$ 0.21
Ammonium, $\text{NH}_4^+$ ( $\mu\text{mol L}^{-1}$ )	1.51 $\pm$ 0.12	3.49 $\pm$ 1.64	8.53 $\pm$ 14.26	1.83 $\pm$ 0.32	3.03 $\pm$ 1.19	12.17 $\pm$ 10.91
Dissolved Organic Carbon, DOC ( $\mu\text{mol L}^{-1}$ )	1009.2 5 $\pm$ 236.88	1015.0 0 $\pm$ 256.75	1032.9 8 $\pm$ 157.96	1063.20 $\pm$ 248.10	1030.73 $\pm$ 261.91	1081.02 $\pm$ 147.70
Microcystin ( $\mu\text{g L}^{-1}$ )	0.17 $\pm$ 0.03	0.16 $\pm$ 0.01	0.70 $\pm$ 0.93	0.19 $\pm$ 0.04	0.19 $\pm$ 0.06	0.87 $\pm$ 1.27
<b>Biological Parameters</b>						
Total Phytoplankton Biovolume ( $\text{mm}^3 \text{L}^{-1}$ )	4.43 $\pm$ 3.87	2.55 $\pm$ 1.38	35.31 $\pm$ 28.91	2.64 $\pm$ 1.21	2.56 $\pm$ 1.41	28.13 $\pm$ 37.08
Potentially Toxicogenic Cyanophyta Biovolume ( $\text{mm}^3 \text{L}^{-1}$ )	0.12 $\pm$ 0.16	0.02 $\pm$ 0.02	17.94 $\pm$ 16.60	0.14 $\pm$ 0.20	0.00 $\pm$ 0.01	4.27 $\pm$ 6.65
Non-toxin Producing Cyanophyta Biovolume ( $\text{mm}^3 \text{L}^{-1}$ )	0.19 $\pm$ 0.18	0.17 $\pm$ 0.17	10.23 $\pm$ 11.60	0.06 $\pm$ 0.03	0.13 $\pm$ 0.14	2.34 $\pm$ 2.24
Chlorophyta Biovolume ( $\text{mm}^3 \text{L}^{-1}$ )	3.17 $\pm$ 3.49	1.51 $\pm$ 1.13	2.08 $\pm$ 1.30	1.56 $\pm$ 1.49	0.57 $\pm$ 0.32	1.46 $\pm$ 1.62
Euglenophyta Biovolume ( $\text{mm}^3 \text{L}^{-1}$ )	0 $\pm$ 0	0 $\pm$ 0	0 $\pm$ 0	0 $\pm$ 0	0.01 $\pm$ 0.01	0.07 $\pm$ 0.18
Cryptophyta + Dinoflagellate Biovolume ( $\text{mm}^3 \text{L}^{-1}$ )	0.41 $\pm$ 0.30	0.54 $\pm$ 0.55	3.75 $\pm$ 5.12	0.61 $\pm$ 0.46	1.10 $\pm$ 0.82	19.50 $\pm$ 36.49
Chrysophyta (including Chrysophytes, Bacillariophytes, Ochromyces, and Haptophytes) Biovolume ( $\text{mm}^3 \text{L}^{-1}$ )	0.54 $\pm$ 0.37	0.32 $\pm$ 0.30	1.31 $\pm$ 2.47	0.26 $\pm$ 0.23	0.75 $\pm$ 1.10	0.49 $\pm$ 0.82
Chlorophyll- <i>a</i> , Chl- <i>a</i> ( $\mu\text{g L}^{-1}$ )	3.54 $\pm$ 1.21	2.97 $\pm$ 2.30	48.70 $\pm$ 39.85	2.09 $\pm$ 1.07	1.53 $\pm$ 1.02	63.52 $\pm$ 79.94
Maximum Quantum Yield of Photosystem II, $\phi_{\text{PSII}}$ (unitless)	0.57 $\pm$ 0.11	0.61 $\pm$ 0.11	0.34 $\pm$ 0.15	0.53 $\pm$ 0.03	0.56 $\pm$ 0.02	0.48 $\pm$ 0.13

Light saturation threshold normalized for Chl- <i>a</i> , $E_k^B$ ( $\mu\text{mol photons } [\mu\text{g Chl-}a^{-1}] \text{ m s}^{-1}$ )	153.23 $\pm$ 177.98	428.24 $\pm$ 728.62	80.90 $\pm$ 174.58	377.22 $\pm$ 430.44	388.69 $\pm$ 360.81	32.34 $\pm$ 33.67
Alpha normalized for Chl- <i>a</i> , $\alpha^B$	0.21 $\pm$ 0.10	0.48 $\pm$ 0.53	0.07 $\pm$ 0.14	0.58 $\pm$ 0.54	0.65 $\pm$ 0.43	0.05 $\pm$ 0.06
Maximum relative electron transport rate, $rETR_{MAX}$ (photons reemitted photons absorbed <sup>-1</sup> )	315.69 $\pm$ 359.98	175.63 $\pm$ 150.92	136.12 $\pm$ 47.95	291.40 $\pm$ 265.33	222.69 $\pm$ 138.22	197.21 $\pm$ 46.31
Light deficiency parameter, $\bar{E}_{24}/E_k$	0.85 $\pm$ 0.70	0.55 $\pm$ 0.28	0.20 $\pm$ 0.15	0.45 $\pm$ 0.21	0.43 $\pm$ 0.20	0.18 $\pm$ 0.07
Gross Primary Productivity normalized to Chl- <i>a</i> , $GPP^B$ ( $\text{mmol O}_2 [\mu\text{g Chl-}a^{-1}] \text{ m day}^{-1}$ )	25.9 $\pm$ 13.0	15.4 $\pm$ 13.7	15.2 $\pm$ 9.5	33.3*	18.2 $\pm$ 15.5	22.8 $\pm$ 12.3
Total Zooplankton Abundance (Individuals $L^{-1}$ )	70.85 $\pm$ 57.89	79.56 $\pm$ 51.45	211.84 $\pm$ 149.78	111.87 $\pm$ 90.99	31.78 $\pm$ 17.90	126.04 $\pm$ 95.11
Adult Copepod Abundance (Individuals $L^{-1}$ )	14.82 $\pm$ 9.13	17.36 $\pm$ 9.66	89.05 $\pm$ 82.69	16.00 $\pm$ 3.75	12.73 $\pm$ 9.92	59.59 $\pm$ 74.25
Copepod Nauplii Abundance (Individuals $L^{-1}$ )	26.73 $\pm$ 25.39	31.46 $\pm$ 39.62	63.54 $\pm$ 54.43	16.59 $\pm$ 6.57	12.75 $\pm$ 8.20	39.01 $\pm$ 55.49
Cladoceran Abundance (Individuals $L^{-1}$ )	29.30 $\pm$ 23.47	30.75 $\pm$ 28.30	59.25 $\pm$ 75.82	79.27 $\pm$ 80.83	6.30 $\pm$ 3.28	27.43 $\pm$ 36.79

\*There was only one control tank for day 9  $GPP^B$

†There were only 7 cyanophyte dominated tanks for day 9 DOC

**Table 2.4:** Statistical analyses for each parameter. Analyses were evaluated on the difference between day 9 and day 0 (i.e., day 9 - day 0). We used a one-way analysis of variance (ANOVA) when the parameter followed a normal distribution, or when a normal distribution resulted from a transformation. A Kruskal-Wallis test (KW) was used when the data did not follow a normal distribution. Statistically significant differences between groups ( $p < 0.05$ ) are denoted by different letters, while same letters indicate that no significant difference exists. Post Hoc tests were used to identify when the change in each parameter was different between control (Con), chlorophyte- (Chloro), and cyanophyte- (Cyano) dominated mesocosm tanks. A Tukey *post hoc* test was used to identify significant differences for parameters that followed a parametric distribution while Dunn's test was used on non-parametric parameters.

	Test	p	Test Statistic	Post Hoc		
				Con	Chloro	Cyano
<b>Physical Parameters</b>						
Temperature	ANOVA	$p=0.08$	$F_{2,14} = 3.05$			
Total Suspended Solids, TSS	KW	$p=0.97$	$\chi^2 = 0.07$ df= 2			
Particulate Inorganic Matter, PIM	KW	$p=0.43$	$\chi^2 = 1.67$ df= 2			
Particulate Organic Matter, POM	ANOVA	$p=0.93$	$F_{2,14} = 0.08$			
Mean daily mixed layer irradiance, $\bar{E}_{24}$	ANOVA	$p=0.61$	$F_{2,14} = 0.52$			
<b>Chemical Parameters</b>						
Total Nitrogen:Total Phosphorus, ln(TN:TP)	ANOVA	$p=0.10$	$\chi^2 = 2.10$ df= 2			
Total Phosphorus, TP	KW	$p=0.03$	$\chi^2 = 7.16$ df= 2	ab	a	b
Total Dissolved Phosphorus, TDP	KW	$p=0.87$	$\chi^2 = 0.23$ df= 2			
Total Nitrogen, TN	KW	$p=0.27$	$\chi^2 = 2.63$ df= 2			

Total Dissolved Nitrogen, TDN	ANOVA	$p=0.90$	$F_{2,14} = 0.11$			
Nitrate, $\text{NO}_3^-$	KW	$p=0.45$	$\chi^2 = 1.58$ df= 2			
Ammonium, $\text{NH}_4^+$	KW	$p=0.20$	$\chi^2 = 3.18$ df= 2			
Dissolved Organic Carbon, DOC	ANOVA	$p=0.05$	$F_{2,13} = 3.92$	ab	a	b
Microcystin	KW	$p=0.12$	$\chi^2 = 4.26$ df= 2			
<b>Biological Parameters</b>						
Total Phytoplankton Biovolume	KW	$p=0.20$	$\chi^2 = 3.18$ df= 2			
Potentially Toxigenic Cyanophyta Biovolume	KW	$p=0.00$	$\chi^2 = 12.61$ df= 2	a	a	b
Non-toxin Producing Cyanophyta Biovolume	KW	$p=0.78$	$\chi^2 = 0.51$ df= 2			
Chlorophyta Biovolume	KW	$p=0.99$	$\chi^2 = 0.02$ df= 2			
Euglenophyta Biovolume	KW	$p=0.79$	$\chi^2 = 0.47$ df= 2			
Cryptophyta + Dinoflagellate Biovolume	KW	$p=0.74$	$\chi^2 = 0.60$ df= 2			
Chrysophyta (including Chrysophytes, Bacillariophytes, Ochrophytes, and Haptophytes) Biovolume	KW	$p=0.11$	$\chi^2 = 4.46$ df= 2			
Chlorophyll- <i>a</i> , Chl- <i>a</i>	KW	$p=0.44$	$\chi^2 = 1.64$ df= 2			
Maximum Quantum Yield of Photosystem II, $\Phi_{\text{PSII}}$	ANOVA	$p=0.06$	$F_{2,14} = 3.43$			

Light saturation threshold normalized for Chl- <i>a</i> , $E_k^B$	ANOVA	$p=0.26$	$F_{2,14} = 1.50$
Alpha normalized for Chl- <i>a</i> , $\alpha^B$	ANOVA	$p=0.71$	$F_{2,14} = 0.36$
Maximum relative electron transport rate, $rETR_{MAX}$	ANOVA	$p=0.28$	$F_{2,14} = 1.40$
Light deficiency parameter, $\bar{E}_{24}/E_k$	ANOVA	$p=0.70$	$F_{2,14} = 0.36$
Gross Primary Productivity normalized for Chl- <i>a</i> , $GPP^B$	ANOVA	$p=0.16$	$F_{2,9} = 2.26$
Total Zooplankton Abundance	ANOVA	$p=0.45$	$F_{2,14} = 0.85$
Adult Copepod Abundance	KW	$p=0.51$	$\chi^2 = 1.35$ df= 2
Copepod Nauplii Abundance	KW	$p=0.88$	$\chi^2 = 0.27$ df= 2
Cladoceran Abundance	ANOVA	$p=0.06$	$F_{2,14} = 3.42$

FIGURES

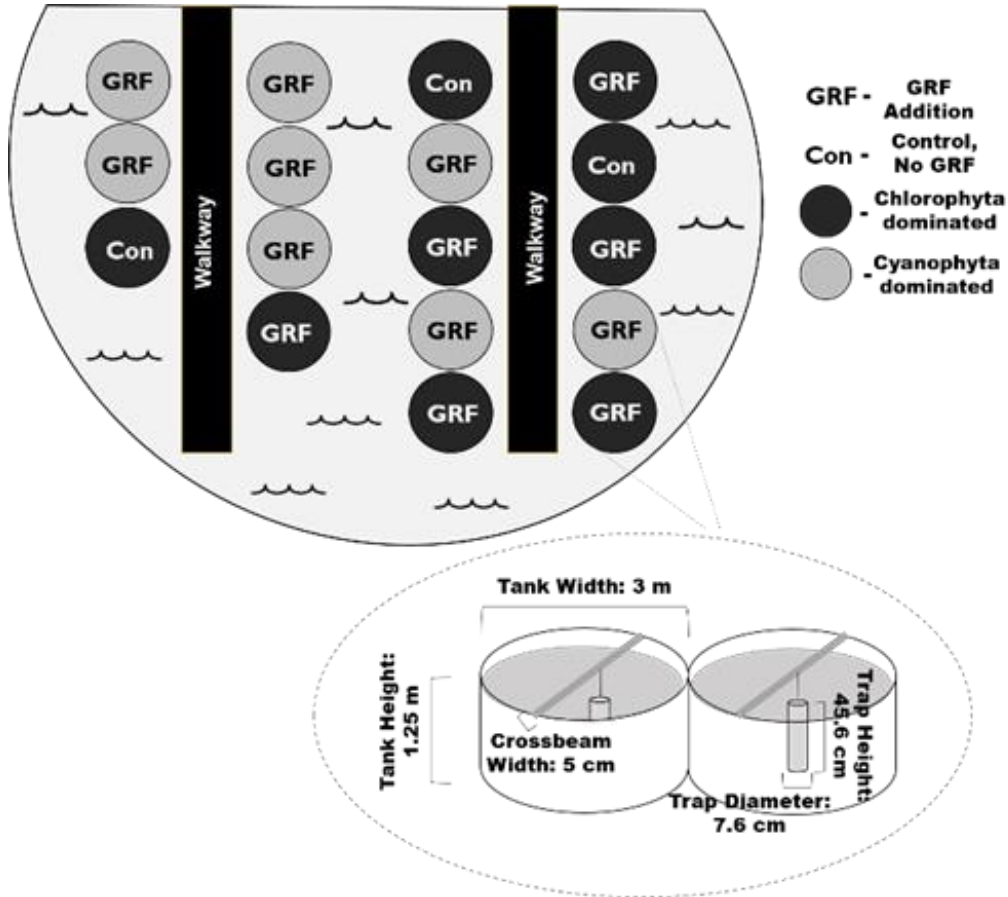


**Figure 2.1:** Birds-eye view of mesocosm tank set-up. We added glacial rock flour (GRF) to 14 of the 17 mesocosm tanks used in this experiment. Phytoplankton communities were dominated by either chlorophytes or cyanophytes ( $n= 8$ ) at the beginning of the experiment. Of the 9 chlorophyte dominated tanks, a subset ( $n= 3$ ) did not receive any nutrient nor GRF amendments and were treated as a control (Con). The remaining chlorophyte dominated tanks ( $n= 6$ ) received daily GRF additions. Tanks were kept in a  $\sim 1300 \text{ m}^2$  shallow pond that was  $\sim 1 \text{ m}$  deep to insulate for changes in air temperatures. The pond was surrounded by low vegetation. Mesocosm tanks were  $\sim 3 \text{ m}$  across,  $1.25 \text{ m}$  high, and volume of  $11,000 \text{ L}$ . Crossbeams were placed across each mesocosm. Sediment traps were suspended from each crossbeam.

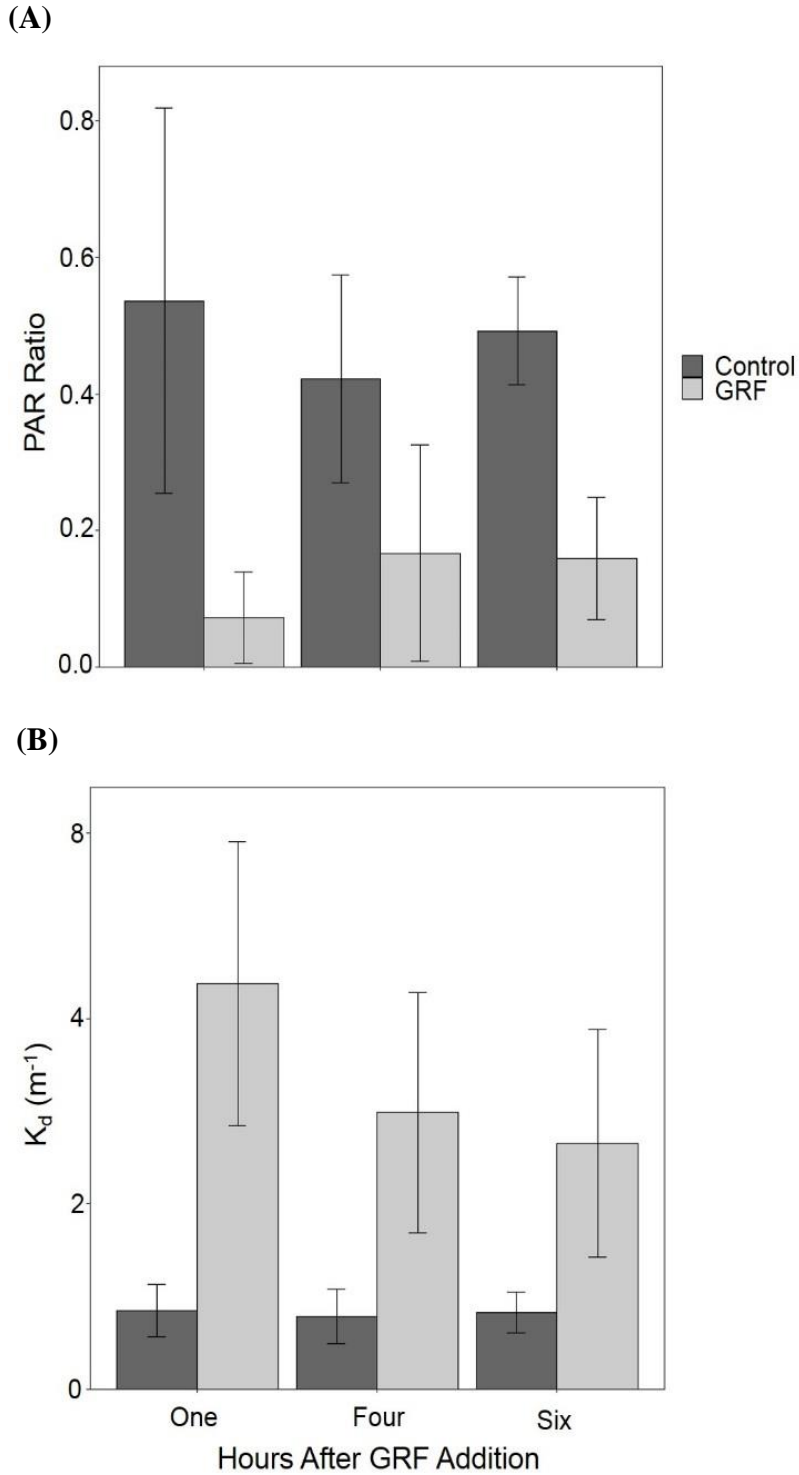
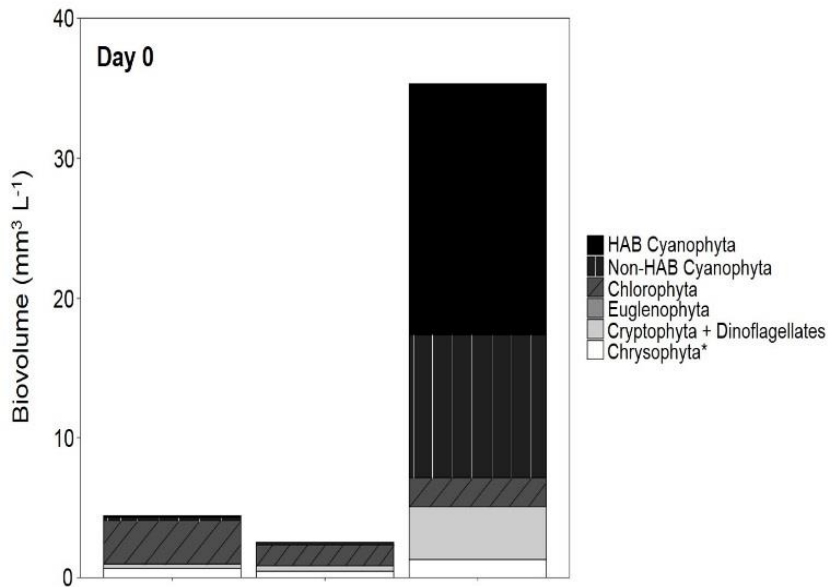


**Figure 2.2:** Comparison of the light environment between tanks that received glacial rock flour (GRF) and tanks that did not receive GRF. PAR ratio (0.5 m water/air reading; A) and vertical light attenuation coefficient ( $K_d$ ; B) were measured in all tanks after GRF was added to all ( $n=14$ ) but the control tanks ( $n=3$ ). Both the PAR ratio and  $K_d$  were

measured one hour after GRF addition every day of the experiment, 4 hours after addition on days 0, 5, 6, and 7, and 6 hours after addition on day 4. The light ratio was determined by dividing photosynthetically active radiation (PAR) measurements made at 0.5 m depth by PAR measurements from above the water's surface in the air. Among GRF tanks, the light ratio was significantly lower one hour after GRF addition than 4 (Kruskal-Wallis  $p < 0.0001$ ,  $df = 2$ ,  $\chi^2 = 26.46$ ) or 6 hours (Kruskal-Wallis  $p = 0.0002$ ,  $df = 2$ ,  $\chi^2 = 26.46$ ), but not significantly different between 4 and 6 hours (Kruskal-Wallis  $p = 0.1709$ ,  $df = 2$ ,  $\chi^2 = 26.46$ ; Figure 2).  $K_d$  was significantly higher one hour after GRF addition (Kruskal-Wallis  $p < 0.0001$ ,  $df = 2$ ,  $\chi^2 = 37.10$ ), but not 4 nor 6 hours after addition (Kruskal-Wallis  $p = 0.2347$ ,  $df = 2$ ,  $\chi^2 = 37.10$ ). For each time, the light ratio was significantly lower (Kruskal-Wallis  $p < 0.0001$ ,  $df = 1$ ,  $\chi^2 = 75.99$ ) in tanks that received GRF compared to control tanks that did not. For each time,  $K_d$  was significantly higher (Kruskal-Wallis  $p < 0.0001$ ,  $df = 1$ ,  $\chi^2 = 87.88$ ) in tanks that received GRF compared to control tanks that did not.

(A)



(B)

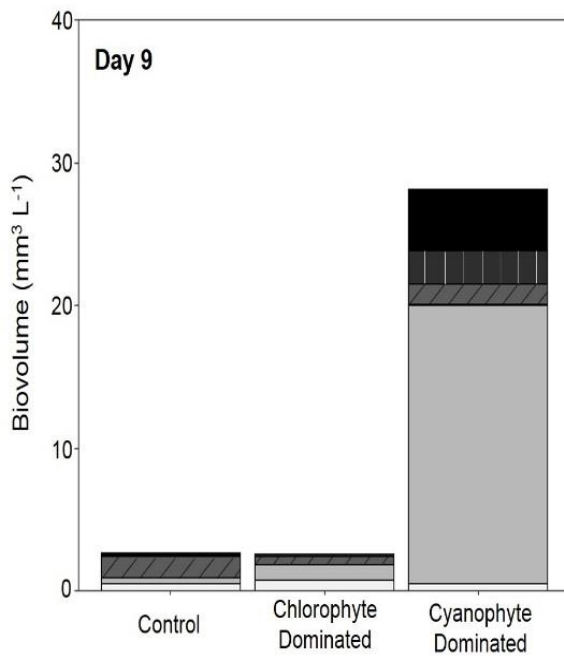


**Figure 2.3:** Phytoplankton biovolume categorized by functional group. Biovolume for day 0 (A) and day 9 (B) for control tanks, tanks dominated by chlorophytes at the beginning of the experiment, and tanks dominated by cyanophytes at the beginning of the experiment. The chrysophyta\* group includes chrysophyta, bacillariophyta, haptophyta, and ochrophyta.

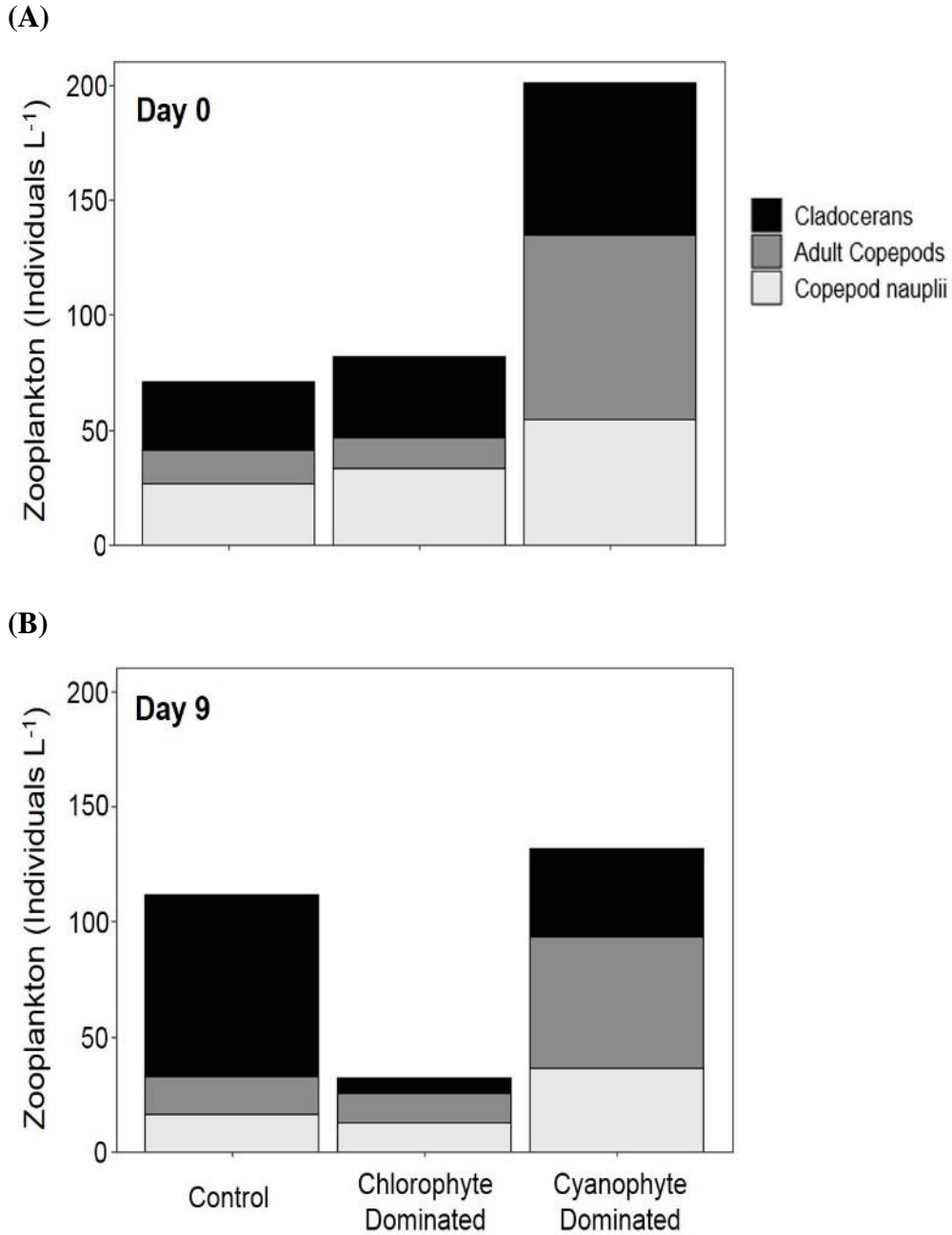


**Figure 2.4:** Zooplankton abundance in mesocosm tanks. Abundance was measured on day 0 (A) and day 9 (B) for control tanks, tanks dominated by chlorophytes at the beginning of the experiment, and tanks dominated by cyanophytes at the beginning of the experiment.

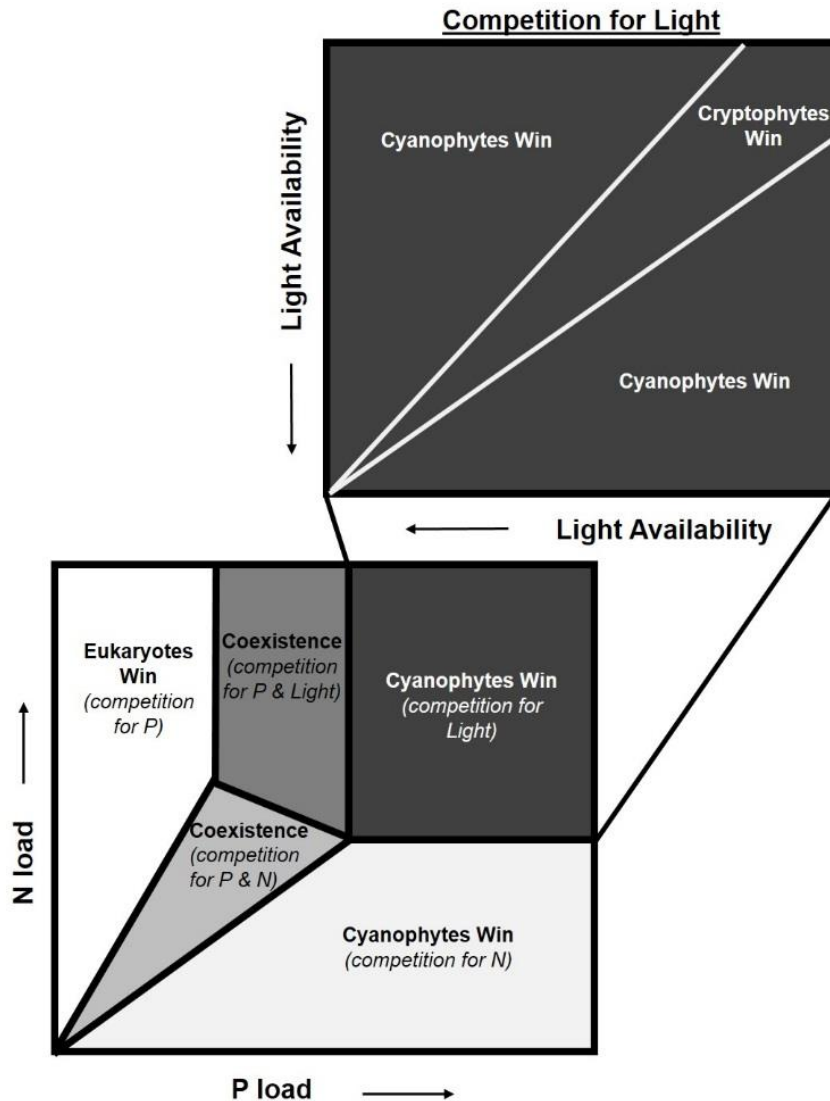


**Figure 2.5:** Adaptation of the nutrient load hypothesis from Brauer et al., (2012). This hypothesis predicts which phytoplankton dominate based on competition for nitrogen (N), phosphorus (P), and light. The nutrient load hypothesis is based on the assumption that cyanobacteria are superior competitors for light and are able to dominate when N and P concentrations are high (Brauer et al., 2012). We add an additional box to highlight the nuance that functional traits can add to competition for these resources, specifically light. Our added box, above, connects to Brauer et al. original figure in the area where there is competition for light. While cyanobacteria often dominate when light is the limiting resource, our findings suggest that cryptophytes can outcompete cyanobacteria under specific light levels due to functional traits. Our box shows this by introducing cryptophytes to this figure, showing that as light availability declines, cryptophytes outcompete cyanophytes.

## CHAPTER 3

### MONITORING MICROCYSTIN ACCUMULATION IN TWO POPULAR SPORTFISH OVER THE COURSE OF A YEAR

#### ABSTRACT

Cyanobacterial blooms sometimes create secondary metabolites that can be transferred between trophic levels and accumulate in fish, where they pose a potential health risk to anglers. We examine microcystin in the muscle, liver, and kidney of bluegill and largemouth bass on 8 sampling dates over a 12 month period. We identify drivers of microcystin accumulation in tissues from fish characteristics and water parameters. Microcystin in bluegill were significantly higher than largemouth bass and in both species, microcystin was highest in livers (bluegill mean= 57.6 ng g<sup>-1</sup>, largemouth bass mean= 71.8 ng g<sup>-1</sup> wet weight [ww]), then kidneys (bluegill mean= 27.1, largemouth bass mean= 22.7 ng g<sup>-1</sup> ww), and muscles (bluegill mean= 7.6, largemouth bass mean= 5.7 ng g<sup>-1</sup> ww). Adult bluegill feed on benthic macroinvertebrates and zooplankton, which may explain their higher microcystin concentrations compared to largemouth bass, which are primarily piscivorous. Harvest date emerged as the best predictor of microcystin in muscles and kidneys, with highest concentrations occurring in April before decreasing throughout the year. Behavioral or physiological response related to spawning may explain this pattern. Microcystin in water also emerged as a significant predictor for microcystin in fish, although its signal was much weaker than harvest date. This suggests that low but persistent microcystin concentrations in the water can lead to accumulation of this cyanotoxin in fish tissues. This study is the first to look at microcystin in fish from

the North American Great Plains and one of only 3 studies that investigate microcystin in bluegill and largemouth bass.

## INTRODUCTION

Cyanobacteria are a group of prokaryotic phytoplankton that sometimes form dense blooms, often in the presence of high nutrient concentrations (Smith and Schindler 2009), warm water temperatures (Paerl and Huisman 2008), and low wind conditions (Cao et al. 2006). Some cyanobacteria can produce secondary metabolites that are harmful to humans (Azevedo et al. 2002; Rao et al. 2002; Stewart et al. 2006). Microcystin, the most common cyanotoxin found in most fresh water bodies, is a hepatotoxin that inhibits protein phosphatases 1 and 2A (Carmichael 1994). In extreme instances, exposure to cyanotoxins can result in death for humans (Li et al. 2011), pets (Backer et al. 2013), livestock (Van Halderen et al. 1995), and wildlife (Miller et al. 2010).

Microcystin accumulates in aquatic organisms such as fish by direct exposure to microcystin dissolved in water (Sieroslawska et al. 2012) and through consumption of contaminated food items (Smith and Haney 2006). This hepatotoxin occurs in the water column most often during summer months when cyanobacterial blooms are traditionally most common (Huisman et al. 2018). Microcystin has been detected in fish collected throughout the year, even times when it is not present in the water (de Magalhães et al. 2001; Zhang et al. 2013). Natural degradation of dissolved microcystin through photolysis (Wörmer et al. 2010) and microbial activity (Park et al. 2001) usually occurs within 8 days (Christoffersen et al. 2002), but fish may continue to be exposed afterwards through their diet. Water parameters like nutrients (Vézie et al. 2002) and chlorophyll-*a*

(chl-*a*; Yuan et al. 2014) have been linked with water microcystin concentrations, but whether they are secondarily linked to microcystin accumulation in fish has not been investigated. General consensus is that microcystin concentrations decline at higher food web trophic levels (Ibelings et al. 2005; Ferrão-Filho and Kozlowsky-Suzuki 2011; Pham and Utsumi 2018), although there have been reports of higher microcystin in fish that feed from high trophic levels compared to organisms from lower trophic levels (Zamora-Barrios et al. 2019). The negative relationship between microcystin and trophic level could be because microcystin can be eliminated in fish via the glutathione metabolic pathway, although the factors that influence this metabolization are poorly understood (Schmidt et al. 2014). Microcystin concentrations are highest in fish livers and kidneys because microcystin is metabolized and eliminated at these sites (Malbrouck and Kestemont 2006; Papadimitriou et al. 2013). Factors and mechanisms behind the toxicodistribution of microcystin in fish muscles and organs are not well understood, and we do not know if differences in metabolic rate among fish species would result in microcystin variability in tissues.

Fish can be a route of toxin exposure for anglers who consume their catch because microcystin covalently binds to proteins in fish muscles (Smith et al. 2010). Covalently-bound microcystins are 3 to 10 times less toxic than free toxins (Campos and Vasconcelos 2010), but can be released into tissues through enzyme cleaving (Smith et al. 2010). During digestion, enzyme cleaving can release formally bound microcystin, increasing the potential health risk to consumers (Díez-Quijada et al. 2019). This potential human health risk has prompted the creation of microcystin fish consumption advisories (Ibelings and Chorus 2007; Anderson-Abbs et al. 2016). The frequency and

magnitude of cyanobacterial blooms and exposure to the toxins they can produce likely play a role in determining how much microcystin has accumulated in a fish at any given time (Jia et al. 2014; Gurbuz et al. 2016). The Missouri Department of Health and Senior Services (MDHSS) recommends that anglers do not consume fish from reservoirs that have experienced a visible bloom within the previous 2 weeks. The presence of a cyanobacterial bloom is sometimes a misleading indicator of microcystin in fish tissues because toxin production is highly variable across space and time (Sabart et al. 2010). Fish collected from lakes that often experience cyanobacterial blooms do not always contain microcystin. For example, despite water microcystin concentrations frequently exceeding  $40 \mu\text{g L}^{-1}$  in Grand Lakes St. Mary's (OH, USA) during the spring, summer, and fall of 2012, microcystin was only measured in 6 % of the fish sampled, and was never greater than  $70.43 \text{ ng g}^{-1} \text{ ww}$  in black crappie (*Pomoxis annularis*; Schmidt et al. 2013). In other instances, microcystin in fish muscles can be as high as  $27.0 \text{ ng g}^{-1} \text{ dw}$  (dry weight) despite below detection water microcystin concentrations (de Magalhães et al. 2001). Understanding seasonal variation in visible blooms and their relationship to microcystin in fish is needed to inform consumption guidelines. Knowing how other variables that might be related to microcystin accumulation in fish, such as individual fish characteristics or water parameters, could provide anglers and government agencies with a more suitable proxy for determining which fish are safe to consume and when.

This study identifies variables that contribute to microcystin in fish over a 12-month period in a recreational reservoir with a history of cyanobacterial blooms. We do not have a clear understanding of how microcystin accumulation changes temporally, and if the factors linked with accumulation are consistent over time. The concentration of

microcystin in muscles, livers, and kidneys were examined in 2 recreationally favored sportfish species to examine potential differences in the accumulation and toxicodistribution of microcystin in intermediate (bluegill, *Lepomis macrochirus*) and high trophic level (largemouth bass, *Micropterus salmoides*) feeders. We examine whether microcystin in fish tissues varied with time of fish collection from April, 2018 to March, 2019, while accounting for fish characteristic variables (i.e., age, length, mass, organosomatic index for liver and gonad, body conditioning index, and sex). We hypothesize that microcystin concentrations will differ between bluegill and largemouth bass because these species feed from different trophic levels. We also hypothesize that microcystin will differ between tissue types, and between harvest dates. Results from this study represent the first assessment of microcystin concentrations in fish tissues collected from the North American Great Plains and contribute to our broader knowledge of accumulation of this toxin in aquatic food webs.

## METHODS

### *Site description*

Dairy Farm Lake #1 is a hypereutrophic reservoir, according to chl-*a* trophic status thresholds previously established for Missouri reservoirs (Jones et al. 2008). It is located in central Missouri, USA (W 38.994156° N -92.488833°) at the University of Missouri Foremost Dairy Research Center and was impounded in 1993. From bathymetric measurements (Figure A2.1), we determined the reservoir has a surface area of 56,084 m<sup>2</sup> and a volume of 123,921 m<sup>3</sup>. The maximum depth is 4.6 m and mean depth is 2.2 m. The watershed, which is 550,370 m<sup>2</sup>, is composed of 70 % crops, 28 % pasture grass, 1 % forest, and <1 % each of wetland, herbaceous or shrub rangeland, and barren

land (Dewitz 2019). Dairy Farm Lake #1 has been periodically stocked by the Missouri Department of Conservation (MDC) with bluegill and largemouth bass and was open to the public for angling during the study period. The reservoir has no inflowing tributary and overland and subsurface flow are the primary input into the reservoir. Outflowing water exits through an outflow valve. This reservoir has been part of a long-term surveillance program through the Missouri Department of Natural Resources (MDNR) to monitor water quality in waterbodies statewide. Dairy Farm Lake #1 was chosen for this study based on DNR's historic reports of cyanobacterial blooms, based on high chl-*a* concentrations as well as visual surface scums, and fish kills in the summer months. Prior to this study, between June, 2017 and December, 2018, phytoplankton samples were collected and biovolume was measured to characterize the composition of phytoplankton in Dairy Farm Lake #1. Cyanobacterial biovolume of 17 samples collected during summer months (June, 2017 to September, 2018) averaged 69.6 % of the total phytoplankton biovolume (Figure A2.2). Potential microcystin producers (procedures described in Chapman and Foss 2019) composed 28.7 % of the cyanobacterial biovolume and estimated nitrogen (N) fixation rates averaged  $0.32 \mu\text{g N L}^{-1} \text{ day}^{-1}$ , based on the number of heterocysts counted (procedures described in Findlay et al. 1994). Cyanobacterial biovolume of 3 samples collected during winter months (October to December) of 2017 and 2018 represented 37.8 % of the total phytoplankton biovolume and 3.4 % of these were potential microcystin producers). Estimated N fixation rates of these non-summer samples were  $0.12 \mu\text{g N L}^{-1} \text{ day}^{-1}$ ) based on a single sample taken on October 3, 2018. Phytoplankton collection, preservation, and enumeration methods are described in the supplemental information.

## *Field collection*

### *Water*

During this study, water parameters were measured approximately twice per month from Dairy Farm Lake #1 between April 19, 2018 and March 25, 2019.

Additionally, archival water data measured in the field and lab from the waterbody were available from twice per month testing over a year prior to fish collection (June 9, 2017 to December 20, 2019). All water quality samples were collected from a site located at the deepest point in the reservoir, directly in front of the earthen dam (Figure A2.1).

During each water quality sampling, we measured Secchi disk depth and used a Yellow Springs Instruments (YSI) EXO 3 sonde to record a vertical profile of temperature, dissolved oxygen (DO), pH, phycocyanin, and chl-*a*. The sonde was calibrated weekly using a 2 point calibration for DO and yearly for chl-*a* and phycocyanin using a known standard. In the field, we determined whether the reservoir was stratified or isothermal by a temperature change greater than 1 °C per meter. We record parameters from the sonde, including temperature (resolution is 0.02 °C, accuracy is  $\pm 0.01$  °C), DO (resolution is 0.1 mg L<sup>-1</sup>, accuracy is  $\pm 0.1$  mg L<sup>-1</sup>), pH (resolution is 0.1, accuracy is  $\pm 0.2$ ), and the ratio of phycocyanin to chl-*a* (PC:Chl-*a*; resolution is 0.01 RFU, accuracy is 0.1 RFU for both), as the average of measurements taken every 0.1 m throughout the mixed layer when the reservoir was stratified, or throughout the entire water column when the reservoir was isothermal. We record hypolimnetic DO as the mean of measurements taken every 0.1 m below the metalimnion to the sediment when the reservoir was stratified. A light profile was taken using a Li-Cor cosine underwater quantum sensor (LI-192) which recorded photosynthetically active radiation (PAR) at

0.25 m intervals throughout the water column. We used PAR to determine the light attenuation coefficient ( $K_d$ ) by taking the natural logarithm of irradiance versus depth (Kirk 1994).

Water cyanotoxin samples were collected using an integrated sampler from the water surface to 0.5 m, and with a van Dorn discrete sampler from 1 m above the sediment. Anatoxin-a and saxitoxin were preserved per Abraxis instructions immediately after collection. All cyanotoxin samples were stored frozen in amber glass vials until analysis. Composite water samples were collected from the surface to 1 m above the thermocline under stratified conditions, or when the reservoir was isothermal from the surface to 1 m above the sediment using a peristaltic pump. After collection, these samples were kept in the dark and transported back to the lab in acid-washed HDPE bottles and processed immediately.

### *Fish*

Largemouth bass ( $n= 117$ ) and bluegill ( $n= 89$ ) were harvested from the study site by MDC fisheries staff using diurnal boat electro-shocking. Fish were harvested on 8 sampling dates including April 23, 2018 (bluegill  $n= 10$ , largemouth bass  $n= 20$ ), May 30, 2018 (bluegill  $n= 13$ , largemouth bass  $n= 19$ ), July 16, 2018 (bluegill  $n= 10$ , largemouth bass  $n= 20$ ), August 21, 2018 (bluegill  $n= 11$ , largemouth bass  $n= 19$ ), October 11, 2018 (bluegill  $n= 10$ , largemouth bass  $n= 10$ ), November 27, 2018 (bluegill  $n= 11$ , largemouth bass  $n= 10$ ), February 4, 2019 (bluegill  $n= 14$ , largemouth bass  $n= 9$ ), and March 18, 2019 (bluegill  $n= 10$ , largemouth bass  $n= 10$ ). Target size of fish during collection were based on sizes most consumed by anglers (largemouth bass < 381 mm; bluegill < 127 mm), but actual size of fish collected was limited by fish availability at

time of sampling. All fish were kept in a live tank with reservoir water while being transported to the lab for processing. Fish mass and total body length, measured from the anterior edge of the mouth to the tip of the tail fin with lobes pressed together, were recorded and fish were euthanized by cervical cut. During dissection, muscles, kidneys, livers, and gonads were extracted. The masses of the liver and gonad were recorded and the organosomatic index was calculated as the mass of the organ divided by the total body mass, multiplied by 100. Muscles, livers, and kidneys were wrapped in aluminum foil and stored at -80 °C until microcystin analysis. Body condition index was calculated for Fulton's condition factor, which equals 100 times fish mass divided by the total length raised to the 3<sup>rd</sup> power (Froese 2006). Additionally, sagittae otoliths were collected during dissection for determination of fish age, with each ring counting as one year. All fish with the same number of rings were considered to be in the same age class, with the next age class beginning on January 1<sup>st</sup> of the next year (Devries and Fire 1996).

### *Laboratory analyses*

#### *Physiochemical analyses of water samples*

From integrated water samples from the mixed layer (when the reservoir was stratified), or from the surface to 1 m above the sediment (when the reservoir was isothermal), we measured total phosphorus (TP), total dissolved phosphorus (TDP), total nitrogen (TN), total dissolved nitrogen (TDN), nitrate + nitrite (NO<sub>3</sub><sup>-</sup>), ammonium (NH<sub>4</sub><sup>+</sup>), dissolved organic carbon (DOC), chl-*a*, total suspended solids (TSS), particulate inorganic matter (PIM), and particulate organic matter (POM) concentrations. Whole water was stored in glass digestion tubes for total nutrient analyses (TP, TN). Filtrate from 0.7 µm glass fiber filters (GFF) was used to measure total dissolved nutrients (TDP,

TDN) which were also stored in glass digestion tubes. TP and TDP were measured spectrophotometrically using the ascorbic acid colorimetric method (Method 4500P B5 [persulfate digestion] and Method 4500P E [ascorbic acid]; APHA, 2017). Phosphorus analyses had a detection limit of  $0.03 \mu\text{mol P L}^{-1}$ . We measured TN and TDN with the second derivative spectroscopy method (Crumpton et al., 1992; Method 4500-N C; APHA, 2017), which had a detection limit of  $2.50 \mu\text{mol N L}^{-1}$ . Total and total dissolved P and N samples were analyzed in triplicate.  $\text{NO}_3^-$  and  $\text{NH}_4^+$  were analyzed from  $0.7 \mu\text{m}$  GFF whole water filtrate using a Lachat QuikChem Flow Injection Analyzer.  $\text{NO}_3^-$  methodology (Method 4500- $\text{NO}_3^-$  I; APHA 2017) has a detection limit of  $0.36 \mu\text{mol NO}_3^- \text{L}^{-1}$  and reports  $\text{NO}_3^-$  as  $\text{NO}_3^-$  plus nitrite ( $\text{NO}_2^-$ ) based on the assumption that environmental  $\text{NO}_2^-$  concentrations are minimal. The lab detection limit for  $\text{NH}_4^+$  is  $0.71 \mu\text{mol NH}_4^+ \text{L}^{-1}$  (Method 4500- $\text{NH}_3$  G; APHA 2017).  $\text{NO}_3^-$  and  $\text{NH}_4^+$  were both analyzed in duplicate. We measured DOC from the filtrate of pre-combusted,  $0.7 \mu\text{m}$  GFF using a Shimadzu total organic C analyzer with the high-temperature combustion method (Method 5310B; APHA, 2017). DOC samples were analyzed in duplicate and had a limit of detection of  $16.7 \mu\text{mol C L}^{-1}$ . Chl-*a* concentrations were quantified from the material retained on  $1.0 \mu\text{m}$  Pall AE GFF using a Turner Design Fluorometer (TD-700) after ethanol extraction and pheophytin acid-correction (Sartory and Grobbelaar, 1984). Pheophytin is a chromophore produced when chlorophyll is digested and can be indicative of grazing rates. The chl-*a* detection limit was  $0.3 \mu\text{g L}^{-1}$ . We used standard methods (Method 2540 D and E; APHA 2017) to measure TSS by drying pre-weighed  $1.5 \mu\text{m}$  Whatman 934-AH filters at  $105 \text{ }^\circ\text{C}$  for 30 minutes. Filters were weighed and then incinerated at  $550 \text{ }^\circ\text{C}$  for 20 minutes to burn off organic material, allowing us to quantify

the portion of TSS that was PIM and POM. TSS, PIM, and POM had a detection limit of 0.1 mg L<sup>-1</sup>.

We calculated mean daily mixed layer irradiance ( $\bar{E}_{24}$ ) using the formula:

$$\bar{E}_{24} = \bar{E}_0 \times (1 - \exp(-1 \times K_d \times Z_{mix})) \times (K_d \times Z_{mix})^{-1}$$

where  $\bar{E}_0$  is incident irradiance and  $Z_{mix}$  is mixing depth.  $\bar{E}_0$  was calculated from the estimated shortwave radiation at the coordinates and date of sampling in Program R (R Core Team 2019) using the phytotools package (Silsbe and Malkin 2015), where it was modeled at 1 minute increments and scaled to PAR, while  $Z_{mix}$  was calculated from temperature profiles using the rLakeAnalyzer package in Program R (Winslow et al. 2017).

#### *Enzyme-immunoassay for microcystin in water and fish*

We used enzyme linked immunosorbent assay (ELISA, Abraxis LLC) to quantify microcystin concentrations in water sampled from the upper 0.5 m of the water's surface, water from 1 m above the sediment, and from fish tissues (i.e., muscles, livers, kidneys). The ELISA we used is an indirect, polyclonal anti-MC-Adda competitive assay based on the recognition of the cyanotoxins by specific biotinylated antibodies. The ELISA kit is approved by the US Environmental Protection Agency (EPA) to quantify microcystin in surface waters (Zaffiro et al. 2016). While cyanotoxins can occur in a variety of different congeners with differing levels of toxicity, ELISA is not able to distinguish between these congeners (Van Apeldoorn et al. 2007). The ELISA procedure measures total microcystin as MC-LR equivalent, meaning that our reported microcystin concentrations are a conservative assessment of potential health risk. We also used ELISA kits from

Abraxis LLC to quantify anatoxin-a, cylindrospermopsin, and saxitoxin in water samples. Before analyses, water samples were thawed and refrozen 3 times and filtered through 0.45  $\mu\text{m}$  GFF. The detection limits for water microcystin, anatoxin-a, cylindrospermopsin, and saxitoxin in water samples were 0.10, 0.10, 0.04, and 0.015  $\mu\text{g L}^{-1}$ , respectively.

Microcystin extraction methods for fish tissues followed published methods (Wood et al. 2006; Smith and Boyer 2009; Preece et al. 2015). Briefly, fish tissues were stored at  $-80\text{ }^{\circ}\text{C}$  between dissection and extraction. Whole tissues were cut up, weighed, and lyophilized to dryness. After lyophilization, whole tissues were weighed again and percent moisture was calculated by:  $(\text{mass before lyophilization} - \text{mass after lyophilization})/\text{mass before lyophilization}$ . Dried tissue subsets were ground using a mortar and pestle and combined with 4 mL of 80 % aqueous methanol in a scintillation vial. Positive controls were spiked with 5  $\mu\text{g L}^{-1}$  microcystin standard from the Abraxis kit. Next, we used a tissue distributor (D160 model from Scilogex) to homogenize samples for 60 seconds, and a probe sonicator (Q500 model with a saw-tooth probe from Qsonica) at 18 – 21 hertz frequency to sonicate samples for 60 seconds in 20 second on/off pulses. Both homogenization and sonication were conducted on ice. In between samples, both units were cleaned with 10 % bleach solution and rinsed with deionized water to prevent cross-contamination. Extracted fish samples were stored at room temperature and in the dark for 24 hours and then centrifuged for 20 minutes, after which the supernatant was passed through 0.45  $\mu\text{m}$  PES syringe filters (Environmental Express). Filters were pre-conditioned with 80 % methanol before the supernatant was passed through, and then rinsed with 80 % methanol. The rinse methanol was retained

and combined with our sample extraction. We then dried the samples at room temperature and in the dark using compressed air until all methanol was evaporated. After drying, we reconstituted the samples with 5 % aqueous methanol, which is the methanol threshold for the Abraxis Microcystin-Adda ELISA kit, and vortexed them for 60 seconds. We stored the samples at 4 °C if they were to be analyzed within 48 hours, or at -20 °C if it was going to be more than 48 hours before analysis. Immediately before analysis with ELISA, samples were brought to room temperature and vortexed for 60 seconds. Thereafter, detection of microcystin followed methods described in the ELISA kit instructions. We calculated the microcystin concentration per wet weight (ww) of each fish tissue using the ELISA output, the mass of the tissue subset, and the percent moisture of each tissue subset and report microcystin in fish tissues as concentrations per ww in  $\text{ng g}^{-1}$ .

While ELISA is a common technique used to measure microcystin concentrations in fish tissues, it can be associated with false positives because other components in the sample, like humic substances, proteins, and other biological macromolecules, can cross-react or interfere with the antibodies in each well (Meriluoto and Spoof 2007). To account for this potential inaccuracy, we included several quality assurance measures, including the use of fish raised in a hatchery with a groundwater source and no history of cyanotoxin exposure as positive (with addition of spike), and negative controls. We determined the detection limit for fish tissues to be the concentration where negative controls, which had no microcystin, were above the detection limit and attributed these false positives to matrix effects. Fish tissue detection limits were 1.6, 14.6, and 10.9  $\text{ng g}^{-1}$  ww for muscles, livers, and kidneys, respectively. There were 12 muscles (all

largemouth bass), 4 livers (2 bluegill and 2 largemouth bass), and 11 kidneys (5 bluegill and 6 largemouth bass) that were below the detection limit, which never represented more than 50 % of the samples collected on a single date for the same species. Our extraction efficiencies, based on spiked recoveries, were 95.4, 114.1, and 89.0 % for muscles, livers, and kidneys, respectively (Table A2.1) and are consistent with microcystin recoveries reported elsewhere (Preece et al. 2015). Intra assay variation was assessed by including the same fish tissue sample at the beginning and end of each ELISA run and was 13.7 % based on the average of each run. Inter assay variation was assessed for both bluegill and largemouth bass for all 3 tissue types by including the same sample in multiple runs. Bluegill inter assay variation was 25.4, 18.1, and 19.3 % for muscles, livers, and kidneys, respectively (Table A2.1). Largemouth bass inter assay variation was 13.8, 15.0, and 7.5 % for muscles, livers, and kidneys, respectively (Table A2.1).

We contracted 17 of our samples representing both species and all 3 tissue types to an external lab (Dr. Greg Boyer, Syracuse, NY), allowing us to compare our analysis with a lab that uses liquid chromatography coupled with tandem mass spectrometry (LC-MS/MS) to measure cyanotoxins in fish. LC-MS/MS is a specialized technique that is less susceptible to false positives than ELISA, especially when quantifying microcystin in organic tissues (Schmidt et al. 2013). LC-MS/MS was used to detect the molecular ion of 11 microcystin congeners, including RR, LR, dLR, LA, YR, hYR, WR, LY, LF, LW, and NOD. While our assay results reported microcystin concentrations ranging from 7.0 – 2592.8 ng g<sup>-1</sup> dry weight (1.6 – 614.6 ng g<sup>-1</sup> ww), results from LC-MS/MS were below the detection limit (2 ng g<sup>-1</sup>) for all samples. One reason for this could be because of false

positives in the Adda ELISA kit we used, which can arise when other compounds contain amino acids that are similar to the Adda moiety (3-amino-9-methoxy-2,6,8-trimethyl-10-phenyl-deca-4,6-dienoic acid; Moreno et al. 2011). Another possible explanation is that we are measuring degradation products from the glutathione metabolic pathway, which occur when microcystin is metabolized and are often not detected with LC-MS/MS (Schmidt et al. 2014).

### *Statistical analyses*

Unless otherwise stated, all statistical tests were performed in the base package of Program R (R Core Team 2019) and all figures were created with the package ggplot2 (Wickham 2016). For all statistical analyses,  $\alpha$  was set at 0.05. For microcystin in fish tissue toxin concentrations that were below the detection limit, we used half the detection limit in statistical analyses. Water samples were not collected on the same date that fish were harvested. For each fish harvest date, we calculated the associated water parameter values by taking the mean of samples collected immediately before, and immediately after each harvest date.

We modeled variables associated with microcystin concentrations in 6 species by tissue combinations (2 fish species and 3 tissue types). We created a separate model for each species tissue combination because existing work shows that microcystin accumulation in fish can vary by trophic level (Ibelings et al. 2005) and tissue type (Ferrão-Filho and Kozlowsky-Suzuki 2011) and we did not want these previously established patterns to drive our results. We began with 31 predictor variables, including 9 fish characteristics and a single temporal measure (harvest date; Table 3.1), hereon collectively referred to as fish characteristics, and 21 water parameters (Table 3.2).

Harvest date was treated as a categorical variable with 8 levels and was included with the fish characteristics because it was correlated with many of the water parameters. We screened fish characteristics and water parameters separately because we wanted to ensure that potential drivers of fish microcystin were not overlooked by considering so many predictors together. To determine which fish characteristics (Table 3.1) to include in our final, combined models, we used multiple linear regression. For all but largemouth bass livers, harvest date emerged as the only variable contributing to the best model to determine microcystin and was retained for inclusion in our combined models. We found no significant fish characteristic variables for microcystin concentrations in largemouth bass livers, so none of these predictors were retained. Total length, age, total mass, BCI, sex, liver mass, liver organosomatic index, gonad mass, and gonad organosomatic index were not significant variables and were not included in our first set of final, combined models.

We used a correlation-based principal components analysis (PCA) with no rotation to limit the number of variables in in our final, combined models. Water quality parameters are often correlated within a sampling period and would therefore exhibit multicollinearity in linear regression models. We considered water variables to be strongly correlated if absolute values were  $\geq 0.6$  within the first 3 component loadings (Table 3.2). We retained one variable from the group of correlated variables within each component loading. For the first component, we retained chl-*a* because it had a high component loading value and the relationship between chl-*a* and microcystin in fish was of ecological interest for this study. Water microcystin was retained for the second component loading. It also had a high component loading value and was of interest due to

its relationship with microcystin in fish tissues (Flores et al. 2018). None of the correlated parameters in the third component loading were more ecologically relevant than the others, so we retained TDN because it had the highest component loading value. We also retained parameters that had absolute values  $< 0.6$  for all 3 component loadings. These parameters did not display multicollinearity with each other nor the other water parameters and were DOC and TDP. To summarize, we retained chl-*a*, TDP, TDN, DOC, and water microcystin and included them in our final, combined model set to determine contribution to fish tissue microcystin value because our PCA showed us that they did not display multicollinearity.

We created a final, combined multiple linear regression model for each of our 6 species tissue combinations using harvest date and the 5 water parameters retained previously. We compared forward and backward stepwise selection and selected the model that had the lowest AIC. Our 6 final models assume a linear relationship between the predictor variables and fish microcystin concentrations and that our water parameters taken at a single site reflect conditions throughout the reservoir. After our final models were developed, we repeated this process, but excluded harvest date to examine whether there were other parameters related to fish microcystin concentrations that were being excluded by the strong harvest date signal. This left us with 2 final model sets, the first being 6 species and tissue models that considered harvest date, while the second was 6 species and tissue models that did not include harvest date.

Harvest date was identified as a significant variable in our models of microcystin in fish tissues. It was categorical, so we applied a 2-way analysis of variance (ANOVA) from the “car” package in Program R (Fox and Weisberg 2019) to identify the differences

between harvest date and fish species. Microcystin concentrations in all 3 tissue types were log transformed and outliers greater than 1.5 times the inter quartile range were removed in order to meet the assumptions of normality and homoscedasticity required for a 2-way ANOVA. Normality and homoscedasticity were verified for muscles (bluegill  $n= 85$ , largemouth bass  $n= 113$ ), livers (bluegill  $n= 89$ , largemouth bass  $n= 111$ ), and kidneys (bluegill  $n= 71$ , largemouth bass  $n= 105$ ) with a Shapiro-Wilk test and a Levene's test, respectively. When appropriate, we applied a Tukey HSD post hoc test from the R package "agricolae" (de Mendiburu 2020).

We also looked for correlations between microcystin in muscles and livers, muscles and kidneys, and livers and kidneys for each fish species. All but bluegill kidneys did not follow a normal distribution (Shapiro-Wilk  $p < 0.05$ ) even after transformation. Kidneys were homoscedastic, but muscles and livers were heteroscedastic (Levene's test  $p < 0.05$ ), even after transformation. For these reasons, a Spearman's rank correlation test was selected to measure correlations between microcystin in muscles (bluegill  $n= 89$ , largemouth bass  $n= 116$ ), livers (bluegill  $n= 88$ , largemouth bass  $n= 116$ ), and kidneys (bluegill  $n= 73$ , largemouth bass  $n= 108$ ). We also looked for correlations in fish total length and age as these parameters are related in most naturally occurring fish populations (Quist and Isermann 2017). Age did not follow a normal distribution (Shapiro-Wilk  $p < 0.05$ ) and was not homoscedastic (Levene's test  $p < 0.05$ ) even after transformation. For these reasons, a Spearman's rank correlation test was used to examine the relationship between fish length and age for bluegill ( $n= 89$ ) and largemouth bass ( $n= 116$ ).

## RESULTS

### *Reservoir characteristics*

Dairy Farm Lake #1 is a hypereutrophic reservoir located in an agricultural watershed. TP concentrations ranged from 1.56 – 3.92  $\mu\text{mol P L}^{-1}$  and were highest in August (Table 3.3). TN concentrations were lowest in May and highest in August, ranging from 65.81 – 141.28  $\mu\text{mol N L}^{-1}$  (Table 3.3). The natural log of the TN:TP ratio is reported to reduce bias resulting from calculating the mean of a ratio (Isles 2020). When the  $\ln(\text{TN:TP})$  ratio is above 3.91, the phytoplankton community is considered to be P-deficient, while  $\ln(\text{TN:TP})$  ratios below 3.00 suggest N-deficiency (Guildford and Hecky 2000). In October and November,  $\ln(\text{TN:TP})$  was above 3.91, suggesting that the phytoplankton community was P-deficient. Between  $\ln(\text{TN:TP})$  3.00 and 3.91, as was the case throughout the rest of the study period, factors other than N and P or both N and P could be restricting growth (Guildford and Hecky 2000).  $\text{NH}_4^+$  was higher than  $\text{NO}_3^-$  on all dates except November 27, 2018. At no time during the study did  $\text{NO}_3^-$  plus  $\text{NH}_4^+$  make up more than half of TDN, indicating that dissolved organic N was the dominant form of dissolved N. DOC was highest in July and lowest in March (Table 3.3).

We observed the clearest water in April and May when sampling dates were characterized most strongly by Secchi disk depth according to the PCA (Figure 3.1). Maximum Secchi disk depth (1.47 m), minimum TSS (4.4  $\text{mg L}^{-1}$ ) and PIM (0.8  $\text{mg L}^{-1}$ ) occurred during May, while minimum  $K_d$  (1.07  $\text{m}^{-1}$ ) was in April (Table 3.3). Maximum TSS (20.0  $\text{mg L}^{-1}$ ) and PIM (12.2  $\text{mg L}^{-1}$ ) occurred in February and, along with higher TDP and DO, characterized February and March sampling (Figure 3.1). PIM made up 17 – 29 % of TSS between May 30, 2018, and October 11, 2018, whereas it represented ~60 % throughout the rest of the study (Table 3.3).  $\bar{E}_{24}$  was highest in the May (271.11  $\mu\text{mol}$

photons  $\text{m}^{-2} \text{s}^{-1}$ ), before declining throughout the rest of the year. The only time that  $\bar{E}_{24}$  was below the light deficiency threshold (Table 3.3; Hecky and Guildford 1984) occurred in February when the reservoir was ice covered. Dairy Farm Lake #1 was stratified between May 30 and August 21, 2018 and was isothermal after November 27, 2018 (Table 3.3). Mean DO concentrations throughout the epilimnion when the reservoir was stratified, or entire water column when the reservoir was isothermal, were lowest in the July and highest in February. When the reservoir was stratified, hypolimnetic DO concentrations ranged from 0.2 – 1.7  $\text{mg L}^{-1}$  (Table 3.3).

POM and chl-*a* were both lowest in April (2.3  $\text{mg L}^{-1}$  and 9.61  $\mu\text{g L}^{-1}$ , respectively) and highest in August (12.9  $\text{mg L}^{-1}$  and 100.89  $\mu\text{g L}^{-1}$ , respectively). Pheophytin was also highest in August when maximum concentrations were 40.4  $\mu\text{g L}^{-1}$ , but lowest (2.8  $\mu\text{g L}^{-1}$ ) in November. The percentage of PC relative to chl-*a* (PC:Chl-*a*) is an indicator of how much of the total phytoplankton community is composed of cyanobacteria. In May, 0 % of the phytoplankton were cyanobacteria, increasing to a maximum of 25.49 % in July (Table 3.3). These 4 parameters (POM, chl-*a*, pheophytin, and PC:Chl-*a*) are positively correlated, which suggests that photoacclimation is not occurring and that chl-*a* and POM are representative of phytoplankton biomass. According to our PCA, high POM, chl-*a*, pheophytin, PC:Chl-*a*,  $K_d$ , pH, and TN are characteristic of July and August sampling dates (Figure 3.1).

#### *Water cyanotoxins*

The highest surface water microcystin concentration was 3.82  $\mu\text{g L}^{-1}$  on September 11, 2017 which was over 7 months before our first fish harvest date (Figure 3.2). We observed low (0.54 – 0.95  $\mu\text{g L}^{-1}$ ) but persistent concentrations of microcystin

in the water throughout the first 5 fish harvest dates (Table 3.3). The highest microcystin concentration collected from 1 m above the sediment between October 17, 2017 and March 25, 2019 was  $1.01 \mu\text{g L}^{-1}$  on May 31, 2018. Surface microcystin concentrations from the upper 0.5 m were similar to those 1 m above the sediment throughout the study period (Table 3.3). Anatoxin-a was detected in the surface and bottom waters from October 11, 2018 until March 18, 2019, but never in concentrations greater than  $0.23 \mu\text{g L}^{-1}$  (Table 3.3). Cylindrospermopsin was never measured above the detection limit and saxitoxin was only measured above the detection limit in the bottom waters on July 16, 2018 (Table 3.3).

#### *Fish characteristics*

Bluegill and largemouth bass were both smallest by mass and length in May (Table 3.1). Mean fish mass was variable over time, especially for largemouth bass (Table 3.1), but individual total mass ranged from 25.0 – 245.0 g for bluegill and 15.0 – 1737.5 g for largemouth bass. Mean total fish length over time varied little for both bluegill and largemouth bass (Table 3.1). Age was also similar across dates for both species, and total length and age were correlated for both bluegill and largemouth bass (Table A2.2). Individual fish lengths ranged from 12.6 – 16.6 cm for bluegill and from 11.0 – 49.0 cm for largemouth bass and individual ages ranged from 1 – 7 years for bluegill and from 0 – 11 years for largemouth bass. Mean Body Condition Index (BCI) displayed little variation throughout the year for both species (Table 3.1). BCI for individual bluegill and largemouth bass was more variable and ranged from 1.2 – 2.4 and 0.5 – 1.6, respectively. Mean liver organosomatic index for both species was not

consistent over time while gonad organosomatic index was highest in May for bluegill and April for largemouth bass (Table 3.1).

#### *Microcystin in fish by harvest date, species, and tissue*

The highest concentration of microcystin in both bluegill and largemouth bass occurred in fish livers, followed by kidneys, and muscles. Microcystin concentrations in muscles and kidneys were correlated (Table 3.4, Figure A2.3), and varied similarly over time. For bluegill, a positive correlation was identified for muscles and livers, muscles and kidneys, and livers and kidneys (Table 3.4). For largemouth bass, a positive correlation was identified for muscles and livers, and muscles and kidneys (Table 3.4).

For muscles and kidneys, the highest microcystin concentrations of both species were measured at the beginning of the study period on April 23, 2018. On each subsequent date, the concentrations were either lower, or not significantly different from the previous date, with the exception of muscle concentrations measured in February which was significantly higher than the preceding 2 dates. Conversely, liver microcystin concentrations for both species did not consistently decrease over time. Maximum liver microcystin concentrations for both bluegill and largemouth bass occurred in April, but after this date there was no consistent pattern in liver microcystin concentrations (Table A2.3).

#### *Fish characteristic cofactors contributing to microcystin variation in fish tissues*

We used multiple linear regression to assess which fish characteristics (Table 3.1) were related to microcystin accumulation in fish tissues. Significant variables were included in a final, combined model of fish characteristics and water parameters. When it

was included in the models, harvest date emerged as the only significant variable for microcystin in bluegill muscle, liver, kidneys, and largemouth bass muscle and kidneys. For largemouth bass liver microcystin concentrations, water microcystin was the only significant predictor variable (Table A2.4). Total fish length, age, BCI, sex, liver mass, liver organosomatic index, gonad mass, and gonad organosomatic index were not significant variables in any of our models that also included harvest date.

When we removed harvest date from the models, some fish characteristics emerged as predictive variables (Table A2.4). Liver organosomatic index was the only variable for the bluegill liver model ( $R^2\text{-adj} = -0.116$ ;  $p < 0.001$ ), and gonad organosomatic index was the only variable for both the largemouth bass muscle ( $R^2\text{-adj} = -0.117$ ;  $p < 0.001$ ) and kidney models ( $R^2\text{-adj} = -0.044$ ;  $p = 0.020$ ). None of the remaining fish characteristics contributed to significant models for bluegill muscles, bluegill kidneys, nor largemouth bass livers.

#### *Combined drivers of microcystin in fish tissues*

We applied multiple linear regression to determine which fish characteristics (Table 3.1) and water parameters (Table 3.2) contributed to microcystin in fish tissues. Harvest date emerged as the only variable in our final models for microcystin in bluegill muscle ( $R^2\text{-adj} = 0.698$ ,  $p < 0.001$ ), bluegill liver ( $R^2\text{-adj} = 0.266$ ,  $p < 0.001$ ), bluegill kidney ( $R^2\text{-adj} = 0.384$ ,  $p < 0.001$ ), largemouth bass muscle ( $R^2\text{-adj} = 0.763$ ,  $p < 0.001$ ), and largemouth bass kidney ( $R^2\text{-adj} = 0.433$ ;  $p < 0.001$ ), while water microcystin was the only variable in our final model for largemouth bass liver ( $R^2\text{-adj} = 0.035$ ;  $p = 0.024$ ).

The strong signal from harvest date likely prevented other variables from emerging as significant variables in our combined models, so we re-analyzed our variables without harvest date (Table A2.4). In the second set of combined models, we included the 5 water parameters identified from our PCA including chl-*a*, TDP, TDN, DOC, and microcystin from the upper 0.5 m of the surface. We also included liver organosomatic index for bluegill livers and gonad organosomatic index for largemouth bass muscles and kidneys. When harvest date was not considered, these variables were identified as significant predictors for multiple linear regression models which considered only fish characteristics. No fish characteristics were included in combined models for bluegill muscles, bluegill kidneys, nor largemouth bass livers because the fish characteristics did not yield a significant model. In all of our 6 combined models that did not consider harvest date, water microcystin emerged as a significant variable (Figure A2.4), and was the only variable for bluegill kidneys and all largemouth bass tissues. For these, the final model structure was:

$$\textit{Fish Microcystin} = \textit{Water Microcystin} + b$$

The models for bluegill kidneys ( $R^2\text{-adj}= 0.100$ ;  $p= 0.004$ ), largemouth bass muscles ( $R^2\text{-adj}= 0.259$ ;  $p< 0.001$ ), largemouth bass livers ( $R^2\text{-adj}= 0.035$ ;  $p= 0.024$ ), and largemouth bass kidneys ( $R^2\text{-adj}= 0.175$ ;  $p< 0.001$ ) were all significant. For bluegill muscles, final model structure was:

$$\textit{Bluegill Muscle Microcystin} = \textit{Water Microcystin} + \textit{chl} + \textit{TDN} + b$$

where chl refers to chlorophyll-*a* concentrations in  $\mu\text{g L}^{-1}$  and TDN is total dissolved nitrogen concentrations in  $\mu\text{mol N L}^{-1}$ . This model was significant ( $p < 0.001$ ) and had an  $R^2$ -adj of 0.459. Final model structure for bluegill livers was:

$$\text{Bluegill Liver Microcystin} = \text{Water Microcystin} + \text{Liver OSI} + \text{TDP} + b$$

where Liver OSI is the liver organosomatic index as a percent and TDP is total dissolved phosphorus in  $\mu\text{mol P L}^{-1}$ . This model was significant ( $p < 0.001$ ) and had an  $R^2$ -adj of 0.299.

#### *The effect of harvest date and species on microcystin in fish tissues*

Multiple linear regression identified harvest date as an important categorical variable of microcystin in fish tissues, but this test does not differentiate differences between individual dates, so further analyses were required. Two-way ANOVAs were conducted to compare the main effects of harvest date and species as well as their interaction on wet weight microcystin concentrations in fish muscles, livers, and kidneys (Table 3.5, Figure 3.3). For muscles and kidneys, the interaction term between harvest date and species was not significant because microcystin was correlated in these tissues (Table 3.5).

Individually, both harvest date and species were significant for muscles and kidneys indicating that microcystin concentrations in these tissues were significantly different between bluegill and largemouth bass, and that microcystin concentrations in these tissues differed between harvest dates (Table 3.5). For livers, the interaction between harvest date and species was significant, indicating that differences between microcystin in these 2 species depended on harvest date.

## DISCUSSION

Harvest date emerged as the most important variable explaining microcystin accumulation in fish tissues, although microcystin concentrations in the water also played a role. After removing harvest date, water microcystin emerged as a predictor variable of microcystin in fish for all 6 of our final, combined models, suggesting that low but persistent concentrations in the environment can lead to accumulation in fish. *Chl-a* and TDN were also included in our final model for bluegill muscles, but the  $R^2$ -adj for this model was only 0.175. Likewise, TDP and liver organosomatic index were significant predictors for bluegill livers, but the final  $R^2$ -adj for this model was only 0.299. While these variables could explain some of the temporal variation we observed in fish microcystin concentrations, the low  $R^2$ -adj values suggests that the link between these predictors and microcystin in fish tissues is weak. Microcystin concentrations in fish tissues were highest in April in the muscles and kidneys of both bluegill and largemouth bass and declined throughout the rest of the year. This decline could be due to cooler water temperatures in the fall and winter slowing down fish consumption and thus microcystin exposure (Block et al. 2020), or because there is an unidentified link between microcystin accumulation and spawning. Behavioral changes associated with spawning, such as consuming more food or spending more time in the littoral zone, may influence microcystin accumulation. Liver microcystin concentrations were more variable than microcystin in muscles and kidneys throughout the year for both species, possibly because microcystin elimination rates are much slower in livers than in muscles or kidneys (Adamovský et al. 2007). Microcystin concentrations were higher in bluegill than in largemouth bass, and concentrations in muscles and kidneys were positively

correlated for both species. Trophic transfer of microcystin is well documented (Ibelings et al. 2005) and we believe that differences in diet offer an explanation for the patterns we observed. Bluegill feed at lower trophic levels than largemouth bass, which could explain why microcystin in bluegill muscles and kidneys were higher than in largemouth bass. This study, measuring microcystin accumulation in 2 recreationally valuable species, is the first to quantify cyanotoxins from fish in the Great Plains, a region where cyanobacterial blooms are common due to high agricultural land use and fertilizer application. This study helps inform the potential microcystin related health risks of consuming the muscles of sportfish in a region where harmful cyanobacterial blooms are common.

#### *Temporal patterns of microcystin in fish*

Diet and feeding habits may contribute to the differences in microcystin concentrations we observed among dates. For warm-water fish like bluegill and largemouth bass, foraging rates are positively correlated with temperature (Block et al. 2020), which could explain the temporal patterns that we observed in microcystin in muscles and kidneys. Bluegill feeding, for example, starts to decline below 10 °C, and ceases when temperatures drop below 3.3 °C (Carlander 1977). Warmer temperatures and increased foraging in the spring and summer contribute to increases in fish growth (McCauley and Kilgour 1990) and could explain the temporal patterns we observed in our study. If fish mass increases at a higher rate than microcystin accumulation, it might appear that microcystin concentrations in fish were decreasing over time. A similar “dilution” effect occurs in mercury uptake by fish (Pickhardt et al. 2002). Ultimately, decreased foraging rates during colder periods could reduce fish exposure to microcystin

if, as we suspect, diet is important to explaining microcystin concentrations in fish from our study site.

Spawning may also play a role in explaining the temporal trends we observed in microcystin accumulation. In Missouri, bluegill typically spawn from late May through August, while largemouth bass spawn from mid-April through late May (Pflieger et al. 1997), roughly corresponding with the sampling dates where we measured the highest microcystin concentrations in muscles and kidneys in both species. The link between spawning and microcystin accumulation could be behavioral, such as consuming more food to offset the high energetic cost of spawning (Jennings et al. 1997; Brown and Murphy 2004) or spending more time in shallow, littoral waters during spawning and nest protection (Gosch et al. 2006; Lawson et al. 2011), which could increase exposure if a surface bloom has been blown close to shore. Either of these behaviors could explain the higher April microcystin concentrations in fish, although we also might have expected to see higher concentrations of liver microcystin concentrations in the spring. Microcystin in the water can reduce spawning activity and success (Baganz et al. 1998), but additional work is required before a definitive link can be made between spawning and microcystin accumulation.

#### *Differences in microcystin by species*

Species-specific dietary patterns likely explain the significant difference we observed in muscle and kidney microcystin concentrations between bluegill and largemouth bass. Consumed food items are a primary route of microcystin exposure for fish (Zamora-Barrios et al. 2019), and these 2 species usually feed from different trophic levels. Bluegill feed primarily on benthic macroinvertebrates and zooplankton (Olson et

al. 2003). Zooplankton are an important component for bluegill diets throughout their lives, even for adults over 200 mm (Harris et al. 1999). In our study, bluegill ranged from 80 – 224 mm, so it is likely that zooplankton made up at least a portion of their diet. Adult largemouth bass above 80 – 100 mm rarely consume zooplankton and primarily feed on fish (Carlander 1977), although benthic macroinvertebrates can also be an important component of their diet (Phillips et al. 1995; Olson 1996; Dibble and Harrel 1997). It is likely that largemouth bass did not consume zooplankton as the smallest bass we sampled was 110 mm. As piscivores (Carlander 1977), largemouth bass probably fed primarily on bluegill as these were the most abundant prey species in the reservoir. While there is some evidence that microcystin biomagnification can occur for planktivorous fish, the ability of organisms to metabolize this toxin mean that it often declines as trophic level increases (Kozlowsky-Suzuki et al. 2012; Pham and Utsumi 2018). Food web studies have revealed that zooplankton contain higher concentrations of microcystin than the fish that consume them, in part because microcystin can be eliminated through the glutathione metabolic pathway (Ibelings et al. 2005; Schmidt et al. 2014). This would explain why microcystin in bluegill was higher than in largemouth bass, despite the likelihood that largemouth bass are consuming bluegill.

The difference between microcystin in bluegill and largemouth bass livers varied temporally, but not by species alone. There is some evidence that fish at higher trophic levels have smaller differences in microcystin in livers and muscles than do fish at lower trophic levels (Flores et al. 2018). This finding is not ubiquitous (Ferrão-Filho and Kozlowsky-Suzuki 2011) and does not explain the significant interaction between date and species. While broad patterns in microcystin accumulation exist based on trophic

level, our study re-emphasizes that individual species may accumulate microcystin differently (Jia et al. 2014) and at different temporal scales. Fish organ size changes over time and in our study, liver OSI was negatively related to microcystin in bluegill livers (Table A2.4). This could suggest that a loss in liver mass concentrates microcystin in bluegill livers.

#### *Microcystin toxicodistribution in fish*

For both bluegill and largemouth bass, microcystin accumulation was highest in livers, followed by kidneys, and then muscles. This order has been previously reported, although there is some evidence to suggest that microcystin accumulation is higher in kidneys than in livers for carnivorous fish like largemouth bass (Ferrão-Filho and Kozlowsky-Suzuki 2011). We observed a positive correlation between microcystin in muscles and kidneys for both bluegill and largemouth bass, which is consistent with previous studies (Mohamed et al. 2003; Chen et al. 2006a). The gut is the primary location for microcystin to be transferred into the bloodstream (Cazenave et al. 2005). Once in the blood, microcystin is transported throughout the body but is not evenly retained across all tissue types, and toxicodistribution can vary by species (Xie et al. 2004). Microcystin retention varies based on several factors including the type of microcystin congener present, type of microcystin exposure, and the amount of blood within the organ (Cazenave et al. 2005; Steiner et al. 2016). The existence of such a strong correlation between microcystin in muscles and kidneys, despite the fact that the kidney is blood-rich while the muscle is not, suggests that the mechanism behind microcystin retention might be similar for these tissue types.

In our study, microcystin concentrations in fish livers were dissimilar to those observed for muscles and kidneys, which is inconsistent with previous work (Mohamed et al. 2003; Chen et al. 2006a). Unlike muscles and kidneys, liver microcystin concentrations did not decrease consistently throughout the study and correlations between livers and other tissues, while present, were never strong ( $\rho$  value  $\leq 0.38$ ). Microcystin is eliminated at a much slower rate in fish livers compared to muscles. The half-life for microcystin in carp livers was estimated to be 8.4 days, compared to 0.7 days for muscles (Adamovský et al. 2007). One explanation for the apparent lack of pattern in liver microcystin accumulation could be that repeated exposure may roughly equal elimination because it takes longer for fish to eliminate microcystin from their liver. We measured detectable microcystin in the water on 6 of 8 harvest dates. Another explanation is that the microcystin congener changed throughout the study period. There is evidence to suggest that the quantity of microcystin absorbed across the intestinal epithelia varies by congener, as does the transport of microcystin throughout fish (Xie et al. 2004; Chen et al. 2006a). Cyanobacterial blooms can be temporally heterogeneous in the type of microcystin congener they produce (Greene et al. 2021). If this temporal heterogeneity was present during our study, it might explain why microcystin accumulation in fish livers followed different patterns than in muscles and kidneys. Further research is needed to better understand species differences in the accumulation of microcystin congeners.

To the best of our knowledge, this is the first study to assess microcystin concentrations in bluegill and largemouth bass kidneys, the first to measure microcystin in the muscles and livers of these two species over a 12 month period, and the first to

investigate microcystin concentrations in the North American Great Plains (Table 3.6). In the US Midwest, bluegill and largemouth bass are frequently targeted by anglers and are recreationally valuable. In 2019, boating and fishing contributed \$23.6 billion to the United States gross domestic product, so maintaining a healthy fishery has important economic implications (BEA 2020). By measuring microcystin concentrations in fish over the course of 12 months, we acquired a better understanding of how microcystin accumulation varies temporally. We found that microcystin impacts are not ubiquitous across taxa. This study also provides regional context for microcystin concentrations in the tissues of 2 fish species that have been largely overlooked when it comes to measuring microcystin accumulation. The microcystin concentrations we observed in these species are consistent with the small number of largemouth bass and *Lepomis* sp. previously assessed for cyanotoxins. For example in Washington, mean microcystin concentrations in largemouth bass were 2.4 and 75.0 ng g<sup>-1</sup> ww for muscles and livers, respectively, based on quantification with ELISA (Hardy et al. 2015), and 4.8 ng g<sup>-1</sup> ww in Lake Ontario bluegill muscles (Table 3.6; Poste et al. 2011). In pumpkinseed sunfish (*Lepomis gibbosus*), a close relative to bluegill, microcystin ranged from 1.9 to 8.7 ng g<sup>-1</sup> ww in muscles from Lake Ontario and Washington fish, respectively (Table 3.6; Poste et al. 2011; Hardy et al. 2015). Liver microcystin concentrations from New Hampshire pumpkinseed sunfish were 3.8 ng g<sup>-1</sup> ww, an order of magnitude lower than the microcystin concentrations from bluegill livers measured in our study (Table 3.6; Smith and Haney 2006). Overall, the range of microcystin concentrations we measured generally fell within previously reported microcystin concentrations from *Lepomis* sp. and largemouth bass tissues in other regions.

### *Microcystin in water and fish*

Water microcystin concentrations explained the differences we observed in fish tissue microcystin concentrations only when harvest date was not included in our models. It was a significant predictor in all 6 of our final models and was the only predictor for bluegill kidneys and all 3 largemouth bass models. A positive relationship between microcystin in water and in fish has previously been reported when concentrations in the water are as high as  $13.4 \mu\text{g L}^{-1}$  (Amrani et al., 2014; Nchabeleng et al. 2014; Flores et al. 2018). Our surface water microcystin concentrations were comparably low ( $<1.0 \mu\text{g L}^{-1}$ ; Table 3.3). While chl-*a* concentrations were high ( $\sim 100 \mu\text{g L}^{-1}$ ) during summer sampling, the PC:Chl-*a* ratio was never greater than 25.49 % (Table 3.3), suggesting that cyanobacteria did not dominate the phytoplankton. In other studies where water microcystin is not directly related to microcystin in fish, water microcystin concentrations are also relatively low. In Italy, over a 16 month period, the highest water microcystin concentration was  $4.21 \mu\text{g L}^{-1}$  and there was no relationship between microcystin in fish and water (Bruno et al. 2009). We observed detectable levels of microcystin in the water on 5 of 8 harvest dates. This suggests that water microcystin concentrations do not need to be especially high to result in accumulation in fish as long as they are persistent and occur frequently. Cyanobacteria likely were not a dominant phytoplankton group when we harvested fish. Not all cyanobacteria can produce microcystin (Chapman and Foss 2019), and even potential toxin producers do not always produce cyanotoxins (Carmichael and Boyer 2016).

The rate of microcystin elimination from fish tissues via the glutathione metabolic pathway is likely on the order of days to weeks (Schmidt et al. 2014). On September 11,

2017, we observed water microcystin concentrations of  $3.82 \mu\text{g L}^{-1}$ . We think it is unlikely that the higher concentrations of microcystin in fish during spring 2018 are a result of the higher microcystin concentrations measured on September 11, 2017 because of the 7 month timespan before the first fish harvest date. In previous work, microcystin was eliminated completely from the muscles of silver carp (*Hypophthalmichthys molitrix*) and common carp (*Cyprinus carpio*) and reduced by 96 and 87 %, respectively, in the livers of these 2 species over a 2 week study period (Adamovský et al. 2007). In pumpkinseed sunfish, microcystin was eliminated from the muscle and liver within 9 days (Smith and Haney 2006). We observed a general decline in microcystin in muscles and kidneys over the course of the study, suggesting that microcystin elimination from these tissues was greater than exposure throughout the study period (Soares et al. 2004; Gurbuz et al. 2016). Microcystin concentrations in water can vary 3-fold over the course of a day (Miller et al. 2019), so it is possible that our bimonthly sampling missed periods of high microcystin concentrations that occurred before the first fish harvest date on April 23, 2018. While uncommon, spring cyanotoxin concentrations have been observed (Wiltsie et al. 2018).

High chl-*a* concentrations or visible presence of an algal bloom have been suggested as time periods to avoid consumption of fish due to the potential for toxin accumulation in fish. Our findings suggest that there is not a reliable water parameter to determine elevated microcystin in fish tissues. When harvest date was not included in our models, water microcystin did emerge as a significant predictor variable for both species and for all tissues, and it was the only predictor variable that was significant for more than a single model. These models did not explain much of the variation in microcystin in

fish tissues, but this could be attributed to the fact that the range of water microcystin concentrations we observed was low. It is possible that a bloom occurred and died between water sampling, which may have released a pulse of microcystin into the water (McKindles et al. 2020). Microcystin concentrations measured at the bottom of the reservoir were similar to concentrations measured at the surface. When the reservoir was isothermal, such as November 11, 2018, February 4, 2019, and March 18, 2019, microcystin concentrations in water from above the sediment could have originated from cyanobacteria suspended throughout the water column. The reservoir was stratified on May 30, 2018, July 16, 2018, and August 21, 2018. On these dates, microcystin measured above the sediment was similar to microcystin measured in surface waters. Phytoplankton sedimentation rates would have to be high to account for the similar microcystin concentrations measured at both depths (Wörmer et al. 2011). Alternatively, microcystin near the bottom could be produced by benthic cyanobacteria (Izaguirre et al. 2007). Resuspension of cyanobacterial cells from the sediment (Tsujimura et al. 2000) or sediment particles themselves could be a source of hypolimnetic cyanotoxins as they readily bind to fine particles (Chen et al. 2006b). Microcystin likely degrades at a slower rate in the bottom waters due to reduced temperatures, PAR, and UV (Park et al. 2001; Wörmer et al. 2010). Bottom water microcystin likely does not represent a major route of exposure for fish as the lack of DO in the hypolimnion excludes most fish for extended periods (Vanlandeghem et al. 2010). Hypoxia also excludes some species of zooplankton (Vanderploeg et al. 2009), which further suggests that fish from our study remained in the epilimnion or littoral zone throughout most of the summer.

#### *Ecological implications*

Exposure to microcystin can have negative effects on fish health, causing histological inflammation, and degeneration and necrosis in tissues throughout the body, but especially the liver (Ibelings et al. 2005). Liver damage is reversible for acute exposure through increased activity of antioxidant enzymes like superoxide dismutase, catalase, glutathione reductase, and glutathione peroxidase, but production of these enzyme exerts an energetic cost (Kankaanpää et al. 2002; Prieto et al. 2006). While adult fish can usually meet this cost, embryotic fish sometimes struggle to meet it because of their limited energy reserve within the yolk (Cazenave et al. 2006). We observed the highest concentrations of microcystin in fish tissues during the spring. If intergeneration transfer of microcystin through gametes does occur, as is the case with organochlorine compounds (Miller 1993), and selenium (Coyle et al. 1993), it is possible that embryonic fish spawned during our study period were exposed to microcystin. We are unaware of any study that investigates intergenerational transfer of microcystin in fish, although this transfer does not seem to occur in aquatic insects (Woller-Skar et al. 2020). Younger fish are more susceptible to the negative health effects of microcystin exposure (Saraf et al. 2018), so even a small transfer could have outsized effects on the success of the entire year class. High spring microcystin concentrations could result in ovarian necrosis (Acuña et al. 2012), which could also reduce year class recruitment. Chronic exposure to microcystin can also have a negative effect on fish health, resulting in liver and ovary apoptosis, damaged gills, hepatic steatosis, and increased difficulty in maintaining cation-anion homeostasis (Carbis et al. 1997; Zhan et al. 2020; Zhang et al. 2020). This results in a greater physiological stress response and reduced fish fitness, ultimately degrading the fishery and reducing its utility to anglers (Ferrão-Filho and Kozlowsky-Suzuki 2011).

Impacts from chronic exposure may be especially pronounced in systems like Dairy Farm Lake #1, where microcystin concentrations in the water are usually low but occur often.

Increased susceptibility to predation resulting from behavioral and physiological changes associated with microcystin exposure may also negatively impact fishery health. Fish motility decreases as exposure to microcystin increases (Baganz et al. 2004), hampering a fish's ability to acquire food and ultimately making it more susceptible to predation (Plaut 2000). A fish may also be more susceptible to predation if it is experiencing negative health effects, like those that can result from microcystin exposure (Kankaanpää et al. 2002; Prieto et al. 2006). Bluegill are common prey for largemouth bass in many small, agriculturally dominated reservoirs (Garvey and Stein 1998), and increased bluegill predation could result in a degraded largemouth bass fishery over time as food becomes scarcer. In small, warmwater impoundments where agricultural land use is high, cyanobacterial blooms occur frequently (Straubinger-Gansberger et al. 2014), and bluegill and largemouth bass are the most commonly stocked fish species (Modde 1980). Our study suggests that it is possible cyanotoxins frequently disrupt the fisheries in these systems, especially in the spring when spawning occurs, and additional investigation into the relationship between cyanobacteria and fish health is required.

#### *Management implications*

A quick and easy method for determining cyanotoxin concentrations in fish tissues would be useful to management agencies tasked with advising the public about when fish are safe to eat. Our findings suggest that the time of year fish are caught is an important variable in assessing microcystin in fish muscles and should be considered when setting consumption advisories. We did not find any fish characteristic or water

parameters that can be reliably used to predict microcystin in fish tissues, although water microcystin concentrations appear to be related. It is possible that water microcystin could be used as a proxy if the range in concentrations was greater than what we observed, but additional research is required to properly assess whether this is the case. Despite the fact that it was not a significant variable in any of our regression analyses, total fish length was negatively correlated with microcystin in muscles and kidneys (i.e. smaller fish have higher concentrations of microcystin) for largemouth bass (Table A2.2, Figure A2.5). Fish length is easy to measure in the field and is commonly used as a proxy for pollutant accumulation in fish (Backstrom et al. 2020). The correlations we observed between these parameters were weak, suggesting that length is not a good proxy for microcystin in fish tissues.

Exposure to microcystin poses a risk to human health, so advisories have been developed for safe levels of fish consumption (Ibelings and Chorus 2007). Several factors are considered for consumption advisories, including weight of the consumer, established no observed adverse effect levels (Fromme et al. 2000), and duration of exposure (Ibelings and Chorus 2007). While it is beyond the scope of this study to make any sort of recommendation about what fish are safe to eat, it is important to put the microcystin concentrations we observed into context by comparing them to existing advisories, taking into consideration the microcystin concentrations in consumed tissues and the amount of tissue consumed. For bluegill and largemouth bass, anglers typically consume only the muscle. Using the highest microcystin concentrations we measured in muscles of bluegill (38.0 ng g<sup>-1</sup> ww) and largemouth bass (17.9 ng g<sup>-1</sup> ww), we calculated how much fish a person would have to consume to exceed tolerable daily intakes by dividing tolerable

daily intake (Ibelings and Chorus 2007) by the highest microcystin concentrations we observed in both species. Assuming a child weighs 10 kg and an adult weighs 75 kg, we can compare microcystin in fish from our study with consumption advisories for lifetime tolerable daily intake, which is calculated based on daily exposure for many months and reflects the risk posed to subsistence fishers (Ibelings and Chorus 2007). To exceed the lifetime tolerable daily intake consumption advisory, a child would have to consume 10.5 g of bluegill and 22.3 g of largemouth bass per day, while an adult would have to consume 78.9 g of bluegill and 167.6 g of largemouth bass per day. Assuming a meal size for a child is 85 g of fish and for an adult is 227 g based on American Heart Association recommendations, a single meal of both species would exceed lifetime consumption advisories (Lichtenstein et al. 2006; Ibelings and Chorus 2007). For people who are eating the fish they catch regularly, but for several weeks at a time instead of months, the seasonal tolerable daily intake advisory might be more applicable (Ibelings and Chorus 2007). To exceed the seasonal advisory for daily consumption, a child would have to consume 105.3 g of bluegill and 223.5 g of largemouth bass per day, while an adult would have to consume 789.5 g of bluegill and 1676.0 g of largemouth bass per day. The American Heart Association recommends consuming 1 – 1.5 meals (227–340 g) of fish each week (Lichtenstein et al. 2006), and Missouri anglers typically consume 306 g of fish each meal (McKee et al. 2015). Based on the microcystin concentrations we measured in fish from this study, an adult Missouri angler could consume 18 meals of bluegill, and 38 meals of largemouth bass each week without exceeding microcystin consumption advisories (Ibelings and Chorus 2007). Our calculation represents a conservative, worst-case scenario because we are using the highest microcystin

concentrations we observed in both species, and because many Missourians do not eat fish every day, per the assumptions of the seasonal consumption advisory (McKee et al. 2015).

### *Conclusions*

Microcystin concentrations were highest in the livers of both bluegill and largemouth bass, followed by kidneys and then muscles. Microcystin concentrations in muscles and kidneys were highest in the spring for both species and declined throughout the rest of the year. This pattern could be related to diet, as we observed relatively low concentrations of microcystin in the water. Consumption of contaminated food could be a primary route of microcystin exposure and future work should look for a link in fish diet and microcystin accumulation in tissues. Another reason that fish microcystin concentrations were higher in April could be because there is a link between spawning and microcystin accumulation. Additional work is required to confirm that this relationship exists in other systems, and to identify the mechanism causing higher concentrations of microcystin in fish collected during the spring. We found that microcystin in fish varies by species, and that bluegill have higher microcystin concentrations possibly because they feed more often from lower trophic levels where microcystin concentrations are often higher, than do largemouth bass. Our findings suggest that fish from our study reservoir did not pose an immediate human health concern for anglers. Study of additional species and reservoirs is necessary before conclusions about the health risk of consuming contaminated fish can be made.

## LITERATURE CITED

- Acuña, S., D. Baxa & S. Teh, 2012. Sublethal dietary effects of microcystin producing *Microcystis* on threadfin shad, *Dorosoma petenense*. *Toxicon* 60: 1191-1202.
- Adamovský, O., R. Kopp, K. Hilscherová, P. Babica, M. Palíková, V. Pašková, S. Navrátil & L. Bláha, 2007. Microcystin kinetics (bioaccumulation, elimination) and biochemical responses in common carp and silver carp exposed to toxic cyanobacterial blooms. *Environmental Toxicology and Chemistry* 26: 2687-2693.
- Amrani, A., H. Nasri, A. Azzouz, Y. Kadi & N. Bouaïcha, 2014. Variation in cyanobacterial hepatotoxin (microcystin) content of water samples and two species of fishes collected from a shallow lake in Algeria. *Archives of Environmental Contamination and Toxicology* 66: 379-389.
- Anderson-Abbs B.A., M. Howard, K.M. Taberski & K.R. Worcester, 2016. California freshwater harmful algal blooms assessment and support strategy. California State Water Resources Control Board. Sacramento, CA.
- APHA, 2017. Standard Methods for the Examination of Water and Wastewater, 23rd ed., In: R.B. Baird, R.B., A.D. Eaton & E.W. Rice (Eds.). American Public Health Association, Washington, DC.
- Azevedo, S.M.F.O., W.W. Carmichael, E.M. Jochimsen, K.L. Rinehart, S. Lau, G.R. Shaw & G.K. Eaglesham, 2002. Human intoxication by microcystins during renal dialysis treatment in Caruaru-Brazil. *Toxicology* 181-182: 441-446.
- Backer, L.C., J.H. Landsberg, M. Miller, K. Keel & T.K. Taylor, 2013. Canine cyanotoxin poisonings in the United States (1920s–2012): review of suspected and confirmed cases from three data sources. *Toxins* 5: 1597-1628.
- Backstrom, C.H., K. Buckman, E. Molden & C.Y. Chen, 2020. Mercury levels in freshwater fish: estimating concentration with fish length to determine exposures through fish consumption. *Archives of Environmental Contamination and Toxicology* 78: 604-621.
- Baganz D., G. Staaks & C.E.W. Steinberg, 1998. Impact of the cyanobacteria toxin, MC-LR on behaviour of zebrafish, *Danio rerio*. *Water Research* 3: 948-952.
- Baganz D., G. Staaks, S. Pflugmacher & C.E.W. Steinberg, 2004. Comparative study of microcystin-LR-induced behavioral changes of two fish species, *Danio rerio* and *Leucaspius delineates*. *Environmental Toxicology* 19: 564-570.
- BEA (Bureau of Economic Analysis), 2020. Outdoor recreation satellite account, U.S. and states, 2019. <https://www.bea.gov/news/2020/outdoor-recreation-satellite-account-us-and-states-2019>

- Block, B.D., J.D. Stockwell & J.E. Marsden, 2020. Contributions of winter foraging to the annual growth of thermally dissimilar fish species. *Hydrobiologia* 847: 4325-4341.
- Brown, M.L. & B.R. Murphy, 2004. Seasonal dynamics of direct and indirect condition indices in relation to energy allocation in largemouth bass *Micropterus salmoides* (Lacèpede). *Ecology of Freshwater Fish* 13: 23-26.
- Bruno, M., S. Melchiorre, V. Messineo, F. Volpi, A. Di Corcia, I. Aragona, G. Guglielmone, C. Di Paolo, M. Cenni, P. Ferranti & P. Gallo, 2009. Microcystin detection in contaminated fish from Italian lakes using ELISA immunoassays and LC-MS/MS analysis, in P.M. Gault & H.J. Marler (Eds.), *Handbook on Cyanobacteria: Biochemistry, Biotechnology and Applications*. New York, NY, pp. 191-210.
- Campos, A. & V. Vasconcelos, 2010. Molecular mechanisms of microcystin toxicity in animal cells. *International Journal of Molecular Sciences* 11: 268-287.
- Cao, H., F. Kong, L. Luo, X. Shi, Z. Yang, X. Zhang & Y. Tao, 2006. Effects of wind and wind-induced waves on vertical phytoplankton distribution and surface blooms of *Microcystis aeruginosa* in Lake Taihu. *Journal of Freshwater Ecology* 21: 231-238.
- Carbis, C.R., G.T. Rawlin, P. Grant, G.F. Mitchell, J.W. Anderson & I. McCauley, 1997. A study of feral carp, *Cyprinus carpio* L., exposed to *Microcystis aeruginosa* at Lake Mokoan, Australia, and possible implications for fish health. *Journal of Fish Diseases* 20: 81-91.
- Carlander, K.D., 1977. *Handbook of Freshwater Fishery Biology*. Ames, IA, 431.
- Carmichael, W.W., 1994. The toxins of cyanobacteria. *Scientific American* 270: 78-86.
- Carmichael, W.W. & G.L. Boyer, 2016. Health impacts from cyanobacterial harmful algae blooms: implications for the North American Great Lakes. *Harmful Algae* 54: 194-212.
- Cazenave, J., D.A. Wunderlin, M.D.L.A. Bistoni, M.V. Amé, E. Krause, S. Pflugmacher & C. Wiegand, 2005. Uptake, tissue distribution and accumulation of microcystin-RR in *Corydoras paleatus*, *Jenynsia multidentata* and *Odontesthes bonariensis*: a field and laboratory study. *Aquatic Toxicology* 75: 178-190.
- Cazenave, J., M.A. Bistoni, E. Zwirnmann, D.A. Wunderlin & C. Wiegand, 2006. Attenuating effects of natural organic matter on microcystin toxicity in zebra fish (*Danio rerio*) embryos—benefits and costs of microcystin detoxication. *Environmental Toxicology* 21: 22-32.
- Chapman, A. & A. Foss, 2019. Potentially Toxicogenic (PTOX) Cyanobacteria List. Palatka, FL: GreenWater Laboratories.
- Chen, J., P. Xie, D. Zhang, Z. Ke & H. Yang, 2006a. *In situ* studies on the bioaccumulation of microcystins in the phytoplanktivorous silver carp

- (*Hypophthalmichthys molitrix*) stocked in Lake Taihu with dense toxic *Microcystis* blooms. *Aquaculture* 261: 1026-1038.
- Chen, W., L. Li, N. Gan & L. Song, 2006b. Optimization of an effective extraction procedure for the analysis of microcystins in soils and lake sediments. *Environmental Pollution* 143: 241-246.
- Christoffersen, K., S. Lyck & A. Winding, 2002. Microbial activity and bacterial community structure during degradation of microcystins. *Aquatic Microbial Ecology* 27: 125-136.
- Coyle, J.J., D.R. Buckler, C.G. Ingersoll, J.F. Fairchild & T.W. May, 1993. Effect of dietary selenium on the reproductive success of bluegills (*Lepomis macrochirus*). *Environmental Toxicology and Chemistry* 12: 551-565.
- Crumpton, W.G., T.M. Isehart & P.D. Mitchell, 1992. Nitrate and organic N analyses with second derivative spectroscopy. *Limnology and Oceanography* 37: 907-913.
- de Magalhães V.F., R.M. Soares & S.M.F.O. Azevedo, 2001. Microcystin contamination in fish from the Jacarepaguá Lagoon (Rio de Janeiro, Brazil): ecological implication and human health risk. *Toxicon* 39: 1077-1085.
- de Mendiburu, F., 2020. agricolae: Statistical procedures for agricultural research. R package version 1.3-3. <https://CRAN.R-project.org/package=agricolae>.
- Devries, D.R. & R.V. Fire, 1996. Determination of age and growth, in: Murphy, B.R. & D.W. Willis, (Eds), *Fisheries Techniques*, 2<sup>nd</sup> edition. American Fisheries Society, Bethesda, pp. 483-512.
- Dewitz, J., 2019. National Land Cover Database (NLCD) 2016 Products: U.S. Geological Survey data release. <https://doi.org/10.5066/P96HHBIE>.
- Dibble, E.D. & S.L. Harrel, 1997. Largemouth bass diets in two aquatic plant communities. *Journal of Aquatic Plant Management* 35: 74-78.
- Díez-Quijada, L., M. Puerto, D. Gutiérrez-Praena, M. Llana-Ruiz-Cabello, Á. Jos & A.M. Cameán, 2019. Microcystin-RR: occurrence, content in water and food and toxicological studies. A review. *Environmental Research* 168: 467-489
- Ferrão-Filho, A.S. & B. Kozłowsky-Suzuki, 2011. Cyanotoxins: bioaccumulation and effects on aquatic animals. *Marine Drugs* 9: 2729-2772.
- Findlay, D.L., R.E. Hecky, L.L. Hendzel, M.P. Stainton & G.W. Regehr, 1994. Relationship between N<sub>2</sub>-fixation and heterocyst abundance and its relevance to the nitrogen budget of Lake 227. *Canadian Journal of Fisheries and Aquatic Sciences* 51: 2254-2266.
- Flores, N.M., T.R. Miller & J.D. Stockwell, 2018. A global analysis of the relationship between concentrations of microcystins in water and fish. *Frontiers in Marine Science* 5: 30.

- Fox, J. & S. Weisberg, 2019. An {R} Companion to Applied Regression, Third Edition. Thousand Oaks CA: Sage. URL: <https://socialsciences.mcmaster.ca/jfox/Books/Companion/>
- Froese, R., 2006. Cube law, condition factor and weight-length relationships: history, meta-analysis and recommendations. *Journal of Applied Ichthyology* 22: 241-253.
- Fromme, H., A. Köhler, R. Krause & D. Führling, 2000. Occurrence of cyanobacterial toxins—microcystins and anatoxin-a—in Berlin water bodies with implications to human health and regulations. *Environmental Toxicology* 15: 120-130.
- Garvey, J.E. & R.A. Stein, 1998. Linking bluegill and gizzard shad prey assemblages to growth of age-0 largemouth bass in reservoirs. *Transactions of the American Fisheries Society* 127: 70-83.
- Gosch, N.J.C., Q.E. Phelps & D.W. Willis, 2006. Habitat characteristics at bluegill spawning colonies in a South Dakota glacial lake. *Ecology of Freshwater Fish* 15: 464-469.
- Greene, S.B.D., G.H. LeFevre & C.D. Markfort, 2021. Improving the spatial and temporal monitoring of cyanotoxins in Iowa lakes using a multiscale and multi-modal monitoring approach. *Science of the Total Environment* 760: 143327.
- Guildford, S.J. & R.E. Hecky, 2000. Total nitrogen, total phosphorus, and nutrient limitation in lakes and oceans: is there a common relationship? *Limnology and Oceanography* 45: 1213-1223.
- Gurbuz, F., O.Y. Uzunmehmetoğlu, Ö. Diler, J.S. Metcalf & G.A. Codd, 2016. Occurrence of microcystins in water, bloom, sediment and fish from a public water supply. *Science of the Total Environment* 562: 860-868.
- Hardy, F.J., A. Johnson, K. Hamel & E. Preece, 2015. Cyanotoxin bioaccumulation in freshwater fish, Washington State, USA. *Environmental Monitoring and Assessment* 187: 667.
- Harris, N.J., G.F. Galinat & D.W. Willis, 1999. Seasonal food habits of bluegills in Richmond Lake, South Dakota. *Proceedings of the South Dakota Academy of Science* 78: 79-85.
- Hecky, R.E. & S.J. Guildford, 1984. Primary productivity of Southern Indian Lake before, during, and after impoundment and Churchill River diversion. *Canadian Journal of Fisheries and Aquatic Sciences* 41: 591-604.
- Huisman, J., G.A. Codd, H.W. Paerl, B.W. Ibelings, J.M.H. Verspagen & P.M. Visser, 2018. Cyanobacterial blooms. *Nature Reviews Microbiology* 16: 471-483.
- Ibelings, B.W. & I. Chorus, 2007. Accumulation of cyanobacterial toxins in freshwater “seafood” and its consequences for public health: a review. *Environmental Pollution* 150: 177-192.

- Ibelings, B.W., K. Bruning, J. de Jong, K. Wolfstein, L.M. Dionisio Pires, J. Postma & T. Burger, 2005. Distribution of microcystins in a lake foodweb: no evidence for biomagnification. *Microbial Ecology* 49: 487-500.
- Isles, P.D.F., 2020. The misuse of ratios in ecological stoichiometry. *Ecology* 101: e03153.
- Izaguirre, G., A. Jungblut & B.A. Neilan, 2007. Benthic cyanobacteria (Oscillatoriaceae) that produces microcystin-LR, isolated from four reservoirs in southern California. *Water Research* 41: 492-498.
- Jennings, M.J., J.E. Claussen & D.P. Philipp, 1997. Effect of population size structure on reproductive investment of male bluegill. *North American Journal of Fisheries Management* 17: 516-524.
- Jia, J., W. Luo, Y. Lu & J.P. Giesy, 2014. Bioaccumulation of microcystins (MCs) in four fish species from Lake Taihu, China: assessment of risks to humans. *Science of the Total Environment* 487: 224-232.
- Jones, J.R., D.V. Obrecht, B.D. Perkins, M.F. Knowlton, A.P. Thorpe, S. Watanabe & R.R. Bacon, 2008. Nutrients, seston, and transparency of Missouri reservoirs and oxbow lakes: an analysis of regional limnology. *Lake and Reservoir Management* 24: 155-180.
- Kankaanpää, H., P.J. Vuorinen, V. Sipia & M. Keinänen, 2002. Acute effects and bioaccumulation of nodularin in sea trout (*Salmo trutta* L.) exposed orally to *Nodularia spumigena* under laboratory conditions. *Aquatic Toxicology* 61: 155-168.
- Kirk, J.T., 1994. *Light and Photosynthesis in Aquatic Ecosystems*. Oxford, England.
- Kozłowski-Suzuki, B., A.E. Wilson & A.D.S. Ferrão-Filho, 2012. Biomagnification or biodilution of microcystins in aquatic foodwebs? Meta-analyses of laboratory and field studies. *Harmful Algae* 18: 47-55.
- Lawson, Z.J., J.W. Gaeta & S.R. Carpenter, 2011. Coarse woody habitat, lakeshore residential development, and largemouth bass nesting behavior. *North American Journal of Fisheries Management* 31: 666-670.
- Li, Y., J. Chen, Q. Zhao, C. Pu, Z. Qiu, R. Zhang & W. Shu, 2011. A cross-sectional investigation of chronic exposure to microcystin in relationship to childhood liver damage in the Three Gorges Reservoir Region, China. *Environmental Health Perspectives* 119: 1483-1488.
- Lichtenstein, A.H., L.J. Appel, M. Brands, M. Carnethon, S. Daniels, H.A. Franch, B. Franklin, P. Kris-Etherton, W.S. Harris, B. Howard, N. Karanja, M. Lefevre, L. Rudel, F. Sacks, L. Van Horn, M. Wilson & J. Wylie-Rosett, 2006. Diet and lifestyle recommendations revision 2006. *Circulation* 114: 82-96.
- Malbrouck, C. & P. Kestemont, 2006. Effects of microcystin on fish. *Environmental Toxicology and Chemistry* 25: 72-86.

- McKee, M.J., K. Bataille & R.A. Reitz, 2015. Sport-caught fish consumption in Missouri: results from the 2002 mail survey, Resource Science Division, Missouri Department of Conservation.
- McCauley, R.W. & D.M. Kilgour, 1990. Effect of air temperature on growth of largemouth bass in North America. *Transactions of the American Fisheries Society* 119:276-281.
- McKindles, K.M., M.A. Manes, J.R. DeMarco, A. McClure, R.M. McKay, T.W. Davis & G.S. Bullerjahn, 2020. Dissolved microcystin release coincident with lysis of a bloom dominated by *Microcystis* spp. in western Lake Erie attributed to a novel cyanophage. *Applied and Environmental Microbiology* 86: e01397-20.
- Meriluoto, J.A.O. & L.E.M. Spoof, 2007. Cyanotoxins: sampling, sample processing and toxin uptake. In H.K. Hudnel (Ed.) *Cyanobacterial Harmful Algal Blooms State of the Science and Research Needs*. New York, NY, pp. 483-499.
- Miller, M.A., 1993. Maternal transfer of organochlorine compounds in salmonines to their eggs. *Canadian Journal of Fisheries and Aquatic Sciences* 50: 1405-1413.
- Miller, M.A., R.M. Kudela, A. Mekebri, D. Crane, S.C. Oates, M. T. Tinker, M. Staedler, W.A. Miller, S. Toy-Choutka, C. Dominik, D. Hardin, G. Langlois, M. Murry, K. Ward & D.A. Jessup, 2010. Evidence for a novel marine harmful algal bloom: cyanotoxin (microcystin) transfer from land to sea otters. *PLoS ONE* 5: e12576.
- Miller, T.R., S.L. Bartlett, C.A. Weirich & J. Hernandez, 2019. Automated subdaily sampling of cyanobacterial toxins on a buoy reveals new temporal patterns in toxin dynamics. *Environmental Science and Technology* 53: 5661-5670.
- Modde, T., 1980. State stocking policies for small warmwater impoundments. *Fisheries*. 5: 13-17.
- Mohamed, Z.A., W.W. Carmichael & A.A. Hussein, 2003. Estimation of microcystins in the freshwater fish *Oreochromis niloticus* in an Egyptian fish farm containing a *Microcystis* bloom. *Environmental Toxicology* 18: 137-141.
- Moreno, I., A. Herrador, L. Atencio, M. Puerto, A.G. González & A.M. Cameán, 2011. Differentiation between microcystin contaminated and uncontaminated fish by determination of unconjugated MCs using an ELISA Anti-Adda test based on receiver-operating characteristic curves threshold values, application to *Tinca tinca* from natural ponds. *Environmental Toxicology* 26: 45-56.
- Nchabeleng, T., P. Cheng, P. Oberholster, A.-M. Botha, W. Smit & W. Luus-Powell, 2014. Microcystin-LR equivalent concentrations in fish tissue during a postbloom *Microcystis* exposure in Loskop Dam, South Africa. *African Journal of Aquatic Science* 39: 459-466.
- Olson, M.H., 1996. Ontogenetic niche shifts in largemouth bass: variability and consequences for first-year growth. *Ecology* 77: 179-190.

- Olson, N.W., C.P. Paukert, D.W. Willis & J.A. Klammer, 2003. Prey selection and diets of bluegill *Lepomis macrochirus* with differing population characteristics in two Nebraska natural lakes. *Fisheries Management and Ecology* 10: 31-40.
- Paerl, H.W. & J. Huisman, 2008. Blooms like it hot. *Science* 320: 57-58.
- Papadimitriou, T., M. Katsiapi, K.A. Kormas, M. Moustaka-Gouni & I. Kagalou, 2013. Artificially-born “killer” lake: phytoplankton based water quality and microcystin affected fish in a reconstructed lake. *Science of the Total Environment* 1: 116-124.
- Park, H., Y. Sasaki, T. Maruyama, E. Yanagisawa, A. Hiraishi & K. Kato, 2001. Degradation of the cyanobacterial hepatotoxin microcystin by a new bacterium isolated from a hypertrophic lake. *Environmental Toxicology* 16: 337-343.
- Pflieger, W.L., M. Sullivan & L. Taylor, 1997. *The Fishes of Missouri*. Missouri Department of Conservation, Jefferson City, MO.
- Pham, T.L. & M. Utsumi, 2018. An overview of the accumulation of microcystins in aquatic ecosystems. *Journal of Environmental Management* 213: 520-529.
- Phillips, J.M., J.R. Jackson & R.L. Noble, 1995. Hatching date influence on age-specific diet and growth of age-0 largemouth bass. *Transactions of the American Fisheries Society* 124: 370-379.
- Pickhardt, P.C., C.L. Folt, C.Y. Chen, B. Klaue & J.D. Blum, 2002. Algal blooms reduce the uptake of toxic methylmercury in freshwater food webs. *PNAS* 99:4419-4423.
- Plaut, I., 2000. Effects of fin size on swimming performance, swimming behavior and routine activity on zebrafish *Danio rerio*. *Journal of Experimental Biology* 203: 813-820.
- Poste, A.E., R.E. Hecky & S.J. Guildford, 2011. Evaluating microcystin exposure risk through fish consumption. *Environmental Science and Technology* 45: 5806-5811.
- Preece, E.P., B.C. Moore, M.E. Swanson & F.J. Hardy, 2015. Identifying best methods for routine ELISA detection of microcystin in seafood. *Environmental Monitoring and Assessment* 187: 12.
- Prieto, A.I., A. Jos, S. Pichardo, I. Moreno & A.M. Cameán, 2006. Differential oxidative stress responses to microcystins LR and RR in intraperitoneally exposed tilapia fish (*Oreochromis* sp.). *Aquatic Toxicology* 77: 314-321.
- Quist, M.C., & D.A. Isermann, 2017. *Age and Growth of Fishes: Principals and Techniques*. American Fisheries Society, Bethesda, MD.
- R Core Team, 2019. *R: A language and environment for statistical computing*. R Foundation for Statistical Computing, Vienna, Austria. URL: <https://www.R-project.org/>.

- Rao, P.V., N. Gupta, A.S. Bhaskar & R. Jayaraj, 2002. Toxins and bioactive compounds from cyanobacteria and their implications on human health. *Journal of Environmental Biology* 23: 215-224.
- Sabart, M., D. Pobel, E. Briand, B. Combourieu, M.J. Salençon, J.F. Humbert & D. Latour, 2010. Spatiotemporal variations in microcystin concentrations and in the proportions of microcystin-producing cells in several *Microcystins aeruginosa* populations. *Applied and Environmental Microbiology* 76: 4750-4759.
- Saraf, S.R., A. Frenkel, M.J. Harke, J.G. Jankowiak, C.J. Gobler & A.E. McElroy, 2018. Effects of *Microcystis* on development of early life stage Japanese medaka (*Oryzias latipes*): comparative toxicity of natural blooms, cultured *Microcystis* and microcystin-LR. *Aquatic Toxicology* 194: 18-26.
- Sartory, D.P. & J.U. Grobbelaar, 1984. Extraction of chlorophyll-*a* from freshwater phytoplankton for spectrophotometric analysis. *Hydrobiologia* 114: 177-187.
- Schmidt, J.R., M. Shaskus, J.F. Estenik, C. Oesch, R. Khidekel & G. Boyer, 2013. Variations in the microcystin content of different fish species collected from a eutrophic lake. *Toxins* 5: 992-1009.
- Schmidt, J.R., S.W. Wilhelm & G.L. Boyer, 2014. The fate of microcystins in the environment and challenges for monitoring. *Toxins* 6: 3354-3387.
- Sieroslawska, A., A. Rymuszka, J. Velisek, B. Pawlik-Skowrońska, Z. Svobodova & T. Skowroński, 2012. Effects of microcystin-containing cyanobacterial extract on hematological and biochemical parameters of common carp (*Cyprinus carpio* L.). *Fish Physiology and Biochemistry* 38: 1159-1167.
- Silsbe, G.M. & S.Y. Malkin, 2015. phytotools: Phytoplankton Production Tools. R package version 1.0. Available online at: <https://CRAN.R-project.org/package=phytotools>
- Smith, J.L. & G.L. Boyer, 2009. Standardization of microcystin extraction from fish tissues: a novel internal standard as a surrogate for polar and non-polar variants. *Toxicon* 53: 238-245.
- Smith, J.L. & J.F. Haney, 2006. Foodweb transfer, accumulation, and depuration of microcystins, a cyanobacterial toxin, in pumpkinseed sunfish (*Lepomis gibbosus*). *Toxicon* 48: 580-589.
- Smith, J.L., K.L. Schulz, P.V. Zimba & G.L. Boyer, 2010. Possible mechanism for the foodweb transfer of covalently bound microcystins. *Ecotoxicology and Environmental Safety* 73: 757-761.
- Smith, V.H. & D.W. Schindler, 2009. Eutrophication science: where do we go from here? *Trends in Ecology and Evolution* 24: 201-207.
- Soares, R.M., V.F. Magalhães & S.M.F.O. Azevedo, 2004. Accumulation and depuration of microcystins (cyanobacteria hepatotoxins) in *Tilapia rendalli* (Cichlidae) under laboratory conditions. *Aquatic Toxicology* 70: 1-10.

- Steiner, K.L., B. Zimmermann, B. Hagenbuch & D. Dietrich, 2016. Zebrafish Oatp-mediated transport of microcystin congeners. *Archives of Toxicology* 90: 1129-1139.
- Stewart, I., P.M. Webb, P.J. Schluter & G.R. Shaw, 2006. Recreational and occupational field exposure to freshwater cyanobacteria – a review of anecdotal and case reports, epidemiological studies and the challenges for epidemiologic assessment. *Environmental Health* 5: 6.
- Straubinger-Gansberger, N., M.N. Kaggwa & M. Schagerl, 2014. Phytoplankton patterns along a series of small man-made reservoirs in Kenya. *Environmental Monitoring and Assessment* 186: 5153-5166.
- Tsujimura, S., H. Tsukada, H. Nakahara, T. Nakajima & M. Nishino, 2000. Seasonal variations of *Microcystis* populations in sediments of Lake Biwa, Japan. *Hydrobiologia* 434: 183-192.
- Van Apeldoorn, M.E., H.P. van Egmond, G.J.A. Speijers & G.J.I. Bakker, 2007. Toxins of cyanobacteria. *Molecular Nutrition and Food Research* 51: 7-60.
- Van Halderen, A., W.R. Harding, J.C. Wessels, D.J. Schneider, E.W.P. Heine, J. Van Der Merwe & J.M. Fourie, 1995. Cyanobacterial (blue-green algae) poisoning of livestock in the Western Cape Province of South Africa. *Journal of the South African Veterinary Association* 66: 260-264.
- Vanderploeg, H.A., S.A. Ludsin, J.F. Cavaletto, T.O. Höök, S.A. Pothoven, S.B. Brandt, J.R. Liebig & G.A. Lang, 2009. Hypoxic zones as habitat for zooplankton in Lake Erie: refuges from predation or exclusion zones? *Journal of Experimental Marine Biology and Ecology* 381: S108-S120.
- Vézie, C., J. Rapala, J. Vaitomaa, J. Seitsonen & K. Sivonen, 2002. Effect of nitrogen and phosphorus on growth of toxic and nontoxic *Microcystis* strains and on intracellular microcystin concentrations. *Microbiological Ecology* 43: 443-454.
- Wickham, H., 2016. *ggplot2: Elegant Graphics for Data Analysis*. Springer-Verlag New York, NY.
- Wiltsie, D., A. Schnetzer, J. Green, M. Vander Borgh & E. Fensin, 2018. Algal blooms and cyanotoxins in Jordan Lake, North Carolina. *Toxins* 10: 92.
- Winslow, L., J. Read, R. Woolway, J. Brentrup, T. Leach, J. Zward, S. Albers & D. Collinge, 2017. *rLakeAnalyzer: Lake Physics Tools*. Available online at: <https://cran.r-project.org/package=rLakeAnalyzer>
- Woller-Skar, M.M., A.L. Russell, J.A. Gaskill & M.R. Luttenton, 2020. Microcystin in multiple life stages of *Hexagenia limbata*, with implication for toxin transfer. *Journal of Great Lakes Research* 46: 666-671.
- Wood, S.A., L.R. Briggs, J. Sprosen, J.G. Ruck, R.G. Wear, P.T. Holland & M. Bloxham, 2006. Changes in concentrations of microcystins in rainbow trout, freshwater mussels, and cyanobacteria in Lakes Rotoiti and Rotoehu. *Environmental Toxicology* 21: 205-222.

- Wörmer, L., M. Huerta-Fontela, S. Cirés, D. Carrasco & A. Quesada, 2010. Natural photodegradation of the cyanobacterial toxins microcystin and cylindrospermopsin. *Environmental Science and Technology* 44: 3002-3007.
- Wörmer, L., S. Cirés & A. Quesada, 2011. Importance of natural sedimentation in the fate of microcystins. *Chemosphere* 82: 1141-1146.
- Xie, L., P. Xie, K. Ozawa, T. Honma, A. Yokoyama & H-D Park, 2004. Dynamics of microcystins-LR and -RR in the phytoplanktivorous silver carp in a sub-chronic toxicity experiment. *Environmental Pollution* 127: 431-439.
- Yuan, L.L., A.I. Pollard, S. Pather, J.L. Oliver & L. D'Anglada, 2014. Managing microcystin: identifying national-scale thresholds for total nitrogen and chlorophyll *a*. *Freshwater Biology* 59: 1970-1981.
- Zaffiro, A., L. Rosenblum & S.C. Wendelken, 2016. Method 546: Determination of total microcystins and nodularins in drinking water and ambient water by adda enzyme-linked immunosorbent assay, United States Environmental Protection Agency. Available at: <https://www.epa.gov/sites/production/files/2016-09/documents/method-546-determination-total-microcystins-nodularins-drinking-water-ambient-water-adda-enzyme-linked-immunosorbent-assay.pdf> [accessed March 13, 2021].
- Zamora-Barrios, C.A., S. Nandini & S.S.S. Sarma, 2019. Bioaccumulation of microcystins in seston, zooplankton and fish: a case study in Lake Zumpango, Mexico. *Environmental Pollution* 249: 267-276.
- Zhan, C., W. Liu, F. Zhang & X. Zhang, 2020. Microcystin-LR triggers different endoplasmic reticulum stress pathways in the liver, ovary, and offspring of zebrafish (*Danio rerio*). *Journal of Hazardous Materials* 386: 121939.
- Zhang, D., W. Lin, Y. Liu, H. Guo, L. Wang, L. Yang, L. Li, D. Li & R. Tang, 2020. Chronic microcystin-LR exposure induces abnormal lipid metabolism via endoplasmic reticulum stress in male zebrafish. *Toxins* 12: 107.
- Zhang, D., X. Deng, P. Xie, J. Chen & L. Guo, 2013. Risk assessment of microcystins in silver carp (*Hypophthalmichthys molitrix*) from eight eutrophic lakes in China. *Food Chemistry* 140: 17-21.

TABLES

**Table 3.1** Characteristics of fish collected from Dairy Farm Lake #1. The sample size (*n*) for bluegill (BLG) and largemouth bass (LMB) are listed underneath each harvest date (month/day/year). For continuous variables, the top value in each cell is the mean of all fish collected on each harvest date, while the bottom value in parentheses is the standard deviation. For sex, which is a categorical variable, the total number of male (m) and female (f) fish are shown for each date. When sex was unable to be determined, fish are reported as undetermined (UD).

Fish Characteristic	Units	Species	4/23/18	5/30/18	7/16/18	8/21/18	10/11/18	11/27/18	2/4/19	3/18/19
			BLG <i>n</i> =10; LMB <i>n</i> =20	BLG <i>n</i> =13; LMB <i>n</i> =18	BLG <i>n</i> =10; LMB <i>n</i> =20	BLG <i>n</i> =11; LMB <i>n</i> =19	BLG <i>n</i> =10; LMB <i>n</i> =10	BLG <i>n</i> =11; LMB <i>n</i> =10	BLG <i>n</i> =14; LMB <i>n</i> =9	BLG <i>n</i> =10; LMB <i>n</i> =10
Length	cm	BLG	18.8 (2.7)	16.1 (3.9)	18.9 (1.5)	17.8 (2.5)	19.8 (1.5)	18.7 (3.0)	18.2 (2.1)	17.6 (2.1)
		LMB	31.5 (9.3)	26.6 (11.1)	29.2 (7.9)	29.6 (8.3)	37.6 (6.1)	34.1 (7.2)	35.9 (5.2)	36.3 (5.2)
Age	years	BLG	4 (1)	3 (1)	3 (1)	3 (1)	4 (2)	3 (2)	3 (1)	3 (1)
		LMB	4 (2)	3 (3)	3 (2)	3 (2)	4 (2)	4 (2)	5 (2)	5 (2)
Mass	g	BLG	263.8 (59.9)	105.5 (66.5)	149.5 (38.1)	115.5 (46.4)	160.5 (36.8)	140.9 (61.8)	126.6 (50.1)	111.9 (52.1)
		LMB	508.5 (406.3)	374.2 (399.3)	410.5 (349.8)	413.7 (345.1)	737.9 (362.0)	621.8 (483.9)	643.3 (280.3)	682.3 (315.8)
Body Condition Index	n/a	BLG	2.0 (0.2)	1.9 (0.3)	2.1 (0.1)	2.0 (0.3)	2.0 (0.2)	2.0 (0.1)	2.0 (0.1)	1.9 (0.2)
		LMB	1.2 (0.2)	1.2 (0.2)	1.3 (0.1)	1.2 (0.2)	1.3 (0.1)	1.3 (0.1)	1.3 (0.1)	1.3 (0.1)
Sex	n/a	BLG	5 m / 5 f	5 m / 6 f 2 UD	7 m / 3 f	7 m / 4 f	4 m / 6 f	1 m / 10 f	8 m / 6 f	6 m / 4 f
		LMB	11 m / 9 f	8 m / 7 f 3 UD	3 m / 12 f 5 UD	4 m / 9 f 6 UD	4 m / 6 f	6 m / 4 f	6 m / 3 f	7 m / 3 f
Liver Mass	g	BLG	1.6 (0.7)	1.0 (0.7)	1.3 (0.5)	1.4 (1.0)	1.2 (0.4)	1.4 (0.6)	1.5 (0.4)	1.3 (0.5)
		LMB	5.7 (5.6)	3.3 (5.8)	3.8 (3.4)	2.6 (1.8)	4.5 (1.8)	6.3 (5.0)	6.6 (3.8)	6.3 (2.4)
Gonad Mass	g	BLG	1.0 (1.0)	2.2 (1.6)	1.4 (1.0)	1.1 (1.4)	1.0 (1.0)	1.2 (1.5)	0.6 (0.5)	0.4 (0.4)

		LMB	13.0 (21.2)	1.4 (1.6)	0.9 (1.3)	1.1 (2.0)	4.4 (4.0)	4.5 (8.5)	5.4 (7.0)	4.5 (6.2)
Liver		BLG	1.15 (0.19)	0.85 (0.24)	0.85 (0.16)	1.12 (0.37)	0.73 (0.13)	1.00 (0.16)	1.29 (0.35)	1.15 (0.25)
Organosomatic	%	LMB	1.06 (0.39)	0.88 (0.36)	1.01 (0.23)	0.85 (0.77)	0.65 (0.16)	1.03 (0.19)	0.99 (0.26)	0.92 (0.39)
Index		BLG	0.66 (0.58)	1.98 (2.13)	1.04 (0.84)	0.75 (0.72)	0.62 (0.54)	0.79 (0.73)	0.46 (0.37)	0.41 (0.43)
Gonad		LMB	1.70 (2.16)	0.36 (0.25)	0.22 (0.23)	0.25 (0.26)	0.56 (0.35)	0.58 (0.52)	0.65 (0.67)	0.65 (0.75)
Organosomatic	%									
Index										

**Table 3.2** Classification of component loadings for annual water parameters using a correlation based principal component analysis (PCA). The percent total variation in the whole dataset that can be described by the included factors is listed next to each component loading (CL). Bold values indicate strongly correlated parameters within each CL. One correlated parameter from each CL was retained for statistical analyses. For CL 1, we retained chl-*a* because of its high loading value and relevance to our research questions. We retained water microcystin from CL 2 because of its high loading value and relationship with microcystin in fish. We retained TDN from CL 3 because it had the highest loading value. We also retained DOC and TDP because they had an absolute value < 0.6 for all CLs, indicating that they did not exhibit multicollinearity with each other or any other water parameters. Retained parameters were included in our final, combined model set and are italicized.

Water Parameters	CL 1 (39.9 %)	CL 2 (24.9 %)	CL 3 (23.3 %)
Particulate Organic Matter (POM)	<b>0.991</b>	-0.104	0.008
Pheophytin	<b>0.976</b>	0.038	0.139
Light Attenuation Coefficient ( $K_d$ )	<b>0.969</b>	-0.030	-0.086
<i>Chlorophyll-a (chl-a)</i>	<b>0.953</b>	0.155	0.043
PC:Chl	<b>0.847</b>	0.316	-0.333
pH	<b>0.825</b>	0.012	0.022
Total Phosphorus (TP)	<b>0.824</b>	-0.465	0.212
Total Nitrogen (TN)	<b>0.794</b>	0.255	-0.549
Secchi Disk Depth	<b>-0.667</b>	0.346	0.474
Total Suspended Solids (TSS)	<b>0.640</b>	<b>-0.765</b>	-0.064
ln(TN:TP)	-0.567	<b>0.603</b>	-0.514
Dissolved Oxygen (DO)	-0.521	<b>-0.750</b>	-0.288
Temperature	0.499	<b>0.714</b>	0.456
<i>Dissolved Organic Carbon (DOC)</i>	0.458	0.528	-0.543
Nitrate ( $\text{NO}_3^-$ )	-0.332	0.002	<b>-0.852</b>
Ammonium ( $\text{NH}_4^+$ )	-0.254	0.273	<b>-0.795</b>
Mean Daily Mixed Layer Irradiance ( $\bar{E}_{24}$ )	-0.192	<b>0.639</b>	<b>0.697</b>
<i>Surface Water Microcystin</i>	0.072	<b>0.832</b>	0.307

<i>Total Dissolved Phosphorus (TDP)</i>	-0.048	-0.487	0.423
Particulate Inorganic Matter (PIM)	-0.035	<b>-0.992</b>	-0.100
<i>Total Dissolved Nitrogen (TDN)</i>	-0.005	0.218	<b>-0.933</b>

---

**Table 3.3** Water parameters measured in Dairy Farm Lake #1. Water parameters, including profiles, are the mean of the sampling date immediately before and immediately after the fish harvest date listed in the top row. “BDL” indicates that parameter was below the detection limit. When fish harvest date fell in between a water sampling date that showed the reservoir to be isothermal and the other to be stratified, we were unable to determine mixing depth nor hypolimnetic dissolved oxygen. This is indicated by “n/a”. We report the maximum depth for mixing depth when the reservoir was isothermal. Parameters measured with a YSI EXO 3 sonde, indicated by “\*”, are averages of the epilimnion when the reservoir was stratified or of the entire water column when the reservoir was isothermal. Hypolimnetic dissolved oxygen is a sonde profile average of the hypolimnion when the reservoir was stratified. Surface water cyanotoxins were integrated samples between 0 and 0.5 m while bottom water cyanotoxins were collected 1 m above the sediment.

Water Parameter	Units	4/23/18	5/30/18	7/16/18	8/21/18	10/11/18	11/27/18	2/4/19	3/18/19
<b>Chemical</b>									
Total Phosphorus (TP)	$\mu\text{mol P L}^{-1}$	1.560	2.137	3.214	3.925	2.234	1.751	3.587	3.136
Total Dissolved Phosphorus (TDP)	$\mu\text{mol P L}^{-1}$	0.605	0.943	0.782	0.735	0.573	0.785	0.920	0.846
Total Nitrogen (TN)	$\mu\text{mol N L}^{-1}$	73.79	65.81	141.28	136.84	123.63	110.31	91.33	77.99
Total Dissolved Nitrogen (TDN)	$\mu\text{mol N L}^{-1}$	59.90	52.54	66.30	71.59	76.92	97.48	61.86	49.05
Nitrate ( $\text{NO}_3^-$ )	$\mu\text{mol NO}_3^- \text{ L}^{-1}$	BDL	0.70	BDL	2.05	5.18	15.69	1.89	0.79
Ammonium ( $\text{NH}_4^+$ )	$\mu\text{mol NH}_4^+ \text{ L}^{-1}$	1.5420	3.9145	BDL	4.6048	15.2620	14.1890	2.5877	0.9103
ln(TN:TP)	unitless	3.86	3.43	3.78	3.55	4.01	4.14	3.24	3.21
Dissolved Organic Carbon (DOC)	$\mu\text{mol C L}^{-1}$	670.3	690.0	823.3	749.3	770.4	764.7	702.6	581.3

Dissolved Oxygen (DO)*	mg L <sup>-1</sup>	9.8	7.3	4.7	7.7	8.7	11.9	12.9	11.5
Hypolimnetic DO	mg L <sup>-1</sup>	n/a	1.3	0.2	1.7	n/a	isothermal	isothermal	isothermal
pH*	unitless	7.9	7.6	8.1	8.7	8.0	7.7	7.8	8.1
Surface Water Microcystin	µg L <sup>-1</sup>	0.95	0.87	0.54	0.87	0.91	BDL	BDL	0.13
Bottom Water Microcystin	µg L <sup>-1</sup>	0.92	0.97	0.66	0.76	0.96	BDL	0.13	BDL
Surface Water Anatoxin-a	µg L <sup>-1</sup>	BDL	BDL	BDL	0.18	0.18	0.21	0.19	0.18
Bottom Water Anatoxin-a	µg L <sup>-1</sup>	BDL	BDL	BDL	BDL	0.23	0.17	0.21	0.20
Surface Water Cylindrospermopsin	µg L <sup>-1</sup>	BDL	BDL	BDL	BDL	BDL	BDL	BDL	BDL
Bottom Water Cylindrospermopsin	µg L <sup>-1</sup>	BDL	BDL	BDL	BDL	BDL	BDL	BDL	BDL
Surface Water Saxitoxin	µg L <sup>-1</sup>	BDL	BDL	BDL	BDL	BDL	BDL	BDL	BDL
Bottom Water Saxitoxin	µg L <sup>-1</sup>	BDL	BDL	0.047	BDL	BDL	BDL	BDL	BDL
Secchi Disk Depth	m	0.76	1.47	0.44	0.47	0.63	0.74	0.50	0.68
Light Attenuation Coefficient (K <sub>d</sub> )	m <sup>-1</sup>	1.07	1.14	3.37	2.79	2.16	1.32	2.01	2.03
Mixing Depth	m	n/a	2.1	2.0	1.7	n/a	4.6	4.6	4.6

Mean Daily Mixed Layer Irradiance ( $\bar{E}_{24}$ )	$\mu\text{mol photons m}^{-2} \text{ s}^{-1}$	168.73	271.11	104.39	140.16	65.04	42.57	31.48	58.96
Water Temperature*	$^{\circ}\text{C}$	14.43	25.81	27.59	26.91	13.69	3.76	1.60	8.11
Total Suspended Solids (TSS)	$\text{mg L}^{-1}$	5.5	4.4	15.1	16.5	9.9	9.8	20.0	18.7
Particulate Inorganic Matter (PIM)	$\text{mg L}^{-1}$	3.2	0.8	2.5	3.6	2.9	6.1	12.2	11.0
Particulate Organic Matter (POM)	$\text{mg L}^{-1}$	2.3	3.7	12.6	12.9	7.0	3.7	7.9	7.7
<b>Biological</b>									
Chlorophyll- <i>a</i> (chl- <i>a</i> )	$\mu\text{g L}^{-1}$	9.6	30.3	78.0	100.9	52.7	13.3	43.6	30.4
Pheophytin	$\mu\text{g L}^{-1}$	3.2	8.5	38.7	40.4	10.7	2.8	17.4	14.2
Phycocyanin:Chl- <i>a</i> *	percent	2.00	0.00	25.49	12.68	16.06	10.75	3.61	6.03

---

**Table 3.4** Correlations between microcystin in muscles, livers, and kidneys for both bluegill and largemouth bass. Spearman’s rank correlation test was used to measure correlations between tissue type. The degrees of freedom (df), p-value, and correlation coefficient (rho) are reported for each correlation. Significance, based on an  $\alpha$  value of 0.05, is indicated by \*. For both species, the correlation between muscles and kidneys (Figure A2.3) was stronger than for any other tissue combination.

<b>Tissues Being Compared</b>	<b>Species</b>	<b>df</b>	<b>p-value</b>	<b>rho</b>
Muscle to Liver	Bluegill	84	< 0.001*	0.38
Muscle to Kidney	Bluegill	66	< 0.001*	0.57
Liver to Kidney	Bluegill	66	0.001*	0.38
Muscle to Liver	Largemouth Bass	105	0.007*	0.25
Muscle to Kidney	Largemouth Bass	101	< 0.001*	0.69
Liver to Kidney	Largemouth Bass	101	0.050	0.19

**Table 3.5** Two-way analysis of variance results showing differences in microcystin concentrations between harvest date and species (Figure 3.3). Degrees of freedom for harvest date and the interaction between harvest date and species are 7. Degrees of freedom for species is one. Significance, based on an  $\alpha$  value of 0.05, is indicated by \*.

	<b>Muscle</b> <b>(residuals= 172)</b>		<b>Liver</b> <b>(residuals= 182)</b>		<b>Kidney</b> <b>(residuals= 159)</b>	
	F statistic	p-value	F statistic	p-value	F statistic	p-value
Harvest Date	85.19	< 0.001*	4.64	< 0.001*	34.31	< 0.001*
Species	31.04	< 0.001*	1.23	0.270	28.37	< 0.001*
Harvest Date $\times$ Species	1.39	0.210	3.15	0.004*	1.05	0.396

**Table 3.6** Microcystin concentrations in the tissues of largemouth bass and *Lepomis* sp. from this study in comparison to those reported in the literature. Microcystin is reported as wet weight concentrations in ng g<sup>-1</sup>. ELISA was used to quantify microcystin in all studies. Sample size (*n*) is reported for each study, as well as the range in parentheses underneath. “UDL” indicates that the minimum sample was measured under the detection limit. Some studies (\*) pooled tissues from multiple fish. We do not report the range of these fish as it only reflects inter-assay variation.

Species	<i>n</i>	Tissue	Microcystin (range)	Source
Largemouth bass	1–3*	Muscle	2.5	Hardy et al. (2015)
Largemouth bass	1–3*	Liver	75.0	Hardy et al. (2015)
Largemouth bass	116	Muscle	5.7 (UDL–17.9)	This study
Largemouth bass	116	Liver	71.8 (UDL–614.6)	This study
Largemouth bass	116	Kidney	22.7 (UDL–79.8)	This study
Bluegill	1	Muscle	2.4	Poste et al. (2011)
Bluegill	89	Muscle	7.6 (UDL–38.0)	This study
Bluegill	88	Liver	57.6 (UDL–208.1)	This study
Bluegill	73	Kidney	27.1 (UDL–86.7)	This study
Pumpkinseed	4	Muscle	1.9 (0.7–2.9)	Poste et al. (2011)
Pumpkinseed	1–3*	Muscle	8.7	Hardy et al. (2015)
Pumpkinseed	9*	Liver	3.8	Smith and Haney (2006)

## FIGURES

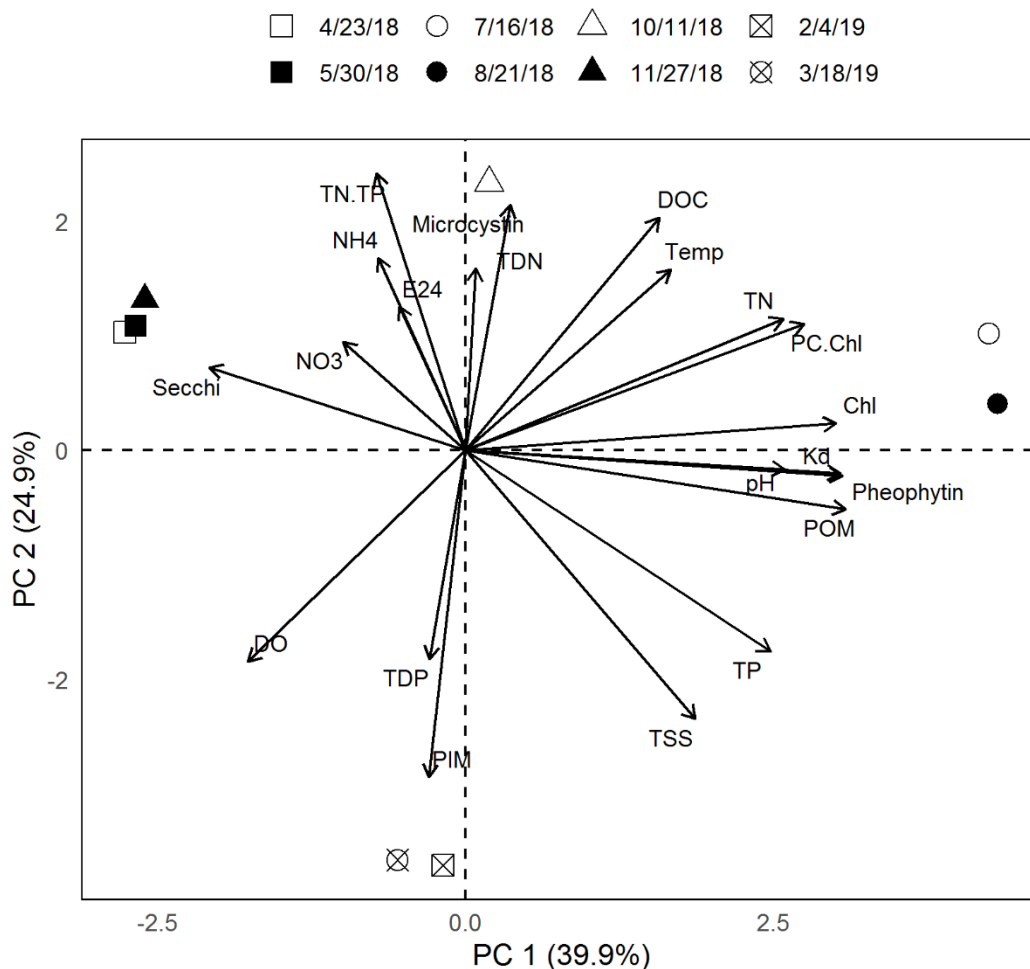


**Figure 3.1** Correlation-based principal component analysis (PCA) used to investigate the relationship between harvest date and 21 water parameters. The first principal component (PC 1) explains 39.9 % of the variation in this dataset, while the second component (PC 2) explains 24.9 % (Table 3.2). Water parameters include: ammonium (NH<sub>4</sub>), chlorophyll-*a* (Chl), dissolved organic carbon (DOC), dissolved oxygen (DO), light attenuation coefficient (K<sub>d</sub>), mean daily mixed layer irradiance (E<sub>24</sub>), microcystin from the upper 0.5 m of the water, natural log of the ratio of total nitrogen to total phosphorus (TN:TP), nitrate (NO<sub>3</sub>), particulate inorganic matter (PIM), particulate organic matter (POM), percent composition of phycocyanin to chlorophyll as measured with a YSI EXO 3 (PC:Chl), pheophytin, pH, Secchi disk depth, temperature (temp), total dissolved nitrogen (TDN), total dissolved phosphorus (TDP), total nitrogen (TN), total phosphorus (TP), and total suspended solids (TSS). Vector length reflects the magnitude of variation explained by that water parameter. Vectors close together are positively correlated while vectors opposite from each other are negatively correlated. Vectors that are orthogonal from each other are unrelated. Harvest date is represented by points.

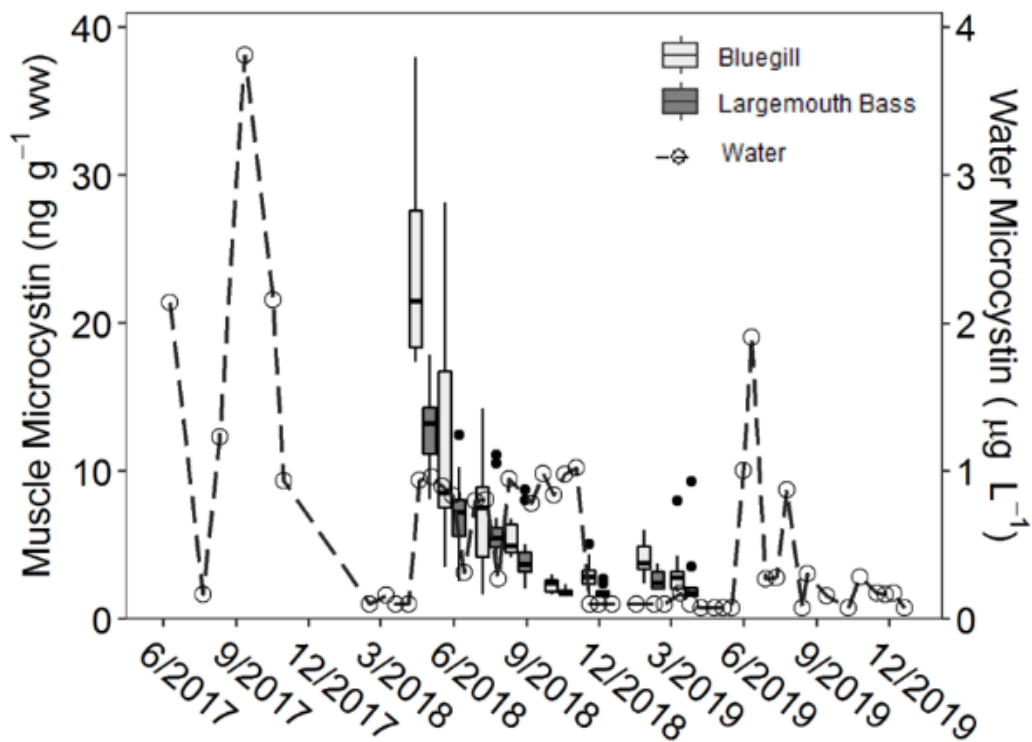
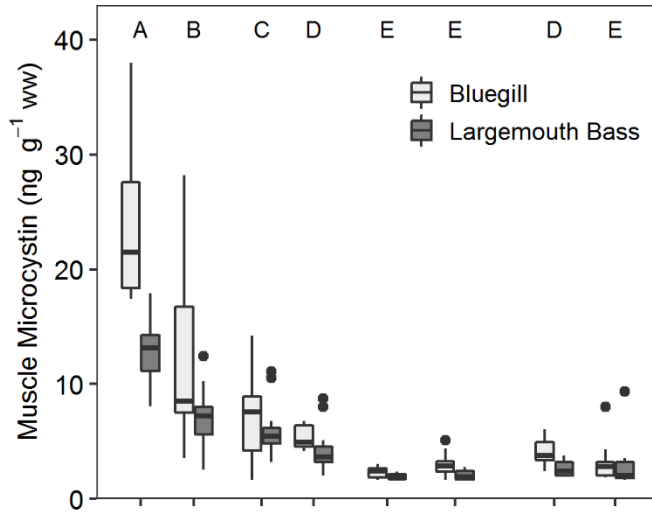
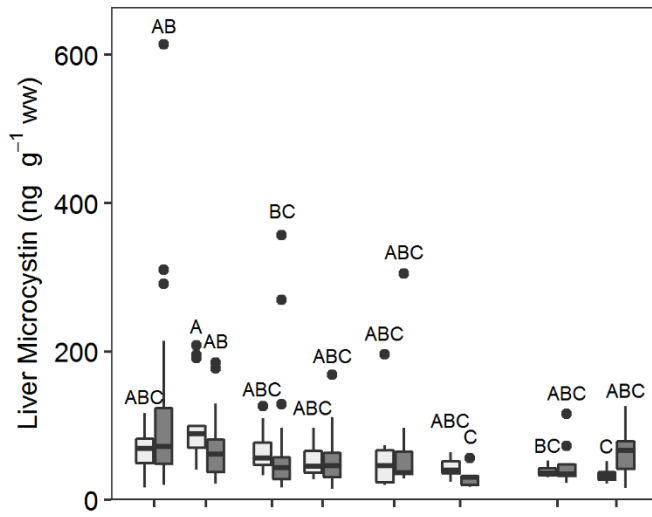


**Figure 3.2** Microcystin in water and fish muscles. Microcystin was measured in the upper 0.5 m of water (dashed lines, open circles, right y-axis) and in bluegill (light grey boxes) and largemouth bass (dark grey boxes) muscles (left y-axis). Standard error for water microcystin was never more than 0.4 per Abraxis Microcystin ELISA guidelines. The boxplots display the 25–75 % quartile with median bar, while the upper (lower) lines show the highest (lowest) values that are not considered outliers. Outliers are indicated by solid, black circles.

A)



B)



C)

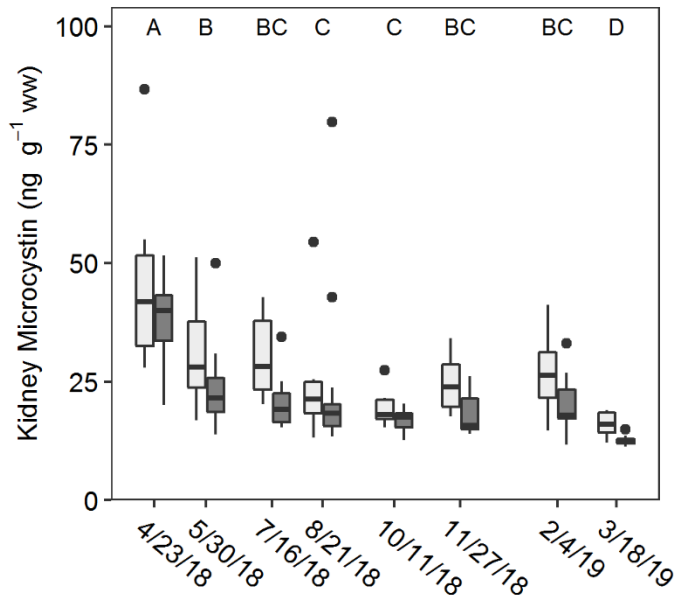


**Figure 3.3** Boxplots showing wet weight microcystin concentrations in fish during each harvest date, by species. A two-way ANOVA was used to evaluate differences in microcystin between dates and species ( $\alpha= 0.05$ ). The central box in the 25 - 75 % quartile with median bar, while the upper (lower) lines show the highest (lowest) values that are not considered outliers. Different letters within each plot indicate significant differences in microcystin concentrations between species per sampling date as indicated by a Tukey's post hoc test. For muscles (A) and kidneys (C), there was a significant difference between microcystin in bluegill and largemouth bass. The interaction effect between harvest date and species is not significant, so letters in these plots show significant differences in harvest date. For livers (B), the interaction effect between harvest date and species is significant, indicating this relationship depends on harvest date. Letters in this plot are placed above each individual box to show significant differences between boxes (Table 3.5).

## CHAPTER 4

# ARE INVASIVE ZEBRA MUSSELS ALWAYS ASSOCIATED WITH AN INCREASE IN WATER CLARITY?

### ABSTRACT

Invasive, filter feeding zebra mussels (*Dreissena polymorpha*) typically cause an increase in water clarity shortly after their establishment. The purpose of this study is to evaluate whether this occurred in Midwest reservoirs, near the southern edge of their North American expansion, using a 40+ year dataset. We look for regime shifts and long-term trends in annual water clarity and compare these to the estimated zebra mussel invasion date for 7 invaded reservoirs in Missouri, USA. We also look at water clarity in 26 non-invaded, reference reservoirs to evaluate if zebra mussel impacts are being masked by changes in external factors. Collectively, our analyses provide a weight of evidence showing that zebra mussel establishment did not increase water clarity, likely because densities are too low to result in a noticeable impact. The highest zebra mussel density we observe is 65 mussels  $m^{-2}$ , an order of magnitude less than in systems where they have had a sustained impact. Low densities could be due to a combination of sublethal environmental conditions for multiple parameters. We identified low particulate inorganic material and low water temperatures as characteristics common to invaded reservoirs. This is the first report where zebra mussel establishment did not cause an increase in water clarity. This study serves as an initial report of factors that may limit zebra mussel densities in Missouri reservoirs.

### INTRODUCTION

The impact of an invasive species is dependent on its adaptability to local conditions and its successful proliferation once established. A successful invader is able to tolerate and adapt to a wide range of environmental conditions, allowing it to expand its distribution and form dense populations (Thompson 1998; Sakai et al. 2001; Lockwood et al. 2013). Many non-native species have established reproducing populations in new areas, but do not always reach densities necessary to cause dramatic, negative impacts because of the environmental conditions (Carey 1996; Kulhanek et al. 2011; Ricciardi et al. 2013). While conditions may not be lethal, they can add increased physiological stress associated with surviving and reproducing in a suboptimal environment (Lockwood et al. 2013). Understanding the parameters that limit a species' spread, resulting in variable densities throughout its distribution, can help managers assess invasion risk and impact (Keller and Perrings 2011).

Zebra mussels (*Dreissena polymorpha*) are one of the most problematic invaders in North America (Lowe et al. 2004). Since their arrival in Lake Erie in 1986 (Carlton 2008), they have spread as far as California (Benson et al. 2021a) and Texas (Churchill et al. 2017), with new water bodies being invaded every year (Benson et al. 2021a). Zebra mussels can reach peak densities 2–4 years after they are introduced (Karatayev et al. 2011) and can have dramatic impacts on native ecosystem processes and function (Schloesser et al. 1991; Ward and Ricciardi 2007; Kim et al. 2015). In the United States, economic impacts are substantial, with an estimated \$11–16 million spent annually to remove zebra mussels from intake pipes at drinking water and power facilities (Connelly et al. 2007).

Given their high filter-feeding capacity (Fanslow et al. 1995), zebra mussel invasions can lead to reductions in phytoplankton biovolume and other suspended particles throughout the water column (Higgins and Vander Zanden 2010; Kirsch and Dzialowski 2012). The magnitude of their impact on water clarity depends on mussel density, which is influenced by several abiotic factors including water temperature (Jost et al. 2015), suspended inorganic solids (Madon et al. 1998), and dissolved oxygen concentrations (McMahon 1996). Zebra mussel densities can fluctuate widely from year to year locally within a water body, but usually do not decline on a lake-wide scale over the long term unless they are replaced by quagga mussels (*Dreissena rostriformis bugensis*; Strayer et al. 2019). To the best of our knowledge, zebra mussel establishment is always associated with an increase in water clarity.

The impact of zebra mussels on Missouri reservoirs is poorly understood. Most North American studies investigating zebra mussel impacts have been conducted in northern, natural lakes (Fahnenstiel et al. 1995; Budd et al. 2001; Higgins and Vander Zanden 2010; Baranowska et al. 2013; North et al. 2013). In contrast, Missouri reservoirs are warmer, have higher concentrations of inorganic particles, and often have longer stratification periods (Jones et al. 2008; Jones et al. 2011). Reservoirs are characterized by longitudinal flow that impacts zebra mussel distributions compared to natural lakes where water movement between nearshore and offshore areas has a greater influence on phytoplankton (Locklin et al. 2020), and consequently sessile filter feeders like zebra mussels (Hecky et al. 2004). These abiotic factors affect zebra mussel survival and persistence (Schneider et al. 1998; Yu and Culver 1999; Elderkin and Klerks 2005), so it is possible that zebra mussel impacts in Missouri reservoirs differ from natural lakes.

The purpose of this study is to determine whether zebra mussels impact water clarity in Missouri reservoirs. Our first objective is to identify whether shifts in water clarity in invaded reservoirs exist, and if so, whether they align with the introduction of zebra mussels using before and after, long-term water clarity data. To accomplish this, we looked for water clarity shifts in non-invaded reference reservoirs and compared them with water clarity in invaded reservoirs over the same time period. We also measured zebra mussel density and biomass in several invaded reservoirs as, to the best of our knowledge, no previous attempt has been made to quantify zebra mussels in Missouri where warmer water temperatures, longer periods of stratification, and higher concentrations of inorganic particles create habitat that differs from lakes to the north. We hypothesize that zebra mussels will affect water clarity and predict that this effect will be similar to that documented in northern latitude lakes. Our results will lend insights into the potential impacts of this aquatic invader near the leading edge of its expansion, which will help inform the potential zebra mussel risk in other regions.

## METHODS

### *Study reservoirs*

This study was conducted in 33 reservoirs throughout the state of Missouri, USA, using data collected between 1976 and 2019. We analyzed water clarity indicators over time in reservoirs invaded by zebra mussels ( $n= 7$ ; Blue Springs, Bull Shoals, Jacomo, Lake of the Ozarks, Lotawana, Smithville, Truman) to assess whether there was a shift in water clarity post-invasion. Three of these reservoirs, Lake of the Ozarks, Lotawana, and Smithville have at least 11 years of data pre-, and 11 years post- zebra mussel invasion. We also measured these parameters over time in reference reservoirs ( $n= 26$ ; Atkinson,

Binder, Bowling Green, Brookfield, Capri, Clearwater, Council Bluff, Deer Ridge, Fellows, Forest, Higginsville, Hunnewell, Kraut Run, Lincoln, Long Branch, Mark Twain, McDaniel, North, Pomme de Terre, Shayne, Stockton, Sugar Creek, Table Rock, Viking, Wappapello, Watkins Mill), which had no known zebra mussel populations. Throughout the state, the Missouri Department of Conservation (MDC) records the first year in which adult zebra mussels are observed in invaded reservoirs. Private citizens report sightings, which are then verified by MDC personnel and reported to the United States Geological Survey (USGS; Benson et al. 2021a). To account for the latency period between when zebra mussels first reached each reservoir and when they were first observed, we report zebra mussel invasion periods as 3 years before initial observation of zebra mussel adults (Burlakova et al. 2006). For this study, we analyzed invaded reservoirs with a minimum of 5 years of data both pre- and post- invasion. All reference reservoirs had at least 26 years of water clarity data spanning the same time period as the zebra mussel reservoirs, and no more than 4 years of non-continuous data for at least one parameter.

Reservoir surface area, volume, and watershed area are from the Missouri Department of Natural Resources (MDNR) and were determined during reservoir impoundment (Missouri DNR 2019). The maximum depth of each reservoir is based on dam height. Mean reservoir depth was calculated from volume and surface area. Flushing rate was calculated by dividing total runoff by reservoir volume, where total runoff was calculated for each reservoir by multiplying watershed area (Missouri DNR 2019) by runoff (Missouri DNR 1986).

While not directly measured in this study, previous reports of calcium concentrations and reservoir use help to give context to Missouri reservoirs. Previous reported calcium concentrations in 80 out of 103 Missouri reservoirs are above 20 mg Ca L<sup>-1</sup> (Wylie and Jones 1991), well above the 12 mg Ca L<sup>-1</sup> threshold necessary for zebra mussel establishment (Cohen 2007). Zebra mussels are still spreading throughout Missouri and the reservoirs that are currently invaded may be related to the amount of boat traffic they receive. Based on a 2013 survey of Missouri anglers, zebra mussel reservoirs are visited 314.1 % more often than reference reservoirs (Reitz 2015). Excluding Lake of the Ozarks, which receives almost twice as many anglers as any other reservoir in the state, invaded reservoirs received 178.7 % more visitors than reference reservoirs (Reitz 2015).

#### *Water clarity parameters*

To assess whether zebra mussel introductions led to a shift in water clarity in Missouri reservoirs, we analyzed chlorophyll-*a* (chl-*a*), total suspended solids (TSS), particulate organic matter (POM), particulate inorganic matter (PIM), and Secchi disk depth in both invaded and non-invaded reference reservoirs. Water samples are collected from the surface of each reservoir at the dam, with the exception of Bull Shoals, which lacked a dam study site. Secchi disk depth and chl-*a* concentrations are measured at 2 locations in Bull Shoals. Site 1 (36.5169°N -92.6235°W), which is 16.4 km up-reservoir of the dam in one of the main arms of the reservoir and has data between 1978 and 2012. TSS and PIM data are also available for site 1. These parameters were never measured in more than 8 consecutive years, so while we were able to include them in our habitat suitability index, we were not able to look for regime shifts nor trends. Site 2 (36.5013°N

-92.9306°W) in Bull Shoals is 36.6 km up-reservoir of the dam, is located in a second main arm of the reservoir, and has data between 2003 and 2019. Each year,  $n= 1$  to  $n= 37$  water samples per reservoir are collected between May 15<sup>th</sup> and September 15<sup>th</sup>. We calculate the annual arithmetic mean for each parameter and use this metric in all statistical analyses.

To measure chl-*a*, water is filtered through 1.0 um PALL AE glass fiber filter (GFF) prior to 2019, and through 0.7 µm Whatman GFF in 2019, and stored frozen until analysis. We quantified chl-*a* concentrations fluorometrically with a Turner Design 700 Fluorometer after ethanol extraction. We report total chl-*a*, which has not been acid corrected for pheophytin (Sartory and Grobbelaar 1984). The chl-*a* detection limit is 0.3 µg L<sup>-1</sup>. We measure TSS following standard methods (Method 2540 D and E; APHA 2017). Water is filtered through pre-weighed 1.5 µm, grade 934-AH Whatman GFF, which are stored frozen until analysis. TSS filters are thawed and dried at 105 °C for 30 minutes, weighed, and then incinerated at 550 °C for 20 minutes to burn off organic material before being weighed again. This loss-on-ignition procedure allowed for the differentiation of TSS by subtracting the mass left after incineration, which is PIM, from the total filter mass before incineration, which is TSS. The difference is POM. TSS, PIM, and POM analyses have a detection limit of 0.1 mg L<sup>-1</sup>. Secchi disk depth is measured with a 20 cm black and white Secchi disk.

#### *Zebra mussel density and biomass*

In summer 2019, we measured zebra mussel density and biomass in Bull Shoals (6/17/2019–6/21/2019), Lake of the Ozarks (5/29/2019, 6/12/2019, 7/11/2019, 7/29/2019, 8/28/2019), Lotawana (10/23/2019), and Smithville (5/22/2019, 6/10/2019, 7/17/2019,

8/19/2019). We did not measure zebra mussel density and biomass in Blue Springs, Jacomo, and Truman because at the time of sampling there were less than 5 years post-invasion water quality data. Zebra mussels were collected from transects placed perpendicular to the shore. The number of transects was based on reservoir size. Twelve transects were sampled in Bull Shoals, 12 in Lake of the Ozarks, 3 in Lotawana, and 10 in Smithville. The first transect was placed at the juncture of the dam and shoreline. Subsequent transects were evenly spaced around the shoreline, although some transects were moved to where previous observations of live mussels have occurred (Figure A3.1; Benson et al. 2021a). To date, quagga mussels have only been observed in Missouri in the Mississippi River (Benson et al. 2021b) and we did not observe this other invasive bivalve during our field sampling.

The number of sites sampled in each transect varied based on the slope of the littoral area, but typically 5 sites were sampled along each transect. Water levels are highly variable from year to year in several reservoirs. Water levels were procured from the Army Corps of Engineers for both Smithville<sup>1</sup> and Bull Shoals<sup>2</sup>, while Lake of the Ozarks<sup>3</sup> were provided by Ameren Corporation. Daily water levels are not recorded for Lotawana but the reservoir was at full pool at the time of sampling. To avoid sampling sites that had been recently dry, we placed our shallowest site at 2 m deeper than the lowest water level recorded over the previous 6 years (Figure A3.1). Each subsequent site along the transect was placed 2 m deeper than the previous site. Sampling ceased when no mussels were collected at the previous 2 sites and the depth was 10 m deeper than the

---

<sup>1</sup> <https://waterdata.usgs.gov/mo/nwis/uv?>

<sup>2</sup> <https://www.swl-wc.usace.army.mil/pages/data/tabular/htm/bulsdam.htm>

<sup>3</sup> <http://apps.ameren.com/HydroElectric/Reports/Osage/HSTBagnellDaily.aspx>

lowest water level recorded throughout the reservoir over the previous 6 years. The 6-year low in water levels for Lotawana is unknown, so we began sampling at 2 m.

At each site, 3 intact grab samples were collected with an Ekman dredge (0.023 m<sup>2</sup>). Samples were rinsed through a 500 µm mesh and any live zebra mussels were retained. Each mussel's length was measured (nearest 1.0 mm) from its umbo to its posterior margin and its weight measured (nearest 0.01 g) after opening its shell to remove water from the mantle cavity. All zebra mussels were counted, measured, and weighed within 48 hrs of collection.

We calculated zebra mussel density and biomass for each sample site based on the area of the Ekman grab. For each reservoir, we report the average density across all sites as individuals per m<sup>2</sup> and the average live-weight biomass as g per m<sup>2</sup>. These reservoir-wide density and biomass estimates reflect the nearshore area where our sampling occurred.

#### *Temperature and dissolved oxygen profiles*

Temperature and dissolved oxygen profiles were measured one to 4 times each year between May 15<sup>th</sup> and September 15<sup>th</sup>. Profiles were taken near the dam at the deepest point in the reservoir using a YSI multi-parameter sonde. No profiles were taken at Bull Shoals site 2. A model 50B was used to take profiles prior to 2000, while a model 85 was used between 2000 and 2006, and a model 550A was used from 2006 to 2016. Prior to 2017, temperature (accuracy: ±0.1–0.3 °C, resolution: 0.10 °C) and dissolved oxygen (accuracy: ±0.03 mg L<sup>-1</sup>, resolution: 0.01 mg L<sup>-1</sup>) measurements were made at discrete, vertical depths (usually 0.5 m intervals). After 2016, dissolved oxygen

(accuracy:  $\pm 0.1 \text{ mg L}^{-1}$ , resolution:  $0.1 \text{ mg L}^{-1}$ ) and temperature (accuracy:  $\pm 0.01 \text{ }^\circ\text{C}$ , resolution:  $0.02 \text{ }^\circ\text{C}$ ) profiles were continuous and collected using a YSI EXO3. Each profile was interpolated to 0.5 m using piecewise cubic hermite interpolating polynomial (PCHIP) with the `pracma` program in R (Borchers 2019). Mixing depth was calculated from the interpolated profile using `rLakeAnalyzer` (Winslow et al. 2019). If mixing depth was not identified in a profile, it was removed unless the profile extended to the reservoir bottom. Epilimnetic temperature and dissolved oxygen were determined for each profile by taking the mean of these parameters above the mixing depth. The depth where anoxia began, or anoxia depth, was considered to be the first depth where dissolved oxygen concentrations were  $\leq 1 \text{ mg L}^{-1}$  (Jones et al. 2011). Annual means of mixing depth, anoxia depth, epilimnetic temperature, and epilimnetic dissolved oxygen were used for statistical analyses.

### *Statistical analyses*

We looked for long-term trends in water clarity parameters for each reservoir. For each year of collection, the mean of each parameter was calculated and analyzed using a sequential t-test analysis of regime shifts (Rodionov 2004). We set the significance level to 0.05, the cut-off length to 10 years, and Huber's Weight Parameter to one. The number of observations with this analysis are not fixed, meaning that a new test is ran on each new data point (Rodionov 2004). This gives it an advantage over other regime shift tests because it is able to identify shifts as soon as they occur, not several years later (Rodionov and Overland 2005). Next, we used a Mann-Kendall trend test before and after each regime shift, or on the entire data series when no regime shift existed, to determine the presence of monotonic trends through time (Pohlert 2020). The year of the

regime shift reported was considered after the shift. If a significant monotonic trend was detected, we determined its magnitude using a Sen's slope calculation (Pohlert 2020). We report significant monotonic trends, as well as the magnitude of these trends for each reservoir and water clarity parameter. We also report the mean of each parameter before and after each regime shift, or on the entire data series if no regime shift existed. The year of the regime shift was included in the calculation of the mean for after the shift.

We determined regime shifts in Secchi disk depth (Table 4.2), TSS (Table 4.3), PIM (Table 4.4), and chl-*a* (Table 4.5) in invaded reservoirs. A regime shift corresponding with the invasion date indicates that zebra mussels could be having an impact, but the direction and trend in water clarity after the shift is indicative of whether that impact is resulting in increased water clarity due to zebra mussel grazing. Increasing water clarity is associated with an increase in Secchi disk depth and a decrease in TSS, PIM, and chl-*a*. An increase in water clarity after the regime shift that corresponds with invasion date could indicate that zebra mussels are having an impact. Likewise, a declining trend in water clarity that is followed by no trend after a regime shift that corresponds with invasion date suggests that zebra mussels could be having a moderating impact. We used a Mann-Kendall test and Sen's slope calculation to determine whether there was an increasing trend in water clarity after the shift occurred, which would further suggest that the introduction of zebra mussels was leading to an increase in water clarity. Considering 4 indicators of water clarity in each invaded reservoir enabled us to establish weight of evidence assessment about the impacts of zebra mussels on invaded reservoirs.

We assessed habitat suitability of invaded and reference reservoirs using a correlation (scaling 2) principal component analysis (PCA) with no rotation. Vectors for

the PCA included mixing depth, anoxia depth, epilimnetic temperature, epilimnetic dissolved oxygen, TSS, PIM, and the ratio of PIM:POM. PIM:POM is reported as a natural log to reduce bias associated with taking the average of ratios (Isles 2020). Bull Shoals site 2 was excluded from the PCA because no epilimnetic temperature nor dissolved oxygen data exists for this site. For each reservoir, the mean for each of these parameters was calculated from the entire long-term dataset and then converted to a z-score to standardize PCA inputs. The PCA was calculated using Program R (R Core Team 2019) and was plotted using the factoextra package (Kassambara and Mundt 2020).

We looked at the relationship between POM and chl-*a* to assess whether photoacclimation was influencing our findings. Phytoplankton can produce increased concentrations of chl-*a* in low light conditions and, if this occurs, chl-*a* may over represent phytoplankton biomass. If light availability has decreased over time in Missouri reservoirs, chl-*a* production may be increasing even though actual biomass is not. This could influence our assessment of temporal trends in chl-*a*. Neither POM nor chl-*a* were normally distributed, even after transformation, so we ran a Spearman's rank correlation test on these parameters in both invaded and reference reservoirs.

## RESULTS

### *Study reservoirs*

All invaded reservoirs are eutrophic except for Bull Shoals, which is classified as mesotrophic (Table 4.1, Jones et al. 2008). Surface area of invaded reservoirs ranged from 1.9 to 217.8 km<sup>2</sup> and volume ranged from 0.0013321584 to 7.416926289 km<sup>3</sup> (Table 4.1). The maximum depth in invaded reservoirs ranges from 17.7 m to 79.6 m and

watershed area ranges from 34.6 to 24,993.3 km<sup>2</sup> (Table 4.1). Flushing rate in invaded reservoirs ranges from 0.363 to 2.835 times per year (Table 4.1). Four invaded reservoirs were located in the Osage Plains, 2 are in the Ozark Highlands, and one is in the Glacial Plains (Jones et al. 2008). Reference reservoirs were located throughout the state and include oligotrophic ( $n= 3$ ), mesotrophic ( $n= 9$ ), and eutrophic ( $n= 14$ ) impoundments (Jones et al., 2008; Table 4.1). These range in size from 0.1 to 161.5 km<sup>2</sup> surface area and 0.000287401 to 3.332862960 km<sup>3</sup> volume (Table 4.1). The maximum depth of reference reservoirs ranges from 6.7 m to 78.6 m and watershed area ranges from 2.1 to 4,852.7 km<sup>2</sup> (Table 4.1). Reference reservoir flushing rates range from 0.190 to 19.201 times per year (Table 4.1). Two reference reservoirs are located in the Osage Plains, 10 are in the Ozark Highlands, 13 are in the Glacial Plains, and one is in the Ozark Border.

Photoacclimation did not have an effect on our findings, as POM and chl-*a* were substantially correlated for the entire long-term dataset in both reference ( $p < 0.0001$ ,  $\rho = 0.91$ ) and invaded reservoirs ( $p < 0.0001$ ,  $\rho = 0.78$ ) and in the latter, both before ( $p < 0.0001$ ,  $\rho = 0.77$ ) and after ( $p < 0.0001$ ,  $\rho = 0.78$ ) invasion. Chl-*a* is representative of phytoplankton biomass.

#### *Regime shifts in invaded reservoirs*

In Blue Springs, a regime shift in PIM occurred during the zebra mussel invasion range. Mean PIM concentrations were lower after the shift than before, and there was no trend before nor after (Figure 4.1). No regime shifts were identified during nor after the zebra mussel invasion range for Secchi disk depth nor TSS. A regime shift in chl-*a* occurred 2 years after the zebra mussel invasion range, but there was only one year post-invasion to detect a trend. While there was no regime shift, an increasing trend of 0.01 m

yr<sup>-1</sup> in Secchi disk depth was identified throughout the study period in Blue Springs. Of the 4 parameters we considered, PIM was the only one that was consistent with what would be expected if zebra mussels were having an impact.

In Bull Shoals, both Secchi disk depth and chl-*a* concentrations were measured from both sites. At site 1, a regime shift occurred in Secchi disk depth 3 years after the zebra mussel invasion range (Figure 4.2). After this regime shift, a trend was not identified because there was only one year post shift to run a Mann-Kendall test (Table 4.2). At Bull Shoals site 2, a regime shift occurred in Secchi disk depth 10 years after the zebra mussel invasion range (Figure 4.2). After this regime shift, a trend was not identified because there was only one year post shift to run a Mann-Kendall test (Table 4.2). No regime shift was identified at site 2 during or after the zebra mussel invasion range for chl-*a*, and there was no trend in this parameter during the study period. Neither of the 2 water clarity parameters we looked at in Bull Shoals sites 1 and 2 increased after the zebra mussel invasion, suggesting that mussels did not have an impact.

In Jacomo, a regime shift in PIM occurred 2 years after the zebra mussel invasion range (Figure 4.3). After this regime shift, a trend was not identified because there was only one year post shift to run a Mann-Kendall test (Table 4.4). No regime shifts nor trends were identified during or after the zebra mussel invasion range for Secchi disk depth, TSS, nor chl-*a*. Of the 4 water clarity parameters we considered in Jacomo, none were consistent with what would be expected if zebra mussels were having an impact.

In Lake of the Ozarks, a regime shift in Secchi disk depth occurred 8 years after the zebra mussel invasion range (Figure 4.4). Mean Secchi disk depth decreased after the shift and there was no trend pre- or post- shift (Table 4.2). A regime shift in TSS and chl-

*a* occurred 8 years after the zebra mussel invasion range (Figure 4.4). Before this shift in TSS, a decreasing trend of  $0.09 \text{ mg L}^{-1} \text{ yr}^{-1}$  was identified (Table 4.3). After the shift, mean TSS increased but there was no trend (Table 4.3). A second shift in TSS occurred 19 years after the zebra mussel invasion range, but there were only 2 years post-shift to measure a trend. For chl-*a*, there was an increasing trend of  $0.16 \text{ g}^{-1} \text{ L}^{-1} \text{ yr}^{-1}$  until the regime shift (Table 4.5). Mean chl-*a* increased after this shift, but no trend was identified. No regime shift nor trend was identified during or after the zebra mussel invasion range for PIM. Of the 4 water clarity parameters examined in Lake of the Ozarks, none were consistent with what would be expected if zebra mussels were having an impact.

In Lotawana, a regime shift in PIM occurred during the zebra mussel invasion range. After the regime shift, mean PIM decreased and a declining trend of  $0.06 \text{ mg L}^{-1} \text{ yr}^{-1}$  was identified (Table 4.4). Regime shifts in TSS occurred one and 10 years after the zebra mussel invasion range (Figure 4.5). Mean TSS decreased after the first shift, but no trend was identified pre- or post- regime shift (Table 4.3). There were only 2 years after the second regime shift and we could not run a Mann-Kendall test. No regime shifts nor trends were identified during or after the zebra mussel invasion range for Secchi disk depth nor chl-*a*. We examined 4 water clarity parameters for Lotawana, 2 of which, TSS and PIM, decreased after the zebra mussel invasion, as would be expected if zebra mussels were having an impact.

In Smithville, no regime shifts occurred during the zebra mussel invasion range. Regime shifts in Secchi disk depth and chl-*a* occurred 6 and 2 years, respectively, after the zebra mussel invasion range (Figure 4.6), although there was not a trend after the

regime shift for either parameter (Tables 4.2, 4.5). For chl-*a*, mean concentrations increased after the shift, which was preceded by an increasing trend of  $0.28 \mu\text{g L}^{-1} \text{yr}^{-1}$  and followed by no trend. Despite no identified regime shift, an increasing trend of  $0.09 \text{mg L}^{-1} \text{yr}^{-1}$  in TSS was identified throughout the study period in Smithville. No regime shifts nor trends were identified during or after the zebra mussel invasion range for Secchi disk depth, TSS and PIM. None of the 4 water clarity parameters we examined in Smithville were consistent with what would be expected if zebra mussels were having an impact.

In Truman, a regime shift occurred during the zebra mussel invasion range for TSS and PIM (Figure 4.7), but the mean of both parameters increased and there was no trend after the shift occurred. A regime shift occurred in chl-*a* 4 years after the zebra mussel invasion range, but there was only one year post-shift (Table 4.5). No regime shift nor trend was identified during or after the zebra mussel invasion range for Secchi disk depth. Of the 4 water clarity parameters we examined in Truman, none provided evidence that zebra mussels were having an effect.

To summarize, an increase in water clarity consistent with what we would expect if zebra mussels were having an impact occurred in 2 out of the 4 water quality parameters in Lotawana, and only one parameter in Blue Springs and Truman. No parameters in Bull Shoals, Jacomo, Smithville, nor Lake of the Ozarks displayed a pattern that was consistent with the expected change in water clarity if zebra mussels were having an impact.

*Regime shifts in reference reservoirs*

We looked for regime shifts in Secchi disk depth, TSS, PIM, and chl-*a* in 26 reference reservoirs to determine whether there were any statewide trends in water clarity that should be accounted for in our analysis of invaded reservoirs and might be indicative of a larger pattern. If water clarity did not increase in invaded reservoirs but decreased in reference reservoirs, it could suggest that zebra mussels were having a moderating effect on water clarity. In other words, water clarity might look static in invaded reservoirs if impacts from zebra mussels were offset by external factors causing water clarity to decrease throughout the state and over time.

A regime shift in Secchi disk depth occurred in 77 % of reference reservoirs. Mean Secchi disk depth increased post shift in 50 % of reservoirs and decreased in 4 % of reservoirs. In 8 % of reservoirs, there were 2 regime shifts. Mean Secchi disk depth increased after the first shift but decreased after the second. Two out of 4 reservoirs saw a significant trend after the regime shift occurred. This trend was positive in Forest, indicating a yearly increase in water clarity, but was negative in Binder.

For TSS, 65 % of reference reservoirs experienced a regime shift, but mean TSS increased in 19 % of these reservoirs and decreased in 8 % of reservoirs. In 8 % of reservoirs, there were 2 regime shifts where mean TSS increased after the first shift and decreased after the second shift. Nineteen percent of reservoirs saw a trend after the regime shift occurred. This trend was positive in Higginsville and Wappapello, indicating a decreasing trend in water clarity, but negative in Deer Ridge, Lincoln, and Viking. Like Secchi disk depth, there was only one reservoir where a regime shift was followed by a trend showing an increase in water clarity.

Fifty-eight percent of reference reservoirs experienced a regime shift in PIM. Mean PIM increased in 19 % of those reservoirs and decreased in 23 %. After the shift, a trend occurred in 35 % of reservoirs. This trend was positive only in Watkins Mill, showing a decrease in water clarity that might be caused by external factors on a statewide scale. A negative trend, and increase in water clarity, occurred after a regime shift in Atkinson, Binder, Bowling Green, Capri, Lincoln, Pomme de Terre, Shayne, and Viking.

For chl-*a*, a regime shift occurred in 69 % of reference reservoirs. Mean chl-*a* increased in 46 % of reservoirs and decreased in 4 %. No trends were observed after a regime shift in any reference reservoirs, but we identified positive trends in chl-*a* before a regime shift in both Clearwater and Table Rock.

To summarize, of the 4 indicators of water clarity that we examined, we did not observe a consistent pattern throughout the reference reservoirs. Water clarity increased in 46, 8, 23, and 4 % for Secchi disk depth, TSS, PIM and chl-*a*, respectively, but decreased in 4, 27, 19, and 46 % of these same parameters. Consistent water clarity decreases in reference reservoirs could suggest that zebra mussels are having a moderating effect in invaded reservoirs, where their impacts are being masked by broader trends. Our weight of evidence shows that no overarching trends exist in reference reservoirs.

#### *Zebra mussel density and biomass*

Zebra mussel density, biomass, and length were measured in Bull Shoals, Lake of the Ozarks, Lotawana, and Smithville (Table 4.6). Lake of the Ozarks had the highest

mean density per site (64.72 mussels  $\text{m}^{-2}$ ), followed by Smithville (25.76 mussels  $\text{m}^{-2}$ ), Lotawana (2.34 mussels  $\text{m}^{-2}$ ), and Bull Shoals (1.75 mussels  $\text{m}^{-2}$ ). Smithville had the greatest mean live weight mussel biomass per site (10.10  $\text{g m}^{-2}$ ), followed by Lake of the Ozarks (6.69  $\text{g m}^{-2}$ ), Bull Shoals (2.28  $\text{g m}^{-2}$ ), and Lotawana (0.20  $\text{g m}^{-2}$ ). Mean zebra mussel length was highest in Bull Shoals (22.6 mm). It was followed by Smithville (10.3 mm), Lotawana (9.5 mm), and Lake of the Ozarks (9.5 mm).

### *Habitat suitability*

We initially included 7 environmental variables in our PCA (Table 4.7) but ultimately removed TSS, PIM:POM, and mixing depth because they explained little of the variance in the data. When TSS was included, the first 2 components only explained an additional 0.4 % of the variation in the study reservoirs. The inclusion of PIM:POM and mixing depth reduced the amount of variation explained by 9.8 and 5.9 %, respectively. When PIM, DO, anoxia depth, and temperature were included in the PCA, the first component explained 50.1 % of the variation in all study reservoirs and was characterized predominantly by PIM, anoxia depth, and epilimnetic temperature (Figure 4.8). The second component, which explained 33.7 % of the variation in the dataset, was characterized by epilimnetic dissolved oxygen. Of the 7 invaded reservoirs we were able to include in the PCA, including only site 1 in Bull Shoals, only one was characterized by higher PIM concentrations and epilimnetic temperatures. Four invaded reservoirs were characterized by lower temperatures, because they were located opposite the temperature vector, while 3 of these were also characterized by lower PIM concentrations and deeper depths for the onset of anoxia because of their location opposite these vectors. Epilimnetic dissolved oxygen concentrations were the primary driver of variation in 2 of

the invaded reservoirs. Reference reservoirs overlapped with invaded reservoirs but displayed much greater variability in the parameters they were characterized by, as indicated by their spread throughout the PCA biplot. Of the 26 reference reservoirs in this study, 7 were located opposite of the epilimnetic temperature vector, compared to 3 located along it, indicating that reference reservoirs were also more often characterized by lower temperatures.

We report the natural log of the ratio of PIM to POM for each study reservoir, despite the fact that it was not included in our PCA (Table 4.7). Throughout all reservoirs, mean  $\ln(\text{PIM}):\ln(\text{POM})$  was -0.2, and on 98 % of sampling events, was below the 1.61.

## DISCUSSION

We looked at 4 water clarity parameters in 6 zebra mussel-invaded reservoirs, and 2 water clarity parameters in Bull Shoals, also invaded by zebra mussels. Our assessment is especially robust in Lake of the Ozarks, Lotawana, and Smithville, where we have at least 11 years of data pre- and post- the zebra mussel invasion date. In 5 out of 7 reservoirs, water clarity did not increase after zebra mussels invaded. Water clarity increased for a single parameter in Blue Springs, and for 2 out of 4 parameters for Lotawana. Our assessment of 26 reference reservoirs shows that water clarity is not changing ubiquitously across the state and suggests that the lack of zebra mussel impact was not a result of the mussels having a moderating effect on trends caused by external factors. Taken collectively, our analyses amass a weight of evidence showing that zebra mussel establishment did not increase water clarity in Missouri reservoirs. These findings are supported by 2019 sampling, which revealed low zebra mussel density and biomass

roughly 10 times lower in Missouri reservoirs compared to northern, natural lakes where zebra mussels were associated with an increase in water clarity (Ozersky et al. 2011; North et al. 2013; Knight et al. 2018; Rudstam and Gandino 2020). One explanation for the low densities could be that one or more habitat suitability parameters are near the tolerable threshold(s) for zebra mussels. It is possible that conditions in Missouri are suboptimal, allowing zebra mussels to survive while preventing them from forming the high densities that cause dramatic increases to water clarity. Invaded reservoirs tend to have cooler epilimnetic temperatures, lower PIM concentrations, and deeper anoxia depths than reference reservoirs. While zebra mussels are able to survive in Missouri reservoirs, these conditions could prevent the mussels from reaching densities great enough to impact water clarity.

#### *Zebra mussel populations*

Zebra mussel density is lower in Missouri than in northern, natural lakes. In 2019, the highest mean density of zebra mussels we found was in Lake of the Ozarks. At each site, there was an average of 65 individuals  $m^{-2}$ , which is over an order of magnitude lower than densities found in northern lakes where zebra mussels cause water clarity to increase. In Lake Champlain (NY-VT), zebra mussel densities were 4,160 individuals  $m^{-2}$  at 5 m depth (Knight et al. 2018). Zebra mussel densities ranged from 1,000 to 10,000 individuals  $m^{-2}$  between 2005 and 2018 in Onondaga Lake (NY, Rudstam and Gandino 2020). In Lake Simcoe (ON, Canada), zebra mussel densities reached as high as 30,000 individuals  $m^{-2}$  at some locations but were more commonly found at densities of 3,300 individuals  $m^{-2}$  (Ozersky et al. 2011; North et al. 2013).

The reservoir with the highest mean zebra mussel biomass we observed in 2019 was Smithville with  $10 \text{ g m}^{-2}$ . Like density, this is lower than what has been observed in northern lakes. Depending on when sampling occurred, mean zebra mussel biomass ranged from 618 to  $1,059 \text{ g m}^{-2}$  in Hargus Lake (OH), and in Lake Erie (ON-NY-PA-OH), zebra mussel biomass was  $1,269 \text{ g m}^{-2}$  before quagga mussels (*Dreissena r. bugensis*) replaced zebra mussels as the dominant dreissenid (Custer and Custer 1997; Yu and Culver 1999). Together, quagga and zebra mussel biomass in Oneida Lake (NY) was  $461 \text{ g m}^{-2}$  (Karatayev et al. 2014). The low biomass we observed in Missouri reservoirs could be why we did not observe an increase in water clarity after zebra mussel establishment.

It is possible that the low zebra mussel density and biomass measurements in 2019 reflected a low year for zebra mussel populations. Zebra mussel populations display high levels of temporal variability and, in extreme cases, can change by more than 10-fold from year to year (Strayer et al. 2019). However, even a 10-fold increase to 2019 measurements would be considerably lower than zebra mussel density and biomass in northern lakes. While additional sampling is required to determine zebra mussel interannual variation, we are confident that zebra mussel density and biomass in Missouri reservoirs are substantially lower than in lakes from more northern latitudes. This could explain why we did not observe a universal increase in water clarity post zebra mussel invasion. Zebra mussels may not be able to form large populations in Missouri because they are living in tolerable but stressful conditions. This is consistent with experimental studies that show zebra mussel mortality is higher when 2 environmental parameters are stressful but sublethal compared to just one (Mathai et al. 2020).

### *Water temperature*

Warm water temperatures could limit zebra mussels from reaching high densities in Missouri reservoirs. Above 30 °C, zebra mussel mortality increases substantially, although specific mortality rates depend on the length of time that temperature remains above 30 °C and thermal tolerance of individual mussels. For example, zebra mussel mortality is 100 % in as little as 2 days or as many as 47 days when temperatures are 31–32 °C (McMahon et al. 1994; Elderkin and Klerks 2005). In Missouri, mean surface water temperatures between May and August are  $\geq 30$  °C in a quarter of the 235 studied reservoirs (Jones et al. 2011). Temperatures above 30 °C could kill some zebra mussels, or could serve to reduce their ability to survive other suboptimal conditions.

Temperatures below the ~30 °C thermal maximum threshold could also have detrimental effects on zebra mussels. Filtration rates begin to decline above 22 °C, and above 25 °C zebra mussel growth rates decline (Thorp et al. 1998), respiration rates increase (Alexander et al. 1994), and byssus thread production and foot activity is reduced (Rajagopal et al. 1997). Surface water temperatures in most Missouri reservoirs are greater than 25 °C throughout most of the summer (Jones et al. 2011). Based on water temperatures and zebra mussel thermal tolerance, it is possible that zebra mussels that settle in the littoral zone are eliminated during the summer, while the surviving mussels are physiologically stressed.

Fluctuating water levels may also reduce zebra mussel densities by exposing mussels at deeper depths to suboptimal water temperatures. In Bull Shoals and Truman Reservoir for example, water levels can fluctuate widely from year to year because these reservoirs are managed by the Army Corps of Engineers to prevent downstream flooding.

August water levels since 2016 have fluctuated by 8.5 m in Bull Shoals<sup>4</sup>, while water level fluctuation in Truman Reservoir<sup>5</sup> have been as high as 5.2 m. Such wide fluctuations could expose zebra mussels that were in deeper, cooler waters the previous year to water temperatures that are suboptimal or lethal. Water level drops could also kill zebra mussels by exposing them to air, and in fact, we observed empty zebra mussel shells above the water line that were attached to permanent boat launch structures in Bull Shoals.

### *Suspended inorganic particles*

Suspended particles can negatively impact zebra mussel fitness by clogging inhalant siphons and gills, reducing rates of respiration, clearance, and ingestion (Madon et al. 1998; Tuttle-Raycraft et al. 2017). Reduced zebra mussel clearance and ingestion rates have been observed in as little as 1 mg L<sup>-1</sup> PIM, especially when food quality is low (Madon et al. 1998). Others have not observed negative effects of suspended particles until PIM concentrations are 27 mg L<sup>-1</sup>, above which zebra mussels increase their pseudofeces production (Lei et al. 1996), and 31 mg L<sup>-1</sup>, which is the concentration above which respiration rates begin to decline (Alexander et al. 1994). The natural log of the ratio of inorganic to organic particles may also influence zebra mussel physiology, with 1.61 as a cutoff under which zebra mussel ingestion, assimilation, water processing, and clearance rates are reduced (Madon et al., 1998; Schneider et al., 1998). PIM concentrations in Missouri are generally higher than lakes at more northern latitudes as median summer concentrations are 3.1 mg L<sup>-1</sup> (Jones et al. 2008). This is above the 1 mg

---

<sup>4</sup> <https://www.swl-wc.usace.army.mil/pages/data/tabular/htm/bulsdam.htm>

<sup>5</sup> [https://waterdata.usgs.gov/mo/nwis/uv?site\\_no=06922440](https://waterdata.usgs.gov/mo/nwis/uv?site_no=06922440)

$L^{-1}$  threshold for negative zebra mussel effects (Madon et al. 1998), but well below some of the other thresholds in the literature (Alexander et al. 1994; Lei et al. 1996). The natural log of PIM to POM was below the 1.6 threshold in 98 % of the sampling events, suggesting that zebra mussels in Missouri reservoirs may be frequently experiencing physiological stress due to suboptimal PIM to POM ratios. Storm events, and the associated increase in PIM from runoff (Hou et al. 2017) and resuspension (Jin and Ji 2001), could increase PIM concentrations and create intermittent periods of increased stress. This would be especially pronounced up-reservoir, and less evident near the dam where our samples were collected. The PIM to POM ratio and PIM concentrations by themselves could be a contributing factor to a suboptimal environment for zebra mussels.

There is evidence that zebra mussels can adapt to chronic levels of high inorganic suspended solids (Ouellette-Plante et al. 2017). Mussels previously exposed to high suspended PIM concentrations are less likely to be affected by future exposures (Summers et al. 1996), possibly because of behavioral techniques such as increasing their palp to gill surface area to facilitate food and non-food particle sorting (Payne et al. 1995), closing their inhalant siphons during periods of high suspended particles (Wiśniewski 1990), and increasing pseudofeces production (Chapman et al. 2017). These adaptations could enable zebra mussels to survive in Missouri reservoirs, despite sub-optimal concentrations of suspended PIM, but they do incur an energetic cost that might reduce overall fitness (Goldsmith et al. 2021). Our comparison of invaded and reference reservoirs showed that 4 of 7 invaded reservoirs were characterized by low PIM concentrations, and only one invaded reservoir was associated with higher PIM concentrations. This suggests that PIM could be an important influence on zebra mussel

densities in Missouri, and the chronic levels of relatively high suspended PIM could be one of multiple factors that ultimately prevents zebra mussels from reaching high densities.

#### *Dissolved oxygen concentrations*

Hypolimnetic oxygen concentrations are probably suboptimal for zebra mussels in Missouri reservoirs throughout most of the summer. Zebra mussels are one of the least tolerant bivalves to low oxygen levels. Their survival thresholds for dissolved oxygen depend on water temperature because of increased metabolic demands associated with warmer temperatures (McMahon 1996; Alexander and McMahon 2004). Under anoxic conditions, 100 % zebra mussel mortality can occur in as little as 4 days when temperatures are 25 °C, but as many as 42 days when temperatures are 5 °C (Mathews and McMahon 1999). By August, temperatures in Missouri hypolimnions often exceed 20 °C (Jones et al. 2020) and approximately 80 % of reservoirs throughout the state experience hypolimnetic anoxia throughout 65 % of the water column (Jones et al. 2011; Petty et al. 2020). Most remain stratified between May and September when the mean summer thermocline depth is  $\leq 5.2$  m in 90 % of reservoirs (Jones et al. 2011). Zebra mussels typically colonize substrate within the upper 9 m when oxygen levels are favorable (Burlakova et al. 2006; Hetherington et al. 2019), but in Missouri, where the thermocline is near 5 m and hypolimnetic oxygen levels are reduced throughout much of the summer, they may be limited to shallower depths. Zebra mussels at shallower depths are more susceptible to drops in water levels, which could leave the mussels dry or expose them to warmer surface waters. Rising water levels may also further reduce habitat by changing the depth above which remains oxygenated. The mixing depth could

establish at a shallower depth than where zebra mussels have settled in the littoral zone. It is possible that during some years, when water levels are high and the depth of the hypolimnion is greater, dissolved oxygen plays a very important role in zebra mussel survival. During years when water levels are low, oxygen concentrations may not be as important because zebra mussels are exposed to the oxygenated epilimnion.

Deeper anoxia depths, which were characteristic of 4 invaded reservoirs, may provide an indication of the importance of hypolimnetic dissolved oxygen concentrations on zebra mussels. Deeper anoxia depths could expand zebra mussel habitat availability by increasing the depth at which water remains oxygenated throughout the summer. Zebra mussels growing below the anoxia have been killed in other water bodies as a result of low hypolimnetic dissolved oxygen levels (Yu and Culver 1999), so it would be unsurprising if this parameter was an important factor in determining zebra mussel populations in Missouri.

#### *Zebra mussels along the southern extant of their expansion*

Our analysis of habitat suitability suggests that invaded reservoirs are more often characterized by cooler epilimnetic water temperatures, lower PIM concentrations, and larger oxygenated epilimnions. We found that many reference and invaded reservoirs shared these conditions, but this overlap is unsurprising. The absence of an invader does not necessarily mean that conditions prevent that invader from becoming established, especially along the expanding edge of its range as it is possible the invader has not yet arrived. In Missouri, Lake of the Ozarks was the first reservoir where zebra mussels were observed and is also the most visited (Reitz 2015). It could be that the reference reservoirs in this area might be more susceptible to zebra mussel establishment if they are

invaded, while reference reservoirs with warmer temperatures and/or higher PIM concentrations might be less likely to support dense zebra mussel populations if they are invaded. The most consistent pattern we observed in invaded reservoirs was that they were characterized by cooler epilimnetic temperatures and lower PIM concentrations (Figure 4.8). Further investigation is required, but our analysis serves as an initial assessment of the parameters that might be most influential to zebra mussel densities near the end of their range.

Texas represents the southern extant of the zebra mussel invasion in North America and Europe (Locklin et al. 2020). There, zebra mussels have been observed in 39 lakes and reservoirs and are expected to continue their expansion (Robertson et al. 2020). Zebra mussel densities are higher down-reservoir compared to up-reservoir, which could reflect the longitudinal flow of these systems (Locklin et al. 2020). This differs from natural lakes, where zebra mussels cause nutrients to move from the pelagic offshore to the littoral nearshore (Hecky et al. 2004). Warm water temperatures at the southern zebra mussel extant cause growth rates to be faster than anywhere else and enable up to 2 reproductive events per year, compared to a single reproductive event in many northern latitude lakes (Churchill 2013). Mortality in Texas reservoirs is high due to frequent summer temperatures above 30 °C (Churchill et al. 2017; Arterburn 2020). Due to extreme climate events and high mortality rates associated with water temperatures near their thermal tolerance, zebra mussels along the southern edge of their range may experience large population swings (Churchill et al. 2017). If these “boom and bust” cycles are common in zebra mussel population densities at southern latitudes, it would explain why we did not observe a consistent increase in water clarity post

invasion. It is possible that our 2019 sampling may have occurred on a down, or “bust” year. Even if this was the case, zebra mussel densities were over an order of magnitude less in the 4 reservoirs we sampled than in any other invaded lake previously reported, suggesting that not all areas are equally impacted by this invader. In Belton Lake, Texas, zebra mussel densities from the spring cohort were as high as 21,160 mussels  $m^{-2}$  at a single site (Locklin et al. 2020), much greater than the maximum zebra mussel density of 1,682 mussels  $m^{-2}$  that we measured at a site in Lake of the Ozarks, Missouri. The reason why densities vary so dramatically in reservoirs at or near the southern zebra mussel expansion is still unclear, but our study suggests that differences in PIM concentrations and epilimnetic temperatures could play a role.

### *Conclusions*

Using 40+ years of historical water clarity data, we looked for regime shifts in water clarity corresponding with zebra mussel establishment. Considering the 4 water clarity parameters and 7 Missouri reservoirs with zebra mussel populations, we amounted a weight of evidence showing that zebra mussel establishment is not consistently associated with an increase in water clarity. This finding contradicts trends in northern lakes (Higgins and Vander Zanden 2010) and, to the best of our knowledge, is the first record of zebra mussels having an undetectable effect on water clarity. In Missouri reservoirs, epilimnetic temperatures, TSS, PIM, and hypolimnetic dissolved oxygen concentrations are near, or occasionally exceed, zebra mussel survival thresholds. It is possible that living in sublethal conditions prevents zebra mussels from establishing consistently high densities in Missouri reservoirs. This theory was supported by 2019 sampling of 4 invaded reservoirs. We observed zebra mussel densities no greater than

1,682 mussels  $\text{m}^{-2}$  at a single site, over 10 times less than densities in more northern lakes (Ozersky et al. 2011; North et al. 2013; Knight et al. 2018; Rudstam and Gandino 2020). Our habitat suitability assessment of Missouri reservoirs shows that invaded reservoirs were characterized by lower PIM concentrations and cooler epilimnetic temperatures, which could provide some indication about the parameters limiting zebra mussel densities. Additional research is needed to confirm whether or not this is the case, but our findings provide important insights into the impacts of invasive zebra mussels that will help us better understand their impacts as they continue to expand throughout North America.

## LITERATURE CITED

- Alexander JE, Thorp JH, Fell RD (1994) Turbidity and temperature effect on oxygen consumption in the zebra mussel (*Dreissena polymorpha*). *Can J Fish Aquat Sci* 51:179–184
- Alexander JE, McMahon RF (2004) Respiratory response to temperature and hypoxia in the zebra mussel *Dreissena polymorpha*. *Comp Biochem Phys A* 137:425–434
- APHA (2017) Standard Methods for the Examination of Water and Wastewater 23<sup>rd</sup> edn. Baird RB, Eaton AD, Rice EW (eds) Washington DC: American Public Health Association, Denver: American Water Works Association, Alexandria: Water Environment Federation
- Arterburn H (2020) Zebra mussel populations in warmer waters. Dissertation, University of Texas at Arlington
- Baranowska KA, North RL, Winter JG, Dillon PJ (2013) Long-term seasonal effects of dreissenid mussels on phytoplankton in Lake Simcoe, Ontario, Canada. *Inland Waters* 3:285–296
- Benson AJ, Raikow D, Larson J, Fusaro A, Bogdanoff AK, Elgin A (2021a) *Dreissena polymorpha* (Pallas, 1771). United States Geological Survey. <http://nas.er.usgs.gov/taxgroup/mollusks/zebramussel/zebramusseldistribution.aspx>. Accessed 5 April 2021
- Benson AJ, Richardson MM, Maynard E, Larson J, Fusaro A, Bogdanoff AK, Neilson ME, Elgin A (2021b). *Dreissena rostriformis bugensis* (Andrusov, 1897): U.S. Geological Survey. <https://nas.er.usgs.gov/queries/SpeciesAnimatedMap.aspx?speciesID=95>. Accessed 4 June 2021
- Borchers HW (2019) pracma: practical numerical math functions. <https://CRAN.R-project.org/package=pracma>. Accessed 5 April 2021
- Budd JW, Drummer TD, Nalepa TF, Fahnenstiel GL (2001) Remote sensing of biotic effects: zebra mussels (*Dreissena polymorpha*) influence on water clarity in Saginaw Bay, Lake Huron. *Limnol Oceanogr* 46:213–223
- Burlakova LE, Karatayev AY, Padilla DK (2006) Changes in the distribution and abundance of *Dreissena polymorpha* within lakes through time. *Hydrobiologia* 571:133–146
- Carey JR (1996) The incipient Mediterranean fruit fly population in California: implications for invasion biology. *Ecology* 77:1690–1696
- Carlton JT (2008) The zebra mussel *Dreissena polymorpha* found in North America in 1986 and 1987. *J Great Lakes Res* 34:770–773
- Chapman PM, Hayward A, Faithful J (2017) Total suspended solids effects on freshwater lake biota other than fish. *B Environ Contam Tox* 99:423–427

- Churchill CJ (2013). Spatio-temporal spawning and larval dynamics of a zebra mussel (*Dreissena polymorpha*) population in a North Texas Reservoir: implications for invasions in the southern United States. *Aquat Invasions* 8:389–406
- Churchill CJ, Hoeinghaus DJ, La Point, TW (2017) Environmental conditions increase growth rates and mortality of zebra mussels (*Dreissena polymorpha*) along the southern invasion front in North America. *Biol Invasions* 19:2355–2373
- Cohen AN (2007) Potential Distribution of Zebra Mussels (*Dreissena Polymorpha*) and Quagga Mussels (*Dreissena Bugensis*) in California: Phase 1 Report. San Francisco Estuary Institute, Oakland
- Connelly NA, O'Neill CR, Knuth BA, Brown TL (2007) Economic impacts of zebra mussels on drinking water treatment and electric power generation facilities. *Environ Manage* 40:105–112
- Custer CM, Custer TW (1997) Occurrence of zebra mussels in near-shore areas of western Lake Erie. *J Great Lakes Res* 23:180–115
- Elderkin CL, Klerks PL (2005) Variation in thermal tolerance among three Mississippi River populations of the zebra mussel, *Dreissena polymorpha*. *J Shellfish Res* 24:221–226
- Fahnenstiel GL, Lang GA, Nalepa TF, Johengen TH (1995). Effects of zebra mussel (*Dreissena polymorpha*) colonization on water quality parameters in Saginaw Bay, Lake Huron. *J of Great Lakes Res* 21:435–448.
- Fanslow DL, Nalepa TF, Lang GA (1995) Filtration rates of the zebra mussel (*Dreissena polymorpha*) on natural seston from Saginaw Bay, Lake Huron. *J Great Lakes Res* 21:489–500
- Goldsmith AM, Jaber F, Ahmari H, Randklev CR (2021) Clearing up cloudy waters: a review of sediment impacts to unionid freshwater mussels. *Environ Rev* 29:100–108
- Hecky RE, Smith REH, Barton DR, Guildford SJ, Taylor WD, Charlton MN, Howell T (2004) The nearshore phosphorus shunt: a consequence of ecosystem engineering by dreissenids in the Laurentian Great Lakes. *Can J Fish Aquat Sci* 61:1285–1293.
- Hetherington AL, Rudstam LG, Schneider RL, Schneider RL, Holeck KT, Hotaling CW, Cooper JE, Jackson JR (2019) Invader invaded: population dynamics of zebra mussels (*Dreissena polymorpha*) and quagga mussels (*Dreissena rostriformis bugensis*) in polymictic Oneida Lake, NY, USA (1992–2013). *Biol Invasions* 21:1529–1544
- Higgins SN, Vander Zanden MJ (2010) What a difference a species makes: a meta-analysis of dreissenid mussel impacts on freshwater ecosystems. *Ecol Monogr* 80:179–196

- Hou X, Feng L, Duan H, Chen X, Sun D, Shi K (2017) Fifteen-year monitoring of the turbidity dynamics in large lakes and reservoirs in the middle and lower basin of the Yangtze River, China. *Remote Sens Environ* 190:107–121
- Isles PDF (2020) The misuse of ratios in ecological stoichiometry. *Ecology* 101:e03153
- Jin KR, Ji ZG (2001) Calibration and verification of a spectral wind-wave model for Lake Okeechobee. *Ocean Eng.* 28:571–584
- Jones JR, Obrecht DV, Perkins BD, Knowlton MF, Thorpe AP, Watanabe S, Bacon RR (2008) Nutrients, seston, and transparency of Missouri reservoirs and oxbow lakes: an analysis of regional limnology. *Lake Reservoir Manag* 24:155–180
- Jones JR, Knowlton MF, Obrecht DV, Graham JL (2011) Temperature and oxygen in Missouri reservoirs. *Lake Reservoir Manag* 27:173–182
- Jones JR, Thorpe AP, Obrecht DV (2020) Limnological characteristics of Missouri reservoirs: synthesis of a long-term assessment. *Lake Reservoir Manag* 36:412–422
- Jost JA, Soltis EN, Moyer MR, Keshwani SS (2015) Linking zebra mussel growth and survival with two cellular stress indicators during chronic temperature stress. *Invertebr Biol* 134:189–202
- Karatayev AY, Burlakova LE, Mastitsky SE, Padilla DK, Mills EL (2011) Contrasting rates of spread of two congeners, *Dreissena polymorpha* and *Dreissena rostriformis bugensis*, at different spatial scales. *J Shellfish Res* 30:1–9
- Karatayev VA, Karatayev AY, Burlakova LE, Rudstam LG (2014) Eutrophication and *Dreissena* invasion as drivers of biodiversity: a century of change in the mollusk community of Oneida Lake. *PLoS ONE* 9:e101388. doi.org/10.1371/journal.pone.0101388
- Kassambara A, Mundt F (2020). factoextra: extract and visualize the results of multivariate data analyses. <https://CRAN.R-project.org/package=factoextra>
- Keller RP, Perrings C (2011) International policy options for reducing the environmental impacts of invasive species. *Bioscience* 61:1005–1012
- Kim TY, North RL, Guildford SJ, Dillon P, Smith REH (2015) Phytoplankton productivity and size composition in Lake Simcoe: the nearshore shunt and the importance of autumnal production. *J Great Lakes Res* 41:1075–1086
- Kirsch KM, Dzialowski AR (2012) Effects of invasive zebra mussels on phytoplankton, turbidity, and dissolved nutrients in reservoirs. *Hydrobiologia* 686:169–179
- Knight JC, O'Malley BP, Stockwell JD (2018) Lake Champlain offshore benthic invertebrate community before and after zebra mussel invasion. *J Great Lakes Res* 44:283–288

- Kulhanek SA, Leung B, Ricciardi A (2011) Using ecological niche models to predict the abundance and impact of invasive species: application to the common carp. *Ecol Appl* 21:203–213
- Lei J, Payne BS, Wang SY (1996) Filtration dynamics of the zebra mussel, *Dreissena polymorpha*. *Can J Fish Aquat Sci* 53:29–37
- Locklin JL, Corbitt DN, McMahon RF (2020) Settlement, density, survival and shell growth of zebra mussels, *Dreissena polymorpha*, in a recently invaded low latitude, warm water Texas reservoir. *Aquat Invasions* 15:408–434
- Lockwood JL, Hoopes MF, Marchetti MP (2013) *Invasion Ecology* 2<sup>nd</sup> Edition. Wiley-Blackwell, Chichester
- Lowe S, Browne M, Boudjelas S, De Poorter M (2004) 100 of the world's worst invasive alien species: a selection from the Global Invasive Species Database. International Union for the Conservation of Nature, Auckland
- MacIsaac HJ, Rocha R (1995) Effects of suspended clay on zebra mussel (*Dreissena polymorpha*) faeces and pseudofaeces production. *Arch Hydrobiol* 135:53–64
- Madon SP, Schneider DW, Stoeckel JA, Sparks RE (1998) Effects of inorganic sediment and food concentrations on energetic processes of the zebra mussel, *Dreissena polymorpha*: implications for growth in turbid rivers. *Can J Fish Aquat Sci* 55:401–413
- Mathai PP, Bertram JH, Padhi SK, Singh V, Tolo IE, Primus A, Mor SK, Phelps NBD, Sadowsky MJ (2020) Influence of environmental stressors on the microbiota of zebra mussels (*Dreissena polymorpha*). *Microb Ecol* 707: <https://doi.org/10.1007/s00248-020-01642-2>
- Mathews MA, McMahon RF (1999) Effects of temperature and temperature acclimation on survival of zebra mussels (*Dreissena polymorpha*) and Asian clams (*Corbicula fluminea*) under extreme hypoxia. *J Molluscan Stud* 65:317–325
- McMahon RF (1996) The physiological ecology of the zebra mussel, *Dreissena polymorpha*, in North America and Europe. *Amer Zool* 36:339–363
- McMahon RF, MA Matthews, Ussery TH, Chase R, Clarke M (1994) Further studies of heat tolerance in zebra mussels: Effects of temperature acclimation and chronic exposure to lethal temperatures. In *Proceedings: Fourth international zebra mussel conference '94*, pp. 251–272. Wisconsin Sea Grant Institute, Madison
- Missouri DNR (2019) *MO 2019 Dams*. Rolla, MO: Missouri Geological Survey, Dam and Reservoir Safety Program
- Missouri DNR (1986) *Missouri Water Atlas*. Rolla, MO: Missouri Geological Survey, Division of Geology and Land Survey
- North RL, Barton D, Crowe AS, Dillon PJ, Dolson RML, Evans DO, Ginn BK, Håkanson L, Hawryshyn J, Jarjanazi H, King JW, La Rosa JKL, León L, Lewis CFM, Liddle GE, Lin ZH, Longstaffe FJ, Macdonald RA, Molot L, Ozersky T,

- Palmer ME, Quinlan R, Rennie MD, Robillard MM, Rodé D, Rühland KM, Schwalb A, Smol JP, Stainsby E, Trumpickas JJ, Winter JG, Young JD (2013) The state of Lake Simcoe (Ontario, Canada): the effects of multiple stressors on phosphorus and oxygen dynamics. *Inland Waters* 3:51–74
- Ouellette-Plante J, Morden AL, Johnson LE, Martel AL Ricciardi A (2017) Acclimation by invasive mussels: spatiotemporal variation in phenotypic response to turbidity. *Freshw Sci* 36:325–337
- Ozersky T, Barton DR, Evans DO (2011) Fourteen years of dreissenid presence in the rocky littoral zone of a large lake: effects on macroinvertebrate abundance and diversity. *J N Am Benthol Soc* 30:913–922
- Payne BS, Miller AC, Hubertz ED, Lei J (1995) Adaptive variation in palp and gill size of the zebra mussel (*Dreissena polymorpha*) and Asian clam (*Corbicula fluminea*). *Can J Fish Aquat Sci* 52:1130–1134
- Petty EL, Obrecht DV, North RL (2020) Filling in the flyover zone: high phosphorus in Midwestern (USA) reservoirs results in high phytoplankton biomass but not high primary productivity. *Front Environ Sci* 8:11
- Pohlert T (2020) trend: Non-Parametric Trend Tests and Change-Point Detection. <https://CRAN.R-project.org/package=trend>. Accessed 5 April 2021
- R Core Team, 2019. R: A language and environment for statistical computing. R Foundation for Statistical Computing, Vienna, Austria. URL: <https://www.R-project.org/>
- Rajagopal S, G Van der Velde, HA Jenner (1997) Response of zebra mussel, *Dreissena polymorpha*, to elevated temperatures in the Netherlands. In: FM D'Itri (ed) Zebra mussels and aquatic nuisance species. Ann Arbor Press, Chelsea. pp 257–273
- Reitz RA (2015) Results of the 2013 Missouri statewide angler survey. Resource Science Division, Missouri Department of Conservation
- Ricciardi A, Hoopes MF, Marchetti MP, Lockwood JL (2013) Progress toward understanding the ecological impacts on nonnative species. *Ecol Monogr* 83:263–282
- Robertson JJ, Swannack TM, McGarrity M, Schwalb AN (2020) Zebra mussel invasion of Texas lakes: estimating dispersal potential via boats. *Biol Invasions* 22:3425–3455
- Rodionov SN (2004) A sequential algorithm for testing climate regime shifts. *Geophys Res Lett* 31:L09204. doi:10.1029/2004GL019448
- Rodionov S, Overland JE (2005) Application of a sequential regime shift detection method to the Bering Sea ecosystem. *ICES J of Mar Sci* 52:328–332
- Rudstam LG, Gandino CJ (2020) Zebra or quagga mussel dominance depends on trade-offs between growth and defense—Field support from Onondaga Lake, NY. *PLoS ONE* 15:e0235387. doi.org/10.1371/journal.pone.0235387

- Sakai AK, Allendorf FW, Holt JS, Lodge DM, Molofsky J, With KA, Baughman S, Cabin RJ, Cohen J, Ellstrand NC, McCauley DE, O'Neil P, Parket IM, Thompson JN, Weller SG (2001) The population biology of invasive species. *Ann Rev Ecol Syst* 32:305–332
- Sartory DP, Grobbelaar JU (1984) Extraction of chlorophyll a from freshwater phytoplankton for spectrophotometric analysis. *Hydrobiologia* 114:117–187
- Schloesser DW, Kovalak WP (1991) Infestation of native unionids by *Dreissena polymorpha* in a power plant intake canal in Lake Erie. *J Shellfish Res* 10:355–359
- Schneider DW, Madon SP, Stoeckel JA, Sparks RE (1998) Seston quality controls zebra mussel (*Dreissena polymorpha*) energetics in turbid rivers. *Oecologia* 117:331–341
- Strayer DL, Adamovich BV, Adrian R, Aldridge DC, Balogh C, Burlakova LE, Fried-Petersen HB, -Tóth LG, Hetherington AL, Jones TS, Karatayev AY, Madill JB, Makarevich OA, Marsden JE, Martel AL, Minchin D, Nalepa TF, Noordhuis R, Robinson TJ, Rudstam LG, Schwalb AN, Smith DR, Steinman AD, Jeschke JM (2019) Long-term population dynamics of dreissenid mussels (*Dreissena polymorpha* and *D. rostriformis*): a cross-system analysis. *Ecosphere* 10:e02701. doi:10.1002/ecs2.2701
- Summers RB, Thorp JH, Alexander JE Jr, Fell RD (1996) Respiratory adjustment of dreissenid mussels (*Dreissena polymorpha* and *Dreissena bugensis*) in response to chronic turbidity. *Can J Fish Aquat Sci* 53:1626–1631
- Thompson JN (1998) Rapid evolution as an ecological process. *Trends Ecol Evol* 13:329–332
- Thorp JH, Alexander JE Jr, Bukaveckas BL, Cobbs GA, Bresko KL (1998) Responses of Ohio River and Lake Erie dreissenid molluscs to changes in temperature and turbidity *Can J Fish Aquat Sci* 55:220–229
- Tuttle-Raycraft S, Morris TJ, Ackerman JD (2017) Suspended solid concentration reduces feeding in freshwater mussels. *Sci Total Environ* 598:1160–1168
- Ward JM, Ricciardi A (2007) Impacts of *Dreissena* invasions on benthic macroinvertebrate communities: a meta-analysis. *Divers Distrib* 13:155–65
- Winslow L, Read J, Woolway R, Brentrup J, Leach T, Zwart J, Albers S, Collinge D (2019) rLakeAnalyzer: lake physics tools. <https://CRAN.R-project.org/package=rLakeAnalyzer>. Accessed 5 April 2021
- Wiśniewski R (1990) Shoals of *Dreissena polymorpha* as bio-processor of seston. In: Gulati RD, Lammens EHRR, Meijer ML, van Donk E (eds) *Bio-manipulation Tool for Water Management. Developments in Hydrobiology*, vol. 61. Springer, Dordrecht [https://doi.org/10.1007/978-94-017-0924-8\\_39](https://doi.org/10.1007/978-94-017-0924-8_39). Accessed 5 April 2021
- Wylie GD, Jones JR (1991) Assessment of the sensitivity of Missouri reservoirs to acidification. *J Freshwater Ecol* 6:431–437

Yu N, Culver DA (1999) In situ survival and growth of zebra mussels (*Dreissena polymorpha*) under chronic hypoxia in a stratified lake. *Hydrobiologia* 392:205–215

TABLES

**Table 4.1:** Characterization for all invaded and reference reservoirs. Latitude and longitude refer to the coordinates near the dam. For all reservoirs except Bull Shoals, this is where water samples are collected. Maximum depth is based on the dam height of each reservoir and volume is the volume of each reservoir at full pool. Trophic status was determined from previous work in Missouri reservoirs (Jones et al. 2008). Flushing rate for Bull Shoals is unknown.

	Reservoir	Latitude (°N)	Longitude (°E)	Ecoregion	Trophic Status	Mean Depth (m)	Max. Depth (m)	Surface Area (km <sup>2</sup> )	Flushing Rate (times yr <sup>-1</sup> )	Watershed Area (km <sup>2</sup> )	Volume (km <sup>3</sup> )	
Zebra	Blue Springs	39.0141	-94.3371	Osage Plains	Eutrophic	4.5	16.2	2.9	1.125	86.7	0.013321584	
Mussel	Bull Shoals	36.5308	-92.6047	Ozark Highlands	Mesotrophic	20.4	79.6	194.3		15633.2	7.416926289	
Reservoirs	Jacomo	38.9931	-94.3078	Osage Plains	Eutrophic	7.3	22.6	4.3	0.363	66.8	0.031737440	
	Lake of the Ozarks	38.2039	-92.6236	Ozark Highlands	Eutrophic	12.0	45.1	207.7	2.548	24993.3	2.491629600	
	Lotawana	38.9353	-94.2464	Osage Plains	Eutrophic	7.5	17.7	1.9	0.425	34.6	0.014268897	
	Smithville	39.3631	-94.5567	Glacial Plains	Eutrophic	6.2	32.0	28.7	0.449	543.2	0.178361208	
	Truman	38.2639	-93.4083	Osage Plains	Eutrophic	6.8	38.4	217.8	2.835	18394.7	1.483506396	
	Reference Reservoirs	Atkinson	38.0064	-94.0461	Osage Plains	Eutrophic	1.7	8.5	1.9	1.196	17.0	0.003357533
	Binder	38.6019	-92.3008	Ozark Boarder	Eutrophic	6.9	14.6	0.6	0.963	15.8	0.004085286	
	Bowling Green	39.3420	-91.1531	Glacial Plains	Mesotrophic	19.5	22.3	0.1	0.394	3.4	0.001739207	
	Brookfield	39.7961	-93.0283	Glacial Plains	Eutrophic	5.1	13.1	0.5	0.190	2.7	0.002333744	
	Capri	37.8978	-90.6275	Ozark Highlands	Oligotrophic	8.3	29.6	8.8	0.228	2337.7	0.003488281	
	Clearwater	37.1339	-90.7722	Ozark Highlands	Mesotrophic	30.9	46.9	1.7	3.501	34.6	0.271365600	
	Council Bluff	37.7324	-90.9145	Ozark Highlands	Oligotrophic	9.0	33.5	0.2	0.818	2.4	0.015591187	
	Deer Ridge	40.1803	-91.8269	Glacial Plains	Eutrophic	3.8	11.6	2.9	0.553	51.4	0.000651277	
	Fellows	37.3153	-93.2300	Ozark Highlands	Mesotrophic	11.3	30.5	2.3	0.497	38.3	0.032365282	
	Forest	40.1714	-92.6548	Glacial Plains	Mesotrophic	6.6	20.1	0.6	0.374	8.0	0.015333390	
	Higginsville	39.0617	-93.6700	Glacial Plains	Eutrophic	2.9	10.4	1.9	1.291	17.0	0.002048810	
	Hunnewell	39.7072	-91.8619	Glacial Plains	Eutrophic	3.5	11.0	0.8	0.676	10.3	0.002718590	
	Kraut Run	38.7353	-90.7619	Glacial Plains	Eutrophic	2.2	6.7	0.6	3.320	16.6	0.001270484	
	Lincoln	39.0203	-90.9217	Glacial Plains	Mesotrophic	14.8	21.0	0.1	0.477	4.0	0.001894625	
	Long Branch	39.7514	-92.5150	Glacial Plains	Eutrophic	4.3	21.6	9.9	1.094	270.7	0.042727747	
	Mark Twain	39.5223	-91.6467	Glacial Plains	Eutrophic	8.2	34.1	75.0	1.880	6086.3	0.616789339	
	McDaniel	37.2939	-93.3142	Ozark Highlands	Eutrophic	5.4	14.6	1.0	5.583	100.5	0.005622202	
	North	38.6861	-94.3583	Osage Plains	Eutrophic	1.9	8.5	0.2	3.345	5.1	0.000287401	
	Pomme de Terre	37.9017	-93.3200	Ozark Highlands	Mesotrophic	8.0	47.2	37.7	1.412	1514.8	0.299735640	

Shayne	37.8976	-90.6412	Ozark Highlands	Oligotrophic	10.3	21.9	0.3	0.246	2.1	0.003052863
Stockton	37.6917	-93.7667	Ozark Highlands	Mesotrophic	9.8	49.1	112.3	0.755	2974.2	1.100264160
Sugar Creek	39.4736	-92.4792	Glacial Plains	Eutrophic	4.9	14.9	1.3	0.844	28.7	0.006475770
Table Rock	36.5950	-93.3108	Ozark Highlands	Mesotrophic	20.6	76.8	161.5	0.459	4852.7	3.332862960
Viking	39.9378	-94.0569	Glacial Plains	Mesotrophic	6.5	25.9	2.1	0.383	36.5	0.013568280
Wappapello	36.9311	-90.2806	Ozark Highlands	Eutrophic	2.3	12.8	32.5	19.201	3363.3	0.075636994
Watkins Mill	39.3933	-94.2631	Glacial Plains	Eutrophic	7.3	15.8	0.4	0.370	7.8	0.003207048

---

**Table 4.2:** Regime shifts in Secchi disk depth for invaded and reference reservoirs. The year that a regime shift occurs is identified. When no regime shift occurs in a reservoir, “none” is listed, and when more than one regime shift occurs in a reservoir, multiple years are listed. The number of years is the mean of all years within each period, and the Mann-Kendall p-value indicates whether a significant monotonic trend occurred within a period before and/or after a regime shift, or when no regime shift occurred, the entire data series. When sample size is less than 3, as indicated by “†”, no mean Secchi disk depth nor Mann-Kendall p-value are shown. As an example, Lake of the Ozarks displayed regime shifts in 1986 and 2007. The number of years (10), mean Secchi disk depth of 1.38, and Mann-Kendall p-value of 0.59 correspond with the period before 1986. The sample size of 21, mean Secchi disk depth of 1.65, and Mann-Kendall p-value of 0.65 correspond with the period from 1986 to 2006, and the sample size of 13, mean Secchi disk depth of 1.25, and the Mann-Kendall p-value of 0.08 correspond with the period from 2007 to 2019. When a significant monotonic trend is identified (Mann-Kendall <0.05, “\*”), the Sen’s slope value identifies the direction and magnitude of the trend.

	<b>Reservoir</b>	<b>Invasion Year</b>	<b>Regime Shift Year(s)</b>	<b>Number of Years</b>	<b>Mean Secchi Disk Depth (m)</b>	<b>Mann-Kendall p-value</b>	<b>Sen’s Slope (m yr<sup>-1</sup>)</b>
Zebra Mussel Reservoirs	Blue Springs	2014	none	27	1.12	0.05*	0.01
	Bull Shoals site 1	2006	1996, 2012†	9, 10, 1	2.41, 4.07	0.40, 0.59	-
	Bull Shoals site 2	2006	2019†	16, 1	3.14	0.69	-
	Jacomo	2014	none	29	1.24	0.08	-
	Lake of the Ozarks	1999	1986, 2007	10, 21, 13	1.38, 1.65, 1.25	0.59, 0.65, 0.08	-
	Lotawana	2006	none	22	1.42	0.48	-
	Smithville	2007	2016	30, 4	1.01, 0.81	1, 0.09	-
	Truman	2011	none	34	1.21	0.64	-
Reference Reservoirs	Atkinson	n/a	2018†	29, 1	0.52	0.28	-
	Binder	n/a	1996	10, 23	1.11, 0.80	0.06, 0.05*	-0.01
	Bowling Green	n/a	2006	18, 14	1.95, 1.53	0.16, 0.51	-
	Brookfield	n/a	none	32	1.29	0.53	-
	Capri	n/a	2000	14, 20	4.23, 5.07	0.23, 0.45	-
	Clearwater	n/a	2008	22, 12	1.91, 1.49	0.23, 0.37	-
	Council Bluff	n/a	2019†	30, 1	3.42	0.09	-
	Deer Ridge	n/a	none	32	1.03	0.60	-
	Fellows	n/a	2019†	27, 1	2.77	0.56	-

---

Forest	n/a	2008, 2019 <sup>†</sup>	21, 11, 1	1.39, 1.02	1, 0.04*	0.04
Higginsville	n/a	2015	26, 5	0.64, 0.46	0.08, 0.81	-
Hunnewell	n/a	2003, 2011	15, 8, 9	0.90, 1.28, 0.96	0.20, 0.90, 0.47	-
Kraut Run	n/a	none	26	0.48	0.71	-
Lincoln	n/a	none	33	2.23	1	-
Long Branch	n/a	1992	10, 27	0.85, 0.64	1, 0.36	-
Mark Twain	n/a	none	32	1.00	0.60	-
McDaniel	n/a	2013	22, 3	1.31, 1.75	0.27, 0.30	-
North	n/a	2019 <sup>†</sup>	30, 1	0.68	0.13	-
Pomme de Terre	n/a	2008, 2019 <sup>†</sup>	23, 11, 1	1.80, 1.23	0.56, 0.21	-
Shayne	n/a	2009	19, 11	3.00, 4.09	0.75, 1	-
Stockton	n/a	2008	23, 12	2.94, 1.96	0.40, 0.84	-
Sugar Creek	n/a	none	34	0.82	0.43	-
Table Rock	n/a	1991, 2019 <sup>†</sup>	7, 28, 1	3.79, 2.19	0.23, 0.40	-
Viking	n/a	2012	24, 4	1.35, 1.79	0.14, 0.09	-
Wappapello	n/a	1999	13, 21	1.00, 0.78	0.67, 0.61	-
Watkins Mill	n/a	2018 <sup>†</sup>	28, 2	0.87	0.48	-

---

<sup>†</sup>Indicates that a regime shift was identified in the last 3 years of recorded data. No Mann-Kendall p-value is provided for these dates because this test requires a minimum of 3 values

**Table 4.3:** Regime shifts in total suspended solids (TSS) for invaded and reference reservoirs. The year that a regime shift occurs is identified. When no regime shift occurs in a reservoir, “none” is listed, and when more than one regime shift occurs in a reservoir, multiple years are listed. The number of years is the mean of all years within each period, and the Mann-Kendall p-value indicates whether a significant monotonic trend occurred within a period before and/or after a regime shift, or when no regime shift occurred, the entire data series. When sample size is less than 3, as indicated by “†”, no mean TSS nor Mann-Kendall p-value are. As an example, Lake of the Ozarks displayed regime shifts in 2007 and 2018. The number of years (28), mean TSS of 5.89, and Mann-Kendall p-value of 0.02 correspond with the period before 2007. The sample size of 11, mean TSS of 7.74, and Mann-Kendall p-value of 1 correspond with the period from 2007 to 2017. No mean TSS and Mann-Kendall p-value are reported for the period after 2017 because the sample size for this period is less than 3. When a significant monotonic trend is identified (Mann-Kendall <0.05, “\*”), the Sen’s slope value identifies the direction and magnitude of the trend. In the previous Lake of the Ozarks example, a Sen’s slope calculation was performed on the period before 2007, and a -0.09 mg L<sup>-1</sup> yr<sup>-1</sup> slope was identified.

	<b>Reservoir</b>	<b>Invasion Year</b>	<b>Regime Shift Year(s)</b>	<b>Number of Years</b>	<b>Mean TSS (mg L<sup>-1</sup>)</b>	<b>Mann-Kendall p-value</b>	<b>Sen’s Slope (mg L<sup>-1</sup> yr<sup>-1</sup>)</b>
Zebra Mussel Reservoirs	Blue Springs	2014	none	26	6.49	0.89	-
	Jacomo	2014	none	27	5.55	0.29	-
	Lake of the Ozarks	1999	2007, 2018†	28, 11, 2	5.89, 7.74	0.02*, 1	-0.09
	Lotawana	2006	2010, 2019†	11, 9, 1	5.79, 3.81	0.76, 0.25	-
	Smithville	2007	none	34	8.13	0.03*	0.07
	Truman	2011	2011	27, 7	6.60, 7.58	0.44, 0.55	-
Reference Reservoirs	Atkinson	n/a	2017†	28, 2	16.09	0.57	-
	Binder	n/a	2007, 2018†	20, 10, 2	7.92, 10.74	0.38, 0.86	-
	Bowling Green	n/a	1998, 2019†	10, 20, 1	4.86, 2.91	0.79, 0.87	-
	Brookfield	n/a	none	31	5.72	0.06	-
	Capri	n/a	2000	13, 20	1.60, 1.20	0.95, 0.47	-
	Clearwater	n/a	2005, 2018†	18, 11, 2	3.35, 7.02	0.82, 0.64	-
	Council Bluff	n/a	2018†	29, 2	1.56	0.42	-
	Deer Ridge	n/a	2010	21, 10	6.71, 9.90	0.01*, 0.15	-0.30
Fellows	n/a	2019†	27, 1	2.29	0.82	-	

Forest	n/a	2008, 2016	20, 8, 4	5.57, 11.49, 6.91	0.97, 0.39, 0.31	-
Higginsville	n/a	none	30	14.88	0.01*	0.24
Hunnewell	n/a	none	29	6.81	1	-
Kraut Run	n/a	none	26	16.66	0.52	-
Lincoln	n/a	none	32	3.43	0.05*	-0.03
Long Branch	n/a	none	36	10.58	0.61	-
Mark Twain	n/a	2019†	31, 1	6.94	0.68	-
McDaniel	n/a	2004, 2014†	13, 10, 2	4.64, 5.40	0.33, 0.47	-
North	n/a	2013	24, 7	11.87, 16.90	0.98, 1	-
Pomme de Terre	n/a	2008, 2014	22, 6, 6	3.79, 6.58, 5.04	0.45, 0.06, 1	-
Shayne	n/a	2019†	23, 1	2.03	0.26	-
Stockton	n/a	2008, 2015	22, 7, 5	2.83, 5.97, 9.34	0.35, 0.23, 0.09	-
Sugar Creek	n/a	none	31	9.84	0.93	-
Table Rock	n/a	none	23	2.24	0.63	-
Viking	n/a	none	27	5.73	0.02*	-0.10
Wappapello	n/a	2010	23, 9	9.05, 11.52	0.03*, 0.25	0.15
Watkins Mill	n/a	2018†	28, 2	8.25	0.40	-

†Indicates that a regime shift was identified in the last 3 years of recorded data. No Mann-Kendall  $p$ -value is provided for these dates because this test requires a minimum of 3 values

**Table 4.4:** Regime shifts in particulate inorganic matter (PIM) for invaded and reference reservoirs. The year that a regime shift occurs is identified. When no regime shift occurs in a reservoir, “none” is listed, and when more than one regime shift occurs in a reservoir, multiple years are listed. The number of years is the mean of all years within each period, and the Mann-Kendall p-value indicates whether a significant monotonic trend occurred within a period before and/or after a regime shift, or when no regime shift occurred, the entire data series. When sample size is less than 3, as indicated by “†”, no mean POM nor Mann-Kendall p-value are shown. As an example, Lake of the Ozarks does not display a regime shift in PIM. The number of years (41), mean PIM of 3.63, and Mann-Kendall p-value of 0.16 correspond with the entire period. When a significant monotonic trend is identified (Mann-Kendall <0.05, “\*”), the Sen’s slope value identifies the direction and magnitude of the trend.

	<b>Reservoir</b>	<b>Invasion Year</b>	<b>Regime Shift Year(s)</b>	<b>Number of Years</b>	<b>Mean PIM (mg L<sup>-1</sup>)</b>	<b>Mann-Kendall p-value</b>	<b>Sen’s Slope (mg L<sup>-1</sup> yr<sup>-1</sup>)</b>
Zebra Mussel Reservoirs	Blue Springs	2014	2014	22, 5	3.05, 2.33	0.16, 0.46	-
	Jacomo	2014	2001, 2019†	11, 16, 1	2.84, 1.66	0.88, 0.21	-
	Lake of the Ozarks	1999	none	41	3.63	0.16	-
	Lotawana	2006	2009	10, 11	3.02, 1.15	1, 0.01*	-0.06
	Smithville	2007	none	34	4.42	0.84	-
	Truman	2011	2011	27, 7	3.99, 4.15	0.32, 0.76	-
	Binder	n/a	2019†	31, 1	3.20	0.03*	-0.06

Bowling Green	n/a	none	32	1.68	0.01*	-0.04
Brookfield	n/a	2001, 2018†	13, 16, 2	3.99, 3.23	0.62, 0.30	-
Capri	n/a	none	33	0.60	0.01*	-0.01
Clearwater	n/a	2005, 2014	18, 9, 6	2.01, 4.25, 2.42	0.94, 0.18, 0.71	-
Council Bluff	n/a	none	31	0.68	0.45	-
Deer Ridge	n/a	2002	13, 18	4.83, 2.55	0.50, 0.26	-
Fellows	n/a	none	28	0.85	0.06	-
Forest	n/a	2008	20, 12	4.11, 6.71	0.72, 0.15	-
Higginsville	n/a	none	30	10.08	0.46	-
Hunnewell	n/a	2003, 2019†	14, 16, 1	3.82, 2.38	0.38, 0.26	-
Kraut Run	n/a	none	26	6.57	0.35	-
Lincoln	n/a	none	32	1.70	0.01*	-0.03
Long Branch	n/a	none	36	7.43	1	-
Mark Twain	n/a	none	32	4.22	0.59	-
McDaniel	n/a	2004, 2014†	13, 10, 2	1.56, 2.11	0.27, 0.37	-
North	n/a	2019†	30, 1	5.74	0.75	-
Pomme de Terre	n/a	2008, 2018†	22, 10, 2	1.20, 2.14	0.01*, 0.01*	-0.04, -0.22
Shayne	n/a	2008, 2018†	18, 10, 2	1.44, 0.71	0.45, 0.03*	-0.05
Stockton	n/a	2009, 2015	23, 6, 5	1.30, 3.00, 4.93	0.75, 1, 0.09	-
Sugar Creek	n/a	2014	26, 5	5.80, 4.59	0.19, 1	-
Table Rock	n/a	none	29	0.94	0.46	-
Viking	n/a	none	27	3.50	0.01*	-0.07
Wappapello	n/a	2009, 2019†	22, 10, 1	4.19, 6.01	0.40, 0.37	-
Watkins Mill	n/a	1997, 2018†	9, 19, 2	5.67, 4.15	0.60, 0.02*	0.10

†Indicates that a regime shift was identified in the last 3 years of recorded data. No Mann-Kendall  $p$ -value is provided for these dates because this test requires a minimum of 3 values

**Table 4.5:** Regime shifts in chlorophyll-*a* uncorrected for pheophytin (chl-*a*) for invaded and reference reservoirs. The year that a regime shift occurs is identified. When no regime shift occurs in a reservoir, “none” is listed, and when more than 1 regime shift occurs in a reservoir, multiple years are listed. The number of years is the mean of all years within each period, and the Mann-Kendall p-value indicates whether a significant monotonic trend occurred within a period before and/or after an regime shift, or when no regime shift occurred, the entire data series. When sample size is less than 3, as indicated by “†”, no mean chl-*a* nor Mann-Kendall p-value are shown. As an example, Lake of the Ozarks displayed regime shifts in 2007 and 2018. The number of years (31), mean chl-*a* of 15.58, and Mann-Kendall p-value of 0.03 correspond with the period before 2007. The sample size of 11, mean chl-*a* of 23.34, and Mann-Kendall p-value of 0.88 correspond with the period from 2007 to 2017. No mean chl-*a* and Mann-Kendall p-value are reported for the period after 2017 because the sample size for this period is less than 3. When a significant monotonic trend is identified (Mann-Kendall <0.05, “\*”), the Sen’s slope value identifies the direction and magnitude of the trend. In the previous Lake of the Ozarks example, a Sen’s slope calculation was performed on the period before 2007, and a 0.16  $\mu\text{g L}^{-1} \text{ yr}^{-1}$  slope was identified.

	<b>Reservoir</b>	<b>Invasion Year</b>	<b>Regime Shift Year(s)</b>	<b>Sample Size</b>	<b>Mean Chl-<i>a</i> (<math>\mu\text{g L}^{-1}</math>)</b>	<b>Mann-Kendall p-value</b>	<b>Sen’s Slope (<math>\mu\text{g L}^{-1} \text{ yr}^{-1}</math>)</b>
Zebra Mussel Reservoirs	Blue Springs	2014	2019†	20, 1	18.53	0.13	-
	Bull Shoals site 1	2006	none	12	3.68	0.45	-
	Bull Shoals site 2	2006	none	17	4.04	0.84	-
	Jacomo	2014	none	20	15.53	0.21	-
	Lake of the Ozarks	1999	2007	21, 13	14.46, 20.42	0.02*, 0.43	0.25
	Lotawana	2006	none	15	16.67	0.69	-
	Smithville	2007	2012	16, 8	18.35, 27.26	0.30, 0.54	-
	Truman	2011	2005, 2018†	9, 12, 1	13.64, 20.09	0.05*, 0.45	1.10
Reference Reservoirs	Atkinson	n/a	none	23	41.21	0.38	-
	Binder	n/a	2009, 2018†	13, 8, 2	28.42, 52.45	0.10, 1	-
	Bowling Green	n/a	none	24	6.53	0.73	-
	Brookfield	n/a	2011	13, 9	8.87, 5.77	1, 0.40	-
	Capri	n/a	none	24	1.58	0.01*	0.03
	Clearwater	n/a	none	24	6.27	0.33	-
	Council Bluff	n/a	2018†	22, 2	2.22	0.05*	-0.04

Deer Ridge	n/a	2009, 2018†	11, 9, 2	13.22, 39.99	0.88, 0.75	-
Fellows	n/a	none	21	4.68	0.86	-
Forest	n/a	2006, 2016	7, 10, 4	4.22, 9.03, 5.67	0.37, 0.86, 1	-
Higginsville	n/a	2010, 2019†	12, 9, 1	28.48, 54.71	0.03*, 0.47	2.12
Hunnewell	n/a	2012	14, 8	17.69, 27.44	0.08, 0.06	-
Kraut Run	n/a	2004	8, 11	48.59, 82.19	0.06, 0.76	-
Lincoln	n/a	none	23	4.55	0.46	-
Long Branch	n/a	none	24	18.30	0.13	-
Mark Twain	n/a	none	21	17.11	0.83	-
McDaniel	n/a	2019†	21, 1	15.05	0.45	-
North	n/a	2015	19, 5	47.88, 81.69	0.09, 0.81	-
Pomme de Terre	n/a	2019†	23, 1	15.88	0.56	-
Shayne	n/a	2014	17, 6	1.22, 1.75	0.23, 0.13	-
Stockton	n/a	2008, 2019†	12, 11, 1	7.24, 19.12	0.45, 0.64	-
Sugar Creek	n/a	2019†	22, 1	23.96	0.26	-
Table Rock	n/a	2019†	23, 1	11.45	1	-
Viking	n/a	2015†	18, 1	7.96	1	-
Wappapello	n/a	none	24	29.85,	0.08	-
Watkins Mill	n/a	2018†	20, 2	18.99	0.09	-

†Indicates that a regime shift was identified in the last 3 years of recorded data. No Mann-Kendall  $p$ -value is provided for these dates because this test requires a minimum of 3 values

**Table 4.6:** Zebra mussel density and biomass from 4 invaded Missouri reservoirs. Density (individuals m<sup>-2</sup>) and biomass (live weight, g m<sup>-2</sup>) are means of all sampling sites within each reservoir. Standard error is also reported. Mussels were collected in the summer of 2019.

<b>Invaded Reservoir</b>	<b>Number of Sampling Sites</b>	<b>Density (mussels m<sup>-2</sup>)</b>	<b>Biomass (g m<sup>-2</sup>)</b>
Bull Shoals	58	1.75 ± 1.07	2.28 ± 1.54
Lake of the Ozarks	58	64.72 ± 32.42	6.69 ± 2.83
Lotawana	11	2.34 ± 1.77	0.20 ± 0.14
Smithville	36	25.76 ± 14.92	10.10 ± 10.10

**Table 4.7:** Parameters considered for habitat suitability using a principal component analysis (PCA). The top number is the mean for each reservoir, while the bottom number in parentheses is the range (min-max). Temperature and dissolved oxygen (DO) are means of the epilimnion, while total suspended solids (TSS) and particulate inorganic matter (PIM) were measured from surface water samples. We report ratio of PIM to POM as a natural log,  $\ln(\text{PIM})/\ln(\text{POM})$ , to reduce bias associated with calculating the mean from ratios. Anoxia depth is the depth at which DO concentrations are below 1 mg L<sup>-1</sup>. For Bull Shoals, only site 1 was included in the habitat suitability analysis because no temperature nor dissolved oxygen data exists for Bull Shoals site 2.

Reservoir	Mixing Depth (m)	Epilimnetic Temperature (°C)	Epilimnetic DO (mg L <sup>-1</sup> )	Anoxia Depth (m)	TSS (mg L <sup>-1</sup> )	PIM (mg L <sup>-1</sup> )	PIM:POM
Bull Shoals site 1	5.18 (4.13–6.13)	27.30 (24.05–31.07)	8.3 (7.3–9.4)	8.44 (8.00–9.33)	3.32 (2.77–4.13)	1.45 (0.63–2.13)	-0.44 (-1.41–0.21)
Jacomo	3.81 (2.89–5.05)	26.11 (23.24–29.55)	8.1 (7.4–8.8)	6.15 (5.00–7.00)	5.55 (2.50–9.87)	2.15 (1.10–4.48)	-0.51 (-1.40–0.08)
Lotawana	4.23 (3.11–6.15)	25.96 (22.72–29.33)	7.7 (5.5–8.7)	6.43 (6.00–7.125)	4.72 (1.19–8.40)	2.04 (0.66–6.30)	-0.46 (-1.54–1.03)
Lake of the Ozarks	7.75 (2.00–14.61)	25.88 (21.61–29.68)	7.4 (3.8–13.2)	11.79 (6.00–23.50)	6.37 (3.50–11.89)	3.63 (1.35–8.55)	-0.68 (-1.77–0.50)
Smithville	5.35 (3.64–10.30)	25.73 (22.92–28.13)	7.7 (4.8–10.5)	7.71 (5.00–11.00)	8.13 (4.65–20.40)	4.42 (2.20–6.99)	0.25 (-0.48–1.12)
Truman	5.41 (1.01–8.21)	25.98 (21.27–29.31)	7.4 (4.7–11.5)	7.73 (5.00–9.67)	6.80 (3.60–13.68)	4.02 (1.43–10.13)	0.18 (-0.96–1.49)
Reference Reservoirs	Atkinson 1.82 (0.96–2.86)	27.85 (23.67–33.00)	7.4 (4.1–10.1)	3.57 (2.50–5.80)	15.71 (7.47–30.93)	9.14 (3.55–19.37)	0.26 (-0.84–1.07)
	Binder 2.65 (1.59–3.80)	26.14 (23.79–28.81)	7.4 (4.1–9.5)	3.91 (3.13–5.00)	8.85 (4.00–15.70)	3.14 (1.05–10.47)	-0.70 (-2.37–1.07)

Bowling Green	2.35 (1.48–5.51)	25.16 (22.8–28.9)	7.5 (4.8–10.2)	6.35 (3.38–14.50)	3.55 (1.55–12.20)	1.68 (0.55–8.43)	-0.37 (-1.33–0.81)
Brookfield	3.07 (2.14–4.27)	25.30 (21.56–27.66)	7.6 (5.3–10.2)	5.46 (4.33–7.50)	5.66 (2.77–9.07)	3.59 (1.53–5.83)	0.56 (-0.03–1.16)
Capri	4.57 (2.75–5.95)	25.58 (23.26–28.09)	7.9 (5.2–10.8)	15.01 (8.00–20.00)	1.36 (0.80–2.90)	0.60 (0.20–1.80)	-0.38 (-1.40–1.30)
Clearwater	3.73 (1.50–5.79)	26.82 (21.44–30.12)	8.2 (4.9–11.9)	6.87 (4.00–9.00)	4.32 (2.27–9.10)	2.74 (1.13–6.77)	0.38 (-0.55–0.85)
Council Bluff	3.43 (1.38–5.39)	25.73 (21.21–30.94)	7.5 (4.9–10.0)	10.02 (4.50–20.00)	1.47 (0.88–2.15)	0.68 (0.33–1.20)	-0.31 (-1.12–0.57)
Deer Ridge	1.57 (1.10–2.30)	26.43 (22.67–31.20)	7.4 (4.9–10.6)	3.28 (2.25–5.63)	7.74 (2.57–12.73)	3.51 (0.74–8.67)	-0.40 (-1.51–0.80)
Fellows	3.99 (2.50–5.51)	26.04 (22.79–29.58)	8.1 (5.1–10.8)	9.44 (5.00–14.00)	2.37 (1.63–3.27)	0.91 (0.33–1.60)	-0.60 (-1.81–0.00)
Forest	2.91 (1.97–4.16)	25.50 (21.63–29.72)	7.7 (5.1–9.7)	5.96 (4.50–7.33)	6.89 (2.90–14.40)	5.08 (1.80–11.63)	0.94 (0.15–1.98)
Higginsville	2.34 (1.08–3.75)	26.40 (20.52–30.67)	6.9 (2.2–11.4)	3.83 (2.50–6.00)	15.44 (7.83–50.60)	10.08 (4.63–41.67)	0.54 (-0.56–1.77)
Hunnewell	2.24 (1.54–3.44)	25.88 (22.43–29.08)	8.0 (4.9–11.1)	3.95 (3.00–4.75)	6.77 (3.34–11.38)	3.07 (0.93–5.25)	-0.21 (-1.09–0.83)
Kraut Run	1.76 (0.50–2.44)	27.56 (24.18–30.54)	7.9 (4.4–11.3)	3.13 (2.50–4.00)	16.85 (10.80–28.57)	6.57 (3.43–19.63)	-0.53 (-1.23–0.41)
Lincoln	2.05 (1.24–3.44)	26.29 (22.41–29.03)	7.6 (4.7–10.4)	5.63 (2.17–10.33)	3.28 (1.58–17.83)	1.70 (0.50–13.17)	-0.23 (-1.05–1.02)
Long Branch	3.77 (0.77–6.37)	24.98 (19.96–29.79)	7.1 (5.0–10.8)	6.59 (4.83–9.25)	10.58 (4.05–32.62)	7.42 (2.60–22.60)	0.76 (-0.36–1.73)
Mark Twain	4.09 (1.35–6.45)	25.45 (22.0–28.77)	7.6 (4.8–11.5)	8.89 (4.00–14.50)	6.99 (3.10–15.80)	4.22 (1.00–13.20)	0.20 (-0.93–1.60)

McDaniel	2.54 (1.13–3.50)	26.42 (22.72–29.26)	8.0 (4.6–12.9)	5.45 (3.00–28.00)	4.96 (2.58–7.50)	1.81 (0.45–3.63)	-0.67 (-1.75–0.09)
North	1.90 (1.27–2.87)	26.42 (22.49–29.04)	7.4 (4.1–11.0)	3.27 (2.50–4.50)	13.01 (4.87–21.73)	5.84 (2.37–14.55)	-0.33 (-1.46–0.73)
Pomme de Terre	5.00 (2.77–7.70)	26.79 (23.54–29.75)	8.0 (4.9–11.9)	8.15 (5.33–12.00)	4.50 (2.70–8.13)	1.48 (0.59–3.82)	-0.86 (-1.57–0.02)
Shayne	3.41 (2.20–4.77)	26.38 (23.58–29.25)	7.7 (5.0–10.2)	13.00 (9.50–16.00)	1.92 (0.98–3.13)	1.18 (0.35–2.30)	0.33 (-1.57–1.15)
Stockton	6.98 (4.43–9.39)	26.21 (22.66–29.50)	8.4 (5.6–10.8)	11.18 (7.25–15.75)	4.43 (1.55–11.89)	2.13 (0.53–6.61)	-0.35 (-1.26–0.81)
Sugar Creek	2.38 (1.14–3.95)	26.11 (22.59–31.58)	8.6 (7.9–10.4)	5.14 (3.70–7.00)	9.84 (7.23–13.80)	5.57 (3.90–7.62)	0.25 (-0.22–0.95)
Table Rock	5.52 (2.50–7.05)	26.64 (20.78–30.59)	8.9 (6.4–11.4)	9.30 (6.75–12.00)	2.31 (0.96–4.70)	0.94 (0.23–2.93)	-0.51 (-2.46–1.01)
Viking	6.13 (1.85–27.35)	24.77 (8.05–29.00)	7.2 (5.0–9.2)	6.85 (4.50–10.00)	5.41 (3.03–10.20)	3.50 (1.90–7.60)	0.56 (-0.30–1.10)
Wappapello	2.26 (0.75–4.83)	27.52 (24.00–31.20)	8.3 (4.4–12.8)	4.60 (2.50–8.50)	9.80 (3.77–15.80)	4.70 (1.73–8.70)	-0.09 (-0.75–0.67)
Watkins Mill	2.59 (1.03–3.99)	26.09 (20.78–29.47)	7.5 (5.5–9.8)	4.35 (3.00–8.00)	8.02 (4.40–12.28)	4.47 (1.50–8.63)	0.17 (-0.61–0.89)

## FIGURES

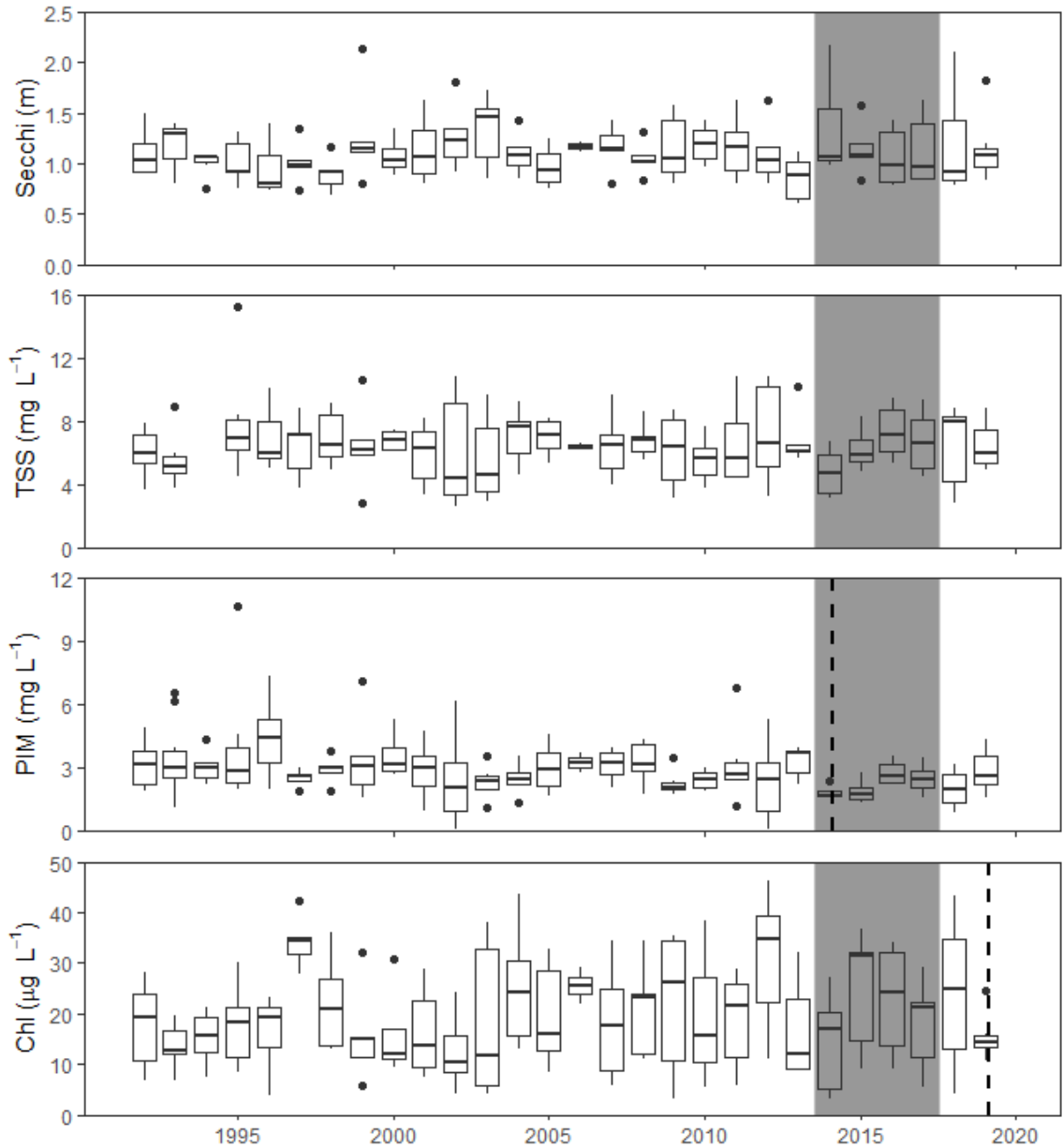
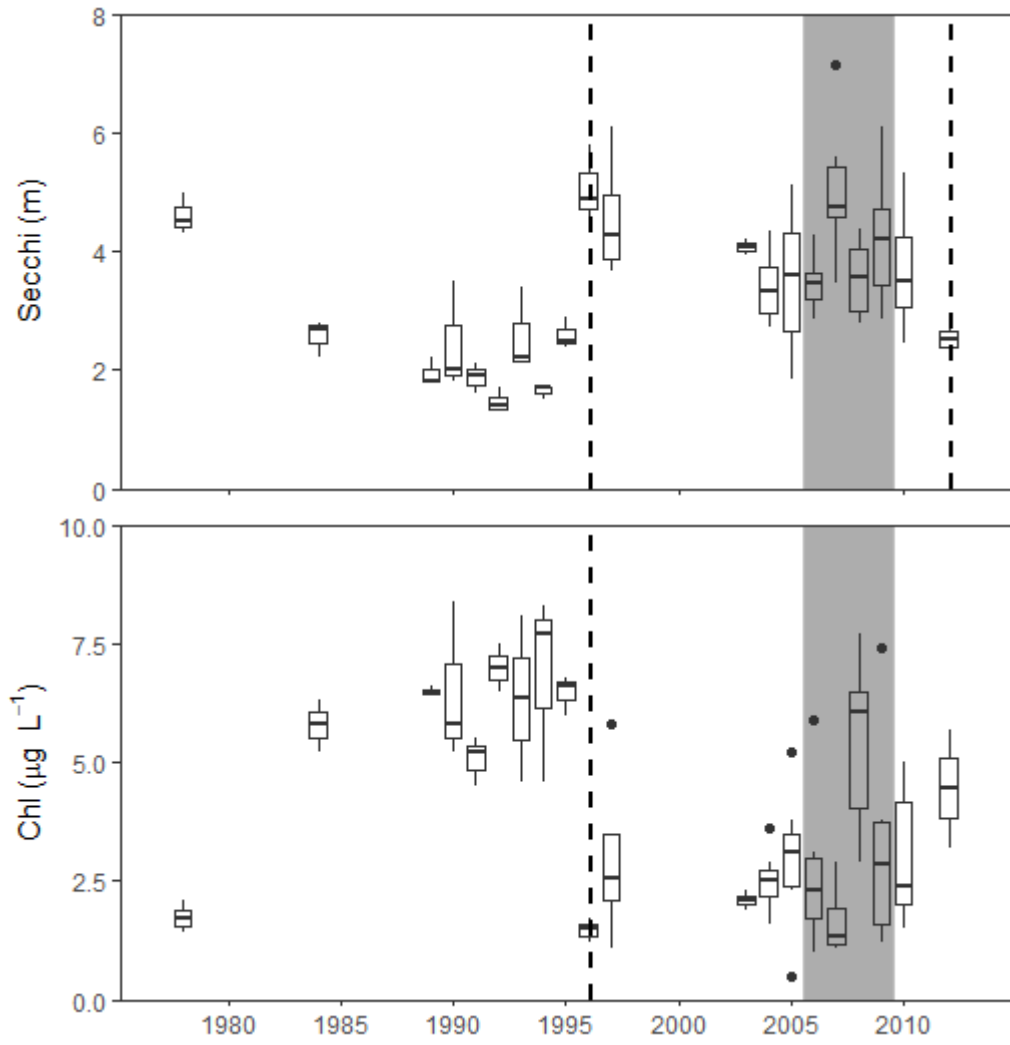


**Figure 4.1:** Boxplots showing parameters of water clarity for Blue Springs Reservoir. The box shows the 25–75% quartile with median bar, while the upper (lower) lines show the highest (lowest) values that are not considered outliers, which are indicated by black circles. Secchi disk depth (Secchi), total suspended solids (TSS), particulate inorganic matter (PIM), and chlorophyll-*a* uncorrected for pheophytin (chl-*a*) are shown. Vertical, dashed lines indicate where a regime shift was identified. Gray shading show the probable invasion period for zebra mussels, with the right edge of the box indicating the year when zebra mussels were first observed.

A)



B)

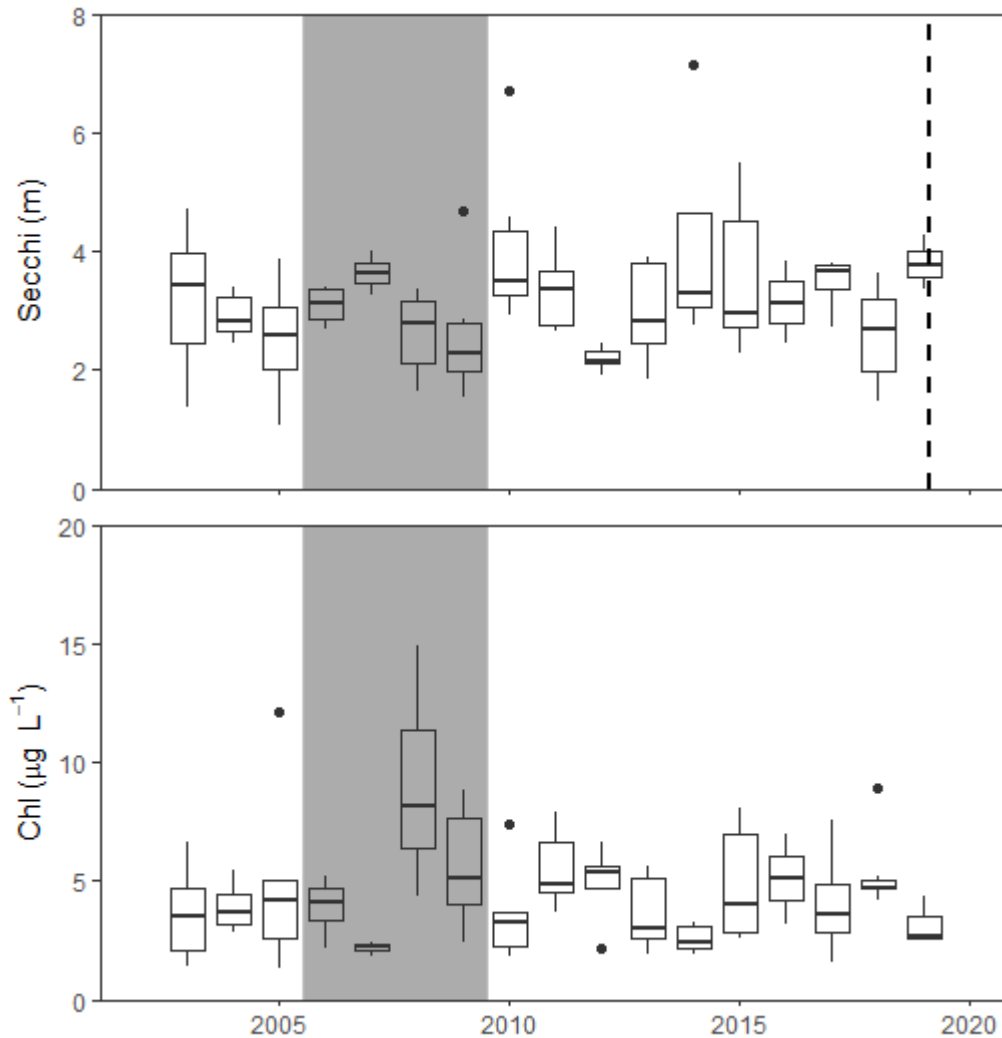


**Figure 4.2:** Boxplots showing parameters of water clarity at 2 sites in Bull Shoals Reservoir. The box shows the 25–75% quartile with median bar, while the upper (lower) lines show the highest (lowest) values that are not considered outliers which are indicated by black circles. Monitoring at site 1 (A), which is closer to the dam than site 2 (B), ended in 2012. Secchi disk depth (Secchi), and chlorophyll-*a* uncorrected for pheophytin (chl-*a*) are shown. Vertical, dashed lines indicate where a regime shift was identified. Gray boxes show the probable invasion period for zebra mussels, with the right edge of the box indicating the year when zebra mussels were first observed.

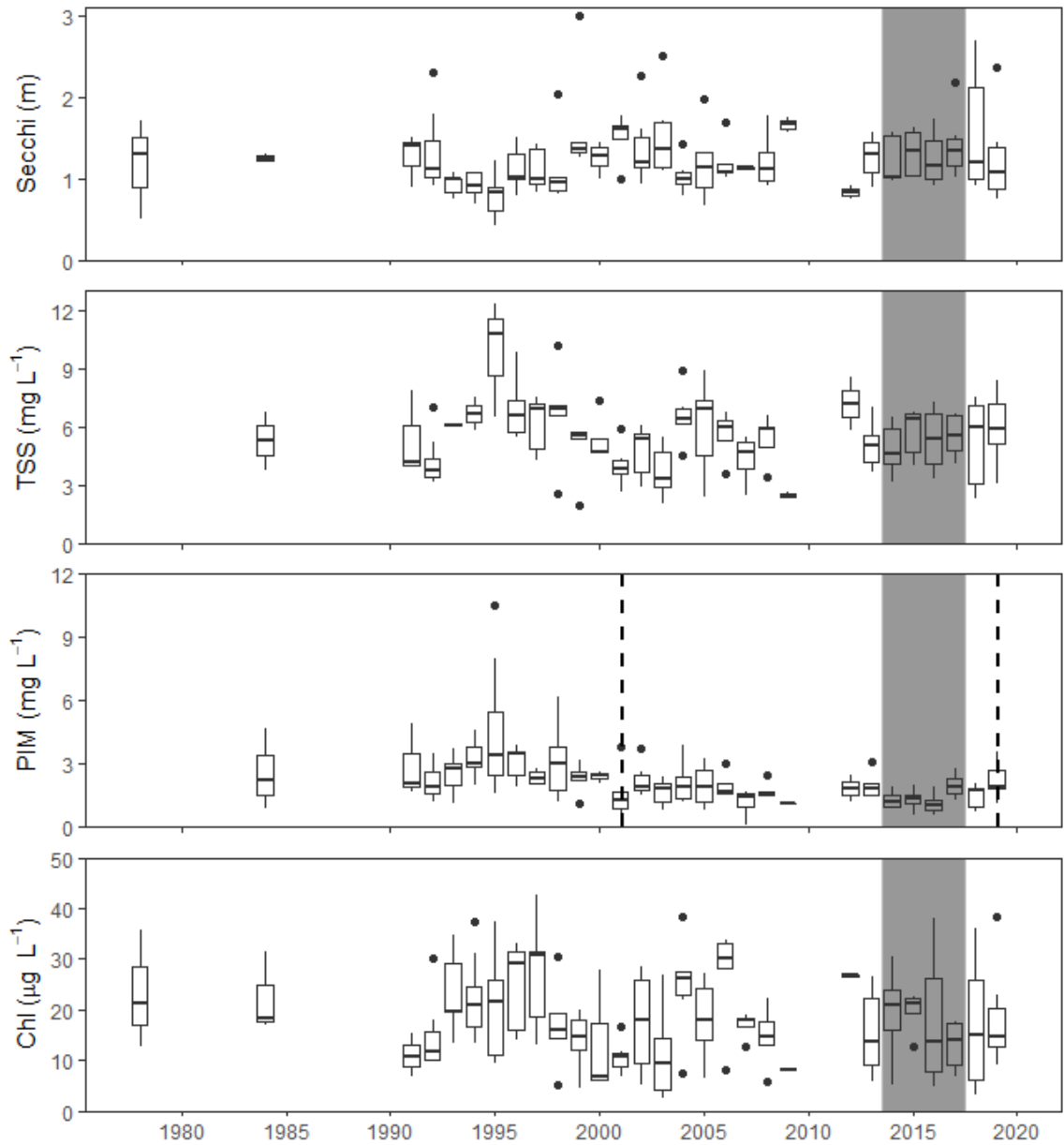


**Figure 4.3:** Boxplots showing parameters of water clarity in Jacomo Reservoir. The box shows the 25–75% quartile with median bar, while the upper (lower) lines show the highest (lowest) values that are not considered outliers. Secchi disk depth (Secchi), total suspended solids (TSS), particulate inorganic matter (PIM), and chlorophyll-*a* uncorrected for pheophytin (chl-*a*) are shown. Vertical, dashed lines indicate where a regime shift was identified. Gray boxes show the probable invasion period for zebra mussels, with the right edge of the box indicating the year when zebra mussels were first observed.

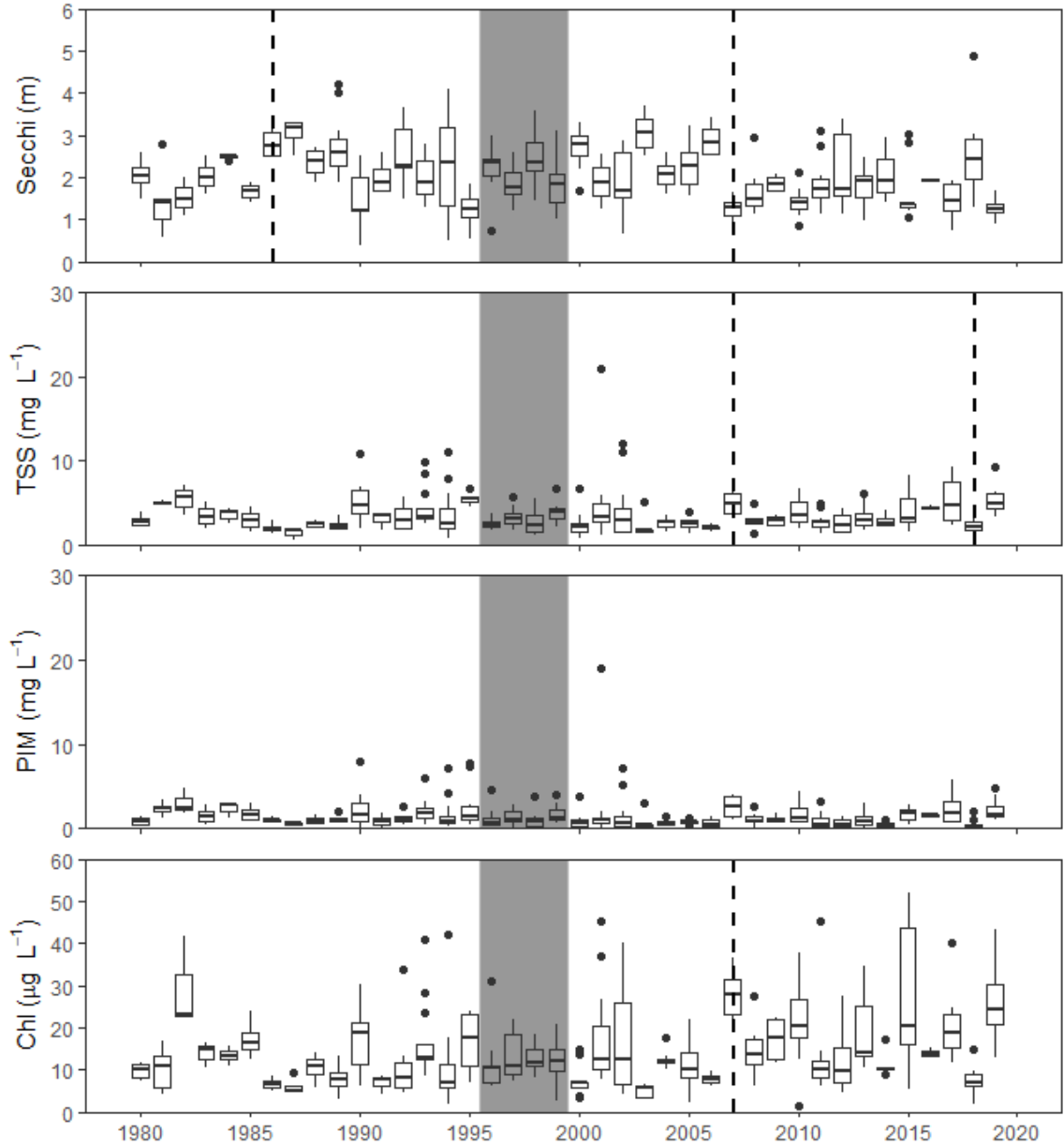


**Figure 4.4:** Boxplots showing parameters of water clarity in Lake of the Ozarks. The box shows the 25–75% quartile with median bar, while the upper (lower) lines show the highest (lowest) values that are not considered outliers, which are indicated by black circles. Secchi disk depth (Secchi), total suspended solids (TSS), particulate inorganic matter (PIM), and chlorophyll-*a* uncorrected for pheophytin (*chl-a*) are shown. Vertical, dashed lines indicate where a regime shift was identified. Gray boxes show the probable invasion period for zebra mussels, with the right edge of the box indicating the year when zebra mussels were first observed.

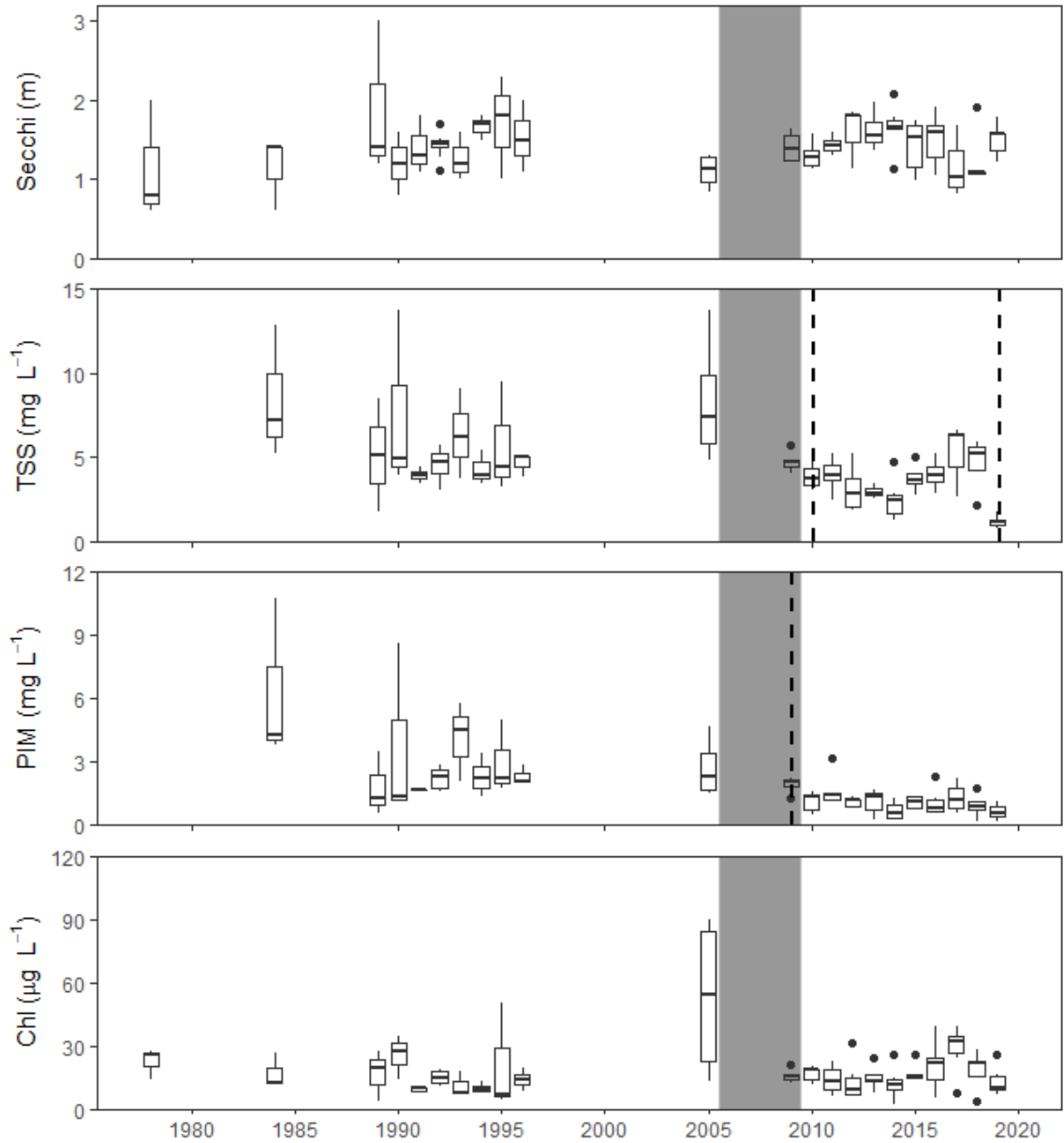


**Figure 4.5:** Boxplots showing parameters of water clarity in Lotawana Reservoir. The box shows the 25–75% quartile with median bar, while the upper (lower) lines show the highest (lowest) values that are not considered outliers, which are indicated by black circles. Secchi disk depth (Secchi), total suspended solids (TSS), particulate inorganic matter (PIM), and chlorophyll-*a* uncorrected for pheophytin (*chl-a*) are shown. Vertical, dashed lines indicate where a regime shift was identified. Gray boxes show the probable invasion period for zebra mussels, with the right edge of the box indicating the year when zebra mussels were first observed.

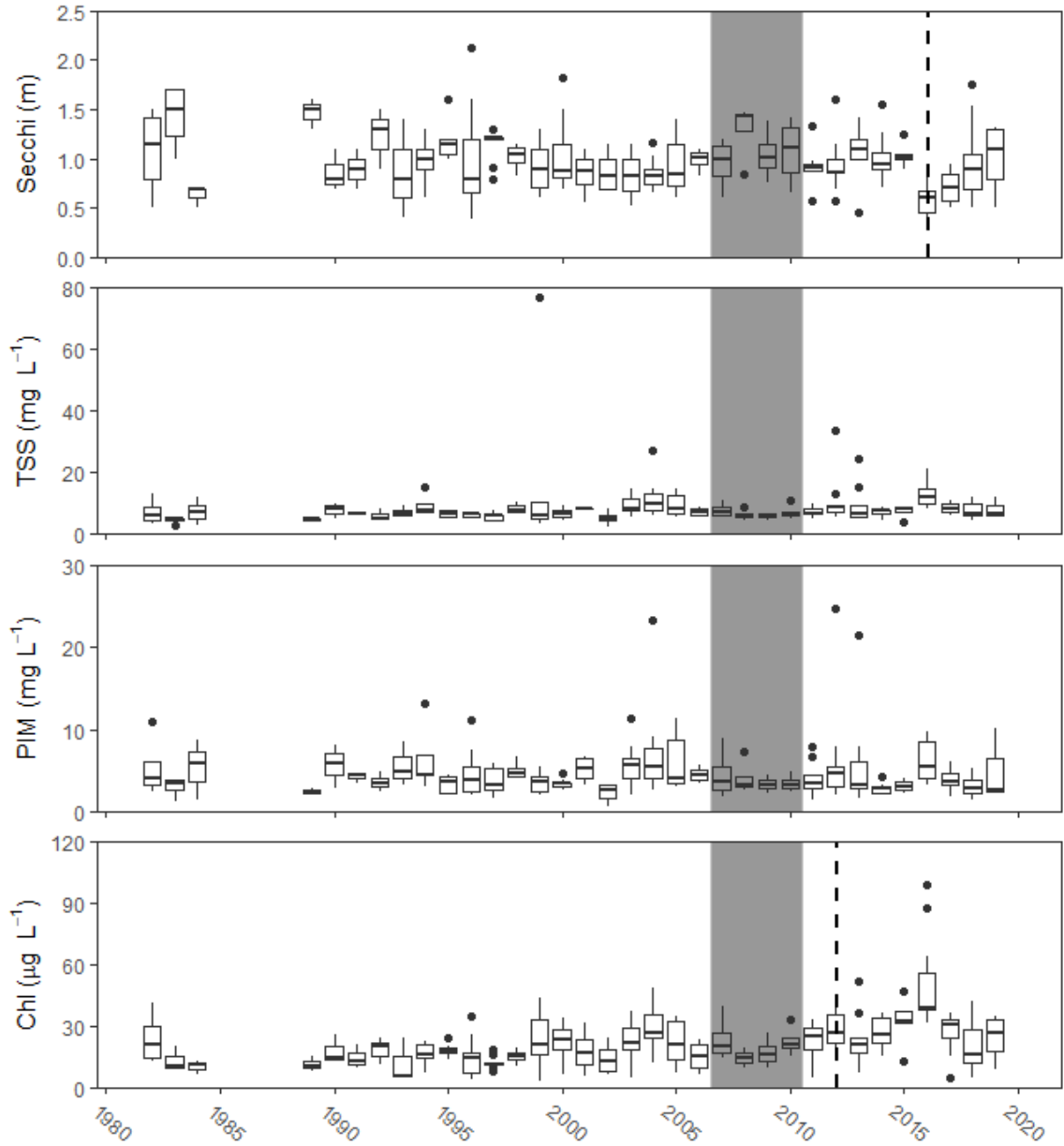


**Figure 4.6:** Boxplots showing parameters of water clarity in Smithville Reservoir. The box shows the 25–75% quartile with median bar, while the upper (lower) lines show the highest (lowest) values that are not considered outliers, which are indicated by black circles. Secchi disk depth (Secchi), total suspended solids (TSS), particulate inorganic matter (PIM), and chlorophyll-*a* uncorrected for pheophytin (chl-*a*) are shown. Vertical, dashed lines indicate where a regime shift was identified. Gray boxes show the probable invasion period for zebra mussels, with the right edge of the box indicating the year when zebra mussels were first observed.

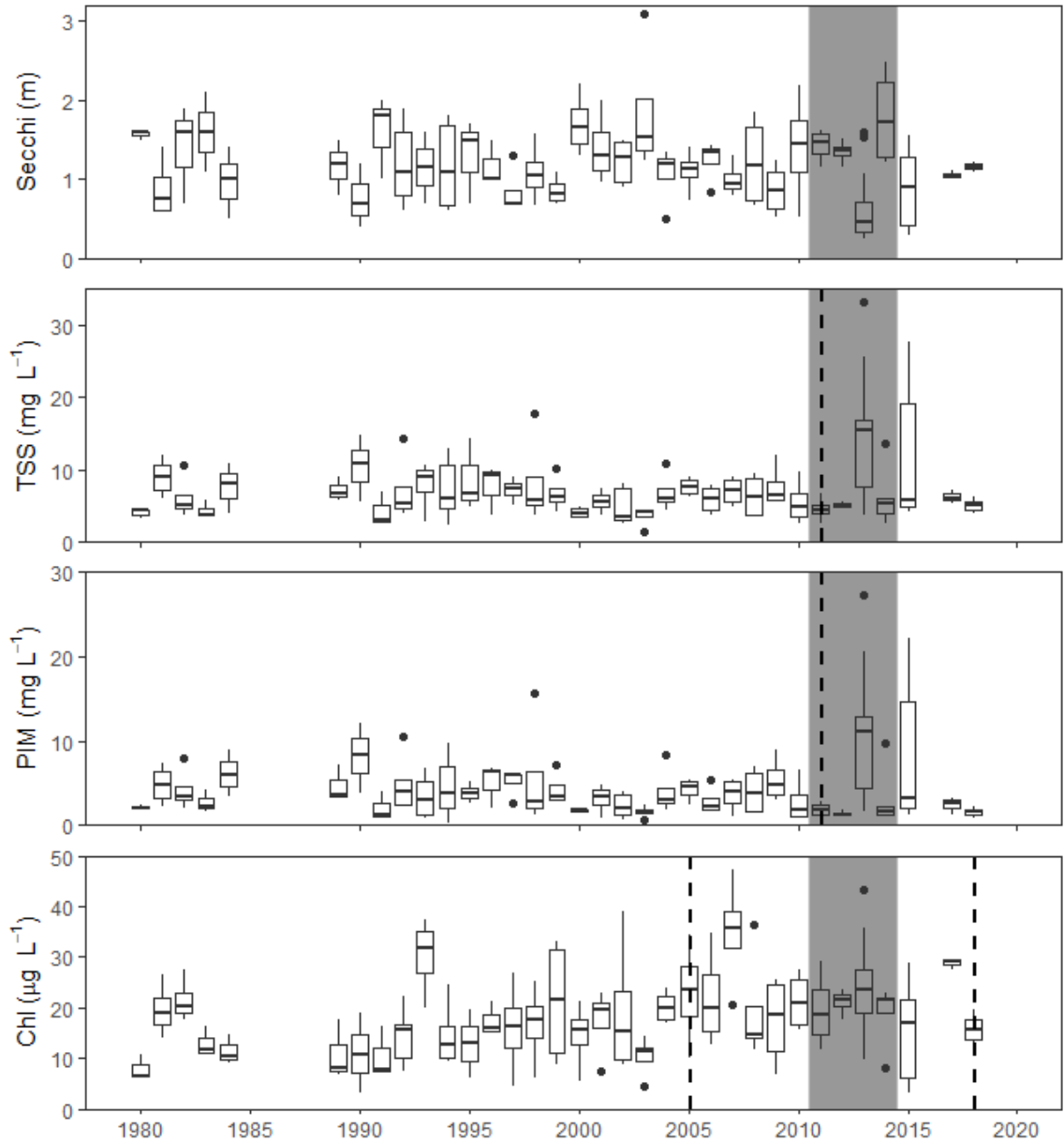


**Figure 4.7:** Boxplots showing parameters of water clarity in Truman Reservoir. The box shows the 25–75% quartile with median bar, while the upper (lower) lines show the highest (lowest) values that are not considered outliers, which are indicated by black circles. Secchi disk depth (Secchi), total suspended solids (TSS), particulate inorganic matter (PIM), and chlorophyll-*a* uncorrected for pheophytin (*chl-a*) are shown. Vertical, dashed lines indicate where a regime shift was identified. Gray boxes show the probable invasion period for zebra mussels, with the right edge of the box indicating the year when zebra mussels were first observed.

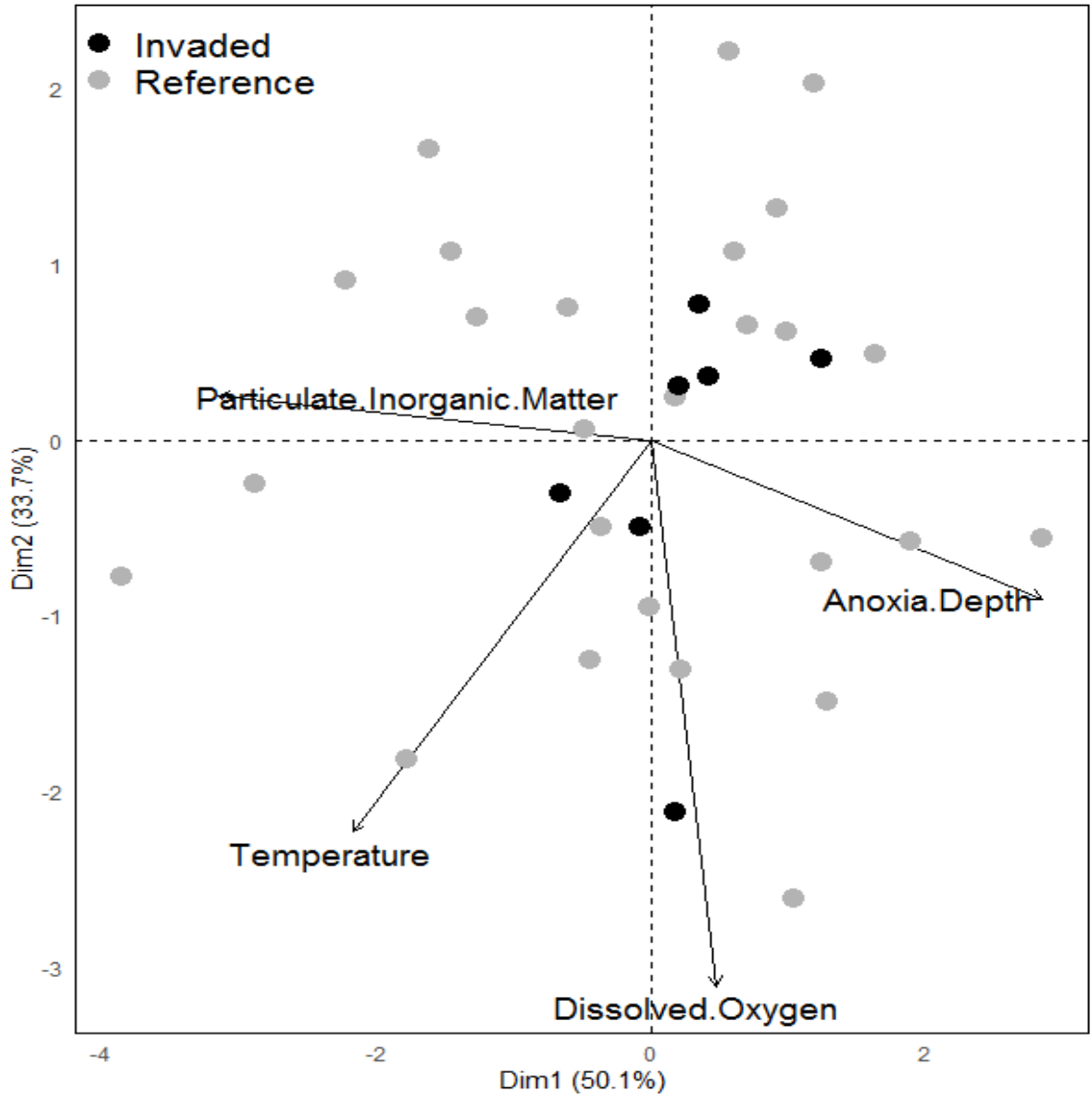


**Figure 4.8:** Correlation-based principal component analysis (PCA) biplot. The first principal component explains 50.1 % of the variation in this dataset, while the second component explains 33.7 %. Vectors represent environmental parameters that could influence zebra mussel survival and density. Vector length reflects the amount of variance in the dataset explained by each environmental parameter. Dissolved oxygen and temperature were measured in the epilimnion, while particulate inorganic matter measurements were made in surface water. Anoxia depth is the depth where dissolved oxygen measurements drop below 1 mg L<sup>-1</sup>. Each point represents mean long-term conditions in each study reservoir. Bull Shoals site 2 is not depicted because it lacks dissolved oxygen, temperature, mixing depth, and anoxia depth data. Reservoirs that have been invaded by zebra mussels are indicated by black circles while reservoirs with no known zebra mussels are shown with grey circles.

## CHAPTER 5

### EXECUTIVE SUMMARY

Freshwater ecosystems are under threat now more than ever. Anthropogenically derived stressors have resulted in greater biodiversity losses in freshwater compared to marine and terrestrial environments (Collen et al., 2009). As we proceed further into the 21<sup>st</sup> century, threats to water quality will include traditional issues like pollution, changes in land use, harmful cyanobacterial blooms, regulated flow regimes, the introduction of invasive species, and climate change, but also emerging threats like microplastics and engineered nanomaterials (Dudgeon et al., 2019). The interactions between stressors also pose unique challenges that may not have occurred previously (Craig et al., 2017). Growing human populations will only increase the pressure to stressors resulting from these threats (Settele et al., 2014), especially as the availability of high quality freshwater resources declines (Vörösmarty et al., 2013). Two threats to freshwater systems, harmful cyanobacterial blooms and invasive zebra mussels (*Dreissena polymorpha*), are investigated in this dissertation.

Harmful cyanobacterial blooms have been increasing in frequency and magnitude in recent decades, largely from anthropogenically derived eutrophication and climate change (Paerl and Huisman, 2008; O'Neil et al., 2012; Huisman et al., 2018). Cyanobacterial blooms are unsightly and pose a health risk because of the secondary metabolites called cyanotoxins that they sometimes produce (Grosse et al., 2006). Due to cyanotoxins, freshwater resources are often closed to the public when blooms occur. Decreased property values, beach closures, interrupted drinking water facilities, and lost recreational opportunities put financial strain on local economies (Dodds et al., 2009;

Bingham et al., 2015; Carmichael and Boyer, 2016). Cyanobacterial blooms have resulted in wildlife mortality (Miller et al., 2010), livestock and pet deaths (Van Halderen et al., 1995; Backer et al., 2013), and human fatalities (Carmichael et al., 2001). For humans, routes of cyanotoxin exposure can be through swallowing small amounts of water while swimming (Lévesque et al., 2014), inhalation of cyanotoxin aerosols (Cheng et al., 2007), consumption of contaminated food items such as fish (Poste et al., 2011) or produce irrigated with contaminated water (Corbel et al., 2016). Due to the associated health risks of harmful cyanobacterial blooms, a lot of research has been conducted into ways to manage cyanobacteria in freshwater systems.

A variety of techniques and strategies exist for mitigating harmful cyanobacterial blooms and the cyanobacteria that are the primary freshwater cause of these blooms (Ibelings et al., 2016). Many of these focus on reducing external nutrient loading (Sharpley et al., 2000). These strategies can be effective over the long term, but there are instances when a quick reduction in cyanobacteria is required (Osgood, 2017). Nutrient reductions may also not be feasible in some areas, such as in the agriculturally dominated Midwest. In Chapter 2, we tested a novel geoengineering strategy designed to reduce cyanobacteria by limiting light availability. We applied a fine particulate called glacial rock flour to 11,000 L mesocosm tanks that were dominated by either cyanobacteria or chlorophytes. The glacial rock flour we used was composed of 70.7 % silt and 11.2 % clay, and a large portion of it remained floating or in suspension for 24 hours. After 9 consecutive days of glacial rock flour additions, we observed a 77.9 % decline in cyanobacteria in tanks that began the experiment with cyanobacteria dominated communities, and a 49.4 % decline in cyanobacteria in tanks that began the experiment

with chlorophyte dominated communities. Cyanobacteria were mostly replaced by cryptophytes, which are more nutritious and highly sought after by planktivores (Stemberger and Gilbert, 1985; Sarnelle, 1993). Cryptophytes are flagellated mixotrophs that can supplement their energetic and nutritional requirements through heterotrophy (Porter, 1988; Urabe et al., 2000) and have been found at high densities in other low-light environments such as perennially ice-covered Antarctic lakes (Marshall and Laybourn-Parry, 2002). Previously, cyanobacteria were viewed as the primary beneficiaries relative to other taxa in the phytoplankton community of reduced light availability (Brauer et al., 2012), but our study suggests that functional traits, like mixotrophy or possessing flagella, enable cryptophytes to thrive under low-light conditions. While glacial rock flour might not be a feasible management strategy in large systems due to the large quantity of glacial rock flour required for daily additions, our experiment demonstrated that light can be a viable management strategy for cyanobacteria even in the presence of high nutrient concentrations.

Cyanotoxins can accumulate in the tissues of aquatic organisms where they can then be transferred to higher trophic levels like fish, which can also be exposed to cyanotoxins dissolved in water (Smith and Haney, 2006; Sieroslawska et al., 2012). The accumulation of cyanotoxins in fish can pose a health risk for anglers who consume the fish they catch (Poste et al., 2011). In Chapter 3, we examined accumulation of the cyanotoxin microcystin in the fillets, livers and kidneys of 2 recreationally valuable sportfish, bluegill (*Lepomis macrochirus*) and largemouth bass (*Micropterus salmoides*). We measured water quality parameters, including microcystin in water, and microcystin in fish over a 12-month period to see if we could identify the factors driving microcystin

accumulation in fish tissues. We found that the date when fish were collected was the most important factor in determining microcystin in fish tissues. When date was removed, microcystin concentrations in the water were a significant predictor for all species and tissue type combinations, but often explained little of the variation in fish microcystin concentrations. Microcystin concentrations were highest in April and May for fillets and kidneys, before decreasing throughout the rest of the year. The higher microcystin concentrations we observed in spring could be due to some behavioral or physiological fish response to spawning, although this relationship requires further investigation. Our findings suggest that date when fish are caught could be an important factor in assessing microcystin in fish and might be an important consideration for managers setting consumption advisories. Of the 31 water parameters and fish characteristics that we examined besides fish harvest date, only water microcystin emerged as a significant predictor for more than a single model. Even then, the models it was part of contained low  $R^2$ -adj and did not explain much of the variation in fish microcystin. We did not find a proxy for microcystin in fillets, livers, and kidneys among fish characteristics and water parameters, suggesting that there is not a quick, easy indicator to assess which fish are safe to consume. Bluegill had significantly higher microcystin concentrations than did largemouth bass, which is consistent with literature showing that microcystin often decreases as trophic level increases (Ibelings et al., 2005). That we observed microcystin concentrations in fish throughout the study, even while microcystin in the water was never measured above  $0.95 \mu\text{g L}^{-1}$ , suggests that low but persistent exposure to microcystin can lead to accumulation in fish tissues. Based on the highest microcystin concentrations from a fillet in our study, and assuming daily

consumption over the course of several weeks, a child would have to consume 105.3 g and an adult would have to consume 789.5 g of fish every day to exceed microcystin consumption guidelines (Ibelings and Chorus, 2007). To the best of our knowledge, this is the first study to look at microcystin in fish from the Great Plains, and one of only a few studies that quantifies microcystin concentrations in the tissues of bluegill and largemouth bass.

Zebra mussels were first observed in North America in 1986 in Lake Erie (Carlton, 2008). Since then, they have spread as far west as California and as far south as Texas, although their current North American range is mostly confined to east of the Rocky Mountains (Benson et al., 2021). Throughout their current range, they have formed dense populations associated with a dramatic increase in water clarity, especially in the upper Midwest (Higgins and Vander Zanden, 2010). In Chapter 4, we looked at the effects of zebra mussels on water clarity along this filter feeder's southern extant. Zebra mussels were first observed in Missouri reservoirs in 2001 and since then, there has been no formal assessment of their effects on water clarity. In the 7 reservoirs we examined, we did not observe a consistent increase in water clarity corresponding with zebra mussel invasion that was greater than the interannual variability of these systems (Jones et al., 2020). In 3 of these reservoirs, our assessment was especially robust as we had at least 11 years pre- and post- invasion data. Zebra mussels are unable to maintain high densities in Missouri like they do at northern latitudes. Lower mussel densities mean that the collective filtering capacity of this filter feeder would not be as high. In 2019, we sampled zebra mussel densities in 4 invaded reservoirs. The highest densities we observed were 64.7 mussels m<sup>-2</sup>, much lower than in lakes in more northern latitudes,

where densities can be as high as 30,000 mussels  $\text{m}^{-2}$  (North et al., 2013). Densities may be lower in Missouri because numerous environmental parameters, including water temperature (McMahon, 1996), suspended inorganic solids (Lei et al., 1996), and dissolved oxygen concentrations (Karatayev et al., 1998) could all be near the limits of this species' tolerable range. Species survival declines as more parameters near its tolerable limits, causing that species increased physiological stress (Lockwood et al., 2013). We performed a habitat suitability assessment by comparing conditions in invaded and non-invaded reservoirs to see if we could detect any factors influencing zebra mussels. Low concentrations of particulate inorganic materials and cooler epilimnetic temperatures were characteristic of invaded reservoirs. While preliminary and requiring additional study, this analysis suggests that these parameters may be limiting zebra mussel densities in Missouri reservoirs. To the best of our knowledge, this is the first study to assess the impacts of zebra mussels in Missouri and its results will inform the potential impacts this invader will have as it continues to spread throughout North America.

This work investigates several aquatic threats and their relationship to light, including harmful cyanobacterial blooms, the transfer of cyanotoxins into fish, and invasive zebra mussels. As harmful cyanobacterial blooms continue to increase in frequency and magnitude, the need for a variety of mitigation strategies will be necessary to accommodate a variety of settings and situations (Ibelings et al., 2016). Reducing light availability, which has previously not received enough research, should be considered as cyanobacterial bloom management strategy in situations where a quick reduction in cyanobacterial biomass is necessary or it is not feasible to reduce external nutrient

loading (Osgood, 2017). Mitigating cyanobacterial blooms will help reduce cyanotoxins in the environment, but knowing how cyanotoxins accumulate throughout the food web will continue to be important to ensure the safety of humans and animals (Ibelings and Chorus, 2007). Zebra mussels, which are having dramatic impacts at more northern latitudes, are not increasing water clarity nor light penetration in Missouri. This could be because conditions in Missouri reservoirs are sub-optimal and prevent zebra mussels from achieving the densities, and reaching the collective filtering capacity, they have reached in areas where they have previously invaded (Higginds and Vander Zanden, 2010). Understanding how aquatic resources are impacted by threats helps managers prioritize scarce resources and assess how threats will affect other systems. As increasing human populations continue to put pressure on freshwater resources (Settele et al., 2014), maintaining high water quality for aquatic life and human use will continue as a primary challenge for scientists and managers.

The objective of this dissertation was to examine how changes in light influence phytoplankton. Our null hypothesis was that light does not control phytoplankton biomass and our alternative hypothesis was that light does control phytoplankton biomass independent of nutrient concentrations, water temperature, and grazing. In chapter 2, we showed that decreased light does lead to a reduction in algal biomass. Increased light availability, resulting from increased grazing by invasive zebra mussels, did not result in an impact to the phytoplankton community in chapter 3. In chapter 4, light contributed to the growth of cyanobacteria and subsequent microcystin production. We found that low but persistent concentrations of microcystin can result in accumulation in fish tissues.

## LITERATURE CITED

- Backer, L.C., J.H. Landsberg, M. Miller, K. Keel & T.K. Taylor, 2013. Canine cyanotoxin poisonings in the United States (1920s–2012): Review of suspected and confirmed cases from three data sources. *Toxins* 5:1597–1628.
- Benson, A.J., D. Raikow, J. Larson, A. Fusaro, A.K. Bogdanoff & A. Elgin, 2021, *Dreissena polymorpha* (Pallas, 1771): U.S. Geological Survey, <https://nas.er.usgs.gov/queries/FactSheet.aspx?speciesID=5>.
- Bingham, M., S.K. Sinha & F. Lupi, 2015. Economic benefits of reducing harmful algal blooms in Lake Erie: Environmental Consulting and Technology Inc., Technical Report.
- Brauer, V.S., M. Stomp & J. Huisman, 2012. The nutrient-load hypothesis: patterns of resource limitation and community structure driven by competition for nutrients and light. *American Naturalist* 179:721–740.
- Carlton, J.T., 2008. The zebra mussel *Dreissena polymorpha* found in North America in 1986 and 1987. *Journal of Great Lakes Research* 34:770–773.
- Carmichael, W.W., S.M. Azevedo, J.S. An, R.J. Molica, E.M. Jochimsen, S. Lau, K.L. Renhart, G.R. Shaw & G.K. Eaglesham, 2001. Human fatalities from cyanobacteria: chemical and biological evidence for cyanotoxins. *Environmental Health Perspectives* 109:663–668.
- Carmichael, W.W. & G.L. Boyer, 2016. Health impacts from cyanobacteria harmful algae blooms: Implications for the North American Great Lakes. *Harmful Algae* 54:194–212.
- Cheng, Y.S., Y. Zhou, C.M. Irvin, B. Kirkpatrick & L.C. Backer, 2007. Characterization of aerosols containing microcystin. *Marine Drugs* 5:136–150.
- Collen, B., J. Loh, S. Whitmee, L. McRae, R. Amin & J.E.M. Baillie, 2009. Monitoring change in vertebrate abundance: the Living Planet Index. *Conservation Biology* 23:317–327.
- Corbel, S., C. Mougín, S. Nélieu, G. Delarue & N. Bouaïcha, 2016. Evaluation of the transfer and the accumulation of microcystins in tomato (*Solanum lycopersicum* cultivar MicroTom) tissues using a cyanobacterial extract containing microcystins and the radiolabeled microcystin-LR (<sup>14</sup>C-MC-LR). *Science of The Total Environment* 541:1052–1058.
- Craig, L.S., J.D. Olden, A.H. Arthington, S. Entekin, C.P. Hawkins, J.J. Kelly, T.A. Kennedy, B.M. Maitland, E.J. Rosi, A.H. Roy, D.L. Strayer, J.L. Tank, A.O. West & M.S. Wooten, 2017. Meeting the challenge of interacting threats in freshwater ecosystems: a call to scientists and managers. *Elementa Science of the Anthropocene* 5:72.
- Dudgeon, D., 2019. Multiple threats imperil freshwater biodiversity in the Anthropocene. *Current Biology* 29:R960–R967.

- Dodds, W. K., W.W. Bouska, J.L. Eitzmann, T.J. Pilger, K.L. Pitts, A.J. Riley, J.T. Schloesser & D.J. Thornbrugh, 2009. Eutrophication of U.S. freshwaters: analysis of potential economic damages. *Environmental Science and Technology* 43:12–19.
- Grosse, Y., R. Baan, K. Straif, B. Secretan, F.E. Ghissassi & V. Cogliano, 2006. Carcinogenicity of nitrate, nitrite, and cyanobacterial peptide toxins. *The Lancet Oncology* 7:628–629.
- Higgins, S.N. & M.J. Vander Zanden, 2010. What a difference a species makes: a meta-analysis of dreissenid mussel impacts on freshwater ecosystems. *Ecological Monographs* 80:179–196.
- Huisman, J., G.A. Codd, H.W. Paerl, B.W. Ibelings, J.M.H. Verspagen & P.M. Visser, 2018. Cyanobacterial blooms. *Nature Reviews Microbiology* 16:471–483.
- Ibelings, B.W., K. Bruning, J. de Jong, K. Wolfstein, L.M. Dionisio Pires, J. Postma & T. Burger, 2005. Distribution of microcystins in a lake foodweb: no evidence for biomagnification. *Microbial Ecology* 49:487–500.
- Ibelings, B.W. & I. Chorus, 2007. Accumulation of cyanobacterial toxins in freshwater “seafood” and its consequences for public health: A review. *Environmental Pollution* 150:177–192.
- Ibelings, B.W., M. Bormans, J. Fastner & P.M. Visser, 2016. CYANOCOST special issue on cyanobacterial blooms: synopsis – a critical review of the management options for their prevention, control and mitigation. *Aquatic Ecology*: 50:595–605.
- Jones, J.R., A.P. Thorpe & D.V. Obrecht, 2020. Limnological characteristics of Missouri reservoirs: synthesis of a long-term assessment. *Lake and Reservoir Management* 36:412–422.
- Karatayev, A.Y., L.E. Burlakova & D.K. Padilla, 1998. Physical factors that limit the distribution and abundance of *Dreissena polymorpha* (PALL.). *Journal of Shellfish Research* 17:1219–1235.
- Lei J., B.S. Payne & S.Y. Wang, 1996. Filtration dynamics of the zebra mussel, *Dreissena polymorpha*. *Canadian Journal of Fisheries and Aquatic Sciences* 53:29–37.
- Lévesque, B., M. Gervais, P. Chevalier, D. Gauvis, E. Anassour-Laouan-Sidi, S. Gingras, N. Fortin, G. Brisson, C. Greer & D. Bird, 2014. Prospective study of acute health effects in relation to exposure of cyanobacteria. *Science of the Total Environment* 466/467:397–403.
- Lockwood, J.L., M.F. Hoopes & M.P. Marchetti, 2013. *Invasion Ecology* 2<sup>nd</sup> Edition. Wiley-Blackwell, Chichester, 466 pp.
- Marshall, W. & J. Laybourn-Parry, 2002. The balance between photosynthesis and grazing in Antarctic mixotrophic cryptophytes during summer. *Freshwater Biology* 47:2060–2070.

- McMahon, R.F., 1996. The physiological ecology of the zebra mussel, *Dreissena polymorpha*, in North America and Europe. *Amer. Zool.* 36:339–363.
- Miller, M.A., R.M. Kudela, A. Mekebri, D. Crane, S.C. Oates, M. T. Tinker, M. Staedler, W.A. Miller, S. Toy-Choutka, C. Dominik, D. Hardin, G. Langlois, M. Murry, K. Ward & D.A. Jessup, 2010. Evidence for a novel marine harmful algal bloom: cyanotoxin (microcystin) transfer from land to sea otters. *PLoS ONE* 5:e12576.
- North, R.L., D. Barton, A.S. Crowe, P.J. Dillon, R.M.L. Dolson, D.O. Evans, B.K. Ginn, L. Håkanson, J. Hawryshyn, H. Jarjanazi, J.W. King, J.K.L. La Rosa, L. León, C.F.M. Lewis, G.E. Liddle, Z.H. Lin, F.J. Longstaffe, R.A. Macdonald, L. Molot, T. Ozersky, M.E. Palmer, R. Quinlan, M.D. Rennie, M.M. Robillard, D. Rodé, K.M. Rühland, A. Schwalb, J.P. Smol, E. Stainsby, J.J. Trumpickas, J.G. Winter & J.D. Young, 2013. The state of Lake Simcoe (Ontario, Canada): the effects of multiple stressors on phosphorus and oxygen dynamics. *Inland Waters* 3:51–74.
- O’Neil, J.M., T.W. Davis, M.A. Burford & C.J. Gobler, 2012. The rise of harmful cyanobacteria blooms: potential role of eutrophication and climate change. *Harmful Algae* 14:313–334.
- Osgood, R.A., 2017. Inadequacy of best management practices for restoring eutrophic lakes in the United States: guidance for policy and practice. *Inland Waters* 7:401–407.
- Paerl, H.W. & J. Huisman, 2008. Blooms like it hot. *Science* 320:57–58.
- Porter, K.G., 1988. Phagotrophic phytoflagellates in microbial food webs. *Hydrobiologia* 159:89–97.
- Poste, A.E., R.E. Hecky & S.J. Guildford, 2011. Evaluating microcystin exposure risk through fish consumption. *Environmental Science and Technology* 45:5806–5811.
- Sarnelle, O., 1993. Herbivore effects on phytoplankton succession in a eutrophic lake. *Ecological Monographs* 63:129–149.
- Settele, J., R. Scholes, R. Betts, S. Bunn, P. Leadley, D. Nepstad, J.T. Overpeck, & M.A. Taboada, 2014. Terrestrial and inland water systems. In B. Field, V.R. Barros, D.J. Dokken, K.J. Mach, M.D. Mastrandrea, T.E. Bilir, M. Chatterjee, K.L. Ebi, Y.O. Estrada, R.C. Genova, B. Girma, E.S. Kissel, A.N. Levy, S. MacCracken, P. R. Mastrandrea & L.L. White (eds.), *Climate Change 2014: Impacts, Adaptation, and Vulnerability. Part A: Global and Sectoral Aspects*. pp. 271–359. Contribution of Working Group II to the Fifth Assessment Report of the Intergovernmental Panel on Climate Change, Cambridge University Press, Cambridge, UK.
- Sharpley, A., B. Foy & P. Withers, 2000. Practical and innovative measures for the control of agricultural phosphorus losses to water: an overview. *Journal of Environmental Quality* 29:1–9.

- Sieroslawska, A., A. Rymuszka, J. Velisek, B. Pawlik-Skowrońska, Z. Svobodova & T. Skowroński, 2012. Effects of microcystin-containing cyanobacterial extract on hematological and biochemical parameters of common carp (*Cyprinus carpio* L.). *Fish Physiology and Biochemistry* 38:1159–1167.
- Smith, J.L. & J.F. Haney, 2006. Foodweb transfer, accumulation, and depuration of microcystins, a cyanobacterial toxin, in pumpkinseed sunfish (*Lepomis gibbosus*). *Toxicon* 48:580–589.
- Stemberger, R. S. & J.J. Gilbert, 1985. Body size, food concentration, and population growth in planktonic rotifers. *Ecology* 66:1151–1159.
- Urabe, J., T.B. Gurung, T. Yoshida, T. Sekino & M. Nakanishi, 2000. Diel changes in phagotrophy by *Cryptomonas* in Lake Biwa. *Limnology and Oceanography* 45:1558–1563.
- Van Halderen, A., W.R. Harding, J.C. Wessels, D.J. Schneider, E.W.P. Heine, J. Van Der Merwe & J.M. Fourie, 1995. Cyanobacterial (blue-green algae) poisoning of livestock in the Western Cape Province of South Africa. *Journal of the South African Veterinary Association* 66:260–264.
- Vörösmarty, C.J., C. Pahl-Wostl, S.E. Bunn & R. Lawford, 2013. Global water, the Anthropocene and the transformation of a science. *Current Opinion in Environmental Sustainability* 5:539–550.

APPENDIX 1

TABLES

**Table A1.1:** Glacial rock flour (GRF) elemental composition, separated by major and minor elements.

<b>Major Elemental Composition</b>	<b>Percent Composition</b>
SiO <sub>2</sub>	52.02%
Al <sub>2</sub> O <sub>3</sub>	16.61%
Fe <sub>2</sub> O <sub>3</sub>	9.67%
MnO	0.17%
MgO	4.82%
CaO	8.58%
Na <sub>2</sub> O	1.94%
K <sub>2</sub> O	0.75%
TiO <sub>2</sub>	0.55%
P <sub>2</sub> O <sub>5</sub>	0.10%
<b>Minor Elemental Composition</b>	
Sc	0.0041%
V	0.0232%
Cr	0.002%
Co	0.0027%
Ni	0.0011%
Cu	0.0078%
Zn	0.0092%
S	0.113%
Ga	0.0017%
Ge	0.00010%
Rb	0.0009%
Sr	0.0131%
Y	0.00223%
Zr	0.0028%
Nb	0.00008
Cs	0.00009%
Ba	0.0144%
La	0.0002477%
Ce	0.0006800%
Pr	0.0001143%
Nd	0.0006367%
Sm	0.0002327%
Eu	0.00007673%
Gd	0.000301%
Tb	0.000056%

Dy	0.000377%
Ho	0.000082%
Er	0.000241%
Tm	0.0000353%
Yb	0.000245%
Lu	0.0000525%
Hf	0.00009%
Ta	0.000005%
Th	0.000031%
U	0.000024%

**Table A1.2:** Taxonomic composition of phytoplankton within each mesocosm tank. Finest taxonomic identification was down to genus (Guiry and Guiry, 2020). Rare taxa, which are defined as those which total less than 5% of total phytoplankton density in each tank, are excluded. Biovolume (BV) and percent composition is given for all genera that comprise more than 5% of the total phytoplankton biovolume in each tank. Phytoplankton were sampled on day 0 and day 9 in chlorophyte-dominated ( $n= 6$ ), cyanophyte-dominated ( $n= 8$ ) and control ( $n= 3$ ) mesocosm tanks.

Day	Tank	Experimental Group	Functional Group	Division	Genus	Percent Composition	BV (mm <sup>3</sup> L <sup>-1</sup> )
0	1	Cyanophyte-Dominated	Potentially Toxigenic Cyanophyta	Cyanobacteria	<i>Raphidiopsis sp.</i>	35.6	26.89
0	1	Cyanophyte-Dominated	Cryptophyta and Dinoflagellates	Cryptophyta	<i>Cryptomonas sp.</i>	22.1	16.70
0	1	Cyanophyte-Dominated	Potentially Toxigenic Cyanophyta	Cyanobacteria	<i>Aphanizomenon sp.</i>	17.4	13.18
0	1	Cyanophyte-Dominated	Potentially Toxigenic Cyanophyta	Cyanobacteria	<i>Dolichospermum sp.</i>	12.5	9.47
0	2	Control	Cryptophyta and Dinoflagellates	Miozoa	<i>Ceratium sp.</i>	34.1	0.38
0	2	Control	Cryptophyta and Dinoflagellates	Cryptophyta	<i>Cryptomonas sp.</i>	28.9	0.32
0	2	Control	Chlorophyta	Chlorophyta	<i>Sphaerocystis sp.</i>	5.6	0.06

0	3	Chlorophyte-Dominated	Cryptophyta and Dinoflagellates	Miozoa	<i>Peridinium sp.</i>	30.4	0.19
0	3	Chlorophyte-Dominated	Cryptophyta and Dinoflagellates	Cryptophyta	<i>Cryptomonas sp.</i>	24.6	0.16
0	3	Chlorophyte-Dominated	Cryptophyta and Dinoflagellates	Cryptophyta	<i>Plagioselmis sp.</i>	16.3	0.10
0	3	Chlorophyte-Dominated	Potentially Toxigenic Cyanophyta	Cyanobacteria	<i>Microcystis sp.</i>	7.3	0.05
0	4	Chlorophyte-Dominated	Chlorophyta	Chlorophyta	<i>Oocystis sp.</i>	86.9	3.02
0	4	Chlorophyte-Dominated	Cryptophyta and Dinoflagellates	Cryptophyta	<i>Cryptomonas sp.</i>	8.0	0.28
0	5	Chlorophyte-Dominated	Chlorophyta	Chlorophyta	<i>Oocystis sp.</i>	44.3	0.76
0	5	Chlorophyte-Dominated	Non-toxin Producing Cyanophyta	Cyanobacteria	<i>Planktolyngbya sp.</i>	14.1	0.24
0	5	Chlorophyte-Dominated	Non-toxin Producing Cyanophyta	Cyanobacteria	<i>Merismopedia sp.</i>	10.7	0.18
0	5	Chlorophyte-Dominated	Chlorophyta	Chlorophyta	<i>Tetraedron sp.</i>	9.1	0.15

0	6	Chlorophyte-Dominated	Chlorophyta	Chlorophyta	<i>Oocystis sp.</i>	52.9	2.62
0	6	Chlorophyte-Dominated	Cryptophyta and Dinoflagellates	Miozoa	<i>Ceratium sp.</i>	14.7	0.73
0	6	Chlorophyte-Dominated	Cryptophyta and Dinoflagellates	Cryptophyta	<i>Cryptomonas sp.</i>	8.3	0.41
0	7	Cyanophyte-Dominated	Chrysophyta	Ochrophyta	<i>Ochromonas sp.</i>	32.9	7.27
0	7	Cyanophyte-Dominated	Non-toxin Producing Cyanophyta	Cyanobacteria	<i>Planktolyngbya sp.</i>	25.5	5.63
0	7	Cyanophyte-Dominated	Potentially Toxigenic Cyanophyta	Cyanobacteria	<i>Aphanizomenon sp.</i>	17.0	3.77
0	7	Cyanophyte-Dominated	Potentially Toxigenic Cyanophyta	Cyanobacteria	<i>Cylindrospermopsis sp.</i>	11.4	2.53
0	8	Chlorophyte-Dominated	Chrysophyta	Haptophyta	<i>Chrysochromulina sp.</i>	29.2	0.76
0	8	Chlorophyte-Dominated	Chlorophyta	Chlorophyta	<i>Oocystis sp.</i>	20.1	0.52
0	8	Chlorophyte-Dominated	Cryptophyta and Dinoflagellates	Cryptophyta	<i>Cryptomonas sp.</i>	14.5	0.38

0	8	Chlorophyte-Dominated	Non-toxin Producing Cyanophyta	Cyanobacteria	<i>Planktolyngbya sp.</i>	11.5	0.30
0	8	Chlorophyte-Dominated	Cryptophyta and Dinoflagellates	Cryptophyta	<i>Plagioselmis sp.</i>	6.5	0.17
0	9	Cyanophyte-Dominated	Potentially Toxigenic Cyanophyta	Cyanobacteria	<i>Aphanizomenon sp.</i>	39.6	30.92
0	9	Cyanophyte-Dominated	Potentially Toxigenic Cyanophyta	Cyanobacteria	<i>Planktothrix sp.</i>	22.3	17.42
0	9	Cyanophyte-Dominated	Non-toxin Producing Cyanophyta	Cyanobacteria	<i>Pseudanabaena sp.</i>	13.8	10.81
0	9	Cyanophyte-Dominated	Potentially Toxigenic Cyanophyta	Cyanobacteria	<i>Dolichospermum sp.</i>	8.1	6.34
0	9	Cyanophyte-Dominated	Non-toxin Producing Cyanophyta	Cyanobacteria	<i>Limnothrix sp.</i>	6.8	5.31
0	10	Control	Chlorophyta	Chlorophyta	<i>Scenedesmus sp.</i>	35.8	0.94
0	10	Control	Cryptophyta and Dinoflagellates	Cryptophyta	<i>Plagioselmis sp.</i>	18.2	0.48
0	10	Control	Chrysophyta	Haptophyta	<i>Chrysochromulina sp.</i>	12.9	0.34

0	10	Control	Cryptophyta and Dinoflagellates	Cryptophyta	<i>Cryptomonas sp.</i>	12.0	0.31
0	10	Control	Chrysophyta	Ochrophyta	<i>Ochromonas sp.</i>	6.6	0.17
0	11	Cyanophyte- Dominated	Cryptophyta and Dinoflagellates	Cryptophyta	<i>Cryptomonas sp.</i>	39.3	2.70
0	11	Cyanophyte- Dominated	Chlorophyta	Chlorophyta	<i>Scenedesmus sp.</i>	30.7	2.11
0	11	Cyanophyte- Dominated	Non-toxin Producing Cyanophyta	Cyanobacteria	<i>Planktolyngbya sp.</i>	10.1	0.70
0	12	Cyanophyte- Dominated	Potentially Toxigenic Cyanophyta	Cyanobacteria	<i>Aphanizomenon sp.</i>	49.4	30.37
0	12	Cyanophyte- Dominated	Non-toxin Producing Cyanophyta	Cyanobacteria	<i>Pseudanabaena sp.</i>	25.5	15.68
0	12	Cyanophyte- Dominated	Non-toxin Producing Cyanophyta	Cyanobacteria	<i>Limnothrix sp.</i>	9.3	5.72
0	12	Cyanophyte- Dominated	Cryptophyta and Dinoflagellates	Cryptophyta	<i>Cryptomonas sp.</i>	5.4	3.35
0	13	Cyanophyte- Dominated	Potentially Toxigenic Cyanophyta	Cyanobacteria	<i>Aphanizomenon sp.</i>	42.5	3.59

0	13	Cyanophyte-Dominated	Potentially Toxigenic Cyanophyta	Cyanobacteria	<i>Dolichospermum sp.</i>	22.9	1.93
0	13	Cyanophyte-Dominated	Chlorophyta	Chlorophyta	<i>Scenedesmus sp.</i>	5.1	0.43
0	13	Cyanophyte-Dominated	Non-toxin Producing Cyanophyta	Cyanobacteria	<i>Cuspidothrix sp.</i>	12.6	1.07
0	13	Cyanophyte-Dominated	Potentially Toxigenic Cyanophyta	Cyanobacteria	<i>Microcystis sp.</i>	9.6	0.81
0	14	Chlorophyte-Dominated	Chlorophyta	Chlorophyta	<i>Sphaerocystis sp.</i>	17.5	0.33
0	14	Chlorophyte-Dominated	Chlorophyta	Chlorophyta	<i>Chlorella sp.</i>	12.5	0.24
0	14	Chlorophyte-Dominated	Chlorophyta	Chlorophyta	<i>Scenedesmus sp.</i>	12.0	0.23
0	14	Chlorophyte-Dominated	Chrysophyta	Bacillariophyta	<i>Cyclotella sp.</i>	11.4	0.22
0	14	Chlorophyte-Dominated	Chrysophyta	Haptophyta	<i>Chrysochromulina sp.</i>	10.2	0.20
0	14	Chlorophyte-Dominated	Chlorophyta	Chlorophyta	<i>Oocystis sp.</i>	8.4	0.16

0	14	Chlorophyte-Dominated	Chrysophyta	Ochrophyta	<i>Ochromonas sp.</i>	6.3	0.12
0	14	Chlorophyte-Dominated	Chlorophyta	Chlorophyta	<i>Chlamydomonas sp.</i>	5.5	0.11
0	15	Control	Chlorophyta	Chlorophyta	<i>Tetraedron sp.</i>	78.5	7.73
0	16	Cyanophyte-Dominated	Potentially Toxigenic Cyanophyta	Cyanobacteria	<i>Dolichospermum sp.</i>	73.4	10.83
0	16	Cyanophyte-Dominated	Chlorophyta	Chlorophyta	<i>Crucigenia sp.</i>	7.0	1.04
0	16	Cyanophyte-Dominated	Potentially Toxigenic Cyanophyta	Cyanobacteria	<i>Microcystis sp.</i>	5.7	0.84
0	17	Cyanophyte-Dominated	Potentially Toxigenic Cyanophyta	Cyanobacteria	<i>Dolichospermum sp.</i>	56.7	8.51
0	17	Cyanophyte-Dominated	Chlorophyta	Chlorophyta	<i>Desmodesmus sp.</i>	15.5	2.33
0	17	Cyanophyte-Dominated	Potentially Toxigenic Cyanophyta	Cyanobacteria	<i>Microcystis sp.</i>	14.5	2.18
9	1	Cyanophyte-Dominated	Potentially Toxigenic Cyanophyta	Cyanobacteria	<i>Raphidiopsis sp.</i>	34.0	10.41

9	1	Cyanophyte-Dominated	Potentially Toxicogenic Cyanophyta	Cyanobacteria	<i>Aphanizomenon sp.</i>	28.0	8.59
9	1	Cyanophyte-Dominated	Cryptophyta and Dinoflagellates	Cryptophyta	<i>Cryptomonas sp.</i>	11.7	3.58
9	1	Cyanophyte-Dominated	Chlorophyta	Chlorophyta	<i>Vitreochlamys sp.</i>	9.9	3.02
9	1	Cyanophyte-Dominated	Non-toxin Producing Cyanophyta	Cyanobacteria	<i>Pseudanabaena sp.</i>	6.1	1.87
9	2	Control	Cryptophyta and Dinoflagellates	Miozoa	<i>Ceratium sp.</i>	52.9	0.70
9	2	Control	Cryptophyta and Dinoflagellates	Miozoa	<i>Gymnodinium sp.</i>	13.9	0.18
9	2	Control	Cryptophyta and Dinoflagellates	Cryptophyta	<i>Plagioselmis sp.</i>	9.4	0.12
9	3	Chlorophyte-Dominated	Cryptophyta and Dinoflagellates	Cryptophyta	<i>Cryptomonas sp.</i>	57.4	0.58
9	3	Chlorophyte-Dominated	Cryptophyta and Dinoflagellates	Cryptophyta	<i>Plagioselmis sp.</i>	16.6	0.17
9	3	Chlorophyte-Dominated	Chrysophyta	Ochrophyta	<i>Ochromonas sp.</i>	8.5	0.09

9	4	Chlorophyte-Dominated	Cryptophyta and Dinoflagellates	Cryptophyta	<i>Cryptomonas sp.</i>	38.4	0.46
9	4	Chlorophyte-Dominated	Chlorophyta	Chlorophyta	<i>Oocystis sp.</i>	31.7	0.38
9	4	Chlorophyte-Dominated	Cryptophyta and Dinoflagellates	Cryptophyta	<i>Rhodomonas sp.</i>	15.8	0.19
9	5	Chlorophyte-Dominated	Chlorophyta	Chlorophyta	<i>Sphaerocystis sp.</i>	22.4	0.30
9	5	Chlorophyte-Dominated	Chlorophyta	Chlorophyta	<i>Oocystis sp.</i>	16.3	0.22
9	5	Chlorophyte-Dominated	Chlorophyta	Chlorophyta	<i>Drepanochloris sp.</i>	15.6	0.21
9	5	Chlorophyte-Dominated	Cryptophyta and Dinoflagellates	Cryptophyta	<i>Rhodomonas sp.</i>	15.7	0.21
9	6	Chlorophyte-Dominated	Cryptophyta and Dinoflagellates	Cryptophyta	<i>Cryptomonas sp.</i>	63.5	2.33
9	6	Chlorophyte-Dominated	Chlorophyta	Chlorophyta	<i>Oocystis sp.</i>	14.5	0.53
9	6	Chlorophyte-Dominated	Cryptophyta and Dinoflagellates	Cryptophyta	<i>Rhodomonas sp.</i>	10.3	0.38

9	7	Cyanophyte-Dominated	Cryptophyta and Dinoflagellates	Cryptophyta	<i>Cryptomonas sp.</i>	93.0	114.00
9	8	Chlorophyte-Dominated	Chrysophyta	Haptophyta	<i>Chrysochromulina sp.</i>	69.4	3.09
9	8	Chlorophyte-Dominated	Cryptophyta and Dinoflagellates	Cryptophyta	<i>Cryptomonas sp.</i>	13.6	0.61
9	9	Cyanophyte-Dominated	Non-toxin Producing Cyanophyta	Cyanobacteria	<i>Planktothrix sp.</i>	35.2	7.13
9	9	Cyanophyte-Dominated	Non-toxin Producing Cyanophyta	Cyanobacteria	<i>Pseudanabaena sp.</i>	24.8	5.02
9	9	Cyanophyte-Dominated	Potentially Toxicogenic Cyanophyta	Cyanobacteria	<i>Aphanizomenon sp.</i>	10.5	2.12
9	10	Control	Chlorophyta	Chlorophyta	<i>Scenedesmus sp.</i>	32.9	0.77
9	10	Control	Cryptophyta and Dinoflagellates	Cryptophyta	<i>Plagioselmis sp.</i>	25.8	0.60
9	10	Control	Chrysophyta	Haptophyta	<i>Chrysochromulina sp.</i>	24.0	0.56
9	10	Control	Cryptophyta and Dinoflagellates	Cryptophyta	<i>Cryptomonas sp.</i>	5.9	0.14
9	10	Control	Chlorophyta	Chlorophyta	<i>Pandorina sp.</i>	5.2	0.12

9	11	Cyanophyte-Dominated	Cryptophyta and Dinoflagellates	Cryptophyta	<i>Cryptomonas sp.</i>	49.9	6.50
9	11	Cyanophyte-Dominated	Chlorophyta	Chlorophyta	<i>Scenedesmus sp.</i>	19.6	2.56
9	11	Cyanophyte-Dominated	Chrysophyta	Bacillariophyta	<i>Cyclotella sp.</i>	18.4	2.40
9	12	Cyanophyte-Dominated	Cryptophyta and Dinoflagellates	Cryptophyta	<i>Cryptomonas sp.</i>	91.9	24.66
9	13	Cyanophyte-Dominated	Chlorophyta	Chlorophyta	<i>Scenedesmus sp.</i>	52.6	0.17
9	13	Cyanophyte-Dominated	Potentially Toxigenic Cyanophyta	Cyanobacteria	<i>Aphanizomenon sp.</i>	17.4	0.06
9	13	Cyanophyte-Dominated	Chlorophyta	Chlorophyta	<i>Monoraphidium sp.</i>	6.5	0.02
9	13	Cyanophyte-Dominated	Non-toxin Producing Cyanophyta	Cyanobacteria	<i>Eucapsis sp.</i>	7.2	0.02
9	14	Chlorophyte-Dominated	Cryptophyta and Dinoflagellates	Cryptophyta	<i>Cryptomonas sp.</i>	20.2	0.76
9	14	Chlorophyte-Dominated	Cryptophyta and Dinoflagellates	Cryptophyta	<i>Plagioselmis sp.</i>	14.2	0.53

9	14	Chlorophyte-Dominated	Chrysophyta	Haptophyta	<i>Chrysochromulina sp.</i>	13.7	0.51
9	14	Chlorophyte-Dominated	Chlorophyta	Chlorophyta	<i>Sphaerocystis sp.</i>	12.3	0.46
9	14	Chlorophyte-Dominated	Non-toxin Producing Cyanophyta	Cyanobacteria	<i>Planktolyngbya sp.</i>	9.7	0.36
9	14	Chlorophyte-Dominated	Chrysophyta	Ochrophyta	<i>Ochromonas sp.</i>	6.2	0.23
9	14	Chlorophyte-Dominated	Chrysophyta	Bacillariophyta	<i>Cyclotella sp.</i>	5.6	0.21
9	14	Chlorophyte-Dominated	Chlorophyta	Chlorophyta	<i>Scenedesmus sp.</i>	5.6	0.21
9	15	Control	Chlorophyta	Chlorophyta	<i>Tetraedron sp.</i>	68.7	2.92
9	15	Control	Potentially Toxigenic Cyanophyta	Cyanobacteria	<i>Microcystis sp.</i>	10.0	0.42
9	15	Control	Chlorophyta	Chlorophyta	<i>Crucigenia sp.</i>	5.1	0.22
9	16	Cyanophyte-Dominated	Potentially Toxigenic Cyanophyta	Cyanobacteria	<i>Dolichospermum sp.</i>	30.6	1.10
9	16	Cyanophyte-Dominated	Potentially Toxigenic Cyanophyta	Cyanobacteria	<i>Aphanizomenon sp.</i>	22.1	0.80

9	16	Cyanophyte-Dominated	Non-toxin Producing Cyanophyta	Cyanobacteria	<i>Planktolyngbya sp.</i>	19.5	0.70
9	16	Cyanophyte-Dominated	Potentially Toxigenic Cyanophyta	Cyanobacteria	<i>Microcystis sp.</i>	5.1	0.18
9	17	Cyanophyte-Dominated	Chlorophyta	Chlorophyta	<i>Desmodesmus sp.</i>	40.9	3.17
9	17	Cyanophyte-Dominated	Cryptophyta and Dinoflagellates	Cryptophyta	<i>Cryptomonas sp.</i>	17.3	1.35
9	17	Cyanophyte-Dominated	Non-toxin Producing Cyanophyta	Cyanobacteria	<i>Planktolyngbya sp.</i>	13.6	1.05
9	17	Cyanophyte-Dominated	Chlorophyta	Chlorophyta	<i>Scenedesmus sp.</i>	5.1	0.39
9	17	Cyanophyte-Dominated	Potentially Toxigenic Cyanophyta	Cyanobacteria	<i>Microcystis sp.</i>	7.3	0.57
9	17	Cyanophyte-Dominated	Euglenophyta	Euglenophyta	<i>Euglena sp.</i>	6.9	0.54

**Table A1.3:** Phytoplankton categorization based on functional group. Phytoplankton were identified to genus and placed into one of six functional groups: potentially toxigenic cyanophyta (Chapman and Foss 2019), non-toxin producing cyanophyta, chlorophyta, euglenophyta, cryptophyta and dinoflagellates, and chrysophyta, including bacillariophytes, chrysophytes, ochrophytes, and haptophytes.

Division	Genus	Functional Group
Cyanobacteria	<i>Aphanizomenon sp.</i>	potentially toxigenic cyanophyta
Cyanobacteria	<i>Cylindrospermopsis sp.</i>	potentially toxigenic cyanophyta
Cyanobacteria	<i>Dolichospermum sp.</i>	potentially toxigenic cyanophyta
Cyanobacteria	<i>Microcystis sp.</i>	potentially toxigenic cyanophyta
Cyanobacteria	<i>Planktothrix sp.</i>	potentially toxigenic cyanophyta
Cyanobacteria	<i>Raphidiopsis sp.</i>	potentially toxigenic cyanophyta
Cyanobacteria	<i>Anathece sp.</i>	non-toxin producing cyanophyta
Cyanobacteria	<i>Aphanocapsa sp.</i>	non-toxin producing cyanophyta
Cyanobacteria	<i>Chroococcus sp.</i>	non-toxin producing cyanophyta
Cyanobacteria	<i>Cuspidothrix sp.</i>	non-toxin producing cyanophyta
Cyanobacteria	<i>Cyanodictyon sp.</i>	non-toxin producing cyanophyta
Cyanobacteria	<i>Eucapsis sp.</i>	non-toxin producing cyanophyta
Cyanobacteria	<i>Limnothrix sp.</i>	non-toxin producing cyanophyta
Cyanobacteria	<i>Merismopedia sp.</i>	non-toxin producing cyanophyta

Cyanobacteria	<i>Planktolyngbya sp.</i>	non-toxin producing cyanophyta
Cyanobacteria	<i>Pseudanabaena sp.</i>	non-toxin producing cyanophyta
Cyanobacteria	<i>Snowella sp.</i>	non-toxin producing cyanophyta
Chlorophyta	<i>Actinastrum sp.</i>	chlorophyta
Chlorophyta	<i>Ankyra sp.</i>	chlorophyta
Chlorophyta	<i>Asterococcus sp.</i>	chlorophyta
Chlorophyta	<i>Chlamydomonas sp.</i>	chlorophyta
Chlorophyta	<i>Chlorella sp.</i>	chlorophyta
Chlorophyta	<i>Chlorogonium sp.</i>	chlorophyta
Chlorophyta	<i>Coelastrum sp.</i>	chlorophyta
Chlorophyta	<i>Cosmarium sp.</i>	chlorophyta
Chlorophyta	<i>Crucigenia sp.</i>	chlorophyta
Chlorophyta	<i>Desmodesmus sp.</i>	chlorophyta
Chlorophyta	<i>Dictyosphaerium sp.</i>	chlorophyta
Chlorophyta	<i>Drepanochloris sp.</i>	chlorophyta
Chlorophyta	<i>Elakatothrix sp.</i>	chlorophyta
Chlorophyta	<i>Golenkiniopsis sp.</i>	chlorophyta
Chlorophyta	<i>Kirchneriella sp.</i>	chlorophyta
Chlorophyta	<i>Monoraphidium sp.</i>	chlorophyta
Chlorophyta	<i>Oocystis sp.</i>	chlorophyta
Chlorophyta	<i>Pandorina sp.</i>	chlorophyta
Chlorophyta	<i>Pedinomonas sp.</i>	chlorophyta
Chlorophyta	<i>Scenedesmus sp.</i>	chlorophyta
Chlorophyta	<i>Sphaerocystis sp.</i>	chlorophyta
Chlorophyta	<i>Tetraedron sp.</i>	chlorophyta
Chlorophyta	<i>Tetrastrum sp.</i>	chlorophyta

Chlorophyta	<i>Treubaria sp.</i>	chlorophyta
Chlorophyta	<i>Vitreochlamys sp.</i>	chlorophyta
Euglenophyta	<i>Euglena sp.</i>	euglenophyta
Miozoa	<i>Ceratium sp.</i>	cryptophyta and dinoflagellates
Cryptophyta	<i>Chroomonas sp.</i>	cryptophyta and dinoflagellates
Cryptophyta	<i>Cryptomonas sp.</i>	cryptophyta and dinoflagellates
Miozoa	<i>Gymnodinium sp.</i>	cryptophyta and dinoflagellates
Miozoa	<i>Peridinium sp.</i>	cryptophyta and dinoflagellates
Cryptophyta	<i>Plagioselmis sp.</i>	cryptophyta and dinoflagellates
Cryptophyta	<i>Rhodomonas sp.</i>	cryptophyta and dinoflagellates
Bacillariophyta	<i>Achnantheidium sp.</i>	chrysophyta (including bacillariophytes, chrysophytes, ochrophytes, and haptophytes)
Ochrophyta	<i>Chromulina sp.</i>	chrysophyta (including bacillariophytes, chrysophytes, ochrophytes, and haptophytes)
Haptophyta	<i>Chrysochromulina sp.</i>	chrysophyta (including bacillariophytes, chrysophytes, ochrophytes, and haptophytes)
Bacillariophyta	<i>Cocconeis sp.</i>	chrysophyta (including bacillariophytes,

		chrysophytes, ochrophytes, and haptophytes)
Bacillariophyta	<i>Cyclotella sp.</i>	chrysophyta (including bacillariophytes, chrysophytes, ochrophytes, and haptophytes)
Bacillariophyta	<i>Eunotia sp.</i>	chrysophyta (including bacillariophytes, chrysophytes, ochrophytes, and haptophytes)
Bacillariophyta	<i>Fragilaria sp.</i>	chrysophyta (including bacillariophytes, chrysophytes, ochrophytes, and haptophytes)
Bacillariophyta	<i>Geissleria sp.</i>	chrysophyta (including bacillariophytes, chrysophytes, ochrophytes, and haptophytes)
Bacillariophyta	<i>Gomphonema sp.</i>	chrysophyta (including bacillariophytes, chrysophytes, ochrophytes, and haptophytes)
Ochrophyta	<i>Mallomonas sp.</i>	chrysophyta (including bacillariophytes, chrysophytes, ochrophytes, and haptophytes)
Bacillariophyta	<i>Nitzschia sp.</i>	chrysophyta (including bacillariophytes, chrysophytes,

Ochromphyta	<i>Ochromonas sp.</i>	ochrophytes, and haptophytes) chrysophyta (including bacillariophytes, chrysophytes, ochrophytes, and haptophytes)
Bacillariophyta	<i>Planothidium sp.</i>	chrysophyta (including bacillariophytes, chrysophytes, ochrophytes, and haptophytes)
Bacillariophyta	<i>Rhoicosphenia sp.</i>	chrysophyta (including bacillariophytes, chrysophytes, ochrophytes, and haptophytes)
Bacillariophyta	<i>Rhopalodia sp.</i>	chrysophyta (including bacillariophytes, chrysophytes, ochrophytes, and haptophytes)
Bacillariophyta	<i>Staurosira sp.</i>	chrysophyta (including bacillariophytes, chrysophytes, ochrophytes, and haptophytes)
Bacillariophyta	<i>Stephanodiscus sp.</i>	chrysophyta (including bacillariophytes, chrysophytes, ochrophytes, and haptophytes)

**Table A1.4:** Taxonomic composition of zooplankton within each tank. Zooplankton were sampled on days 0 and 9 in chlorophyte-dominated ( $n= 6$ ), cyanophyte-dominated ( $n= 9$ ), and control ( $n= 3$ ) tanks. Copepods were classified as adults or nauplii. Cladocerans were identified to genus, except those in the family Chydoridae (Thorpe and Covich, 2001).

Day #	Tank #	Experimental Group	Division	Taxonomic Classification	Percent Composition	Abundance (individuals L <sup>-1</sup> )
0	1	Cyanophyte-Dominated	Copepoda (adult)		66.67	13.51
0	1	Cyanophyte-Dominated	Copepoda (nauplii)		30.95	6.27
0	1	Cyanophyte-Dominated	Cladocera	<i>Diaphanosoma sp.</i>	2.38	0.48
0	2	Control	Copepoda (nauplii)		31.02	12.95
0	2	Control	Copepoda (adult)		28.52	11.90
0	2	Control	Cladocera	<i>Ceriodaphnia sp.</i>	38.34	16.00
0	2	Control	Cladocera	<i>Diaphanosoma sp.</i>	2.12	0.88
0	3	Chlorophyte-Dominated	Cladocera	<i>Diaphanosoma sp.</i>	28.98	5.71
0	3	Chlorophyte-Dominated	Copepoda (adult)		32.65	6.43
0	3	Chlorophyte-Dominated	Copepoda (nauplii)		23.67	4.66
0	3	Chlorophyte-Dominated	Cladocera	<i>Ceriodaphnia sp.</i>	13.47	2.65
0	3	Chlorophyte-Dominated	Cladocera	Chydoridae	0.82	0.16

0	3	Chlorophyte-Dominated	Cladocera	<i>Simocephalus sp.</i>	0.41	0.08
0	4	Chlorophyte-Dominated	Cladocera	<i>Ceriodaphnia sp.</i>	83.41	84.52
0	4	Chlorophyte-Dominated	Copepoda (adult)		8.33	8.44
0	4	Chlorophyte-Dominated	Copepoda (nauplii)		6.90	7.00
0	4	Chlorophyte-Dominated	Cladocera	<i>Diaphanosoma sp.</i>	1.35	1.37
0	5	Chlorophyte-Dominated	Copepoda (nauplii)		66.01	118.86
0	5	Chlorophyte-Dominated	Cladocera	<i>Ceriodaphnia sp.</i>	16.53	29.76
0	5	Chlorophyte-Dominated	Cladocera	<i>Diaphanosoma sp.</i>	8.98	16.16
0	5	Chlorophyte-Dominated	Copepoda (adult)		8.49	15.28
0	6	Chlorophyte-Dominated	Cladocera	<i>Ceriodaphnia sp.</i>	37.97	24.61
0	6	Chlorophyte-Dominated	Copepoda (adult)		33.62	21.79
0	6	Chlorophyte-Dominated	Copepoda (nauplii)		23.70	15.36
0	6	Chlorophyte-Dominated	Cladocera	<i>Diaphanosoma sp.</i>	4.71	3.06
0	7	Cyanophyte-Dominated	Copepoda (adult)		62.26	278.66
0	7	Cyanophyte-Dominated	Copepoda (nauplii)		33.51	149.99

0	7	Cyanophyte-Dominated	Cladocera	<i>Diaphanosoma sp.</i>	2.32	10.37
0	7	Cyanophyte-Dominated	Cladocera	<i>Ceriodaphnia sp.</i>	1.89	8.44
0	7	Cyanophyte-Dominated	Cladocera	Chydoridae	0.02	0.08
0	8	Chlorophyte-Dominated	Copepoda (adult)		51.56	35.79
0	8	Chlorophyte-Dominated	Copepoda (nauplii)		32.10	22.28
0	8	Chlorophyte-Dominated	Cladocera	<i>Ceriodaphnia sp.</i>	11.82	8.20
0	8	Chlorophyte-Dominated	Cladocera	<i>Diaphanosoma sp.</i>	2.90	2.01
0	8	Chlorophyte-Dominated	Cladocera	Chydoridae	1.62	1.13
0	9	Cyanophyte-Dominated	Cladocera	<i>Ceriodaphnia sp.</i>	49.50	217.38
0	9	Cyanophyte-Dominated	Copepoda (nauplii)		31.07	136.48
0	9	Cyanophyte-Dominated	Copepoda (adult)		18.48	81.15
0	9	Cyanophyte-Dominated	Cladocera	<i>Diaphanosoma sp.</i>	0.95	4.18
0	10	Control	Cladocera	<i>Ceriodaphnia sp.</i>	45.38	8.69
0	10	Control	Copepoda (adult)		28.15	5.39
0	10	Control	Copepoda (nauplii)		25.63	4.91
0	10	Control	Cladocera	<i>Diaphanosoma sp.</i>	0.84	0.16

0	11	Cyanophyte-Dominated	Copepoda (nauplii)		37.28	15.68
0	11	Cyanophyte-Dominated	Copepoda (adult)		35.56	14.96
0	11	Cyanophyte-Dominated	Cladocera	<i>Ceriodaphnia sp.</i>	26.20	11.02
0	11	Cyanophyte-Dominated	Cladocera	<i>Diaphanosoma sp.</i>	0.96	0.40
0	12	Cyanophyte-Dominated	Cladocera	<i>Ceriodaphnia sp.</i>	70.64	142.19
0	12	Cyanophyte-Dominated	Copepoda (adult)		16.86	33.94
0	12	Cyanophyte-Dominated	Copepoda (nauplii)		11.87	23.89
0	12	Cyanophyte-Dominated	Cladocera	<i>Diaphanosoma sp.</i>	0.64	1.29
0	13	Cyanophyte-Dominated	Copepoda (adult)		39.26	51.47
0	13	Cyanophyte-Dominated	Cladocera	Chydoridae	32.70	42.86
0	13	Cyanophyte-Dominated	Copepoda (nauplii)		13.99	18.34
0	13	Cyanophyte-Dominated	Cladocera	<i>Diaphanosoma sp.</i>	7.85	10.29
0	13	Cyanophyte-Dominated	Cladocera	<i>Ceriodaphnia sp.</i>	4.42	5.79
0	13	Cyanophyte-Dominated	Cladocera	<i>Simocephalus sp.</i>	1.78	2.33
0	14	Chlorophyte-Dominated	Copepoda (nauplii)		49.33	20.59

0	14	Chlorophyte-Dominated	Copepoda (adult)		38.54	16.08
0	14	Chlorophyte-Dominated	Cladocera	<i>Ceriodaphnia sp.</i>	8.48	3.54
0	14	Chlorophyte-Dominated	Cladocera	<i>Diaphanosoma sp.</i>	3.47	1.45
0	14	Chlorophyte-Dominated	Cladocera	<i>Simocephalus sp.</i>	0.19	0.08
0	15	Control	Copepoda (nauplii)		41.09	62.33
0	15	Control	Cladocera	<i>Ceriodaphnia sp.</i>	35.31	53.56
0	15	Control	Copepoda (adult)		17.92	27.18
0	15	Control	Cladocera	<i>Diaphanosoma sp.</i>	5.46	8.28
0	15	Control	Cladocera	Chydoridae	0.11	0.16
0	15	Control	Cladocera	<i>Simocephalus sp.</i>	0.11	0.16
0	16	Cyanophyte-Dominated	Copepoda (nauplii)		49.67	103.91
0	16	Cyanophyte-Dominated	Copepoda (adult)		45.25	94.66
0	16	Cyanophyte-Dominated	Cladocera	<i>Diaphanosoma sp.</i>	2.77	5.79
0	16	Cyanophyte-Dominated	Cladocera	<i>Ceriodaphnia sp.</i>	2.31	4.83
0	17	Cyanophyte-Dominated	Copepoda (adult)		70.56	143.96
0	17	Cyanophyte-Dominated	Copepoda (nauplii)		26.37	53.80

0	17	Cyanophyte-Dominated	Cladocera	<i>Ceriodaphnia sp.</i>	2.36	4.83
0	17	Cyanophyte-Dominated	Cladocera	<i>Diaphanosoma sp.</i>	0.71	1.45
9	1	Cyanophyte-Dominated	Copepoda (nauplii)		79.76	181.59
9	1	Cyanophyte-Dominated	Copepoda (adult)		20.24	46.08
9	2	Control	Cladocera	<i>Ceriodaphnia sp.</i>	48.62	22.60
9	2	Control	Copepoda (adult)		28.72	13.35
9	2	Control	Copepoda (nauplii)		22.15	10.29
9	2	Control	Cladocera	<i>Diaphanosoma sp.</i>	0.52	0.24
9	3	Chlorophyte-Dominated	Copepoda (adult)		33.33	4.83
9	3	Chlorophyte-Dominated	Cladocera	<i>Ceriodaphnia sp.</i>	26.11	3.78
9	3	Chlorophyte-Dominated	Cladocera	<i>Diaphanosoma sp.</i>	21.11	3.06
9	3	Chlorophyte-Dominated	Copepoda (nauplii)		19.44	2.81
9	4	Chlorophyte-Dominated	Cladocera	<i>Ceriodaphnia sp.</i>	38.94	3.54
9	4	Chlorophyte-Dominated	Copepoda (nauplii)		30.09	2.73
9	4	Chlorophyte-Dominated	Copepoda (adult)		28.32	2.57
9	4	Chlorophyte-Dominated	Cladocera	<i>Diaphanosoma sp.</i>	2.65	0.24

9	5	Chlorophyte-Dominated	Copepoda (adult)		37.33	11.02
9	5	Chlorophyte-Dominated	Copepoda (nauplii)		31.34	9.25
9	5	Chlorophyte-Dominated	Cladocera	<i>Diaphanosoma sp.</i>	24.80	7.32
9	5	Chlorophyte-Dominated	Cladocera	<i>Ceriodaphnia sp.</i>	5.45	1.61
9	5	Chlorophyte-Dominated	Cladocera	<i>Daphnia sp.</i>	1.09	0.32
9	6	Chlorophyte-Dominated	Copepoda (adult)		51.82	33.21
9	6	Chlorophyte-Dominated	Copepoda (nauplii)		30.11	19.30
9	6	Chlorophyte-Dominated	Cladocera	<i>Ceriodaphnia sp.</i>	17.19	11.02
9	6	Chlorophyte-Dominated	Cladocera	<i>Diaphanosoma sp.</i>	0.88	0.56
9	7	Cyanophyte-Dominated	Copepoda (adult)		52.07	7.08
9	7	Cyanophyte-Dominated	Cladocera	<i>Ceriodaphnia sp.</i>	23.08	3.14
9	7	Cyanophyte-Dominated	Copepoda (nauplii)		18.34	2.49
9	7	Cyanophyte-Dominated	Cladocera	<i>Diaphanosoma sp.</i>	4.73	0.64
9	7	Cyanophyte-Dominated	Cladocera	Chydoridae	1.78	0.24
9	8	Chlorophyte-Dominated	Copepoda (nauplii)		55.79	19.38

9	8	Chlorophyte-Dominated	Copepoda (adult)		32.41	11.26
9	8	Chlorophyte-Dominated	Cladocera	<i>Ceriodaphnia sp.</i>	7.64	2.65
9	8	Chlorophyte-Dominated	Cladocera	<i>Diaphanosoma sp.</i>	2.78	0.97
9	8	Chlorophyte-Dominated	Cladocera	Chydoridae	1.39	0.48
9	9	Cyanophyte-Dominated	Cladocera	<i>Ceriodaphnia sp.</i>	53.98	58.87
9	9	Cyanophyte-Dominated	Copepoda (adult)		27.65	30.16
9	9	Cyanophyte-Dominated	Copepoda (nauplii)		17.33	18.90
9	9	Cyanophyte-Dominated	Cladocera	<i>Diaphanosoma sp.</i>	1.03	1.13
9	10	Control	Cladocera	<i>Ceriodaphnia sp.</i>	43.71	21.23
9	10	Control	Copepoda (nauplii)		28.48	13.83
9	10	Control	Copepoda (adult)		27.48	13.35
9	10	Control	Cladocera	<i>Diaphanosoma sp.</i>	0.33	0.16
9	11	Cyanophyte-Dominated	Copepoda (adult)		48.82	39.97
9	11	Cyanophyte-Dominated	Copepoda (nauplii)		30.06	24.61
9	11	Cyanophyte-Dominated	Cladocera	<i>Ceriodaphnia sp.</i>	20.43	16.73
9	11	Cyanophyte-Dominated	Cladocera	<i>Diaphanosoma sp.</i>	0.69	0.56

9	12	Cyanophyte-Dominated	Copepoda (nauplii)		34.46	27.83
9	12	Cyanophyte-Dominated	Copepoda (adult)		33.37	26.94
9	12	Cyanophyte-Dominated	Cladocera	<i>Ceriodaphnia sp.</i>	31.37	25.33
9	12	Cyanophyte-Dominated	Cladocera	<i>Diaphanosoma sp.</i>	0.80	0.64
9	13	Cyanophyte-Dominated	Cladocera	Chydoridae	53.59	27.02
9	13	Cyanophyte-Dominated	Copepoda (adult)		23.92	12.06
9	13	Cyanophyte-Dominated	Cladocera	<i>Ceriodaphnia sp.</i>	9.73	4.91
9	13	Cyanophyte-Dominated	Cladocera	<i>Diaphanosoma sp.</i>	8.61	4.34
9	13	Cyanophyte-Dominated	Cladocera	<i>Simocephalus sp.</i>	0.32	0.16
9	13	Cyanophyte-Dominated	Copepoda (nauplii)		3.83	1.93
9	14	Chlorophyte-Dominated	Copepoda (nauplii)		59.34	23.00
9	14	Chlorophyte-Dominated	Copepoda (adult)		34.85	13.51
9	14	Chlorophyte-Dominated	Cladocera	<i>Diaphanosoma sp.</i>	2.90	1.13
9	14	Chlorophyte-Dominated	Cladocera	<i>Ceriodaphnia sp.</i>	1.45	0.56
9	14	Chlorophyte-Dominated	Cladocera	Chydoridae	1.24	0.48

9	14	Chlorophyte-Dominated	Cladocera	<i>Simocephalus sp.</i>	0.21	0.08
9	15	Control	Cladocera	<i>Ceriodaphnia sp.</i>	78.50	188.83
9	15	Control	Copepoda (nauplii)		10.67	25.65
9	15	Control	Copepoda (adult)		8.86	21.31
9	15	Control	Cladocera	<i>Diaphanosoma sp.</i>	1.94	4.66
9	15	Control	Cladocera	Chydoridae	0.03	0.08
9	16	Cyanophyte-Dominated	Copepoda (adult)		16.44	29.60
9	16	Cyanophyte-Dominated	Cladocera	<i>Ceriodaphnia sp.</i>	2.23	4.02
9	16	Cyanophyte-Dominated	Copepoda (nauplii)		1.21	2.17
9	16	Cyanophyte-Dominated	Cladocera	<i>Diaphanosoma sp.</i>	0.54	0.97
9	17	Cyanophyte-Dominated	Copepoda (adult)		69.21	124.57
9	17	Cyanophyte-Dominated	Copepoda (nauplii)		8.76	15.76
9	17	Cyanophyte-Dominated	Cladocera	<i>Ceriodaphnia sp.</i>	1.43	2.57
9	17	Cyanophyte-Dominated	Cladocera	<i>Diaphanosoma sp.</i>	0.18	0.32

## FIGURES



**Figure A1.1:** Experimental mesocosm tank set up. The trees in the distance are over 100 m away.

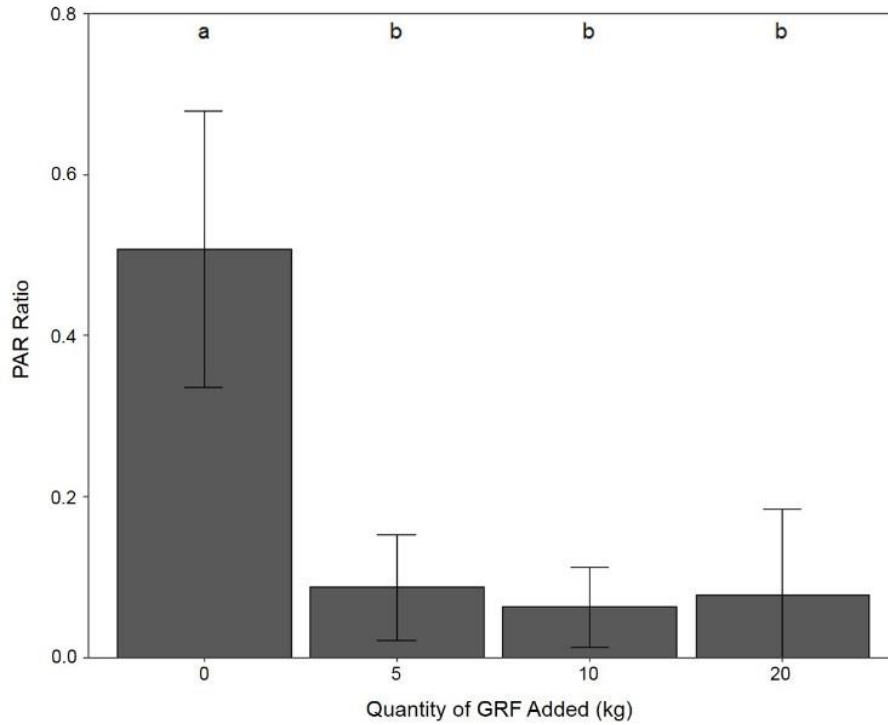


**Figure A1.2:** Comparison of the light environment in tanks that received varying amounts of glacial rock flour (GRF). PAR ratio (0.5 m water/air reading) measured in mesocosm tanks that received 0, 5, 10, and 20 kg of GRF. The light ratio was determined by dividing photosynthetically active radiation (PAR) measurements made at 0.5 m depth by PAR measurements from above the water's surface in the air. Bars with the same letter indicate that no significant difference exists between experimental groups while bars with different letters indicate that there is a significant difference in PAR between groups. We found no significant difference in PAR among tanks that received 5, 10, and 20 kg of GRF (Kruskal-Wallis  $p > 0.05$ ). In this dosing experiment, each experimental group consisted of 2 tanks that were not used in the larger, 9-day experiment.

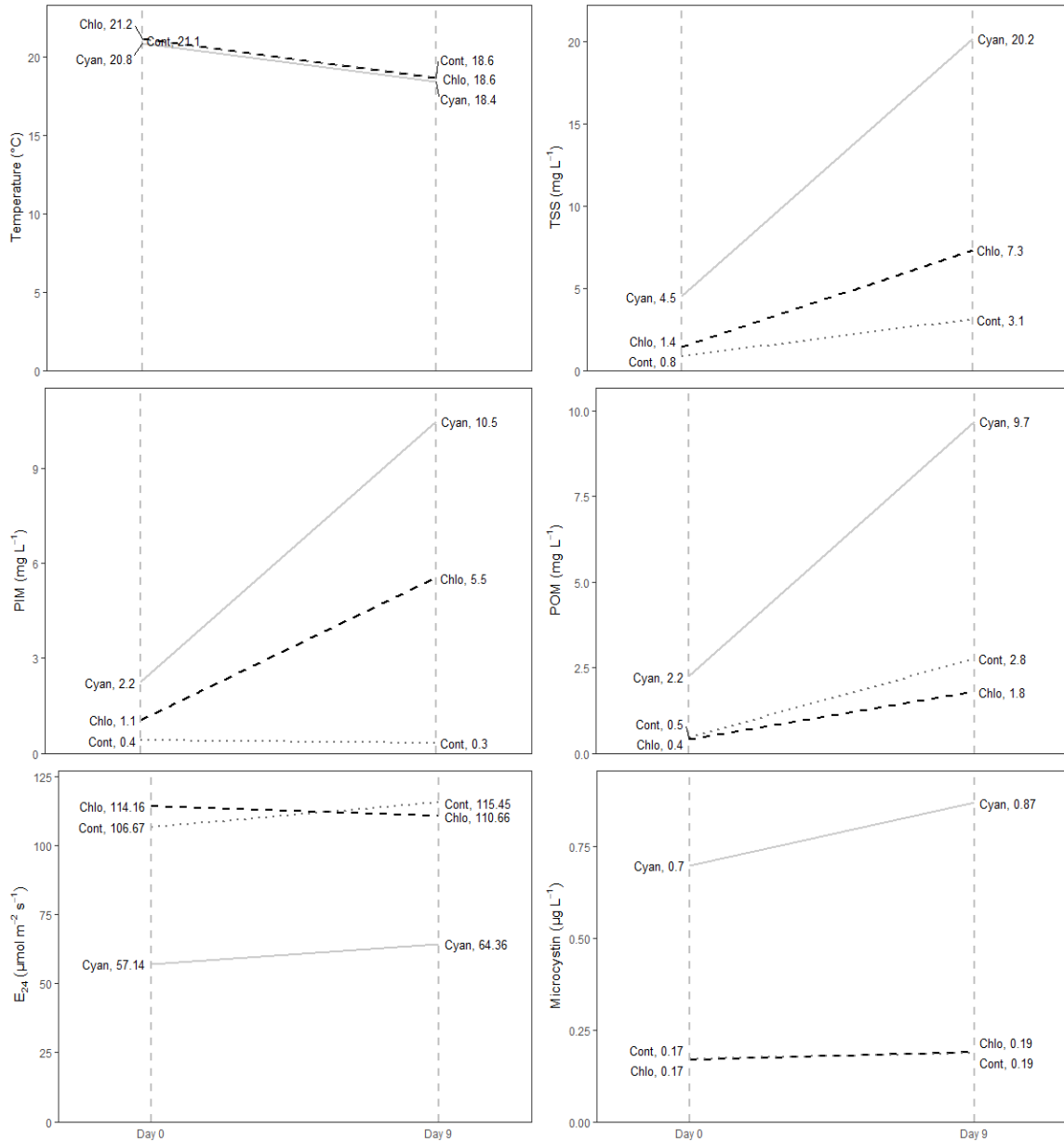


**Figure A1.3:** Slope plots for parameters in experimental mesocosm tanks. Temperature, total suspended solids (TSS), particulate inorganic matter (PIM), particulate organic matter (POM), mean mixed layer irradiance ( $\bar{E}_{24}$ ), and microcystin are presented. Vertical, dashed lines represent measurements taken on day 0 and day 9. Sloped lines represent the change in each parameter for chlorophyte dominated (Chlo, black, dashed line,  $n=6$ ), cyanophyte-dominated (Cyan, light gray solid, line,  $n=8$ ), and control (Cont, dark gray, dotted line,  $n=3$ ) mesocosm tanks. Values to the right of each label are the mean of all tanks within that group.

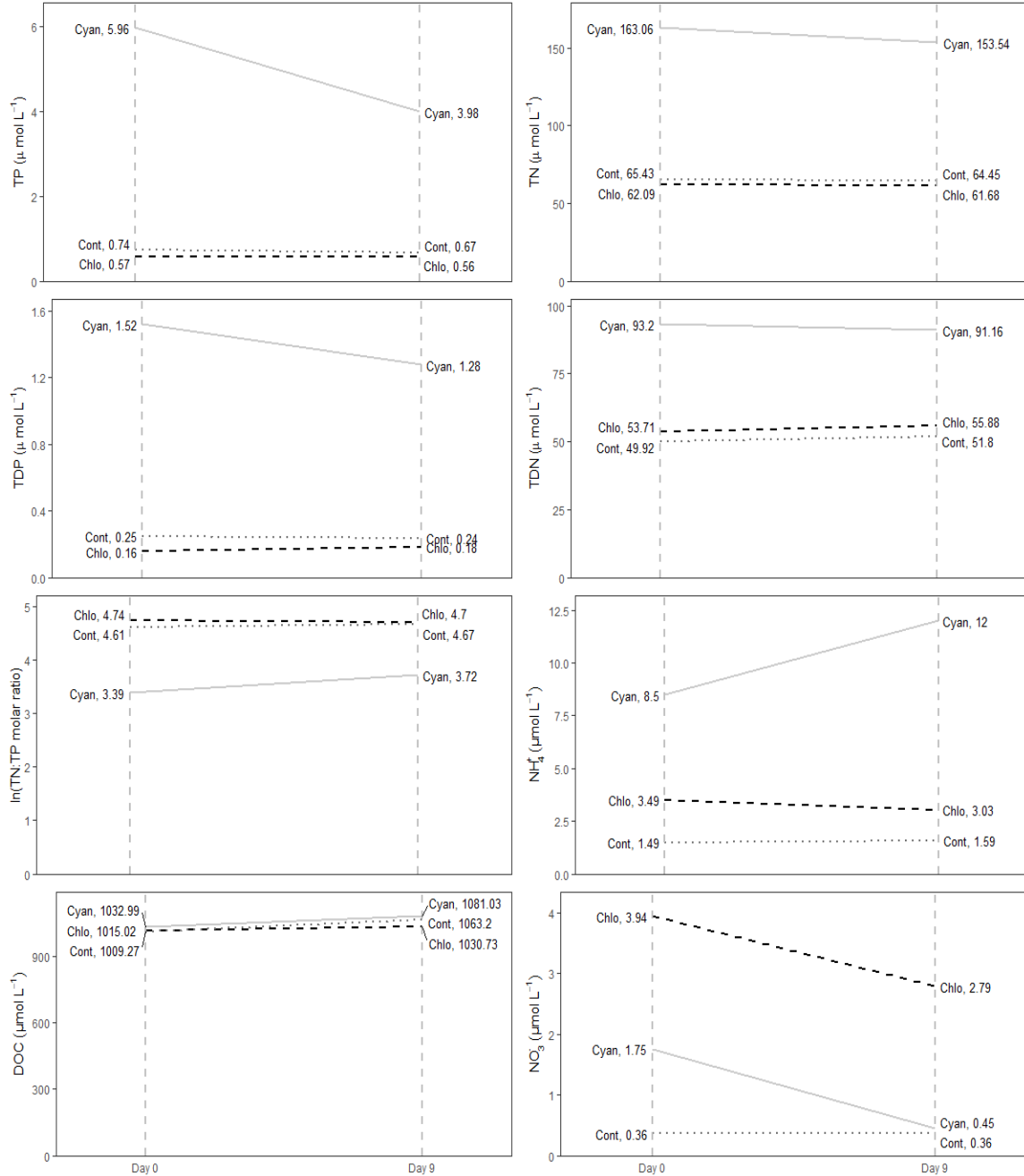


**Figure A1.4:** Slope plots for chemical parameters in experimental mesocosm tanks. Total phosphorus (TP), total nitrogen (TN), total dissolved phosphorus (TDP), total dissolved nitrogen (TDN), the natural log ratio of TN to TP (TN:TP), ammonium ( $\text{NH}_4^+$ ), dissolved organic carbon (DOC), and nitrate ( $\text{NO}_3^-$ ) are presented. Vertical, dashed lines represent measurements taken on day 0 and day 9. Sloped lines represent the change in each parameter for chlorophyte dominated (Chlo, black, dashed line,  $n=6$ ), cyanophyte-dominated (Cyan, light gray, solid line,  $n=8$ ), and control (Cont, dark gray, dotted line,  $n=3$ ) mesocosm tanks. Values to the right of each label are the mean of all tanks within that group.

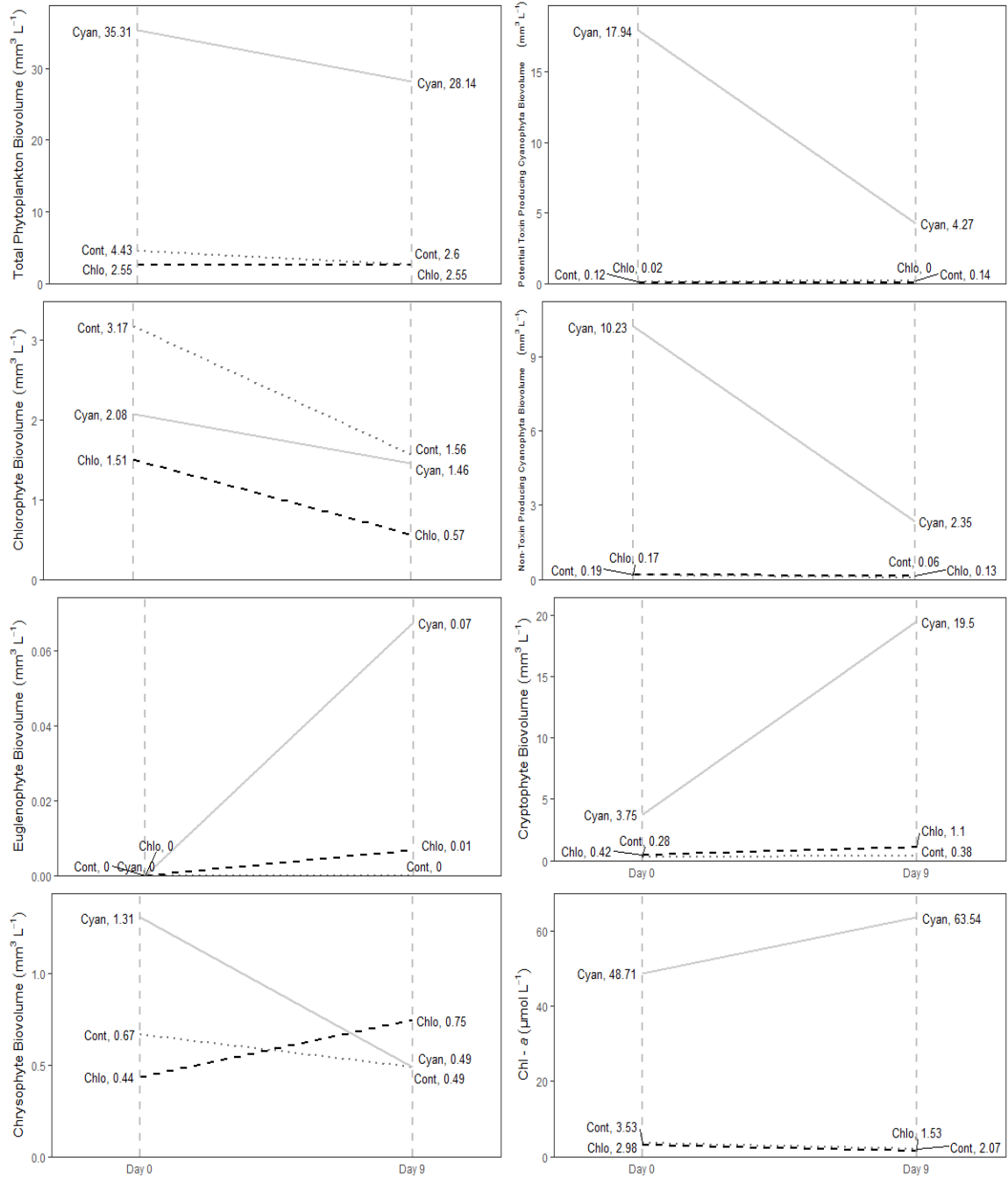


**Figure A1.5:** Slope plots for phytoplankton and chlorophyll-*a* concentrations (Chl-*a*) in experimental mesocosm tanks. Vertical, dashed lines represent measurements taken on day 0 and day 9. Sloped lines represent the change in each parameter for chlorophyte dominated (Chlo, black, dashed line,  $n=6$ ), cyanophyte-dominated (Cyan, light gray, solid line,  $n=8$ ), and control (Cont, dark gray, dotted line,  $n=3$ ) mesocosm tanks. Values to the right of each label are the mean of all tanks within that group.

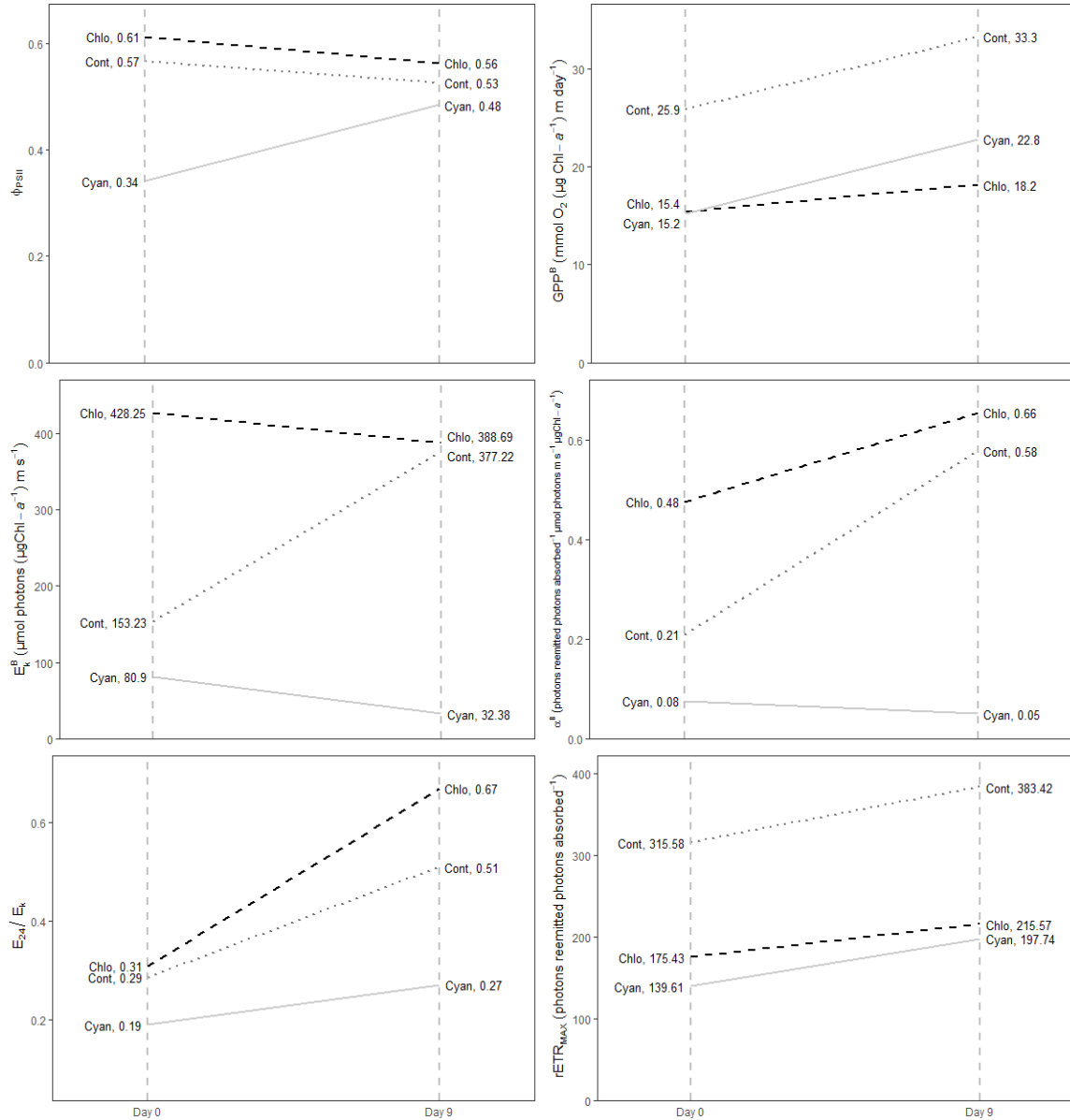


**Figure A1.6:** Slope plots for phytoplankton physiology parameters in experimental mesocosm tanks. Maximum quantum yield of photosystem II ( $\phi_{PSII}$ ), gross primary productivity normalized to chlorophyll-*a* (GPP<sup>B</sup>), light saturation threshold normalized to chlorophyll-*a* ( $E_k^B$ ), alpha normalized to chlorophyll-*a* ( $\alpha^B$ ), light deficiency parameter ( $\bar{E}_{24}/E_k$ ), and maximum relative electron transport rate (rETR<sub>MAX</sub>) are presented. Vertical, dashed lines represent measurements taken on day 0 and day 9. Sloped lines represent the change in each parameter for chlorophyte dominated (Chlo, black, dashed line,  $n=6$ ), cyanophyte-dominated (Cyan, light gray, solid line,  $n=8$ ), and control (Cont, dark gray, dotted line,  $n=3$ ) mesocosm tanks. Values to the right of each label are the mean of all tanks within that group.

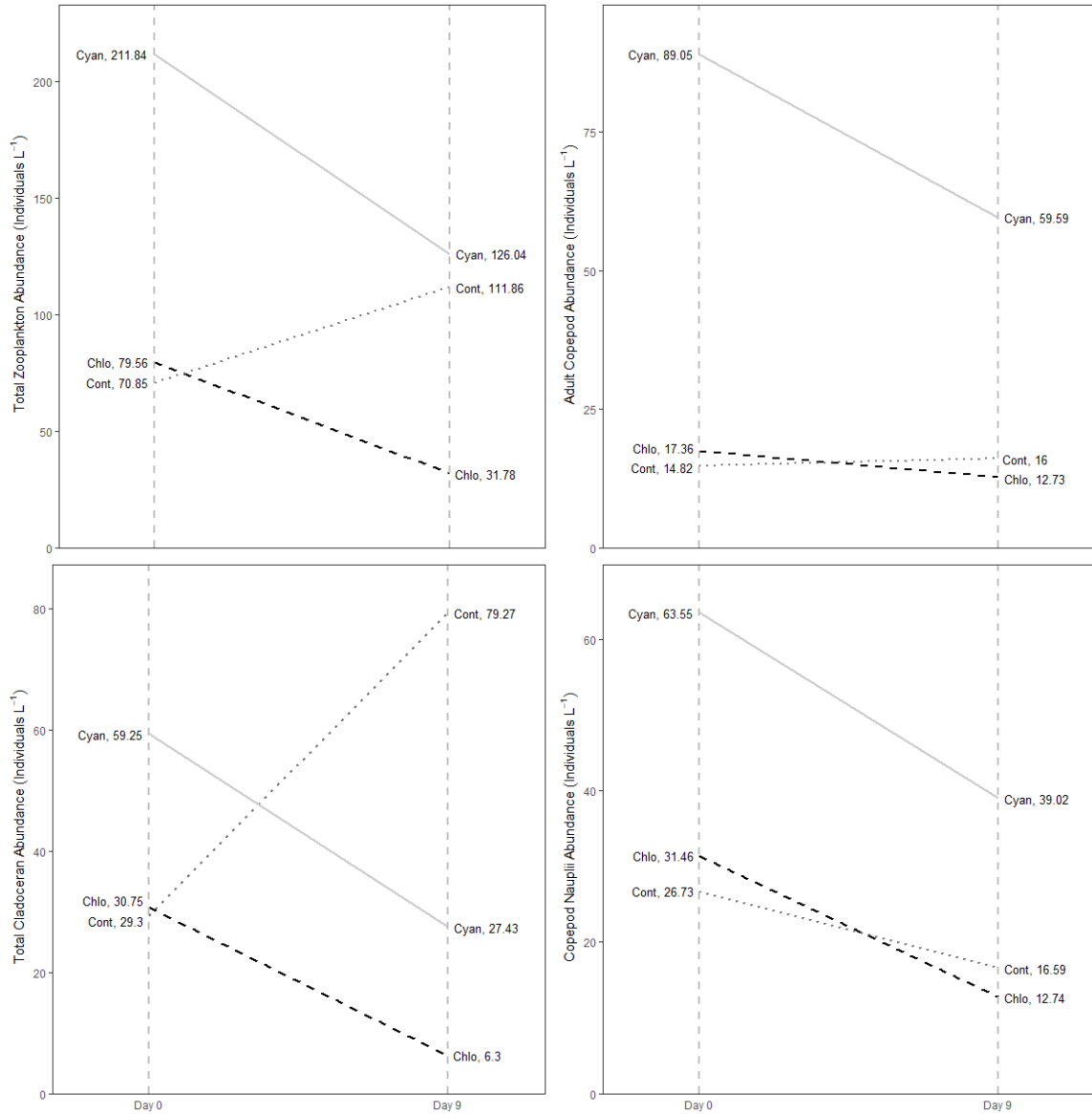


**Figure A1.7:** Slope plots for zooplankton in experimental mesocosm tanks. Vertical, dashed lines represent measurements taken on day 0 and day 9. Sloped lines represent the change in each parameter for chlorophyte dominated (Chlo, black, dashed line,  $n=6$ ), cyanophyte-dominated (Cyan, light gray, solid line,  $n=8$ ), and control (Cont, dark gray, dotted line,  $n=3$ ) mesocosm tanks. Values to the right of each label are the mean of all tanks within that group.

## LITERATURE CITED

- Chapman, A. & A. Foss, 2019. Potentially Toxigenic (PTOX) Cyanobacteria List. GreenWater Laboratories Technical Report.
- Guiry, M.D. & G.M. Guiry, 2020. AlgaeBase. World-wide electronic publication, National University of Ireland, Galway. <https://www.algaebase.org>
- Thorp, J.H. & A.P. Covich, 2001. Ecology and Classification of North American Freshwater Invertebrates. San Diego: Academic Press.

## APPENDIX 2

### SUPPLEMENTARY METHODOLOGY

#### *Bathymetric measurements*

We created a bathymetric map of the reservoir in the summer of 2017 using a Lowrance Elite 7 TI sonar (Figure S1). Continuous, geolocated readings were compiled using ReefMaster software with a depth resolution of 0.01 m.

#### *Phytoplankton identification and enumeration methodology*

Phytoplankton samples were collected 4 times in 2017, including June 16, August 11, October 30, and December 17. In 2018, phytoplankton were collected on 16 dates including June 21, June 29, July 2, July 11, July 16, July 27, August 1, August 6, August 17, August 20, August 28, September 5, September 12, September 21, September 26, and October 3. We used a peristaltic pump to collect composite water samples from the surface to one meter above the mixing depth under stratified conditions, or when the reservoir was isothermal, from the surface to one meter above the sediment. A ~200 mL subset of the water sample was preserved with Lugol's in an amber glass bottle.

Phytoplankton were identified to species using an inverted microscope and the Utermohl method (Karlsson 2003; Komarek and Anagnostidis 2008a; Komarek and Anagnostidis 2008b; Lund et al. 1958; Wehr et al. 2015; John et al. 2017). Phytoplankton were allowed to settle until no phytoplankton were observed in at least 15 fields from subsamples taken from the midpoint of the settling chamber. Phytoplankton were counted at 225× for larger cell and 900× for small cells. Cell biovolume estimates from the first 300 natural units were based on measurements from 30 cells in each taxon and were calculated using the

formula of Hillebrand et al. (1999). Samples collected in 2017 were identified and enumerated by the University of Vermont Rubenstein Ecosystem Science Laboratory. Samples from 2018 were identified and enumerated by H.J. Kling (Algal Taxonomy and Ecology).

#### *Correlation between microcystin and length*

We looked for correlations in microcystin and fish length for all 3 tissue types and both fish species. Length did not follow a normal distribution (Shapiro-Wilk  $p < 0.05$ ) and was not homoscedastic (Levene's test  $p < 0.05$ ) even after transformation. For these reasons, a Spearman's rank correlation test was selected to measure correlations between length and microcystin in muscles (bluegill  $n = 89$ , largemouth bass  $n = 116$ ), livers (bluegill  $n = 88$ , largemouth bass  $n = 116$ ), and kidneys (bluegill  $n = 73$ , largemouth bass  $n = 108$ ).

The relationship between fish length and microcystin in muscles, livers, and kidneys was assessed with a Spearman's rank correlation test for both bluegill and largemouth bass (Table S3). For bluegill, no significant correlation between length and microcystin was identified in muscles, livers, nor kidneys. For largemouth bass, no significant correlation was identified between length and liver microcystin, but a significant, negative correlation was identified for length and microcystin in muscles ( $p = 0.002$ ,  $\rho = -0.28$ ) and in kidneys ( $p = 0.035$ ,  $\rho = -0.20$ ).

TABLES

**Table A2.1:** Assessment of the extraction of microcystin from fish tissue methodology. Both detection limit and extraction efficiency were determined from hatchery raised bluegill, which served as the negative control fish for our study. Negative controls were spiked with a known concentration of microcystin. The extraction efficiency was the percent of this spike that was recovered. We determined the detection limit to be the concentration where negative controls, which are known to lack microcystin came back above the limit of detection, indicating the level where matrix effects are being measured by the analysis. Inter assay variation was determined by including a sample from each species on each plate.

	<b>Muscle</b>	<b>Liver</b>	<b>Kidney</b>
Bluegill Inter Assay Variation	25.4 %	18.1 %	19.3 %
Largemouth Bass Inter Assay Variation	13.8 %	15.0 %	7.5 %
Extraction Efficiency	95.4 %	114.1 %	89.0 %
Detection Limit	1.6 ng g <sup>-1</sup>	14.6 ng g <sup>-1</sup>	10.9 ng g <sup>-1</sup>

**Table A2.2:** Spearman’s rank correlations between fish length and microcystin (MC) in muscles, livers, and kidneys for bluegill and largemouth bass. The degrees of freedom (df) and p-value for each correlation are reported, along with the correlation coefficient (rho) when significant correlations exist.

<b>Parameters Being Compared</b>	<b>Species</b>	<b>df</b>	<b>p-value</b>	<b>rho</b>
Length to Muscle MC	Bluegill	87	0.116	-0.17
Length to Liver MC	Bluegill	86	0.666	0.05
Length to Kidney MC	Bluegill	71	0.248	-0.14
Length to Age MC	Bluegill	87	< 0.001	0.72
Length to Muscle MC	Largemouth Bass	87	0.002	-0.29
Length to Liver MC	Largemouth Bass	86	0.412	-0.08
Length to Kidney MC	Largemouth Bass	71	0.035	-0.20
Length to Age MC	Largemouth Bass	114	< 0.001	0.89

**Table A2.3:** Microcystin concentrations measured in bluegill and largemouth bass over the course of a year. Microcystin concentrations are reported as ng g<sup>-1</sup> ww. The top value in each cell is the mean of microcystin in all tissues from each harvest date. The middle value, in parentheses, is the standard deviation and the bottom value is the samples size (n).

Tissue	Species	4/23/18	5/30/18	7/16/18	8/21/18	10/11/18	11/27/18	2/4/19	3/18/19
Muscle	Bluegill	24.3	12.2	6.9	5.3	2.3	3.0	4.1	2.7
		(7.0)	(8.1)	(3.6)	(1.0)	(0.5)	(1.0)	(1.0)	(2.3)
		n= 10	n= 13	n= 10	n= 11	n= 10	n= 11	n= 14	n= 10
Liver	Bluegill	65.6	103.1	66.1	53.6	58.1	40.0	38.6	64.9
		(27.4)	(55.4)	(29.3)	(22.6)	(49.9)	(17.4)	(6.9)	(32.2)
		n= 10	n= 13	n= 10	n= 11	n= 10	n= 10	n= 14	n= 10
Kidney	Bluegill	45.3	26.8	24.2	14.0	15.6	13.5	24.7	12.1
		(16.5)	(13.5)	(14.3)	(16.2)	(8.4)	(13.0)	(9.9)	(1.2)
		n= 10	n= 12	n= 8	n= 6	n= 8	n= 6	n= 13	n= 10
Muscle	Largemouth Bass	12.9	6.9	5.8	4.1	1.9	1.8	2.6	2.7
		(2.7)	(2.6)	(1.9)	(1.7)	(0.3)	(0.4)	(0.6)	(2.3)
		n= 20	n= 18	n= 20	n= 19	n= 10	n= 10	n= 9	n= 10
Liver	Largemouth Bass	124.4	74.2	69.7	54.1	72.0	28.5	46.3	64.9
		(138.8)	(46.4)	(86.6)	(35.8)	(80.4)	(11.4)	(28.4)	(32.2)
		n= 20	n= 18	n= 20	n= 19	n= 10	n= 10	n= 9	n= 10
Kidney	Largemouth Bass	38.4	23.2	14.2	21.1	17.0	16.7	18.4	12.1
		(7.6)	(8.0)	(10.2)	(15.8)	(2.4)	(6.9)	(7.1)	(1.2)
		n= 20	n= 18	n= 20	n= 19	n= 10	n= 10	n= 9	n= 10

**Table A2.4:** Multiple linear regression models explaining microcystin accumulation in fish filets, livers, and kidneys. Models were created for all three tissue types for both bluegill (BLG) and largemouth bass (LMB). In the “Fish Characteristic” models, only fish characteristics such as length, age, mass, body condition index, sex, liver organosomatic index (OSI), and gonad OSI (Table 1) were included. The “Combined” models included significant parameters identified in the fish characteristic models, as well as water microcystin (MC), total dissolved phosphorus (TDP), total dissolved nitrogen (TDN), chlorophyll-*a* concentrations (chl-*a*), and dissolved organic carbon, which were identified as un-correlated water quality parameters (Table 2). Both model sets were run twice, the first time including harvest date as a categorical variable with 8 levels. We do not report the individual statistics for harvest date because multiple linear regression determines these based on a reference level for categorical variables. We see no ecological nor experimental benefit to setting any individual date as a reference level, indicated by “-,” and instead look for differences in microcystin between dates using a two-way Analysis of Variance (ANOVA, Table 3.5). In the second model set, harvest date was excluded. For each individual model, the p-value and R<sup>2</sup>-adj are listed in the “Species and Tissue” column, while the coefficient, t-value, standard error, and p-value for each significant model parameter are listed in subsequent columns. In each row, “ns” is used to denote when a significant model was not able to be created from the given parameters.

Model	Species and Tissue	Parameter	Coefficient	t-value	Standard Error	p-value
Fish Characteristics - Harvest Date Included	BLG Muscle (R <sup>2</sup> -adj=0.698; <i>p</i> <0.001)	Harvest Date	-	-	-	-
	BLG Liver (R <sup>2</sup> -adj=0.266; <i>p</i> <0.001)	Harvest Date	-	-	-	-
	BLG Kidney (R <sup>2</sup> -adj=0.384; <i>p</i> <0.001)	Harvest Date	-	-	-	-
	LMB Muscle (R <sup>2</sup> -adj=0.763; <i>p</i> <0.001)	Harvest Date	-	-	-	-
	LMB Liver (R <sup>2</sup> -adj=0.021; <i>p</i> =0.063)	ns	ns	ns	ns	ns
	LMB Kidney (R <sup>2</sup> -adj=0.433; <i>p</i> <0.001)	Harvest Date	-	-	-	-
Fish Characteristics - Harvest Date Excluded	BLG Muscle (R <sup>2</sup> -adj=-0.016; <i>p</i> =0.583)	ns	ns	ns	ns	ns
	BLG Liver (R <sup>2</sup> -adj=-0.116; <i>p</i> <0.001)	Liver OSI	-0.046	-3.529	0.013	<0.001
	BLG Kidney (R <sup>2</sup> -adj=-0.024; <i>p</i> =0.101)	ns	ns	ns	ns	ns
	LMB Muscle (R <sup>2</sup> -adj=-0.117; <i>p</i> <0.001)	Gonad OSI	0.001	3.936	<0.001	<0.001

	LMB Liver (R <sup>2</sup> -adj=-0.021; <i>p</i> =0.063)	ns	ns	ns	ns	ns
	LMB Kidney (R <sup>2</sup> -adj=-0.044; <i>p</i> =0.020)	Gonad OSI	0.002	2.372	0.001	0.020
Combined - Harvest Date Included	BLG Muscle (R <sup>2</sup> -adj=0.698; <i>p</i> <0.001)	Harvest Date	-	-	-	-
	BLG Liver (R <sup>2</sup> -adj=0.266; <i>p</i> <0.001)	Harvest Date	-	-	-	-
	BLG Kidney (R <sup>2</sup> -adj=0.384; <i>p</i> <0.001)	Harvest Date	-	-	-	-
	LMB Muscle (R <sup>2</sup> -adj=0.763; <i>p</i> <0.001)	Harvest Date	-	-	-	-
	LMB Liver (R <sup>2</sup> -adj=0.035; <i>p</i> =0.024)	Water MC	0.051	2.280	0.022	0.025
	LMB Kidney (R <sup>2</sup> -adj=0.433; <i>p</i> <0.001)	Harvest Date	-	-	-	-
Combined - Harvest Date Excluded		Water MC	0.018	6.715	0.002	<0.001
	BLG Muscle (R <sup>2</sup> -adj=0.459; <i>p</i> <0.001)	chl- <i>a</i>	-0.125	-5.638	0.022	<0.001
		TDN	< -0.001	-2.719	<0.001	0.008
		Water MC	0.054	0.054	0.011	<0.001
	BLG Liver (R <sup>2</sup> -adj=0.299; <i>p</i> <0.001)	Liver OSI	-0.034	-0.034	0.012	0.006
		TDP	0.113	0.113	0.032	0.001
	BLG Kidney (R <sup>2</sup> -adj=0.100; <i>p</i> =0.004)	Water MC	0.012	2.995	0.004	0.004
	LMB Muscle (R <sup>2</sup> -adj=0.259; <i>p</i> <0.001)	Water MC	0.006	6.422	0.001	<0.001
	LMB Liver (R <sup>2</sup> -adj=0.035; <i>p</i> =0.024)	Water MC	0.051	2.280	0.022	0.025
	LMB Kidney (R <sup>2</sup> -adj=0.175; <i>p</i> <0.001)	Water MC	0.014	4.863	0.003	<0.001

FIGURES

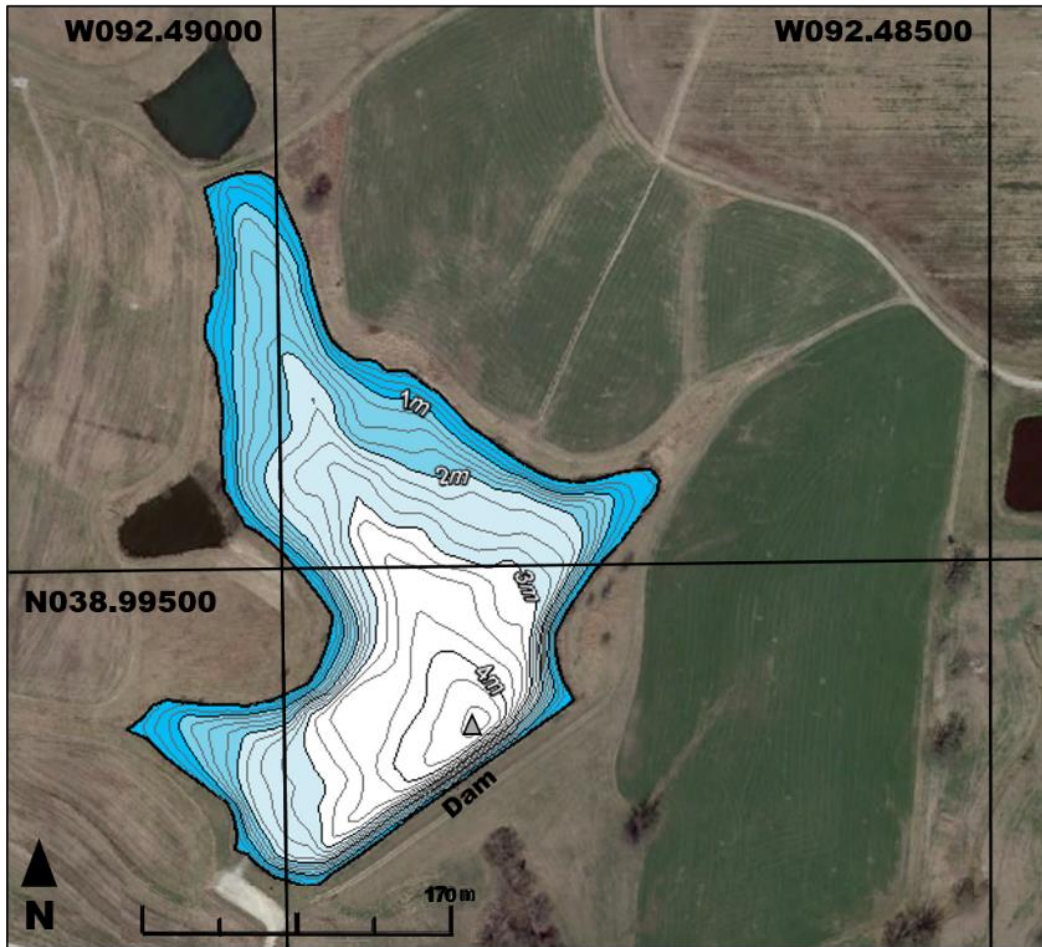


**Figure A2.1:** Bathymetric map of Dairy Farm Lake #1 was created in 2017. Our sampling site for water parameters is indicated by the grey triangle.

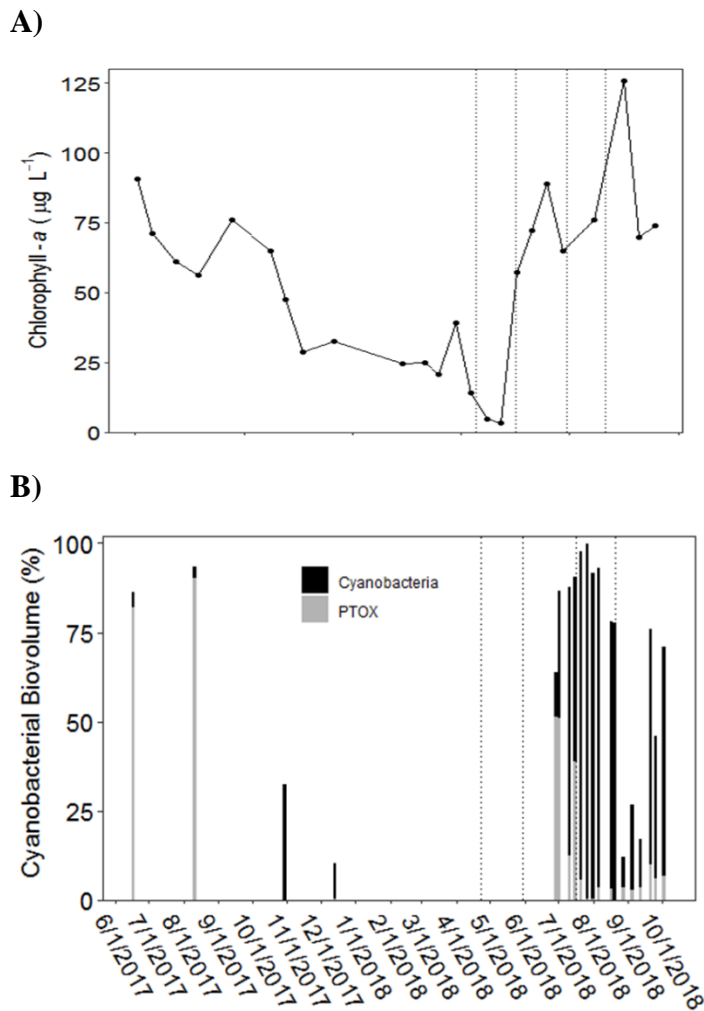


**Figure A2.2:** Chlorophyll-*a*, microcystin, and cyanobacterial biovolume measured in Dairy Farm Lake #1 between June 17, 2017 and October 3, 2018. Chlorophyll-*a* concentrations (A) are from the epilimnion (when the reservoir was stratified) or from the surface to 1 m above the sediment (when the reservoir was isothermal). Cyanobacteria (B) are from the epilimnion (when the reservoir was stratified) or from the surface to 1 m above the sediment (when the reservoir was isothermal). Total cyanobacterial biovolume is reported as the percent of total phytoplankton biovolume that are cyanobacteria, while potentially microcystin producing cyanobacteria (PTOX) is reported as the percent of total cyanobacterial biovolume. Potential microcystin producers were classified following Chapman and Foss (2019). Vertical, dotted lines show fish harvest dates that overlap with phytoplankton enumeration.

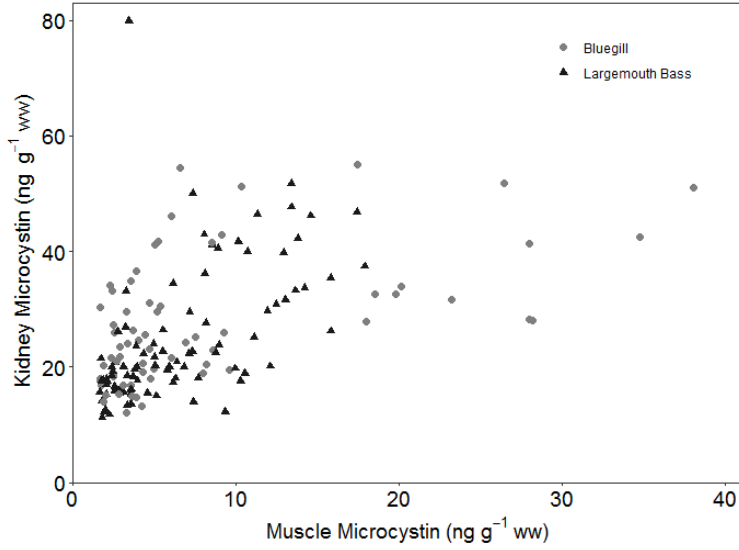
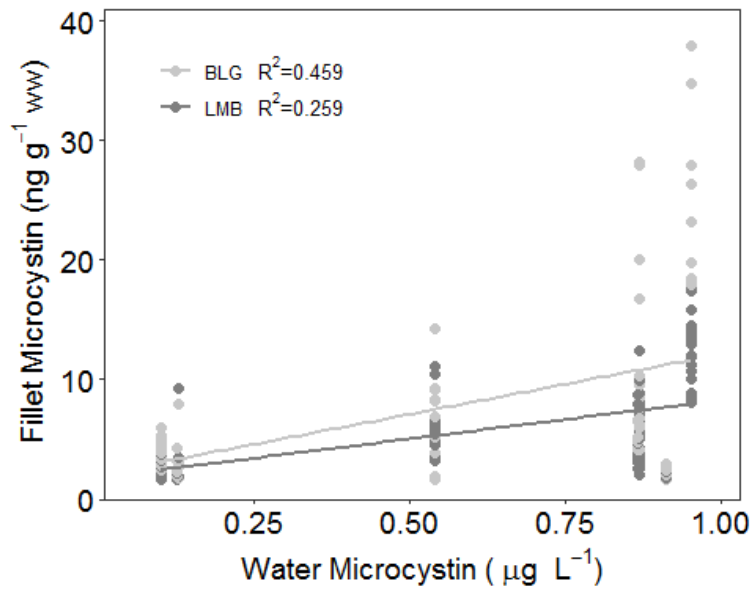
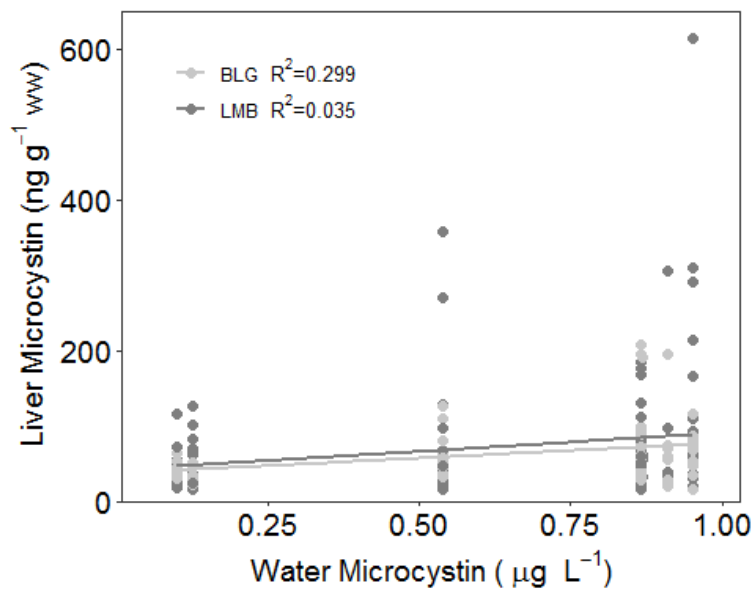


**Figure A2.3:** Scatterplot of muscle and kidney microcystin displayed as wet weight concentrations. Significant and substantial positive correlations exist between these tissues for both and largemouth bass (Table A2.3).

A)



B)



C)

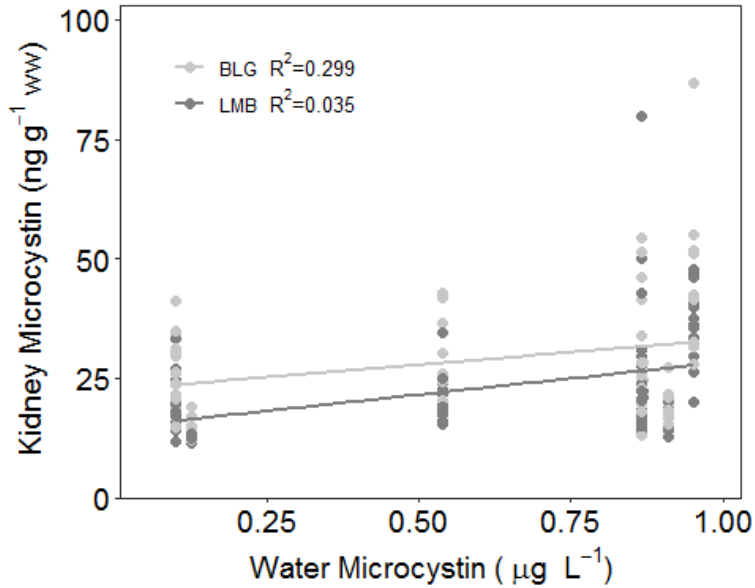
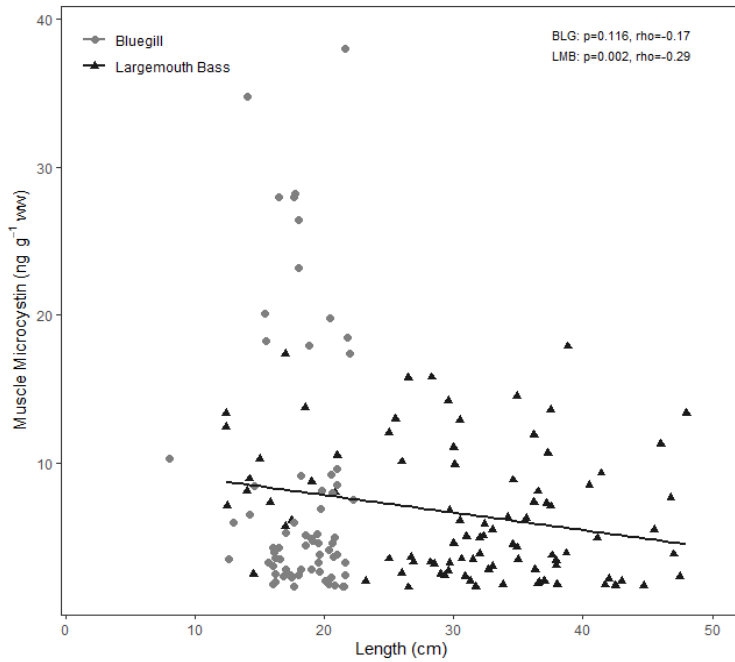


**Figure A2.4:** Scatterplots of water microcystin and microcystin in fish tissues.  $R^2$  values on each plot represent the  $R^2_{\text{adj}}$  for our final, combined multiple linear regression models that excluded harvest date (Table A2.4). Trendlines indicate that water microcystin concentrations were a significant predictor ( $p < 0.05$ ) for microcystin concentrations in fish muscles (A), livers (B), and kidneys (C). We created models for bluegill (BLG, light grey) and largemouth bass (LMB, dark grey).

**A)**



**B)**

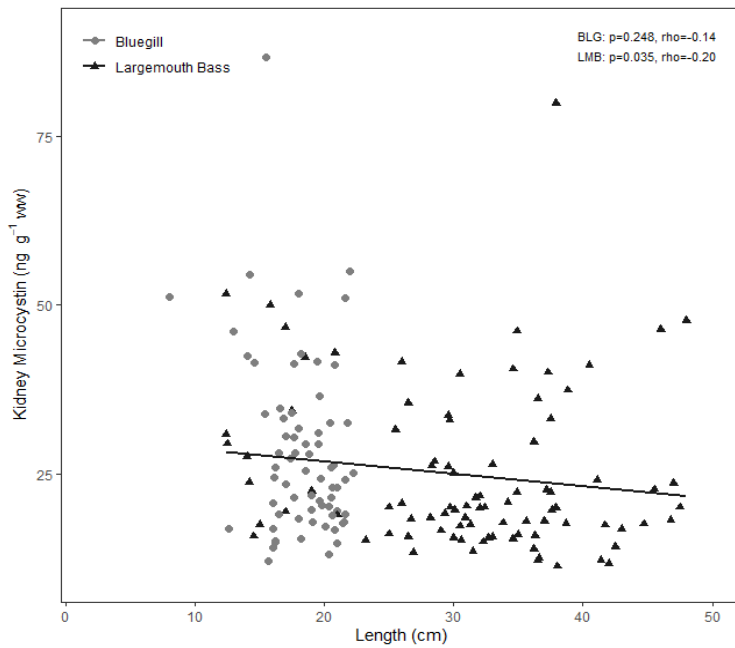


**Figure A2.5:** Scatterplot of microcystin and total fish length. Microcystin is reported in wet weight (ww). Trendlines are included only for largemouth bass, as length and microcystin was significantly correlated for largemouth bass and microcystin in muscles (A) and kidneys (B; Table A2.3).

## LITERATURE CITED

- Chapman, A. & A. Foss, 2019. Potentially Toxigenic (PTOX) Cyanobacteria  
List. Palatka, FL: GreenWater Laboratories.
- Hillebrand, H., C.D. Dürselen, D. Kirschtel, U. Pollinger & T. Zohary, 1999. Biovolume  
calculation for pelagic and benthic microalgae. *Journal of Phycology* 35: 403-424.
- John, D.M., B.A. Whitton & A.J. Brook, 2017. *Freshwater Algal Flora of the British  
Isles*, 2<sup>nd</sup> ed. London, England.
- Karlsson, I., 2003. Benthic growth of *Gloeotrichia echinulata* cyanobacteria.  
*Hydrobiologia* 506-509: 189-193.
- Komarek, J. & K. Anagnostidis, 2008a. *Cyanoprokaryota Part 1: Chroococcales*.  
Spektrum Akademischer Verlag Heidelberg.
- Komarek, J. & K. Anagnostidis, 2008b. *Cyanoprokaryota Part 2: Oscillatoriales*.  
Spektrum Akademischer Verlag Heidelberg.
- Lund, J.W.G., C. Kipling & E.D. LeCren, 1958. The inverted microscope method of  
estimating algal numbers and the statistical basis of estimates by  
counting. *Hydrobiologia* 11: 143-170.
- Wehr, J.D., R.G. Sheath & J.P. Kociolek, 2015. *Freshwater Algae of North America:  
Ecology and Classification*, 2<sup>nd</sup> ed. San Diego, CA.

## APPENDIX 3

FIGURE

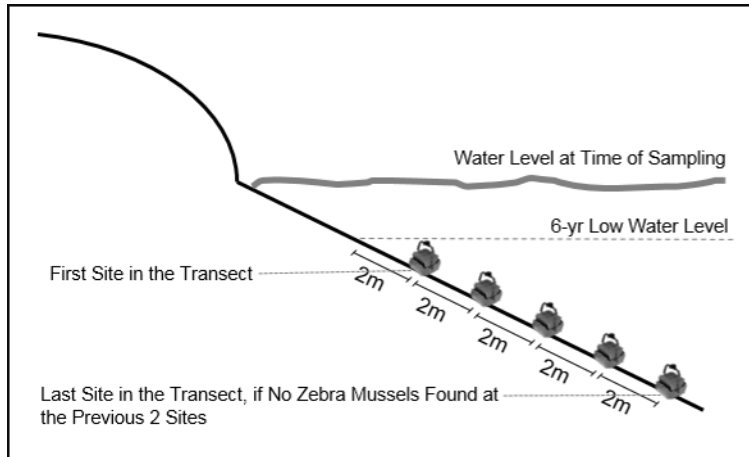


**Figure A3.1:** Example of site selection in each transect. The first site was always 2 m deeper than the lowest water level recorded over the previous 6 years in the reservoir. Each subsequent site was located at 2 m intervals. The last site in each transect occurred when we did not find any zebra mussels at the previous 2 sites and a depth of 10 m deeper than the 6 year low was reached.

## VITA

Jacob Aaron Cianci-Gaskill was born and raised in western New York. He graduated from Brockport High School in Brockport, NY in 2010 before attending the State University of New York College of Environmental Science and Forestry. There, he received his bachelor's of science in Environmental Science, with an emphasis in Renewable Energy, and minors in Urban Ecology and Watershed Science. His honors thesis was entitled "*Examining the effects of pH and macrophyte diversity on benthic macroinvertebrate assemblages in Adirondack lakes.*" He received his master's of science in Biology, with an emphasis in Aquatic Sciences, at Grand Valley State University in 2014. His master's thesis was entitled "*Do invasive dreissenid mussels influence spatial and temporal patterns of toxic Microcystis aeruginosa in a low-nutrient Michigan lake?*"

In 2017, Jacob began his dissertation work at the University of Missouri in the School of Natural Resources, with an emphasis in Water Resources. His doctoral research, entitled "*Phytoplankton response to water quality threats in Midwest reservoirs,*" was completed between 2017 and 2021.